DOCTOR OF PHILOSOPHY

Elucidating the role of bacterial SLC26 transporters

Karinou, Eleni

Award date:
2014

DOCTOR OF PHILOSOPHY

Elucidating the role of bacterial SLC26 transporters

Eleni Karinou

2014

University of Dundee

College of Life Sciences

Division of Molecular Microbiology

Elucidating the role of bacterial SLC26 transporters

Eleni Karinou

March 2014

A thesis submitted to the University of Dundee for the degree of Doctor of Philosophy.

Table of contents

List of Figures

List of Tables

General Abbreviations

5’ RACE	5 prime rapid amplification of cDNA ends
A420	Absorbance measured at wavelength 420 nm
Amp	Ampicillin
APS	ammonium persulfate
cml	chloramphenicol
CRP	cAMP receptor protein
DDM	*n*-Dodecyl-β-D-maltopyranoside
EDTA	ethylene diamine tetraacetic acid
EMSA	electrophoretic mobility shift assay
FNR	fumarate and nitrate regulatory protein
FPLC	fast protein liquid chromatography
gDNA	genomic DNA
IMAC	immobilized metal ion affinity chromatography
LB	Luria-Bertani medium
OD_{600}	optical density measured at wavelength 600 nm
PAGE	polyacrylamide gel electrophoresis
PCR	polymerase chain reaction
RT-PCR	reverse transcription polymerase chain reaction
SDS	sodium dodecyl sulphate
TAE	Tris/acetate/EDTA
TBS	Tris buffered saline
TEMED	N, N, N', N'-tetramethylethylenediamine
U	units

Acknowledgments

First of all, I would like to thank my supervisor Dr Arnaud Javelle for giving me the opportunity to study for a PhD in his lab and trusting me with such an interesting and multifaceted project. We both gained great academic and personal experience the last four years. I would also like to thank BBSRC for funding my project.

Big thanks to all the AJ lab members, past and present. A special thank-you goes to Emma Compton for her unlimited personal and scientific support. I cannot express how grateful I am for all your encouragement, advice and scones that kept me sane.

At this point, I would like to thank Prof Gottfried Unden at the University of Mainz who kindly provided me with strains and plasmids for my experiments and his knowledge on the C_4-dicarboxylate metabolism.

I would like to thank the whole division of Molecular Microbiology, PIs, postdocs and PhD students, for all the help with my project and all the laughs. I consider myself lucky to have been surrounded by people that made me excited being at work every day! Especially, I would like to thank Dr Grant Buchanan for his patience answering all my questions on bacterial genetics as well as for the crash course in Dundonian. Also, I am extremely grateful to Prof Tracy Palmer and Prof Frank Sargent for their constructive advice on my work during the years and their personal support and encouragement.

Every day lab work would not have been possible without our astonishing lab manager, Jacqueline Heilbronn. Thank you so much not only because you are an amazing co-worker but also the warmest hug in Dundee.

I also want to thank Nishal Patel, Ross Fennessy and the rest of the Speedophile society for keeping the “spirit” high. You were a great support!

Last but not least, I would like to thank Daniel Hain for his endless support and comfort even at my darkest moments. Thank you for being there! Above all, I would like to thank my family. Words are not enough to describe their love and encouragement that helped me chase all my dreams.

Declaration

I declare that I am the author of this thesis. Unless otherwise stated, all references cited have been consulted. I declare that the experiments of which the thesis is a record of have been conducted by myself and that any work conducted by other researchers has been noted accordingly. I declare that the thesis has not been previously accepted for a higher degree.

Eleni Karinou

(Candidate)

Arnaud Javelle

(Supervisor)

Publications

Compton, E. L., **Karinou, E**., Naismith, J. H., Gabel, F., & Javelle, A. (2011). Low resolution structure of a bacterial SLC26 transporter reveals dimeric stoichiometry and mobile intracellular domains. *Journal of Biological Chemistry*, ***286***(30), 27058-27067.

Karinou, E., Compton, E. L., Morel, M., & Javelle, A. (2013). The *Escherichia coli* SLC26 homologue YchM (DauA) is a C_4-dicarboxylic-acid transporter. *Molecular microbiology*, ***87***(3), 623-640.

Abstract

The Solute Carrier 26 (SLC26) and Sulphate transporter (SulP) family is a ubiquitous superfamily of transporter proteins conserved from bacteria to man. Proteins within the SLC26/SulP family exhibit a wide variety of functions, transporting anions ranging from halides to bicarbonate. The functional importance of this family is illustrated by the fact that several inherited human diseases are caused by mutations in SLC26 genes. Although these proteins are present in almost all bacteria their physiological function is still unknown. The overall aim of my project was to use a combination of genetic and biochemical approaches to investigate the substrate and physiological role of YchM, the SulP protein found in the bacterial model organism *Escherichia coli*. The work presented here has identified that YchM is an aerobic succinate transporter at acid pH, re-named as DauA (for Dicarboxylic Acid Uptake system A). Using *in vivo* transport assays I studied the apparent kinetics and substrate specificity of DauA. Competition assays showed that DauA apart from succinate can transport fumarate with no preference on the protonation state of the substrate. I identified a further regulatory role for DauA affecting DctA, the main succinate transporter. I showed that DauA and DctA interact physically via their transmembrane domain forming a regulatory unit. More candidate proteins interacting with DauA have been identified by mass spectrometry suggesting a role for DauA in the acid resistance mechanism. Finally, preliminary results on the regulation showed that DauA is produced constitutively regardless of pH or carbon source the cells are grown in. A growth-phase-dependent regulation was observed when cells were grown in glucose and reduction of DauA under anaerobic conditions might indicate a level of regulation. This is the first study reporting that a member of the SLC26/SulP family acts as a bifunctional protein with transport and regulatory activity in the C_4-dicarboxylic acid metabolism.

1 Introduction

1.1 Transporters and Channels

Membrane transporters and channels play crucial roles in fundamental cellular functions and normal physiological processes such as nervous influx conduction, nutrient uptake, removal of waste or oxygen transport during respiration. Therefore studies of solute carrier proteins have had great impact on our understanding of human disease and the design of effective drugs. About 30% of current clinically- marketed drugs have as their targets membrane transporters or channels.

The systems that transfer solutes across the cytoplasmic membrane can be classified into two major categories: channels and transporters, with the latter being subdivided into primary and secondary active transporters based on the energy used for the transport process (Fig. 1-1) (Dubyak, 2004; Saier, 2000).

Channels allow the flow of ions down their electrochemical gradient. Thus, ion movement through channels takes place at rates approaching those of free diffusion (*i.e.* ~ 10^7 ions/sec). Ion channels exhibit two major properties, selectivity and gating. The functions of ion channels require fast switch-on rates and transient open states in the millisecond range. The fast transition from closed to open is achieved by gating of specific chemical, physical and electrical signals (Booth, 2003).

Transporters are characterized by their vectorial reaction which requires selective binding of the transported solute and a conformational change finally leading to the actual movement of the solute across the membrane. The price for this transport against the solute electrochemical gradient is consumption of cellular energy (Dubyak, 2004).

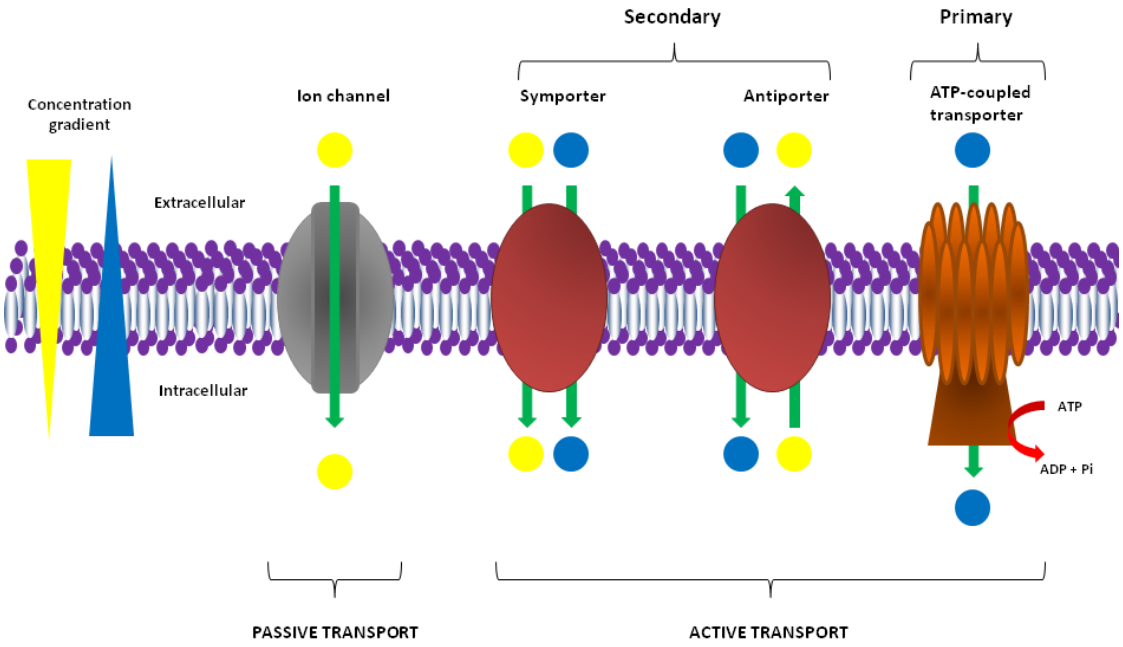

Figure 1- 1: Simplified overview of membrane transport systems.
Ion transport mechanisms across biological membranes can be passive or active. Passive transporters do not utilize any energy source and transport their substrate across an electrochemical gradient. Active transporters can be divided into primary and secondary transporters. In both cases transport across the membrane requires the consumption of cellular energy. In primary transport, hydrolysed ATP provides the necessary energy for the transport of the substrate against the concentration gradient. In secondary transport, the electrochemical potential difference of the substrate transported across the concentration gradient is used as energy source for the transport of the second substrate against the concentration gradient.

Primary active transporters need sources of energy, such as light or chemical energy, for their function. They convert the energy sources into electrochemical energy, which is used to transport their substrates across the membrane (Saier, 2000).

In secondary transport systems, the free energy for accumulation of a solute is provided by the electrochemical gradient of another solute. Two basic classes of secondary active transporters have been identified (Fig.1-1) (Poolman & Konings, 1993; Saier, 2000):

- Symporters: two substrates are transported in the same direction
- Antiporters: two substrates are transported in opposite directions

1.2 The SLC26A/SulP Family

The ubiquitous SLC26A/SulP (Solute carrier 26/ Sulphate Permease) family is a protein family of highly versatile anion transporters/channels with intriguing roles in normal cell physiology and human pathophysiology (Dorwart *et al.*, 2008a; Dorwart *et al.*, 2008b; Mount & Romero, 2004; Ohana *et al.*, 2009). Proteins within this family exhibit a wide-ranged substrate repertoire of monovalent and divalent anions, ranging from halides to carboxylic acids, with low and high affinities.

The first SulP transporter was identified in the filamentous fungus *Neurospora crassa* (Marzluf, 1970), while the SLC26 protein family was defined 20 years ago by expression cloning of a sulphate transporter from rat liver (Bissig *et al.*, 1994). Since then, it has been shown that these transporters form a unique and ubiquitous family (TC 2.A.53) with over 200 sequenced members derived from bacteria to man (Saier *et al.*, 1999; Saier & Paulsen, 1999; Sandal & Marcker, 1994). However, the low level of sequence similarity among the family members does not allow reliable prediction of function or substrate specificity (Dorwart *et al.*, 2008b). Furthermore, there is extremely limited structural and topological information for this family and a number of computer programs using several different algorithms predicts a topology of 10-14 transmembrane spanning α- helices (TMs) depending on the protein, having both N- and C- termini in the cytoplasm (Loughlin *et al.*, 2002). A partial similarity between the transmembrane domain of SLC26 proteins and the *Escherichia coli* ClC (Cl^-/ H^+) transporters has been suggested, even though the two families share a minimal overall sequence similarity (Ohana *et al.*, 2011).

The C-terminus of all SLC26A members and most of the SulP homologues is fused with a Sulphate Transporter and Anti-Sigma factor antagonist (STAS) domain (Fig. 1-2). Many studies point towards a homo-oligomeric and particularly dimeric or

tetrameric assembly state of these transporters (Compton *et al.*, 2011; Currall *et al.*, 2011; Detro-Dassen *et al.*, 2008; Hallworth & Nichols, 2012; Mio *et al.*, 2008; Navaratnam *et al.*, 2005; Zheng *et al.*, 2006; Wang *et al.*, 2010).

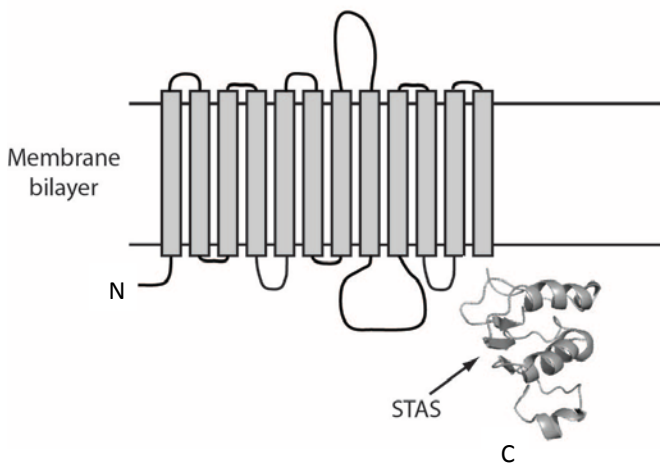

Figure 1- 2: Predicted topological organization of *Yersinia enterocolitica* Yeslc26A2 SulP homologue.
Domain organization of the *Yersinia enterocolitica* SulP homologue, YeSlc26A2, showing a transmembrane region of 12 α-helices and a model of the cytoplasmic STAS domain generated from sequence alignment with the *M. tuberculosis* STAS domain (Compton *et al.*, 2011).

1.2.1 Eukaryotic SLC26A transporters

1.2.1.1 SulP in Fungi

Investigations of sulphate transport in yeast and fungi have revealed the presence of two sulphate permeases in the plasma membrane of high and low affinity. These SulP transporters have been characterised as proton/sulphate symporters (Marzluf, 1997). The SulP proteins are critical in fungi sulphur metabolism, thus *sulP* mutations result in a sulphate auxotrophic phenotype. These permeases are strongly regulated at the transcriptional and posttranslational level (Cherest *et al.*, 1997; Natorff *et al.*, 2003; van de Kamp *et al.*, 1999). The sulphate metabolite repression (SMR) system is responsible for *sulP* regulation and represses *sulP* expression when a preferred reduced sulphur

source is available (Marzluf, 1997; Natorff *et al.*, 2003). In a recent study on Sul2p of *Saccharomyces cerevisiae* it has been proposed that the transporter is autoregulated in a use-dependent manner. This means that the transporter's inactivation depends on the influx of extracellular SO_4^{2-}, as more extracellular substrate is available and being transported, the levels of inactivation and degradation of the transporter increase. This process provides the cells with a protection mechanism against toxic substrates, such as selenate and chromate which can serve also as substrates of these transporters, by preventing excessive uptake (Jennings & Cui, 2012).

Although vacuolar sulphate transport is not well characterised, in *S. cerevisiae*, the protein Ygr125w is localised in the vacuole and has been suggested to act as a sulphate transporter. Ygr125w is a SulP protein which contains a STAS and a cyclic nucleotide monophosphate binding (cNMP-bdg) domain fused with its C-terminus.

Finally, domain prediction programmes such as CDART (Geer *et al.*, 2002), give a list of genes encoding SulP homologues fused to β-carbonic anhydrase (βCA) domains in different fungi species such as *S. cerevisiae*, *Neurospora*, *Aspergillis*, *Candida*, *Penicillium*, *Trichophyton* and *Ustilago*. These results suggest that although no fungal SulP homologue has been functionally characterized so far as a bicarbonate transporter, these proteins may be involved in the carbonate metabolism (Alper & Sharma, 2013).

1.2.1.2 SulP in Plants

The plant SulP transporters have been identified as sulphate/proton symporters (Buchner *et al.*, 2004). Their important role is illustrated by the fact that mutations in these transporters result in sulphate starvation syndrome and in decreased nitrogen fixation efficiency in legumes (Krusell *et al.*, 2005). Plants usually contain multiple

SulP paralogues, for example the model plant *Arabidopsis thaliana* encodes 14 members, subdivided into 5 groups, expressed in different tissues. Group 1 consists of high affinity transporters present solely in root tissue (Yoshimoto *et al.*, 2002). Group 2 has lower affinity for sulphate and shows vascular tissue localization (Takahashi *et al.*, 2000). The role(s) and tissue distribution of the members of Group 3 is still unclear and need to be defined (Krusell *et al*., 2005). Group 4 and 5 are both localized in the tonoplast, with the former playing roles in the vacuolar sulphate efflux, while members of the latter have been characterized as possible molybdate carriers (Hawkesford & De Kok, 2006). While most of the SulP transporters in plants are involved in sulphate metabolism, some of them such as the SHST1 from *Stylosanthes hamata* have a role in molybdate metabolism (Fitzpatrick *et al.*, 2008) and in barley the SulP homologue HvST is involved in the regulation of phytate levels in the cell (Ye *et al.*, 2011).

SulP expression and activity are tightly regulated. Thus, SulP expression in *planta* is controlled by the sulphur status of the cell *i.e.* i) inhibited by low cysteine or glutathione concentration and ii) activated by O-acetylserine, the precursor of the cysteine biosynthesis (Hawkesford & De Kok, 2006). Moreover, additional regulatory control has been shown at the post-translational level, implicating the carboxy-terminal STAS domain (Shibagaki & Grossman, 2006; Shibagaki & Grossman, 2010). In a recent study on the SULTR 1;2 in *A. thaliana*, an additional level of regulation was characterized. It has been shown that the STAS domain of this transporter interacts with the O-acetyl-serine (thiol) lyase (OASTL), an enzyme that catalyzes cysteine biosynthesis. The formation of the complex in between SULTR1.2 and OASTL is controlled by the cellular energy status and inhibits SULTR1.2 activity while activating OASTL activity (Shibagaki & Grossman, 2010).

1.2.1.3 SLC26A in Mammals

The human genome encodes at least 10 SLC26A transporters capable of transporting a wide variety of ions, ranging from halides to carboxylic acids (Table 1-1) (Dorwart *et al.*, 2008b; Mount & Romero, 2004; Ohana *et al.*, 2009). The functional importance of this family is illustrated by the fact that several inherited human diseases are caused by mutations in SLC26 genes (Table 1-1) (Dorwart *et al.*, 2008a; Hastbacka *et al.*, 1996; Prasad *et al.*, 2004; Zheng *et al.*, 2000).

Table 1- 1: The human SLC26A family of transporters (adapted from Alper *et al.*, 2013)

Human gene name	Substrates	Tissue distribution	Disease
SLC26A1	SO_4^{2-}, oxalate, glyoxylate	Hepatocytes, Renal Prox. Tubule Intestine (basolateral)	N/A*
SLC26A2	SO_4^{2-}, oxalate, Cl^-	Chondrocytes, Renal Prox. Tubule, Intestine, Panc duct (apical)	Diastrophic dysplasia, Diastrophic dysplasia, Broad bone-Platyspondylic variant, Atelosteogenesis II, Achondrogenesis IB, Multiple epiphyseal dysplasia type 4, De la Chapelle dysplasia
SLC26A3	Cl^-, HCO_3^-, oxalate	Enterocytes, sperrm Epididymis (apical)	Congenital chloride Diarrhea
SLC26A4	I^-, Cl^-, HCO_3^-	Cochlear, vestibular Epithelial cells,	Pendred syndrome, Deafness (DFNB4),

		Thyrocytes, Type B intercalated cell Airway epithelial cell (apical)	+enlargement of the vestibular acqueduct
SLC26A5	N/A	Cochlear hair cells	Non- syndromic deafness
SLC26A6	Cl^-, HCO_3^-, oxalate, OH^-, formate	Enterocytes, Pancreatic duct, Renal Prox. Tubule, Cardiac myocytes, Sperm	N/A
SLC26A7	Cl^-, HCO_3^-, OH^-, SO_4^{2-}	Gastric parietal cells Type A Intercalated cells, Endothelial cells (apical, lysosome)	N/A
SLC26A8	Cl^-, HCO_3^-, OH^-	Male germ cells, Sperm	N/A
SLC26A9	Cl^-, HCO_3^-	Airway epithelial cells Gastric parietal cells Kidney , Brain	N/A
SLC26A10	N/A	Widespread	N/A
SLC26A11	Cl^-, HCO_3^-, SO_4^{2-}	Renal Intercalated cells (apical), panc. duct Endothelial cells Brain, Widespread	N/A

* N/A: Not Applicable

A variety of different regulatory mechanisms have been described for the human SLC26 transporters, including transcriptional, protein trafficking and post-translational modifications. Unfortunately, most of the regulatory interactions identified are still unclear due to the lack of basic functional information (Dorwart *et al.*, 2008b).

1.2.1.3.1 SLC26A1 (SAT-1)

The first member of the SLC26A family to be cloned and characterized was the SAT-1 protein in rat liver (Bissig *et al.*, 1994). Initially, it was characterised as a sulphate anion transporter and further studies showed that it is capable of oxalate, glyoxylate and chloride transport (Schnedler *et al.*, 2011; Xie *et al.*, 2002). It is localized in the basolateral membrane of hepatocytes, enterocytes and proximal tubular epithelial cells (Regeer & Markovich, 2004). The promoter of the mouse homologue SLC26a1 is under the regulation of thyroxine and AP-1 transcription factor (Markovich, 2011). The human SLC26A1 gene has not been associated with any pathological conditions.

1.2.1.3.2 SLC26A2 (DTDST)

The gene encoding for SLC26A2/DTDST (Diastrophic Dysplasia Sulphate Transporter) was characterised as involved in the autosomal recessive diastrophic dysplasia (Hastbacka *et al.*, 1994). Further analysis showed that various mutations in SLC26A2 cause at least five more recessive chondrodyspalsia syndromes (Jackson *et al.*, 2012). SLC26A2 is mainly a SO_4^{2-} /Cl^- or SO_4^{2-}/ (Cl^- + OH^-) exchanger but can also mediate the transport of I^-, Br^- and NO_3^- (Heneghan *et al.*, 2010; Ohana *et al.*, 2012). It is expressed in renal proximal tubules (Chapman & Karniski, 2010) and in the intestinal tract (Haila *et al.*, 2001; Heneghan *et al.*, 2010) while it shows widespread distribution during development (Haila *et al.*, 2001). Studies of the 5' flanking region upstream of the SLC26A2 gene showed that there are binding sites for the SP-1 and CFBA1 transcriptional factors and that it is induced by the bone morphogenetic protein 2 (BMP-2) via the xenobiotic- responsible element (XRE) (Kobayashi *et al.*, 1997).

Interestingly, it has been shown that SLC26A2 plays a role in colon cancer biology. Cultured cancer cells lacking SLC26A2 showed increased proliferation (Yusa *et al.*, 2010) and the expression of SLC26A2 was decreased in colon cancer biopsies (Galamb *et al.*, 2008). Also, SLC26A2 is suppressed epigenetically in colon cancer cells resulting in unsulphated sialyl groups of the Lewis(x) antigen (Yusa *et al.*, 2010).

1.2.1.3.3 SLC26A3 (DRA, CLD)

SLC26A3 was originally named DRA (Down Regulated in Adenoma) because it was identified as candidate tumour suppressor gene (Schweinfest *et al.*, 2006). However, later it was shown that mutations in this gene are responsible for the recessive congenital chloride diarrhoea (CLD) (Hoglund *et al.*, 2001). SLC26A3 is a Cl^-/HCO_3^- exchanger expressed mainly in the intestine (Chernova *et al.*, 2003; Melvin *et al.*, 1999). Almost 60 different mutations in SLC26A3 have been identified as cause for CLD. Most of these mutations are missense resulting in general loss-of-function (Wedenoja *et al.*, 2011). The C-terminal region of SLC26A3 harbours a STAS domain followed by a PDZ recognition motif. PDZ domains [Post synaptic density protein (PSD95), Drosophila disc large tumour suppressor (Dlg1) and Zonula occludens-1 protein (zo-1)] are commonly found in signalling proteins of viruses, bacteria, fungi, plants and animals. Proper surface expression and protein stabilization requires intact STAS domain and N-glycosylation of SLC26A3 (Dorwart *et al.*, 2008a; Hayashi & Yamashita, 2012; Lamprecht *et al.*, 2009).

Expression of human SLC26A3 is stimulated by butyrate via YY1 and by another unidentified transcriptional factor. Also, it has been shown that expression of SLC26A3

is induced in the presence of Lactobacilli but suppressed by IL-1β and IFN-γ inflammatory mediators (Malakooti *et al.*, 2011).

1.2.1.3.4 SLC26A4 (Pendrin)

Mutations in SLC26A4 have been identified as the causative agent of two types of deafness, for the autosomal non-syndromic deafness DFNB4 and for Pendred syndrome which is characterised by vestibular aqueduct enlargement and euthyroid goitre (Sheffield *et al.*, 1996). SLC26A4 is expressed in a variety of cochlear, vestibular and epithelial cells (Choi *et al.*, 2011) as well as in the apical membranes of the thyrocyte (Bidart *et al.*, 2000; Royaux *et al.*, 2000). It is capable of Cl^-, HCO_3^-, I^-, formate, nitrate and succinate exchange (Reimold *et al.*, 2011; Shcheynikov *et al.*, 2008), although it is not the main I^- transporter in the thyroid follicle (Fong, 2011). In kidney and cochlea, the expression of SLC26A4 is regulated by the transcription factor FOXI1 whereas in the thyroid by TTF-1, thyroglobulin, TSH and iodide (Rozenfeld *et al.*, 2012).

1.2.1.3.5 SLC26A5 (Prestin)

The SLC26A5 protein in humans is unique among the other homologues of this family due to its characterization as a membrane-bound motor protein responsible for the electromobility of outer hair cells in the cochlea (Zheng *et al.*, 2000). However, it has not been clearly associated as a human deafness gene (Minor *et al.*, 2009). Further investigations demonstrated that prestin is capable of oxalate and formate transport in CHO cells (Bai *et al.*, 2009).

1.2.1.3.6 SLC26A6

The SLC26A6 exchanger exhibits widespread expression, being found in kidney, heart, muscle, stomach, oesophagus and placenta with a wide range of substrates, including HCO_3^-, OH^-, oxalate and nitrate (Alvarez *et al.*, 2004; Chernova *et al.*, 2005; Wang *et al.*, 2002; Xie *et al.*, 2002). Recently, it has been shown that SLC26A6 is involved in a pathway with Na^+-dependent dicarboxylate co-transporter (NADC-1) to regulate the citrate/oxalate homeostasis. The SLC26A6 STAS domain interacts with the first intracellular loop of NADC-1 in a mutual reciprocal regulation manner, where SLAC26A is activated and NADC-1 is inhibited (Ohana *et al.*, 2013).

1.2.1.3.7 SLC26A7

SLC26A7 is characterised as both a Cl^-/HCO_3^- exchanger and an increased Cl^- selectivity anion channel (Petrovic *et al.*, 2004; Kosiek *et al.*, 2007). The mouse homologue is localized in the basolateral membrane of gastric parietal cells while in humans is found mainly in the kidney (Petrovic *et al.*, 2004).

1.2.1.3.8 SLC26A8 (Tat1)

The SLC26A8 homologue has been characterised as a modest Cl^-, SO_4^{2-} and oxalate transporter (Lohi *et al.*, 2002; Toure *et al.*, 2001). In mice it is expressed in spermatocytes and mature sperm (Toure *et al.*, 2001). Mice depleted of SLC26a8 showed male infertility as a result of non-mobile sperm (Toure *et al.*, 2007). However, no polymorphisms in SLC26A8 have been identified in infertile men (Makela *et al.*, 2005).

1.2.1.3.9 SLC26A9

SLC26A9 is a highly selective Cl^- channel expressed mainly in brain and on apical membranes of airway epithelial cells (Dorwart *et al.*, 2007; Lohi *et al.*, 2002). In humans SLC26A9 is constitutively active on a CFTR-dependent manner (Bertrand *et al.*, 2009). The regulation and function of this transporter is highly dependent on the expressed tissue and organism.

1.2.1.3.10 SLC26A10

In humans the SLC26A10 predicted polypeptide is considered a pseudogene however in mice it is highly expressed in heart (Alvarez *et al.*, 2004).

1.2.1.3.11 SLC26A11

SLC26A11 is a SO_4^{2-} transporter mainly expressed in kidney, brain and placenta but also in other tissues at lower levels (Vincourt *et al.*, 2003). It has been found in several lyosomal proteomes suggesting that it might function as lyosomal sulphate transporter (Stewart *et al.*, 2011) and the SLC26A11 gene was found adjacent to SGSH, a gene encoding for sulfamidase, mutations in which cause a lyosomal storage disease (Ouesleti *et al.*, 2011).

1.2.2 Prokaryotic SLC26A transporters

While the amount of information on eukaryotic members of the SCL26A/SulP family constantly increases, the role of the prokaryotic homologues so far remains unclear. Many bacterial species have been shown to express multiple SulP homologues,

however, none of the bacterial SulP proteins have been shown to play a direct active role in sulphate transport (Saier & Paulsen, 1999; Zolotarev *et al.*, 2008). Sulphate metabolism has been extensively studied in bacteria; sulphate and organosulphate uptake is catalysed by an ABC transporter from the SulT family (TC 3.A.1.6) (Pilsyk & Paszewski, 2009).

The only comprehensive functional and topological analysis of a bacterial SulP protein concerns the bicarbonate transporter BicA from *Synechococcus (*Shelden *et al., 2010).* Although marine cyanobacteria play a large part in the global CO_2 sequestration and primary production, little is known about the inorganic carbon uptake system. BicA has been characterized as low/medium affinity Na^+/ bicarbonate symporter. BicA is the entry point of CO_2 into *Synechococcus* metabolism and the first step of the photosynthetic CO_2 fixation. The discovery of BicA has significant implications for understanding the important contribution of oceanic strains of cyanobacteria to global CO_2 sequestration processes (Price *et al.*, 2004). It has been shown that this bacterial SulP has 12 transmembrane helices (Fig. 1-3). *bicA* expression is activated under low inorganic carbon conditions (Shelden *et al.*, 2010).

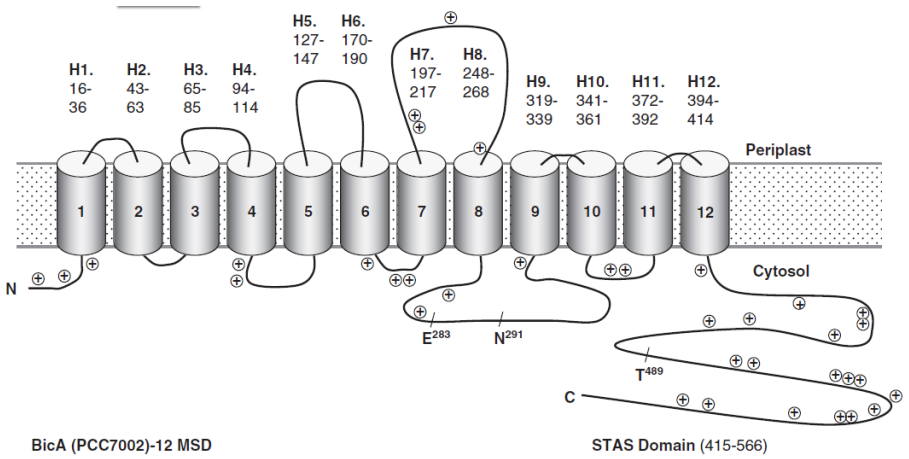

Figure 1- 3: Simplified topology of BicA of Synechococcus PCC7002 (Shelden *et al.*, 2010). PhoA-LacZ mapping of BicA from Synechococcus PCC7002 showed that the transporter has 12 transmembrane helices, with both N- and C- termini inside the cytoplasm. The positions of positive charged residues are indicated. The highly conserved residues E^{283} and N^{291} are implicated in human disease. T^{489} is a putative phosphorylation site.

The *Mycobacterium tuberculosis* genome encodes for three SulP proteins, RV1739c, Rv1707 and Rv3273. Overexpression of Rv1739c in *Escherichia coli* cells increased sulphate uptake but failed to complement the auxotrophic phenotype of a *M. bovis* mutant lacking the primary ABC sulphate transporter (Hatzios & Bertozzi, 2011; Zolotarev *et al.*, 2008). It has been shown that in mycobacteria, outer membrane sulfolipids play a role in pathogenicity and that the expression of Rv1739c and Rv1707 genes is induced in activated macrophages 24 hours after infection, leading to the hypothesis that SulP proteins of *M. tuberculosis* might be necessary for survival in hypoxic or other stress conditions (Hatzios & Bertozzi, 2011). The third mycobacterial SulP homologue, Rv3273, is lacking a C-terminal STAS domain but instead is fused to a β-carbonic anhydrase domain suggesting that it might functions as a HCO_3^- transporter (Nishimori *et al.*, 2010).

In *Escherichia coli* only one SulP homologue, YchM, has been identified. Recently, the crystal structure of the isolated YchM STAS domain was solved in a complex with acyl carrier protein (ACP), leading to the suggestion that YchM is a bicarbonate transporter

involved in fatty acid metabolism (Babu *et al.*, 2010). However, an exhaustive phylogenetic analysis of bacterial SLC26 homologues performed by our group clearly shows that *E. coli* YchM clusters independently from the BicA/BicA-like proteins (Fig. 1-4). The characterisation of the YchM physiological role is the subject of this thesis.

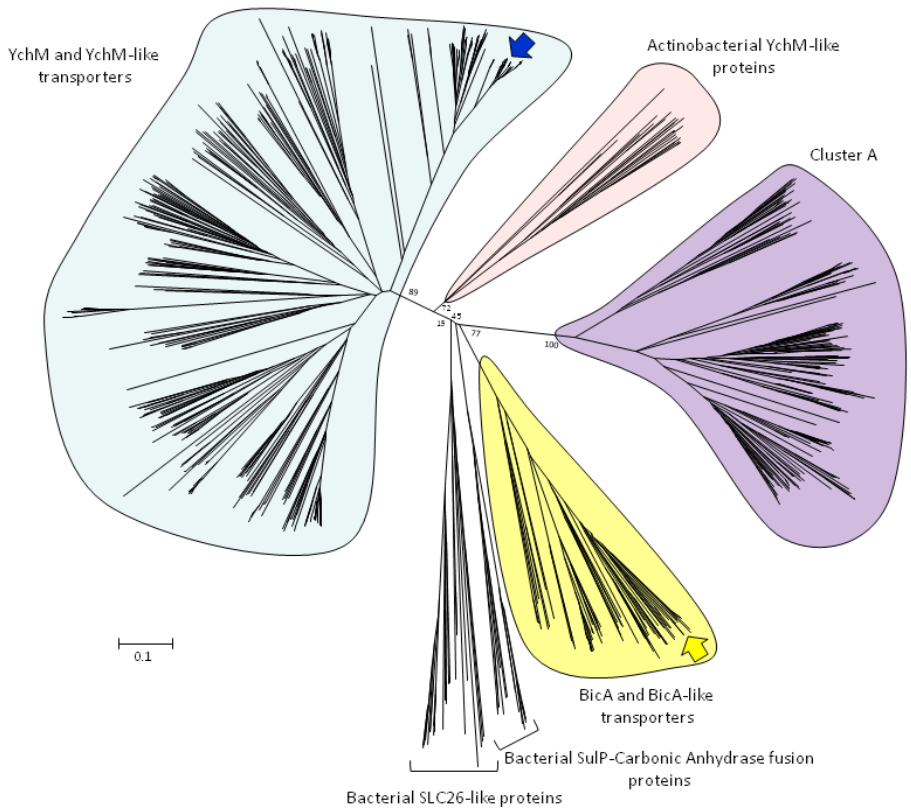

Figure 1- 4: Phylogenetic tree of SulP homologues in bacteria.
Neighbour-joining tree of 766 SulP homologues sequences retrieved from the NCBI database using BLASTP. The blue and yellow arrows refer to YchM from *E. coli* and BicA from *Synechococcus* sp. respectively. Cluster A is a separate group without any functional annotation, composed of sequences from Actinobacteria, Bacteroidetes, Cyanobacteria and Proteobacteria. Bootstrap values are reported only for main clusters. The scale marker represents 0.1 substitutions per residue (analysis performed by Melanie Morel).

In the *Streptomyces* species two SulP encoding genes have been found in bleomycin and penicillin biosynthesis operons (Du *et al.*, 2000), but their function has not been identified yet.

Finally, the human and animal pathogen *Yersinia enterocolitica* encodes multiple SulP transporter proteins. Structural information on YeSlc26A2 generated by small angle neutron scattering (SANS) is available: a low resolution structural model shows that YeSlc26A2 forms homodimers stabilised by the transmembrane core with the STAS domain projecting away from the membrane, not taking part in the dimerization (Fig. 1-5) (Compton *et al.*, 2011).

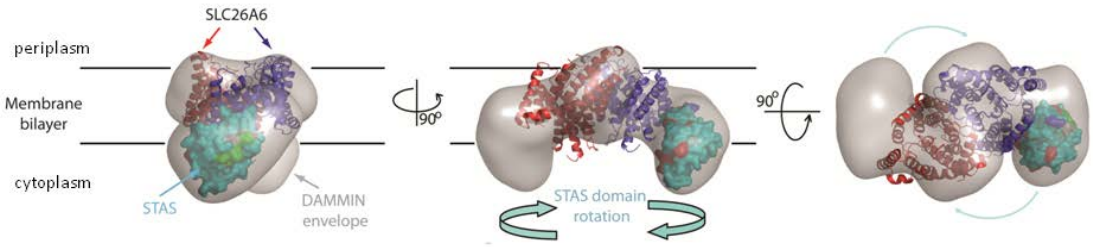

Figure 1- 5: Domain architecture of YeSlc26A2.
Docking of SLC26A6 transmembrane domain (based on ClC-ec1) and STAS domain models into the low resolution envelope, viewed from the plane of the membrane and above the membrane (Compton *et al.*, 2011).

Prokaryotic members of the SulP family appear to be fused to non-transporter domains in the C-terminal. SulP – carbonic anhydrase homologue fusions have been predicted for a small number of bacterial SulP proteins suggesting bicarbonate or carbonate transport functions, but their regulation and function are still unknown. Another interesting group of fusions came up with SulP – rhodanese (a thiosulphate: cyanide sulphotranspherase) suggesting a role in sulphate uptake. Finally, the large majority of bacterial SulPs are fused to a STAS domain (Fig. 1-6) (Felce & Saier, 2004). Other interesting predicted C-terminal domains of bacterial SulP homologues include nuclear pore complex components, t-SNARE-like domains and ADP-ribosyl glycohydrolase domains (Alper & Sharma, 2013). However, further studies will be necessary to identify the function of the bacterial SulP proteins and the role of these domains.

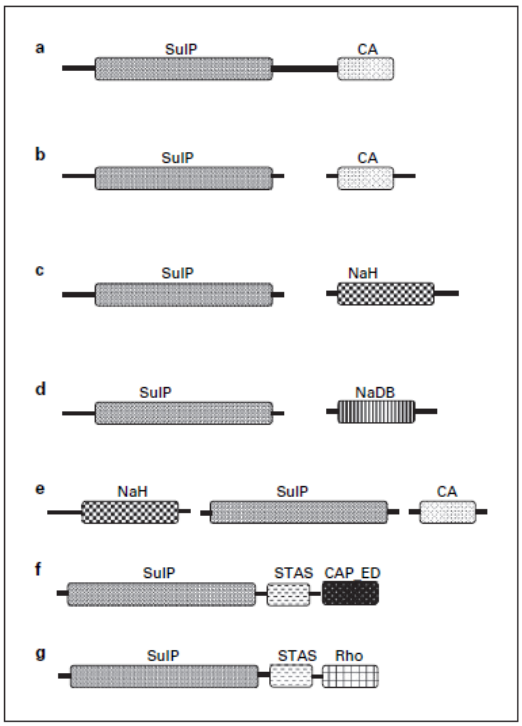

Figure 1- 6: Predicted SulP fusions types.
(a) SulP homologue fused to a carbonic anhydrase (CA) domain. (b) Two adjacent genes encoding for SulP homologue and for carbonic anhydrase homologues. (c) A SulP homologue with an adjacent gene encoding a Na^+ /H^+ antiporter homologue of the NhaD family (TC #2.A.62). (d) A SulP homologue with an adjacent gene encoding a putative Na^+ bicarbonate symporter of the SBT family (TC #2.A.83). (e) A SulP homologue with adjacent genes encoding both a Na^+ /H^+ antiporter homologue of the NhaD family and a carbonic anhydrase. (f) A SulP homologue with fused STAS and a CAP_ED cyclic AMP-binding domain. (g) A SulP homologue with fused STAS and rhodanese domains. The domain/gene combinations shown in a–e and g are exclusively from bacteria, but that shown in f is found in both bacteria and fungi (Felce & Saier, 2004).

Eukaryotic members of the SulP family have quite diverse functions, such as H^+/sulphate symport activity in plants and fungi but anion exchange in mammals, with different members showing different specificities. Given the diversity of functions in eukaryotic members, it is reasonable to expect that the SulP family in prokaryotes can transport or exchange a number of inorganic anions and/or other substrates.

1.3 STAS domain

A very interesting and novel regulatory mechanism may control the activity of the SLC26A/SulP transporters. All the vertebrate SLC26A transporters and almost all the lower organism SulP transporters possess a cytoplasmic C-terminal region named Sulphate Transporter and Anti-Sigma factor antagonist (STAS) domain. The name of this domain came from an unexpected similarity with the bacterial Anti-Sigma factor antagonists (ASA), typified by SpoIIAA in *Bacillus subtilis* (Aravind & Koonin, 2000).

The STAS domain presents a low sequence identity (around 30%) but share a conserved fold of 4β-strands interspersed among 5 α-helices. The unexpected identification of the STAS domain in SLC26A/SulP transporters, as well as disease-associated mutations in this domain, provides functional clues as to the regulation of the transporter (Dorwart *et al.*, 2008a).

1.3.1 STAS domain in eukaryotes

1.3.1.1 Function

In eukaryotes, the STAS domain is only found fused with the C terminal region of the SLC26A/SulP transporters. The mammalian STAS are bigger than homologues in plant and fungi. Indeed, the mammalian STAS domain possesses an intervening sequence (IVS) between helix α1 and strand β3, missing from the STAS domains found in plants and fungi. This region is the main source of variability among the SLC26 STAS domains.

It has been proposed that the STAS domain takes part in protein-protein interactions and is involved in signal transduction given its significant similarity with SpoIIAA (Aravind & Koonin, 2000).

In *Arabidopsis thaliana*, it has been shown that the STAS domain of the sulphate transporter Sultr1;2 forms homodimers and it is essential for correct membrane localization, protein stability and transport kinetics (Shibagaki & Grossman, 2006). Furthermore, Sultr1;2 has been shown to interact, via the STAS domain, with the enzyme O-acetylserine-lyase/cysteine synthase. The activity of the transporter and the enzyme are co-regulated via this interaction in response to the sulphur cellular status (Shibagaki & Grossman, 2010).

Several mammalian members of the SLC26 family have been shown to interact with the CFTR chloride channel. This interaction results in co-regulation of both transporters. In humans, SLC26A3, through its the C-terminal PDZ recognition motif, interacts with the PDZ adaptor proteins PDZK1, E3KARP and IKEPP which form a scaffold that brings SLC26A3 in close proximity with CFTR anion transporters (Lamprecht *et al.*, 2009). It has also been shown that SLC26A3 is able to interact directly through its STAS domain with the R domain of CFTR (Chernova *et al.*, 2003; Ko *et al.*, 2002). In HEK-293 cells the R domain of CFTR is able to interact with the STAS domain of SLC26A6 and SLC26A9 (Ko *et al.*, 2002; Ko *et al.*, 2004). In contrast with the rest of the transporters of the family, interactions between the STAS domain of SLC26A9 and the R domain of CFTR inhibit the transport activity of the former (Chang *et al.*, 2009).

In a recent study, it has been shown that the mouse oxalate transporter Slc26a6 interacts, via its STAS domain, with the first intracellular loop of the citrate transporter

NaDC-1. The interaction is putatively involved in the regulation of Ca^{+}-oxalate stone formation (Ohana *et al.*, 2013).

1.3.1.2 Structure

Recently, the structure of the rat prestin (SLC26a5) STAS domain has been solved by X-ray crystallography (Pasqualetto *et al.*, 2010). The deletion of the IVR and 9 C-terminal residues was necessary in order to obtain diffracting crystals of this domain. This structural analysis reveals that the STAS domain starts immediately after the last transmembrane helix of the transporter. The domain is structurally and topologically similar to the bacterial Anti-Sigma Antagonist (ASA) factor. The authors hypothesised that the STAS domain of the SLC26A transporter is involved in functionally important intra- and inter- molecular interactions (Pasqualetto *et al.*, 2010).

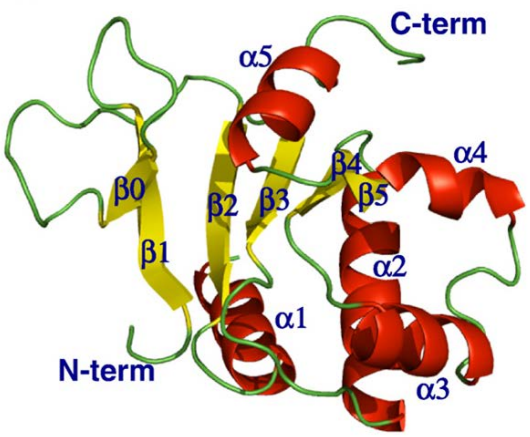

Figure 1- 7: Crystal structure of SLC26A5 (prestin).
In yellow are the β-strands forming the central β-sheet and in red the α-helices. In green are represented the connecting loops (Pasqualetto *et al.*, 2010).

1.3.2 STAS domain in bacteria

Although STAS domains are only present fused with the C-terminal region of SLC26A transporters in eukaryotes, they can also be found in numerous proteins in bacteria. STAS domain containing proteins have been involved mainly in (1) sigma factor regulation, (2) signal transduction and (3) regulation and protein interactions of the SulP anion transporters.

In addition, further functions have been suggested for STAS domain containing proteins. These proteins may be involved in nutrient transport based on their proximity to domains encoding enzymes such as glutaminase, glycosyltransferase, and vitamin-K-dependent carboxylase activity. Also, the STAS domains as such can be adjacent to other domains involved in detoxification of alkalenes and organic solvents (Sharma *et al.*, 2011a).

1.3.2.1 STAS domain in Anti-Sigma factor Antagonists (ASAs)

Under nutritional stress, *Bacillus subtilis* cells resort to sporulation. Sporulation is a highly regulated event which results in a specialized differentiated endospore, resistant to almost all the common anti-bacterial agents. Upon onset of sporulation, sigma factor σ^F, which is responsible for the early forespore-specific gene expression, is activated. Regulation of σ^F involves a series of regulators starting with SpoIIAB, an anti-sigma factor with protein kinase activity. Interaction between SpoIIAB and σ^F prevents the latter from forming the RNA polymerase holoenzyme and thus progressing with the sporulation specific cascade of gene expression. SpoIIAB is inhibited by interaction with the anti-sigma factor antagonist SpoIIAA, a STAS domain containing protein, which releases the sigma factor. SpoIIAB in turn phosphorylates SpoIIAA inactivating

it and starting a new cycle of catalytic interactions (Fig. 1-8) (Errington, 2003; Masuda *et al.*, 2004).

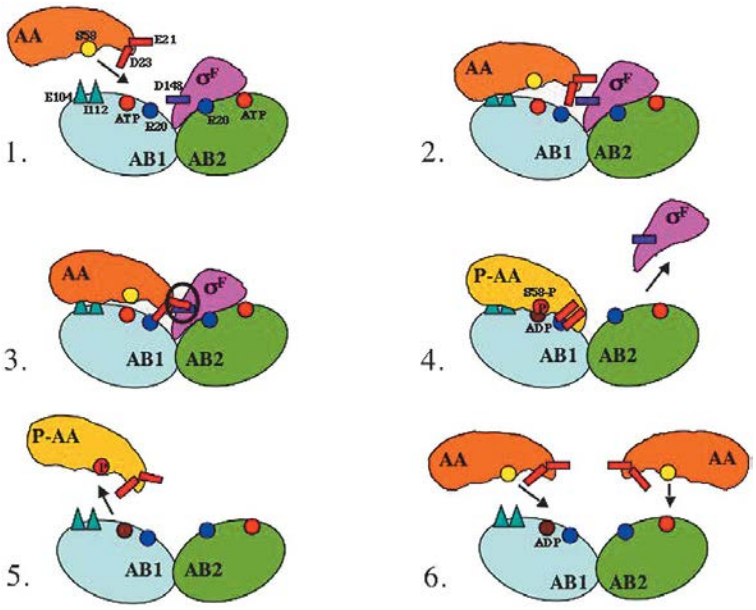

Figure 1- 8: Cartoon illustrating the mechanism of displacement of σ^F from SpoIIAB by SpoIIAA.
SpoIIAB1 and SpoIIAB2 are coloured blue and green, respectively. σ^F is coloured pink and SpoIIAA in orange. (1) AB1 of σ^F:AB2 is the targeted molecule for docking as its surface is more accessible to AA. (2) AA docks onto its initial docking sites on AB1. (3) AA docks into a secondary which is represented by AA-Asp23 interacting with AB-Arg20. Upon the second docking, a clash occurs between σ^F and AA (circled in black). (4) The clash leads to the dissociation of σ^F from AB (ADP). AA then slips into its final docking conformation that is amenable to phosphorylation (represented by AA turning yellow). (5) P-AA dissociates from AB (ADP) due to steric and electrostatic clashes. (6) Unphosphorylated AAs interact with AB1 as an IC and AB2 as a target for phosphorylation. AA, SpoIIAA; AB1, SpoIIAB1; AB2, SpoIIAB2; P-AA, phosphorylated SpoIIAA (Masuda *et al.*, 2004).

1.3.2.2 STAS domain containing proteins in signal transduction

1.3.2.2.1 The stressosome

In *Bacillus subtilis* and related Gram positive bacteria, mild environmental stress (pH, osmolarity, and ethanol) stimulates the σ^B stress response pathway. The sigma factor σ^B is responsible for the signal transduction cascade resulting in entry to stationary phase and starvation response. In the absence of environmental stress, σ^B is inactive in a complex with its cognate anti-sigma factor RsbW. RsbW also acts as a protein kinase towards the anti-sigma factor antagonist RsbV, a STAS domain containing protein. Inactivation of RsbV by phosphorylation can be reversed by the phosphatase RsbU in the presence of stress (Hecker *et al.*, 2007).

The stressosome, a large protein complex, is found upstream of RsbU in the σ^B pathway. It consists of 40 copies of the multidomain STAS containing protein RsbR and 20 copies of the STAS containing protein RsbS. Under normal conditions the stressosome is able to sequester 20 copies of the kinase RsbT. Upon environmental stress, RbsT phosphorylates RsbS and RsbT, releasing itself from the stressosome. This leads to binding of RsbT to RsbU and to an increase in the phosphatase activity of the latter. In turn, RsbU dephosphorylates RsbV which is active now to bind to the σ^B-RsbW complex and to release σ^B, resulting in the induction of the σ^B regulon (Fig. 1-9) (Marles-Wright & Lewis, 2010).

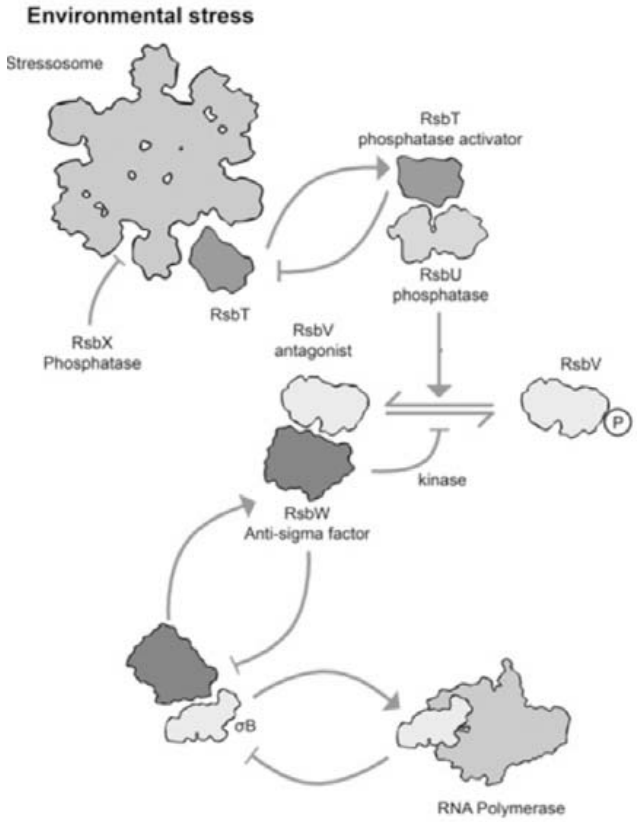

Figure 1- 9: The σ^B regulatory pathway of *B. subtilis.*
The stressosome, a complex made up of multiple copies of STAS proteins RsbR and RsbS, serves to sequester kinase RsbT in normal conditions. Under stress, RsbT phosphorylates both STAS proteins, resulting in its release from the stressosome to bind and activate RsbU phosphatase. The RsbT/RsbU complex-mediated dephosphorylation of anti-anti-σ factor STAS protein RsbV allows it to bind anti-σ factor RsbW, liberating σ^B from its inactivating complex with RsbW, and allowing activation of RNA polymerase (Sharma *et al.*, 2011a).

1.3.2.2.2 Phototransduction

Another environmental stimulus for activation of the σ^B regulatory pathway is blue light. The signal is detected and transmitted via the stressosome to σ^B by the blue light receptor YtvA. YvtA is a chimeric protein with one LOV (Light-Oxygen-Voltage sensing) domain, which binds flavin cofactors (FMN), and one STAS domain.

LOV domains belong to the Per-ARNT-Sim (PAS) domain superfamily. In bacteria they regulate general stress response, cell envelope physiology and virulence (Herrou & Crosson, 2011).

Blue light triggers the decay of LOV-FMN and this conformational change is transduced to the STAS domain via a short J linker connecting the two domains. It is not yet completely understood how the STAS domain of YtvA is involved in σ^B pathway activation via the stressosome but it has been suggested that it might have a direct or indirect role in RsbT kinase activation (Herrou & Crosson, 2011; Tang *et al.*, 2010). A recent paper by Jurk *et al.* showed that YvtA is incorporated permanently in the stressosome independent of the light state, recruited by RsbR. This results to a slight displacement of RsbR which might induce a transient interaction between YvtA and RsbT. Upon illumination slight conformational changes of the YvtA and Rsb proteins STAS domains might trigger the signal transduction cascade (Jurk *et al.*, 2013).

1.3.2.3 STAS domain in SulP transporters

The large majority of bacterial SulPs are fused to a STAS domain (Felce & Saier, 2004). Although the function and topology of the bicarbonate transporter BicA in *Synechococcus* has been elucidated, the role of its STAS domain in the regulation and function is still unknown (Shelden *et al.*, 2010).

To date, the only crystal structures available for bacterial SulP STAS domains have been generated for the homologues in *Wolinella succinogenes*, *Vibrio cholera* and *Escherichia coli*, and by NMR in *Mycobacterium tuberculosis* (Fig. 1-10).

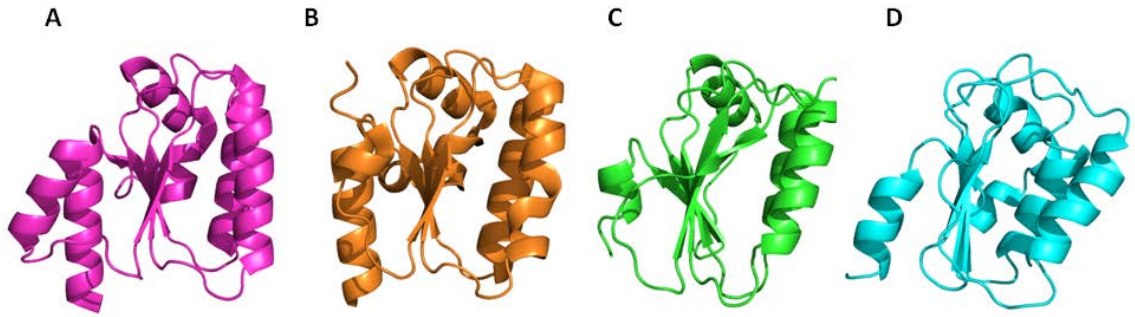

Figure 1- 10: 3D structures of bacterial SulP STAS domains.
(A) *Wolinella succinogenes* (B) *Vibrio cholera* (C) *Escherichia coli* and (D) *Mycobacterium tuberculosis.* Images kindly provided by Emma Compton.

The structures of these STAS domain are very similar, sharing the interspersed β-strands and α-helices characteristic of the bacterial STAS domain and anti-anti-sigma proteins (Fig. 1-10 and 1-11).

In *M. tuberculosis*, the Rv1739c STAS domain is able to bind guanine nucleotides and has a modest GTPase activity, but it is not a phosphoprotein or substrate of any of the defined *M. tuberculosis* Ser/Thr kinases (Sharma *et al.,* 2011b). Backbone dynamics measured by ^{1}H- ^{15}N NMR suggested that guanine nucleotides bound to Rv1739c STAS domain cause conformational changes and that these changes may shift the oligomeric state away from the usual monomeric state of the unliganded STAS domain (Sharma *et al.,* 2012). Many residues of Rv1739c STAS domain found to bind or to be conformationally affected by ligand contact align with disease associated residues in human SLC26 STAS domains, suggesting proper folding and signal related functions for these residues (Sharma *et al.,* 2011b).

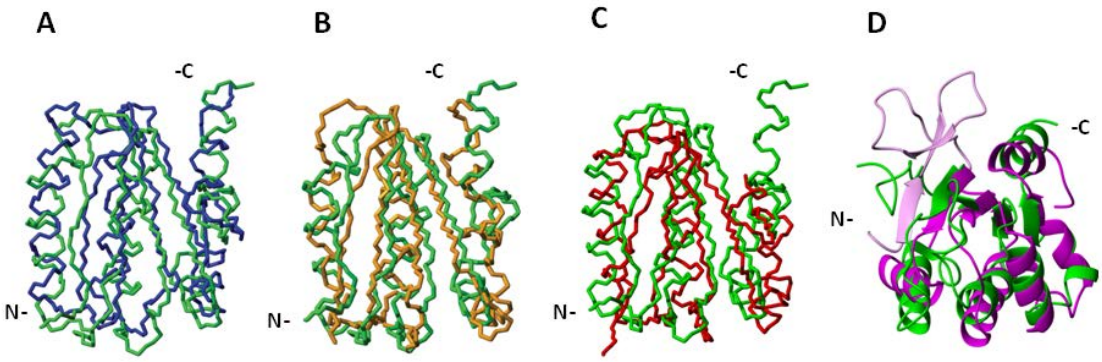

Figure 1- 11: Structural alignment of Rv1739c STAS domain.
A–D, average backbone structure of the Rv1739c STAS domain (green) aligned with: (A) crystal structure of non-phosphorylated SPOIIAA from *B. sphaericus* (blue), (B) solution NMR structure of *B. subtilis* SPOIIAA (orange); (C) solution NMR structure of *T. maritima* TM1442 (red); (D) overlay of a ribbon representation of Rv1739c STAS (green) with the crystal structure of an engineered core STAS domain from rat Slc26A5/prestin (magenta).The region shown in light magenta comprises the N-terminal 15 aa of the prestin STAS (light magenta) extending beyond the Rv1739c STAS N-terminal residues (Sharma *et al.*, 2011b).

In *E.coli*, the STAS domain of the SulP homologue YchM was co-purified and co–crystallised with the acyl carrier protein (ACP). The molonyl-coA moiety attached to ACP defines the contact in between the two proteins. It was showed that the secondary structure sequence (β1-β2-α1-β3-α2-β4-α3-β5-α4) differs from the Rv1739c STAS domain and the anti-sigma factor antagonists, with a switching of α1and β2 and absence of helix α5 (Fig. 1-12) (Babu *et al.*, 2010). Based on the fact that YchM co-crystallised with ACP the authors proposed that YchM is a bicarbonate transporter involved in fatty acid metabolism. However, a later study from the same group failed to reproduce their bicarbonate transport assay and they did not obtain evidence that the full length YchM interacts with ACP (Taddese, 2013). In addition, we have clearly shown that YchM does not belong to the BicA/BicA-like proteins phylogenetic cluster and acts as a succinate transporter (Karinou *et al.*, 2013). Taken together these observations suggest it is likely that the YchM STAS-ACP is a non-functional interaction.

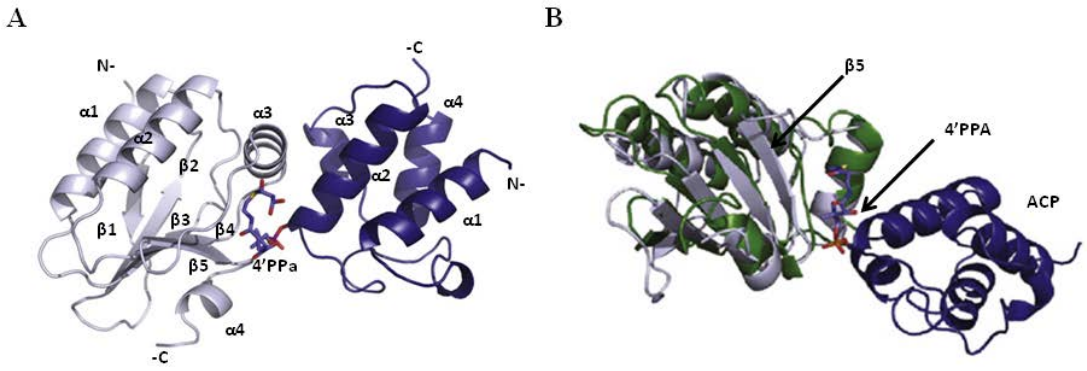

Figure 1- 12: Crystal structure of YchM STAS domain in complex with ACP.
(A) The STAS domain of YchM (residues 436–550) bound to ACP are shown in white and blue, respectively. The 4'PPa is covalently bound to ACP and is located at the interface between STAS and ACP. (B) The structural overlay of YchM-STAS onto SPOIIAA illustrates the position of the additional fifth b strand on YchM that is created to provide a binding pocket for the malonyl 4'PPa (Babu *et al*., 2010).

1.4 Aims

Apart from the bicarbonate transporter BicA from *Synechococcus*, no bacterial SulP homologue has been characterized to date although they are conserved in bacteria. Based on their similarities with homologues in plants and fungi, bacterial SulP are usually classified as sulphate transporters, but no evidence is available to support this hypothesis. Initial phylogenetic analysis (Fig. 1-4) showed that *E. coli* YchM clusters independently from the BicA/BicA-like proteins. Therefore, the overall aim of this project was to use a combination of genetic and biochemical approaches to investigate the substrate(s) and physiological role of YchM, the SulP protein found in the bacterial model organism *Escherichia coli*. Three basic approaches were undertaken:

1) Identification of a YchM-dependent phenotype

2) Identification of proteins that may interact with YchM

3) Analysis of the expression of YchM

2 Materials and Methods

2.1 Bacterial strains, plasmids and oligonucleotides used in this study

2.1.1 E. coli strains used in this study

Table 2-1: Strains used in this work

Strain	Genotype*	Reference
MACH1	F⁻ Φ80*lacZ*ΔM15 Δ*lac*X74 *hsd*R(r_K^-, m_K^+) Δ*rec*A1398 *end*A1 *ton*A	Invitrogen
DH5α	F⁻ *end*A1 *gln*V44 *thi-1 recA1 relA1 gyrA96 deoR nupG* Φ80*lacZ*ΔM15 Δ(*lacZYA-argF*)U169, *hsd*R17(r_K^- m_K^+), λ^-	Promega
MC4100	F⁻ (*araD139*) Δ(*argF-lac*)169 λ^- e14⁻ *flhD5301* Δ(*fruK-yeiR*)725 (*fruA25*) *relA1 rpsL150*(Str^R) *rbsR22* Δ(*fimB-fimE*)632(::IS_1) *deoC1*	(Casadaban & Cohen, 1979)
BTH101	F⁻ *cya-99 araD139 galE15 galK16 rpsL1*(Str^R) *hsdR2 mcrA mcrB1*	(Karimova *et al.*, 1998)
BW25113	F⁻ Δ(*araD-araB*)567 Δ*lacZ*4787(::rrnB-3) λ^- *rph-1* Δ(*rhaD-rhaB*)568 *hsdR*514	(Baba *et al.*, 2006)
JW5189-1	F⁻ Δ(*araD-araB*)567 Δ*lacZ*4787(::rrnB-3) λ^- Δ*ychM*724::kan, *rph-1* Δ(*rhaD-rhaB*)568 *hsdR*514	(Baba et al., 2006)
JW3496-1	F⁻ Δ(*araD-araB*)567 Δ*lacZ*4787(::rrnB-3) λ^- Δ*dctA*783::kan *rph-1* Δ(*rhaD-rhaB*)568 *hsdR*514	(Baba et al., 2006)
JW4085-3	F⁻ Δ(*araD-araB*)567 Δ*lacZ*4787(::rrnB-3) λ^- *rph-1* Δ(*rhaD-rhaB*)568 Δ*dcuR*750::kan *hsdR*514	(Baba et al., 2006)
JW4086-1	F⁻ Δ(*araD-araB*)567 Δ*lacZ*4787(::rrnB-3) λ^- *rph-1* Δ(*rhaD-rhaB*)568 Δ*dcuS*751::kan *hsdR*514	(Baba et al., 2006)
IMW385	MC4100, but λ[Φ(*dctA*–*lacZ*)hyb Amp^R]	(Kleefeld, 2002)
EK9	BW25113, but Δ*dauA*	This study
EK83	BW25113, but Δ*dctA*	This study

EK96	BW25113, but Δ*dctA*Δ*dauA*	This study
EK107	BW25113, but Δ*dcuR*	This study
EK108	BW25113, but Δ*dcuS*	This study
EK111	IMW385, but Δ*dauA*	This study
EK161	EK83 encoding DauA-His**	This study
EK169	BW25113 encoding DauA-His**	This study
EK178	BW25113 encoding DctA-His**	This study
EK180	EK9 encoding DctA-His**	This study
EK182	BW25113 encoding DauA-His** and DctA-FLAG**	This study
EK184	EK182, but Δ*dcuS*	This study
EK187	EK9 encoding DctA-FLAG**	This study
EK197	BW25113 pJL28(Amp^R)	This study
EK201	BW25113 pEK201	This study
EK202	BW25113 pEK202	This study
EK203	BW25113 pEK203	This study
EK208	BW25113, but Δ*cpxR*	This study
EK212	EK182 pJL28(Amp^R)	This study
EK213	EK182 pEK203	This study
EK214	BW25113, but Δ*cpxA*	This study

*: Antibiotic resistance cassettes are indicated as follows: cml, Chloramphenicol resistance; amp, ampicillin resistance; kan, Kanamycin resistance.
**: proteins with in-frame C-terminal His tag or FLAG tag fusions

2.1.2 Plasmids used in this study

Table 2-2: Plasmids used in this work

Plasmid	**Description***	**Reference**
pCP20	FLP^+, λcI857$^+$, λp_R Rep^{ts}, Amp^R, Cam^R	(Datsenko & Wanner, 2000)
pJL28	Vector for transcriptional fusions, Amp^R	Kindly provided by Prof G. Unden (University of Mainz)
pEK201	pJL28:P3	This study
pEK202	pJL28:P2	This study

pEK203	pJL:P1	This study
pBluescriptKS+	Cloning vector, Amp^R	Stratagene
pEK153	pBluescript:DctA-His**	This study
pEK154	pBluescript:DauA-His**	This study
pMAK705	Suicide vector for gene deletion or insertion by homologues recombination Cm^R	Kindly provided by Prof Tracy Palmer
pEK163	pMAK705: Dcta-His**	This study
pEK164	pMAK705:DauA-His**	This study
pEK181	pMAK705:Dcta-FLAG**	This study
Bacterial Two Hybrid plasmids		
pUT18	Encoding the adenylate cyclase domain T18 from *Bordutella pertussis*, C-terminal fusions	Kindly provided by Prof. Tracy Palmer
pUT18:ssNarG		Kindly provided by Prof. Tracy Palmer
pEK158	pUT18:DauA	This study
pEK172	pUT18:$DauA_{1-444}$	This study
pEK193	pUT18:AmtB	This study
pEK211	pUT18:STAS	This study
pT25	Encoding the adenylate cyclase domain T25 from *Bordutella pertussis*, N-terminal fusions	Kindly provided by Prof. Tracy Palmer
pT25: NarJ		Kindly provided by Prof. Tracy Palmer
pEK36	pT25:STAS	This study
pEK167	pT25:DauA	This study
pKNT25	Encoding the adenylate cyclase dpmain T25 from *Bordutella pertussis*, C-terminal fusions	Kindly provided by Prof G. Unden (University of Mainz)
pEK191	pKNT25:DauA	This study
pEK192	pKNT25:AmtB	This study
pEK209	pKNT25:$DauA_{1-444}$	This study
pEK210	pKNT25:STAS	This study

pMW429	pUT18C:DcuS	Kindly provided by Prof G. Unden (University of Mainz)
pMW858	pKNT25:DctA	Kindly provided by Prof G. Unden (University of Mainz)
pMW919	pKNT25:DcuS	Kindly provided by Prof G. Unden (University of Mainz)
pMW428	pUT18:DcuS	Kindly provided by Prof G. Unden (University of Mainz)
pMW917	pUT18C:DctA	Kindly provided by Prof G. Unden (University of Mainz)
pMW918	pUT18:DctA	Kindly provided by Prof G. Unden (University of Mainz)
pMW1647	pKNT25:MalE-DctA$_{362-428}$	Kindly provided by Prof G. Unden (University of Mainz)

*: Antibiotic resistance cassettes are indicated as follows: cml, Chloramphenicol resistance; amp, ampicillin resistance; kan, Kanamycin resistance.
**: proteins with in-frame C-terminal His tag or FLAG tag fusions

2.1.3 Oligonucleotides used in this study

Table 2-3: Oligonucleotides used in this work

Primer	Target	Sequence (5'-3')*	Comments
Sequencing/Screening			
EKO67	*dauA*	atgc**ggatcc**gtgaacaaaatattttcctcacatgtg	Forward
EKO68	*dauA*	atgc**aagctt**ttataaatccgccatcgccgcgcgacg	Reverse
EKO96	pUT18	ttagctcactcattaggcaccc	Forward
EKO97	pUT18	tcgtagcggaactggcgac	Reverse

EKO220	*dctA*	ggagttcgggtggcgctggatg	500bp upstream *dctA*
EKO221	*dctA*	cgtcaaggccaccgctttgcg	500bp downstream *dctA*
EKO239	*dcuR*	ggaagagattggctctctgctg	483bp upstream *dcuR*
EKO240	*dcuR*	actctctggcgatgggtttatag	368bp downstream *dcuR*
EKO241	*dcuS*	gctgacatatcgcagtgttgaaatag	265bp upstream *dcuS*
EKO242	*dcuS*	cggaggagatgacaatcacatc	522bp downstream *dcuS*
EKO320	pBluescript	gtaaaacgacggccagtg	Forward
EKO321	pBluescript	caggaaacagctatgaccatg	Reverse
EKO409	pJL28	ggcgtatcacgaggccctttcg	Forward
EKO410	pJL28	cacgacgttgtaaaacgacggg	Reverse
EKO322	pT25	ccgcatctgtccaacttcc	Forward
EKO323	pT25	ggatgtgctgcaaggc	Reverse
EKO357	pKNT25	acactttatgcttccggctcg	Forward
EKO358	pKNT25	gccagactcccggtcggcggcg	Reverse
Primer	**Target**	**Sequence (5'-3')**	**Position****
RT-PCR analysis for DauA co-transcribed genes			
EKO70	*prs*	ggtgatgcatatcatcggtgacgt	+608 → +632
EKO71	*dauA*	ctcaatcaggcgaccaaagcgtgc	+363 → +387
EKO72	*dauA*	cctttccgcgctctgatcgacgct	+30 → +54
EKO73	*dauA*	gccgagcattgccattgagaatgc	+843 → +867
EKO74	*prs*	cctgatatgaagctttttgctggt	+3 → +27
EKO75	*prs*	cgattcttcgttgctgatacgacg	+900 → +924
EKO87	*dauA*	atgctgctgtgcatgtcgctgacc	+1230 → +1254
EKO88	*pth*	cacgcccgcacataacccactggg	-181 → -205
EKO92	*hemM*	gttgatagggttagtctgcttgcatc	-191 → -165
EKO93	*hemM*	cgtcttatccgcctgctaccgctg	+18 → +42
EKO94	*ychB*	ctgactgggacaggggcctgtgtc	+708 → +732
EKO95	*dauA*	caagcgtcgatcagagcgcggaaagg	+30 → +56
EKO154	*ychB*	atgcggacacagtggccctct	+1 → +21
EKO155	*ychB*	atggatgagctggcggaaatg	+381 → +402
EKO158	*dauA*	ttataaatccgccatcgccgcgcgacg	+1653 → +1680
Primer	**Target**	**Sequence (5'-3')**	**Vector/ Restriction site**
Bacterial Two Hybrid constructs			
EKO63	STAS	atgc**ggatcc**agcaccggtagtcgtagatgttcca	pT25/ *BamH1*
EKO64	STAS	atgc**ggtacc**ttataaatccgccatcgccgcgcg	pT25/ *KpnI*
EKO281	*dctA*	atgc**aagctt**gatgaaaacctctctgtttaaaagc	pUT18/ *HinIII*
EKO282	*dctA*	atgc**tctaga**ggagaggataattcgtgcgttttgcc	pUT18/ *XbaI*
EKO283	*dctA*	atgc**ggatcc**gatgaaaacctctctgtttaaaagc	pT25/ *BamHI*
EKO284	*dctA*	atgc**ggtacc**ttaagaggataattcgtgcgttttgcc	pT25/ *KpnI*

EKO285	*dauA*	atgc**aagctt**ggtgaacaaaatattttcctcacatg	pUT18/ *HindIII*
EKO286	*dauA*	atgc**tctaga**ggtaaatccgccatcgccgcgcgacg	pUT18/ *XbaI*
EKO326	*dauA*	atgc**ctgcag**ggtgaacaaaatattttcctcacatg	pT25/ *PstI*
EKO324	*dauA*	atgc**ggatcc**ttataaatccgccatcgccgcgcgacg	pT25/ *BamHI*
EKO347	$dauA_{1-444}$	cgcacgtcctctagaggatccccgggtaccgagctcgaattc	pUT18
EKO348	$dauA_{1-444}$	ctctagaggacgtgcgatacgacgcataaacagcagcgatg	pUT18
EKO360	*dauA*	atgc**ctgcag**ggtgaacaaaatattttcctcacatg	pKNT25/ *PstI*
EKO361	*dauA*	atgc**gaattc**ggtaaatccgccatcgccgcgcgacg	pKNT25/ *EcoRI*
EKO363	*amtB*	atgc**ctgcag**gatgaagatagcgacgataaaaactggg	pKNT25/ *PstI*
EKO364	*amtB*	atgc**gaattc**ggcgcgttataggcattctcgcc	pKNT25/ *EcoRI*
EKO365	*amtB*	atgc**aagctt**gatgaagatagcgacgataaaaactggg	pUT18/ *HindIII*
EKO366	*amtB*	atgc**tctaga**ggcgcgttataggcattctcgcc	pUT18/ *XbaI*
Primer	**Target**	**Sequence (5'-3')**	**Comments/ Restriction site**
Construction of C-terminal tag insertions			
EKO307	*dauA*	atgc**tctaga**cacaaagtggtcgacttgc	Last 500 bp of *dauA*/ *XbaI*
EKO308	*dauA*	atgc**ggatcc**ttagtggtggtgatgatgatgtaaatccgccatcgc cgc gcg	Last 500 bp of *dauA*, 6xHis/ *BamH1*
EKO309	*dauA*	atgc**ggatcc**gtacgagattgaccagtc	500bp downstream *dauA*/ *BamH1*
EKO310	*dauA*	atgc**ctgcag**actattagaaagtcaaggtg	500bp downstream *dauA*/ *PstI*
EKO311	*dctA*	atgc**tctaga**tactggggacttcatcttccg	Last 500bp of *dctA*/ *XbaI*
EKO312	*dctA*	atgc**ggatcc**ttagtggtggtgatgatgatgagaggataattc gtgcg	Last 500 bp of *dctA*, 6xHis/ *BamH1*
EKO313	*dctA*	atgc**ggatcc**tctcatcacttatgcccgc	500bp downstream *dctA*/ *BamH1*
EKO314	*dctA*	atgc**ctgcag**cgtcaaggccaccgctttgcgttagc	500bp downstream *dctA*/ *PstI*
EKO367	*dctA*	aaagatgatgatgataaataaggatcctctcatcacttatcgccg cac	replace His to FLAG tag in pEK163
EKO368	*dctA*	atcatcatcatctttataatcagaggataattcgtgcgttttgccatc cgg	replace His to FLAG tag in pEK163
Other constructs			
EKO67	*dauA*	atgc**ggatcc**gtgaacaaaatattttcctcacatgtg	*BamH1*
EKO68	*dauA*	atgc**aagctt**ttataaatccgccatcgccgcgcgacg	*HindIII*
EKO411	*dauA* promoter 3	atgc**gaattc**ggcgtcgcgcctgactgggacagg	*P3, 1,377 kb upstream dauA EcoR1*

EKO412	*dauA* promoter 2	atgc**gaattc**ggcccctactttggctatgcgcgcc	P2, 809bp upstream *dauA*/ *EcoR1*
EKO413	*dauA* promoter 1	atgc**gaattc**ggcgtccgcgtgcgaacgtttcacagg	P1, 490bp upstream *dauA*/ *EcoR1*
EKO414	*dauA* promoter	atgc**ggatcc**ggcataataatgtttcatccgtgagcgc	Replace *dauA* start codon

*: Endonuclease restriction cut sites are highlighted.
**: Position of primer is indicated in relation to the translational start site (+1) of the named gene.

2.2 Growth conditions, media and antibiotics used in this study

2.2.1 Growth conditions and media

Luria–Bertani (LB) broth and LB agar were used for routine bacterial growth and genetic studies (Sambrook *et al.*, 1989) at 37^{o}C unless otherwise stated. For growth experiments *E. coli* was cultivated in M9 minimal medium (Yanisch-Perron *et al.*, 1985), enriched M9 (eM9) medium (Kramer *et al.*, 2007) or MOPS minimal medium (Neidhardt *et al.*, 1974) adjusted at the desired pH. All media were supplemented with 50 mM of the specified carbon source. 1.5% (w/v) agar was used to solidify media. For the determination of chromosomal or plasmid encoded β-galactosidase activity and for measuring the uptake rates of [^{14}C]-carbon sources the conditions and media used were specified in each experiment. See Appendix A for detailed compositions of buffers, solutions and media used in this study.

2.2.2 Antibiotics

When required, antibiotics where added at the following final concentrations:

Table 2-4: Antibiotics used in this work

Antibiotics	Dissolved in	Final concentration (μg ml^{-1})
Ampicillin	H_2O	100 μg ml^{-1}
Chloramphenicol	100% ethanol	30 μg ml^{-1}
Kanamycin	H_2O	50 μg ml^{-1}

2.3 Phenotypic Characterisation Methods

2.3.1 Phenotypic Microarrays

As a first attempt of a phenotypic characterization, the technology of Phenotypic Microarrays (Biolog) was used (Bochner, 2009). Briefly, wild type and mutant strains were grown overnight on LB agar. A cell suspension at a standardized cell density was prepared in a minimal medium supplemented with the appropriate nutrient source and a redox dye, tetrazolium violet. 100 μl of this cell suspension were pipetted in a 96-well microtiter plate and measured for 24 and 48 h at 37°C in a microtiter plate reader (OMNILOG instrument). 700 non-redundant trophic conditions were screened (Carbon, Nitrogen, Phosphorus and Sulphur metabolism, nutrient supplements, osmotic and pH sensitivity).

2.3.2 Growth experiments

Escherichia coli strains were cultured overnight in eM9 or MOPS minimal medium supplemented with 50 mM of the appropriate carbon source at 37^{o}C and at the desired pH. The next day the cells were washed twice in eM9 or MOPS (carbon source free) and diluted to an optical density at 600 nm of 0.05 in 150 ml of eM9 medium containing

50 mM of the appropriate carbon source at the appropriate pH into a 96-well microtitre plate. Growth was monitored for 24 h using a Synergy 2 platereader (Biotek).

2.4 General Molecular Biology Methods

2.4.1 Competent cells and transformation

2.4.1.1 Chemically competent cells

A single colony of the appropriate strain was inoculated in 5 ml LB and grown overnight at 37^{o}C. The next day 250 ml of LB medium were incubated with 2.5 ml of the overnight culture and grown for 2 hours at 37^{o}C (until OD_{600} 0.3- 0.4). The culture was then transferred to sterile centrifuge tubes and after incubation for 30 min on ice, the cells were pelleted. The supernatant was removed and the cells resuspended in 30 ml of ice cold sterile 0.1 M $CaCl_2$ and left on ice for 30 min, after which a second centrifugation step was performed. The cells were resuspended in 8 ml ice cold 0.1 M $CaCl_2$ + 15% glycerol, snap-frozen in liquid nitrogen and stored at -80^{o}C.

2.4.1.2 Heat shock transformation method

Genetic material was mixed with 100 µl of chemically competent cells and incubated on ice for 30 min. The cells were heat shocked at 42^{o}C for 75 sec. 1 ml of LB was added and the cells were incubated for at least 1.5 hours at 37^{o}C before they were plated on LB medium supplemented with the appropriate antibiotic and incubated overnight at 37^{o}C.

2.4.2 DNA techniques

2.4.2.1 Genomic DNA extraction

Genomic DNA was extracted from *E. coli* cells using a modified version of the classic phenol/chloroform method for nucleic acid extraction (Harwood & Cutting, 1990). One fresh colony was inoculated in 3 ml LB and grown to an OD_{600} of 1-1.5. Cells were resuspended in lysis buffer (Appendix A) containing 10 mg ml^{-1} lysozyme and incubated for 30 min at 37^{o}C. On visible cell lysis 0.9% (w/v) sarkosyl was added and the cells were left on ice for 5 min. Tris(hydroxymethyl)aminomethane (Tris) buffered phenol was added and after the mixture was well vortexed the organic phenol containing phase was separated from the aqueous DNA-containing layer by centrifugation. Chloroform/isoamyl alcohol (24:1 v/v) was added to the aqueous phase and another round of centrifugation was performed. The aqueous phase formed was removed and the containing DNA was precipitated with the addition of 850 mM sodium citrate and 100% ethanol. The precipitated DNA was washed with 70% ethanol and resuspended in water. DNA concentration was measured using Nanodrop Spectophotometer (Labtech) and aliquots were stored at -20^{o}C.

2.4.2.2 Polymerase Chain Reaction (PCR)

The *in vitro* nucleic acid amplification was performed using Polymerase Chain Reaction (PCR) (Mullis *et al.*, 1986). For all standard PCR reactions Taq DNA polymerase (Roche) was used, cloning fragments were amplified by Expand High Fidelity PCR System (Roche) and Phusion DNA polymerase (Finnzymes) was used in constructs made by site-directed mutagenesis. All PCR reactions were performed in a Veriti® Thermal Cycler (Applied Biosystems®).

Table 2-5: Typical PCR reaction composition used

Component	Final concentration
10x PCR reaction buffer (100 mM Tris-HCl pH8.3, 500 mM KCl, 25 mM $MgCl_2$)	1x
10mM dNTP mix	250 µM each
Primers	1 µM each
Polymerase	2.5 U
DNA template	50-100 ng
H_2O	Up to 50 µl

When bacterial colonies were used as a source of DNA: one colony was resuspended in 100 µl water and boiled for 5 min. Then cells were spun down and 4 µl of supernatant was used as template DNA per 20 µl PCR reaction volume.

Table 2-6: Standard thermal cycler conditions used

Step	Temperature	Time
Initial denaturation (1cycle)	94°C	2 min
35 cycles:		
Denaturation	94°C	15 sec
Annealing	52-60°C*	30 sec
Elongation	72°C	45 sec/ kb
Final elongation	72°C	7 min

* The optimal annealing temperature depends on the melting temperature of the primers

2.4.2.3 Site-directed mutagenesis by PCR

For introduction or deletion mutations in a given plasmid site-directed mutagenesis was used according to the QuikChange protocol (Stratagene). In order to remove methylated DNA with no mutation, 40 U *DpnI* (NEB) restriction enzyme were added in the PCR reaction and incubated for 3 h at 37^{o}C. Buffers and enzymes were removed from the sample using the QIAquick PCR Purification Kit® (Qiagen). Next, the plasmids were transformed into *E. coli* MACH1 competent cells.

2.4.2.4 DNA purification

DNA extracted from agarose gel after electrophoresis using the QIAquick Gel Extraction Kit® (Qiagen), in accordance with manufacturer's instructions. Briefly, DNA fragment was excised from agarose gel, dissolved in Buffer QC (Qiagen) and incubated for 15 min at 50^{o}C. Buffer QC solubilises the agarose gel and provides the appropriate conditions for DNA binging to the silica membrane. In this method DNA is captured to a silica membrane under high-salt conditions. Agarose and buffers were removed from the column with high-salt buffer washes. DNA was eluted from the column using a low-salt buffer.

DNA from PCR and enzymatic reactions was purified using the QIAquick PCR purification Kit® (QIAGEN). DNA samples were resuspended in Buffer PB (Qiagen) (5:1 v/v) and DNA was captured to a silica membrane under high-salt conditions. Impurities and salts were washed away from the membranes using the ethanol-containing PE Buffer (Qiagen). DNA was eluted from the column using a low-salt buffer.

2.4.2.5 Plasmid purification

Cells were grown overnight in LB supplemented with the appropriate antibiotics and plasmids were purified using QIAprep Miniprep Kit® (Qiagen) according to manufacturer's instructions. Briefly, cells were pelleted by centrifugation and lysed under alkaline conditions. Lysates were separated from cell debris by centrifugation and subsequently DNA was bound to the QIAprep silica membrane. RNA and proteins were washed off of the column using high salt buffer. Finally, DNA plasmid was eluted using water at pH 7.

2.4.2.6 Restriction endonuclease digests

All DNA digestions were performed using restriction endonucleases supplied by New England Biolabs® (NEB) in buffers provided by the manufacturer. Digests were incubated for at least 2 hours at the temperature specified by the manufacturer. When two enzymes with incompatible buffers were used, after the first digestion the DNA was purified using QIAquick PCR purification Kit® (QIAGEN) and then the second enzyme and buffer were added. For cloning purposes, restriction enzymes and buffers were removed from PCR products using QIAquick PCR purification Kit® (QIAGEN).

2.4.2.7 Dephosphorylation of DNA vectors

Linear DNA vectors were dephosphorylated to prevent self-ligation using shrimp alkaline phosphatase (SAP) by Roche, which removes phosphate groups from the 5' end of DNA or RNA. Reactions were performed according to manufacturer's instructions. Briefly, 4 U of alkaline phosphatase and 1x reaction buffer were added in the linear vector sample and incubated for 30 min at 37^{o}C. Alkaline phosphatase was inactivated

by incubation at 65^{o}C. For cloning purposes, restriction enzymes and buffers were removed from vector using QIAquick Gel Extraction Kit® (Qiagen).

2.4.2.8 Ligation

A Nanodrop Spectophotometer (Labtech) was used to quantify the DNA fragments in cloning experiments. The inserts were cloned into the appropriate vector with a 5:1 molar ratio using T4 DNA ligase. T4 ligase catalyses the formation of phosphodiester bonds between 5' phosphate and 3' hydroxyl ends in duplex DNA or RNA. In a typical ligation reaction 1x T4 ligase reaction buffer and 400 Units of T4 DNA ligase (NEB) in a total volume of 20 µl was used and incubated for at least one hour at room temperature.

2.4.2.9 Construction of BTH plasmids

Most of the plasmids used in the BTH experiments were constructed by standard cloning procedures using plasmids and primers detailed in Table 2-2 and Table 2-3. Plasmid pEK172 was constructed as follows: primers EKO347 and EKO348 were used to delete by site-directed mutagenesis the STAS domain from plasmid pEK158.

2.4.2.10 Construction of plasmids containing tag fused protein variants

Strains EK169 and EK161 were constructed as follows: a fragment (A) covering the last 501 base pairs (bp) of *dauA* and introducing six histidines before the termination codon was amplified by PCR using primers EKO307 and EKO308 with BW25113 chromosomal DNA as template. The product was digested with *XbaI* and *BamHI*. A

second fragment (B) covering 500 bp sequence downstream of *dauA* was amplified by PCR using primers EKO309 and EKO310 with BW25113 chromosomal DNA as template. The product was digested with *BamHI* and *PstI*. Both fragments were cloned simultaneously into pBluescript to give plasmid pEK154. The *dauA* $(His)_6$-tagged allele was excised by digestion with *XbaI* and *PstI* and subcloned into pMAK705 to give plasmid pEK164. The mutant allele of *dauA* was transferred into the chromosome of BW25113 and EK83 as described (Hamilton *et al.*, 1989) to give strains EK169 and EK161 respectively.

Strains EK178 and EK180 were constructed similarly using the primers EKO311– EKO312 for fragment A and EKO313– EKO314 for fragment B, to give first plasmid pEK153 and then plasmid pEK163. The mutant allele of *dctA* was transferred to the chromosome of BW25113 and EK9 to give strains EK178 and EK180 respectively.

Strain EK182 was constructed as follows: primers EKO367 and EKO368 were used to replace by site-directed mutagenesis the His-tag with a FLAG tag on the pEK163. The FLAG tagged mutate allele was transferred into the chromosome of EK169 as described (Hamilton et al., 1989) to give strain EK182. Strain EK184 was constructed by P1 transduction. A P1 lysate was prepared from JW4086-1 and transduced into EK182 according to standard methods (Miller, 1972). The kanamycin-resistance cassette was then subsequently removed using the pCP20-encoded FLP recombinase (Datsenko & Wanner, 2000).

2.4.2.11 In-frame chromosomal gene deletions and insertions

2.4.2.11.1 pMAK705 vector-based recombination method

For the generation of chromosomal gene deletions and insertions the pMAK705 method developed by Hamilton *et al*. (Hamilton *et al.*, 1989) was used. The desired mutation was cloned into the suicide vector pMAK705 and transformed into a *recA*$^+$ target strain, heat shocking the cells for 5 min at 37^{o}C and recovery for at least 2 h at 30^{o}C. Cells were plated on LB supplemented with chloramphenicol and grown for two days at 30^{o}C. Transformant colonies were used for overnight growth and vector integration onto the chromosome was achieved by serial dilution of the overnight cells onto LB chloramphenicol plates and growth at 44^{o}C. Next, for resolution of co-integrates colonies were inoculated into LB supplemented with chloramphenicol and grown at 30^{o}C for at least 24h three consecutive times. Finally, single colonies were isolated on a LB chloramphenicol plates and inoculated in LB (without chloramphenicol) in order to cure the plasmid at 44^{o}C. Colonies were tested for loss of antibiotic resistance by replica plating onto LB agar with or without the relevant antibiotic. Further confirmation of gene mutation was performed by PCR analysis.

2.4.2.11.2 Bacteriophage P1-mediated transduction method

Generalized phage transduction is a method used to move selectable genetic elements from one “donor” strain to another “recipient” strain with the use of a bacteriophage. The basic principle of this method is that during lysogeny the phage accidentally packs part of the “donor” DNA in its head and lysates can be used to infect another “recipient” strain resulting in the introduction of this packaged DNA through homologous recombination (Weinstock, 2002).

2.4.2.11.2.1Preparation of P1 lysates

E.coli strains carrying kanamycin selection cassettes in the place of the desired gene were used as donor strains for the generation of P1 lysates carrying the marker to be transduced. One fresh colony was grown overnight aerobically in LB at 30^{o}C. The next day, overnight culture was mixed with MC buffer (Appendix A) in 1:1 ration and incubated for 30 min at 37^{o}C. Serial dilutions of P1 phage was mixed with the bacterial suspension and incubated at 37^{o}C for 15 min. Molten LBMC soft agar (Appendix A) was added to the phage-cell mixture and poured over freshly made R plates (Appendix A). After 5-7 hours of incubation at 37^{o}C, the plate with confluent lysis was used to isolate the phage lysate. Chloroform was added and P1 phage lysates were stored at 4^{o}C in the dark.

2.4.2.11.2.2 P1 transduction

Once phage lysate was generated from a donor strain, it could be used to transfer the desired allele to a recipient strain. A really important step at this part of the process is the control of the phage infectivity to avoid lysis of the bacteria transduced with the desired genetic element. Overnight culture of the recipient strain, grown in LB at 30^{o}C, was mixed with MC buffer (Appendix A) in 1:1 ratio and incubated for 30 min at 37^{o}C. Cells were harvested, resuspended in TGYES medium (Appendix A) containing 5 mM $CaCl_2$ and mixed with 100 μl of the desired P1 lysate. $CaCl_2$ is necessary for phage infectivity. After incubation for 30 min at 37^{o}C the calcium chelator sodium citrate was added at a concentration of 1M which is enough to prevent the phages from further infectivity but does not starve the bacterial cells of calcium. Cells were pelleted and washed in LB before being resuspended in TGYES medium (Appendix A) supplemented with 20 mM sodium citrate and incubated for 3 h at 37^{o}C to allow the

expression of the antibiotic resistance marker. Cells were harvested and washed in LB. Finally, resuspended cells in TGYES containing 20 mM sodium citrate were plated on LB supplemented with the appropriate antibiotic and 3.125 mM pyrophosphate, which acts as a calcium chelator.

2.4.2.11.3 FLP- mediated excision of marked mutations

For the generation of in-frame, un-marked and non-polar deletions the following method was used to excise the antibiotic cassette of the desired strains: Antibiotic-resistant cells were transformed by $CaCl_2$ transformation with the temperature sensitive plasmid pCP20 and plated onto LB agar supplemented with chloramphenicol (Datsenko & Wanner, 2000). After incubation for 2 days at 30^{o}C, single transformants were streaked onto fresh LB agar plates and incubated overnight at 42^{o}C. The next day colonies were tested for loss of antibiotic resistance by replica plating onto LB agar with and without the relevant antibiotic. Further confirmation of gene deletion was performed by PCR analysis.

2.4.2.12 DNA sequencing

All new constructs were confirmed by DNA sequencing. The DNA sequencing service was provided by the DNA Sequencing & Service at the University of Dundee (http://www.dnaseq.co.uk/).

2.4.3 RNA techniques

2.4.3.1 RNA extraction

Total RNA was extracted and purified using the RiboPure™- Bacteria Kit (Ambion). Any trace amount of genomic DNA from the eluted RNA was removed by DNase I treatment, as per the manufacturer's instructions. Total RNA concentration was measured at A_{260} with a Nanodrop Spectophotometer (Labtech).

2.4.3.2 RT-PCR

In order to assess if *dauA* forms an operons with neighbouring genes RT-PCR analysis was performed. RNA was isolated from BW25113 wild type and EK9 strains and analysis was performed using the SuperScript™ III One- Step RT- PCR System with Platinum® Taq DNA Polymerase (Invitrogen) according to manufacturer's recommendations. Briefly, gene specific primers are used to synthesize the cDNA to avoid nonspecific products in the one-step procedure.

Table 2-7: The typical reaction composition used for the RT-PCR analysis

Components	**Volume**
2x Reaction mix (40 mM Tris-HCl pH8.4, 100 mM KCl, 0.4 mM of each dNTP, 3.2 mM $MgSO_4$)	10 µl
Template RNA	100 ng
Sense primer (10 µM)	0.4 µl
Anti-sense primer (10 µM)	0.4 µl
SuperScript™ III RT/ Platinum® Taq mix	100 U/2.5 U
Sterile RNase- free water	Up to 20 µl

To verify the absence of genomic DNA in the RNA samples, the SuperScript™ III RT/ Platinum® Taq mix was omitted and substituted with 2 units of Platinum® Taq DNA Polymerase (Invitrogen). The thermal cycler was programmed so that cDNA synthesis is followed immediately by PCR amplification.

Table 2-8: Standard thermal cycler conditions used for RT-PCR

Step	Temperature	Time
cDNA synthesis (1 cycle)	55°C	30 min
Denaturation (1 cycle)*	94°C	2 min
PCR amplification (35 cycles)		
denaturation	94°C	15 sec
annealing	55°C	30 sec
extension	68°C	1 min/kb
Final extension (1cycle)	68°C	5 min

* During 2 min incubation at 94°C, SuperScript™ III RT is inactivated, Platinum® Taq mix is activated and RNA/cDNA hybrid is denaturated.

2.4.4 Bacterial two-hybrid (BTH) system

This genetic screening is based on the reconstitution, in an *E. coli cyaA*$^-$ strain (deficient in endogenous adenylate cyclase), of a signal transduction pathway that takes advantage of the positive control exerted by cAMP. Two putative interacting proteins are genetically fused to two complementary fragments, T25 and T18, which constitute the catalytic domain of *Bordetella pertussis* adenylate cyclase. Association of the two-hybrid proteins results in functional complementation between T25 and T18 fragments and leads to cAMP synthesis. Cyclic AMP then triggers transcriptional activation of catabolic operons, such as lactose or maltose. *E. coli cyaA*$^-$ are unable to ferment

maltose: they form white colonies on MacConkey indicator media containing maltose, while *cyaA*$^{+}$ bacteria form red colonies on the same media (the fermentation of maltose results in the acidification of the medium which is revealed by the colour change of the dye phenol red) (Karimova *et al.*, 1998).

Plasmids harbouring fusion proteins to T18 and T25 were co-transformed in *E. coli cyaA*$^{-}$ strain BTH101 and plated onto MacConkey medium supplemented with maltose, and cultured at 30°C for 48 h. Red colonies signified possible interactions. An average colony was inoculated in 5 ml LB medium supplemented with appropriate antibiotics, and grown overnight at 30^{o}C. The next day potential interactions were quantified measuring β-galactosidase activity.

2.4.5 Biochemical techniques

2.4.5.1 Enzyme Assays

2.4.5.1.1 β-galactosidase activity assay

β-galactosidase assays were performed on toluenized bacterial suspensions, as described by Miller (Miller, 1972). The OD_{600} of cells to be tested was measured and 1 ml aliquots were taken, into which 50 µl toluene was added and left on ice for 30 min. 450 µl of Z-buffer (supplemented with β- mercaptoethanol) and 100 µl of ONPG (4 mg/ ml) were added to 20 µl of toluenized cells and incubated at 28^{o}C. On development of yellow colour 250 µl of Na_2CO_3 was added, the time of reaction was noted and the absorbance at 260nm was measured. One unit of activity corresponds to 1 nmol of o-nitrophenyl b-D-galactoside hydrolyzed per min at 28^{o}C. β-galactosidase activity was calculated based on the following equation:

β-galactosidase activity (Miller Units)=A_{420} x 10^3/ t x V x OD_{600}

t= time of reaction (min)

V= volumes of cells used (ml)

2.4.5.2 Subcellular fractionation

Cells were cultured overnight in M9 minimal medium containing glucose as sole carbon source. The next day the cells were washed twice in M9 (carbon source free) at pH 5 or pH 7 and diluted to an OD_{600} of 0.6 in M9 medium containing the carbon source (50 mM) and pH indicated. After 6 h, cells were harvested by centrifugation and fractionated as described before (Coutts *et al.*, 2002). Pelleted cells were resuspended in 50 mM Tris 10 mM EDTA pH 8. Lysis of the cell was achieved by 5 x 15 sec sonication 15 sec intervals between bursts at 10% amplitude. Cell debris was removed by centrifugation and part of the supernatant was used as the whole cell fraction. The rest of the supernatant was transferred into polycarbonate ultracentrifuge tube (Beckman) and centrifuged at 80,000 rpm for 30 min at 4^{o}C. Part of the supernatant was kept as the soluble fraction and the rest was discarded. The pellet was resuspended in 50 mM Tris 10 mM EDTA pH 8 and centrifuged at 80,000 rpm for 30 min at 4^{o}C. The supernatant was discarded and the pellet of this centrifugation was resuspended in 50 mM Tris 10 mM EDTA pH 8 0.6 M NaCl and centrifuged at 80,000 rpm for 30 min at 4^{o}C. The pellet of the last centrifugation was resuspended in 50 mM Tris 10 mM EDTA pH 8 and used as the membrane fraction. Fractions were stored at -20^{o}C until further use.

2.4.5.3 Protein quantification (Bradford method)

The total protein concentration in each fraction was measured using the DC protein assay kit (Bio-Rad Laboratories) in microplate reader. This is a colorimetric method for measurement of protein concentration similar to the Lowry assay (Lowry *et al.*, 1951). Essentially, the protein is first mixed with an alkaline copper tartrate solution. The alkaline-treated protein can reduce the Folin reagent which lead to the development of blue colour and can be measured at 750 nm. A standard curve was prepared of serial dilutions of bovine serum albumin concentrations ranging from 0.2 mg/ml to about 1.5 mg/ml. Reagent A (alkaline copper tartrate solution) and Reagent B (dilute Folin Reagent) were added to the standards and protein samples and gently mixed. After incubation for 15 min at room temperature absorbance was read at 750 nm.

2.4.5.4 SDS-polyacrylamide gel electrophoresis (PAGE)

For separation of proteins by approximate size, SDS-PAGE was used in Bio-Rad protein gel electrophoresis mini-gel system. Typically resolving gels of acrylamide concentration used was ranging from 10%-15%. Table 2-9 details the resolving and stacking gel components used in this study. Protein samples were resuspended in SDS loading buffer and the gels were run in SDS Running Buffer (Appendix A) for 1 h at 120 V. PageRuler prestained protein ladder (ThermoScientific) was used as size standard.

Table 2-9: Components of a typical SDS-PAGE gel used in this study

	SEPERATING			STACKING	
	10%	12.5%	15%		
Acrylamide	1.625 ml	2.05 ml	2.5 ml	**Acrylamide**	0.375 ml
Solution 2	1.25 ml	1.25 ml	1.25 ml	**Solution 3**	0.625 ml
H_2O	2.125 ml	1.7 ml	1.25 ml	**H_2O**	1.5 ml
10% APS	50 µl	50 µl	50 µl	**10% APS**	25 µl
TEMED	5 µl	5 µl	5 µl	**TEMED**	2.5 µl

2.4.5.5 Coomassie staining

For visualisation of proteins after separation in SDS-PAGE coomassie staining was used (Appendix A). Enough coomassie solution was used to cover the acrylamide gels and microwaved for 30 sec. The gels were incubated with the stain for further 20 min at room temperature with gentle shacking. The coomassie staining was discarded and the gels were rinsed twice with distilled water before transferred to destain solution (Appendix A). Periodically destain solution was replaced with fresh until sufficient level of destaining was achieved. Gels were then scanned.

2.4.5.6 Purification of DauA for mass spectrometry analysis

EK182 cells were grown overnight in 3 L LB medium supplemented with succinate for the induction of DctA. The next day the cells were pelleted by centrifugation, resuspended in lysis buffer (Appendix A) and lysed with a constant cell disrupter (three passes at 20 kpsi). Cell debris was removed by centrifugation at 20,000 g for 45 min and the supernatant was further centrifuged at 20,000 g for 2 h. The pelleted membrane fraction was resuspended in buffer A (Appendix A). Membranes proteins were extracted with 2% DDM for 1 h at 4^{o}C and loaded onto a Co^{2+}-affinity column (HisTrap, GE

Healthcare). The protein was purified using an FPLC (AKTA purifier -GE Healthcare). The column was washed with Wash Buffer (Appendix A) and the protein was eluted using a linear 55–500 mM imidazole gradient.

2.4.5.7 Purification of DauA and DctA for interaction studies

EK182 cells were grown and the membrane proteins were extracted as described above. Solubilized membrane proteins were incubated with cobalt covered sepharose beads and incubated for 1 h at 4^{o}C. DauA-His was purified by immobilized metal ion affinity chromatography (IMAC) and eluted using 500 mM imidazole. The elution fractions were further purified using Anti-FLAG® M2 affinity Gel (Sigma) according to the manufacturer's instructions and protein was eluted using 0.1 M glycine HCl pH 3.5.

2.4.5.8 Western immunoblotting

Subcellular fractions or purified protein samples were used for the detection of tag fused proteins by western immunoblotting. Samples were loaded into SDS-PAGE gels and were run at 120 V. Proteins were transferred onto PVDF membrane using a Trans-Blot® SD Semi-Dry Transfer Cell (Bio-Rad). The membrane was blocked with 5% (w/v) skimmed milk powder in 1x TBST for 1 h. For the detection of the His- and the FLAG-tagget protein, anti-His (Qiagen) and anti-FLAG antibody (Sigma) were used respectively. Rabbit polyclonal anti-TatC antibody raised against purified *E. coli* TatC protein was kindly provided by Prof. Tracy Palmer. Primary antibodies were incubated for 1 h at room temperature. The membrane was washed with TBST (Appendix A) and incubated for 1 h with Goat Anti-Mouse IgG (H+L)-HRP conjugate secondary antibody (Bio-Rad) for the membranes incubated with α-His and α-FLAG antibodies, and with

Goat Anti-Rabbit IgG (H+L)-HRP (Bio-Rad) for α-TatC antibody. After a series of washes with TBST the membrane was developed with Novex® ECL Chemiluminescent Substrate Reagent Kit and exposed to X-ray film.

2.4.5.9 Membrane stripping

The membrane was incubated twice in stripping buffer (Appendix A) and subsequently washed thoroughly with TBST (Appendix A). Then the membrane was re-blocked with 5% (w/v) skimmed milk powder in 1x TBST and incubated with the new primary antibody.

2.4.5.10 Transport assay

In vivo transport assays were adapted from Jack *et al*. (Jack *et al.*, 1999). Briefly, cells were cultured overnight in M9 minimal medium containing glucose as sole carbon source. The next day the cells were washed twice in M9 (carbon source free) at pH 5 or pH 7 and diluted to an OD_{600} of 0.6 in M9 medium containing the carbon source (50 mM) and pH indicated. After 6 h, cells were harvested, washed twice in M9 minimal medium without a carbon source, at the appropriate pH and resuspended in the same medium to give a final OD_{600} of 0.6. At zero time, [^{14}C]-aspartate, -fumarate or -succinate (55 mCi mmol^{-1}) was added to give the final concentration specified for each experiment. Samples of 300 µl were taken at 15 sec, 30 sec, 1, 2, 3, 4, 5 and 6 min and uptake was terminated by filtration through nitrocellulose filters (Millipore type HA; 0.45 mm pore size) under a constant vacuum. The radioactivity present on the filter was determined using a scintillation counter. Data were calibrated by using internal

standards spotted on filters and counted in the same experiment. Bacterial dry weight was calculated using the OD_{600} reading according to the following equation:

OD_{600} = 1 ≈ 1 x 10^9 cells/ml ≈ 1 mg/ml or 1 g/litre wet cell weight ≈ 1/4 g/litre or 0.25 g/litre dry cell weight

For the competition experiments, unlabelled competitor (50-fold excess) was added at the same time as the [^{14}C]-labelled substrate (40 μM). For the uptake experiments at pH 7 and pH 5, the cells were cultured in the same way as for the other transport assays, at pH7 or pH5, after which they were split in two equal batches, washed quickly twice in M9 minimal medium without a carbon source at pH7 or 5 and assayed immediately for uptake activity (10 μM substrate). The pH dependence of the concentrations (expressed as %) of the different protonation states of succinate and fumarate were calculated as follows: $[COOH - COOH] = ([H^+]^2)/([H^+]^2 + K_{a1}[H^+] + K_{a1}K_{a2})$, $[COOH – COO^-] = (K_{a1}[H^+])/([H^+]^2 + K_{a1}[H^+] + K_{a1}K_{a2})$, $[COO^- - COO^-] = (K_{a1} K_{a2})/ ([H^+]^2 + K_{a1}[H^+] + K_{a1}K_{a2})$ with $pKa = -Log_{10}(K_a)$

3 Physiological Characterisation Of The *Escherichia coli* SLC26 Homologue YchM (DauA)

3.1 Introduction

The Solute Carrier 26 (SLC26) and Sulphate transporter (SulP) family is a ubiquitous superfamily of transporter proteins conserved from bacteria to man. 'SLC26' refers to homologues found in animals and 'SulP' more specifically to those found in plants and fungi. Proteins within the SLC26/SulP family exhibit a wide variety of functions, transporting anions ranging from halides to bicarbonate (Dorwart *et al.*, 2008b; Mount & Romero, 2004). The functional importance of this family is illustrated by the fact that several inherited human diseases are caused by mutations in SLC26 genes (Mount & Romero, 2004). In plants and fungi, SulP proteins are primarily sulphate uptake transporters, with mutations in the *sulP* genes leading to starvation syndrome in plants and auxotrophic phenotypes in fungi (Saier & Paulsen, 1999). Although these proteins are present in almost all bacteria their physiological function is completely unknown. They are frequently classified as sulphate transporters based on their homology with the SulP proteins, however there is little experimental evidence to support this (Saier & Paulsen, 1999; Zolotarev *et al.*, 2008). Indeed, in cyanobacteria, these proteins have been characterised as low affinity Na^+-dependent HCO_3^- transporters (Price & Howitt, 2011; Price *et al.*, 2004). However, a phylogenetic analysis of bacterial SulP proteins (Fig. 1-4) showed that YchM (the *E. coli* SLC26 homologue) clusters independently from the BicA and BicA-like proteins. These results indicated that YchM may not act as a bicarbonate transporter.

The main objective of this chapter was to characterise the physiological role of YchM. At first, a global approach was used to identify YchM dependent phenotypes. Next, the growth and protein production was monitored under aerobic and anaerobic conditions. Furthermore, an *in vivo* transport assay was developed for the study of the apparent kinetics of YchM. Also, YchM substrate repertoire was investigated. Finally, the regulatory roles of YchM were explored. In the course of this part of the study, YchM was showed to be an aerobic succinate transporter. Hence, *ychM* was re-named as *dauA* (for dicarboxylic acid uptake system A) and this denomination is used for the rest of this study.

3.2 Results

3.2.1 Identification of a DauA-dependent phenotype

In order to identify the physiological role of DauA, an in-frame, unmarked and non-polar deletion of *dauA* was generated using FLP-mediated excision in the *E. coli* BW25113 background, generating strain EK9.

The technology of phenotypic microarrays (PM) was used as a global approach to compare the metabolic activity of the parent strain (BW25113) versus Δ*dauA* (EK9) strains under various trophic conditions (carbon, nitrogen, phosphate and sulphur sources, nutrient supplements, osmolytes and pH). This system uses the reduction of a dye (tetrazolium violet) to colourimetrically detect cell respiration. BW25113 and mutant cells were grown in minimal medium supplemented with the appropriate nutrient source and the redox dye. If the cell is able to transport and catabolise the nutrient source provided a purple colour develops in the well. The formation of colour in each well is monitored and recorded by a colour video camera attached to a computer (Bochner, 2009).

The bacterial SLC26/SulP proteins are often classified as potential sulphate transporters based on sequence similarities with the SLC26A transporters in plants and fungi. Therefore, the first substrates to be tested were different sulphur sources. However, no significant difference was observed between the wild type and Δ*dauA* (EK9) cells metabolic activity on any of sulphur sources, suggesting that DauA does not have an essential role in sulphur metabolism (Fig. 3.1).

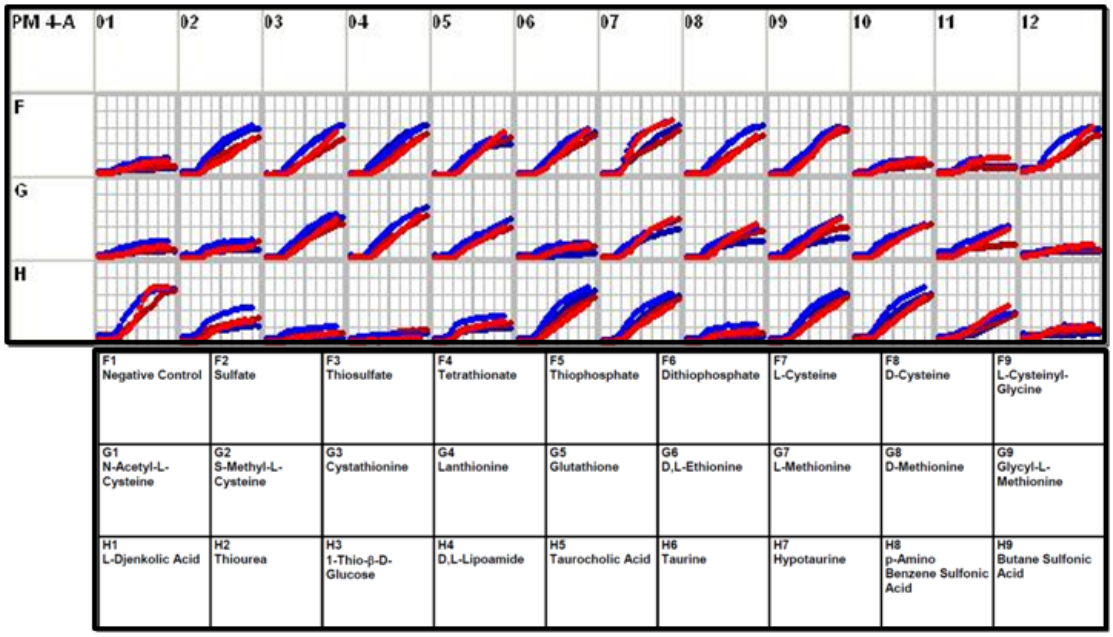

Figure 3-1: Phenotypic microarray analysis of parent strain and Δ*dauA* cells grown with various sulphur sources.

Phenotypic microarray data comparing Δ*dauA* (EK9) strain (red line) with its isogenic parent strain BW25113 (blue line). Cells were cultured with different sulphur sources for 48h and the colour intensity (a measure of cell metabolism) was monitored spectrophotometrically at 590 nm (plotted in arbitrary units). In each well two repetitions for each strain are presented.

The screening for a DauA-dependent phenotype was continued by using different carbon sources as substrates. Interestingly, Δ*dauA* (EK9) cells were metabolically inactive compared to the wild type when succinate was used as the sole carbon source (Fig. 3-2; open symbols). To confirm that the phenotype observed was a result of the Δ*dauA* (EK9) strain's inability to specifically metabolize succinate and not of a general problem in carbon metabolism, other carbon sources (glucose, fructose, maltose and glycerol) were tested (Fig. 3-2; open symbols). Citrate was used as a negative control, since *E. coli* cells are unable to use it as a carbon source aerobically.

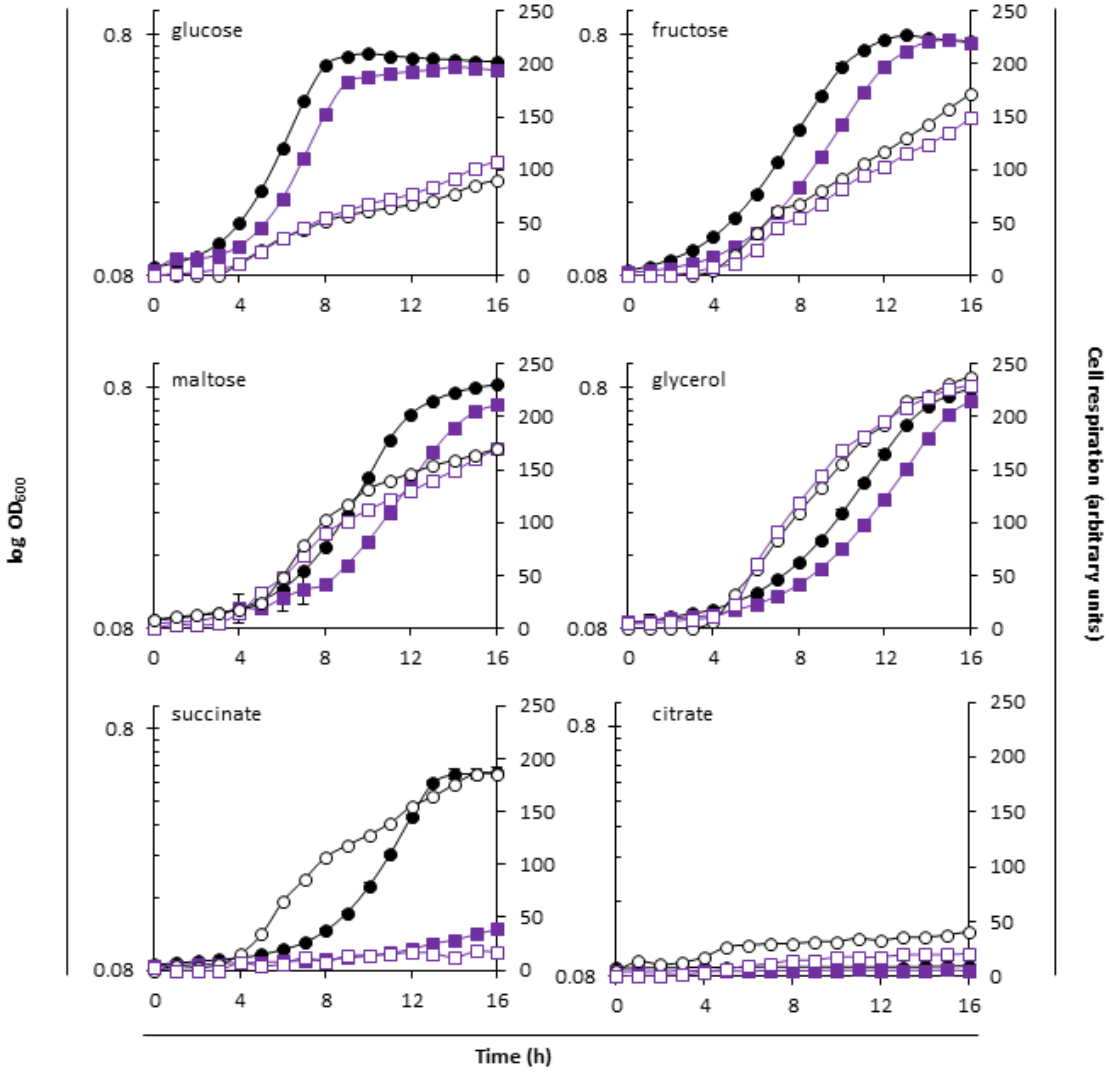

Figure 3- 2: Identification of a DauA-dependent phenotype.

Parent strain (black circles) and Δ*dauA* (EK9) (purple squares) cells were grown in MOPS minimal medium pH 7 supplemented with 50 mM of the indicated carbon source. Growth curves (average of four independent experiments, error bars represent the standard deviation) at 600 nm were recorded using microplates (closed symbols). Cell respiration (open symbols) was measured in a different experiment (data collected from one representative experiment are shown) in a phenotypic microarray by monitoring the colour intensity spectrophotometrically at 590 mm.

To further confirm the phenotype observed in the PM analysis, the growth rates of the parent and Δ*dauA* strains were monitored. Cells were grown in MOPS minimal medium supplemented with different carbon sources (Fig. 3-2; closed symbols). The Δ*dauA* (EK9) strain was not able to grow when succinate was added opposed to the parent

strain, while the growth for both parent and mutant cells was comparable for all the other carbon sources tested.

The phenotypic microarray data combined with the growth curve results indicate that DauA is involved in succinate metabolism.

3.2.1.1 C_4-dicarboxylic acid metabolism in *E.coli*

Succinate is a C_4-dicarboxylic acid. *Escherichia coli* and related bacteria are able to metabolise various C_4-dicarboxylic acids under aerobic and anaerobic conditions. *E. coli* possesses a collection of well characterised systems to meet the requirements for C_4-dicarboxylate metabolism (Janausch *et al.*, 2002).

3.2.1.1.1 C_4-dicarboxylic acid transport systems

Under aerobic conditions C_4-dicarboxylic acids like succinate, fumarate, malate, tartrate, aspartate and the aromatic monocarboxylate orotate are oxidized to CO_2 via the tricarboxylic acid cycle (TCA) and can be used as carbon an energy source (Unden & Kleefeld, 2004).

DctA (TC 2.A.23.1.7) is the main transporter for these solutes under aerobic conditions and belongs to the dicarboxylate/amino acid:cation symporter (DAACS) family of carriers (Saier, 1998; Davies *et al.*, 1999). DctA is conserved in aerobic Gram-negative bacteria and many Gram-positive with low G+C contents, but not in strictly anaerobic bacteria. DctA has a wide repertoire of substrates (succinate, fumarate, malate, aspartate, tartrate, orotate) (Baker *et al.*, 1996; Davies *et al.*, 1999). It has been characterised as cation/C_4-dicarboxylate symporter (Janausch *et al.*, 2002). It has been

shown that *dctA* mutants are still able to grow in succinate as the sole carbon source when acidic pH is applied suggesting the existence of another not yet identified succinate transporter (Janausch *et al.*, 2001).

Under anaerobic conditions, when the TCA cycle is impaired convertion of C_4-dicarboxylates is effected by fumarate respiration and the succinate produced is excreted to the medium (Unden & Bongaerts, 1997). DcuA and DcuB carriers are preferentially fumarate/succinate antiporters, but they can catalyse uptake and efflux of C_4-dicarboxylates and they are present in anaerobic and facultative anaerobic bacteria (Six *et al.*, 1994; Ullmann *et al.*, 2000). DcuB (TC 2.A.13.1.2) is thought to be the most important fumarate/succinate exchanger while DcuA (TC 2.A.13.1.1) is considered to be a backup carrier (Golby *et al.*, 1998). DcuC (TC 2.A.61.1.1) though functionally similar to DcuA/B carriers plays a role in succinate efflux during glucose fermentation (Zientz *et al.*, 1996). No function is attributed to DcuD (TC 2.A. 61.1.2) indicating that it might be a cryptic, unexpressed, transporter (Janausch & Unden, 1999).

Another family of carboxylate:C_4-dicarboxylic acids antiporters has been identified in *E. coli*, which is a subgroup of the divalent anion: Na^+ symporters (DASS). Two members of this family are the citrate: succinate antiporter CitT (TC 2.A.47.3.2) and the putative tartrate:succinate antiporter TtdT (TC 2.A.47.3.3). CitT catalyses citrate exchange or citrate:succinate/fumarate/tartrate exchange during citrate fermentation differentiating it from the specific C_4-dicarboxylic acids Dcu transporters discussed above (Pos *et al.*, 1998).

3.2.1.1.2 Expression and regulation of C_4-dicarboxylate metabolism components

Under aerobic conditions, maximal *dctA* expression is detected during the stationary growth phase in the presence of C_4-dicarboxylates (Davies *et al.*, 1999). The expression of *dctA* by succinate or other C_4-dicarboxylates is induced by the two-component system DcuSR. DcuS is a membrane embedded histidine kinase which is autophosphorylated when bound to C_4-dicarboxylic acids. DcuS phosphorylates the cytoplasmic DNA-binding regulator DcuR which induces the expression of C_4-dicarboxylic acid genes (Davies *et al.*, 1999; Golby *et al.*, 1999; Zientz *et al.*, 1998). Recently it has been shown that helix VIIIb of DctA interacts directly with the cytoplasmic PAS domain of DcuS, forming a sensing unit where the transporter acts as a co-sensor modifying DcuS activity (Fig. 3-3) (Witan *et al.*, 2012a; Witan *et al.*, 2012b). *dctA* expression is strongly repressed (30-fold) in the presence of glucose via the cAMP-CRP complex (carbon catabolite repression, CCR) and under anaerobic conditions via the ArcBA two-component system (Davies *et al.*, 1999).

Under anaerobic conditions, the expression of the Dcu transporters is tightly regulated. The expression of *dcuB* is induced by the fumarate and nitrate reductase regulator (FNR) in response to anoxia and by the DcuSR two component system in the presence of C_4-dicarboxylic acids. On the other hand, *dcuB* expression is repressed by the two-component regulator system NarXL in the presence of nitrate and by carbon catabolite repression (CCR) in the presence of glucose (Golby *et al.*, 1998; Zientz *et al.*, 1999). Similarly to the DctA-DcuS sensor unit, DcuB has been identified to act as a bifunctional protein which interacts with DcuS modifying its activity under anaerobic conditions (Kleefeld *et al.*, 2009). Under the same conditions, *dcuC* expression is induced by FNR but in contrast to *dcuB* the two-component systems DcuSR, NarXL and CCR does not affect *dcuC* induction and/or repression (Zientz *et al.*, 1999).

The regulation of *dcuA* expression has not been clarified yet and the gene seems to be expressed constitutively under the conditions tested. However, there is a 40% decrease in its expression under aerobic conditions (Golby *et al.*, 1998).

Finally, conditions inducing the expression of *dcuD* have not been found yet (Janausch & Unden, 1999).

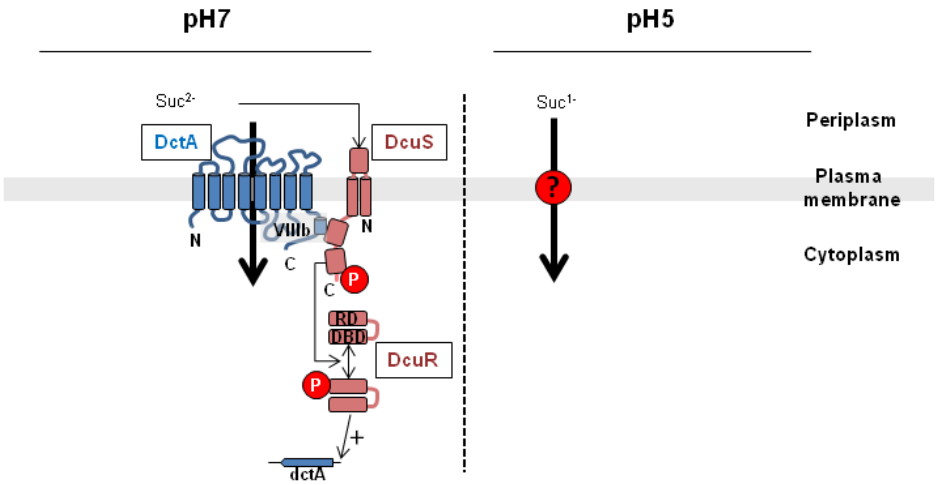

Figure 3- 3: Aerobic succinate uptake in *E. coli.*

Simplified schematic representation of succinate uptake in *E. coli* cells under aerobic conditions. At pH 7 in the presence of succinate DctA is the main uptake system. DctA interacts with DcuS of the two-component regulatory system DcuSR to form a sensing unit. At pH 5 the existence of another succinate transporter has been suggested since *dctA* mutants are still able to grow under these conditions. DBD, DNA-binding domain; RD, receiver domain;

3.2.1.2 Succinate

During the past few years, interest in bacterial succinate metabolism has increased due to the fact that succinate has been identified as an important platform chemical. Succinic acid derivatives such as 1,4-butanediol, maleic anhydride, succinimide, 2-pyrrolidinone and tetrahydrofuran can be used for the production of polymers, industrial solvents and chemicals with wide range of applications. Furthermore, succinate is widely used in the food industry as a flavouring agent or food additive. In pharmaceutical formulations it is used as a counter ion because of its innocuous properties. Currently, succinate is

produced petrochemically from butane and much effort is being put towards bio-succinate production (Thakker *et al.,* 2012). *E. coli* is one of the bacteria used for bio-succinate production, thus in this context, the characterisation of a new family of succinate transporter is of particular importance.

3.2.2 DauA is involved in succinate metabolism

3.2.2.1 Under aerobic conditions

3.2.2.1.1 Phenotypic analysis

The fact that DauA plays a role in succinate metabolism and the existence of a missing succinate transporter active at acidic pH led us to hypothesize that DauA may be involved in this process. To assess whether DauA is involved in succinate metabolism and/or transport, the growth of the parental, Δ*dauA* (EK9), Δ*dctA* (EK83), and Δ*dctA*/Δ*dauA* (EK96) strains was compared on MOPS minimal medium agar plates supplemented with 50 mM glucose or succinate as the sole carbon source. During the first 24 h of incubation at 37^{o}C all mutants were unable to grow on the succinate supplemented plates, while normal growth was observed on the glucose plate (Fig. 3-4; left panel). After 48 h, only very weak growth was observed for the single Δ*dauA* (EK9) and Δ*dctA* (EK83) mutants, whereas the double mutant Δ*dctA*/Δ*dauA* (EK96) showed only residual growth (Fig. 3-4; right panel).

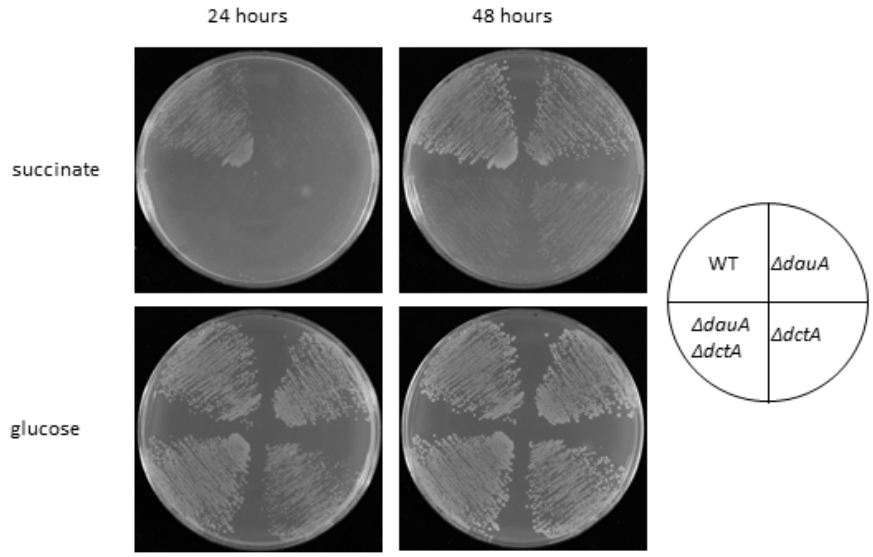

Figure 3-4: DauA is involved in succinate metabolism.

Wild type and isogenic Δ*dauA* (EK9), Δ*dctA* (EK83) and Δ*dctA*/Δ*dauA* (EK96) strains were grown on MOPS minimal medium agar plates supplemented with 50 mM succinate (upper panel) or glucose (lower panel) as the sole carbon sources. The plates were incubated for 24 h (left panel) or 48 h (right panel) at 37^{o}C.

The next step was to study the growth of the above strains under aerobic conditions at different pHs. Cells were inoculated in eM9 minimal medium supplemented with 50 mM glucose or succinate as the sole carbon source, at pH 7 or pH 5 and their growth was monitored. In the succinate medium at pH 7 (Fig. 3-5; upper right panel), the Δ*dauA* (EK9) mutant showed slightly impaired growth compared to the wild type strain, while Δ*dctA* (EK83) cells showed an apparent reduced growth rate as expected. The double mutant cells Δ*dctA*/Δ*dauA* (EK96) presented a more prominent growth defect. Interestingly, in the eM9 minimal medium supplemented with succinate at pH 5 (Fig. 3-5; lower right panel), the growth of the Δ*dctA* (EK83) strains was restored to almost the wild type rate whereas Δ*dauA* (EK9) and Δ*dctA*/Δ*dauA* (EK96) were unable to grow. All strains grew equally well in the glucose supplemented medium at pH 7 (Fig. 3-5; upper left panel). The generally poor growth presented by all four strains in eM9

glucose at pH 5 (Fig. 3-5; lower left panel) is due to glucose repression of the acid resistance system (Castanie-Cornet *et al.*, 1999). These results suggest that DauA plays a role in the aerobic C_4-dicarboxylate metabolism and specifically in the succinate metabolism under acidic conditions.

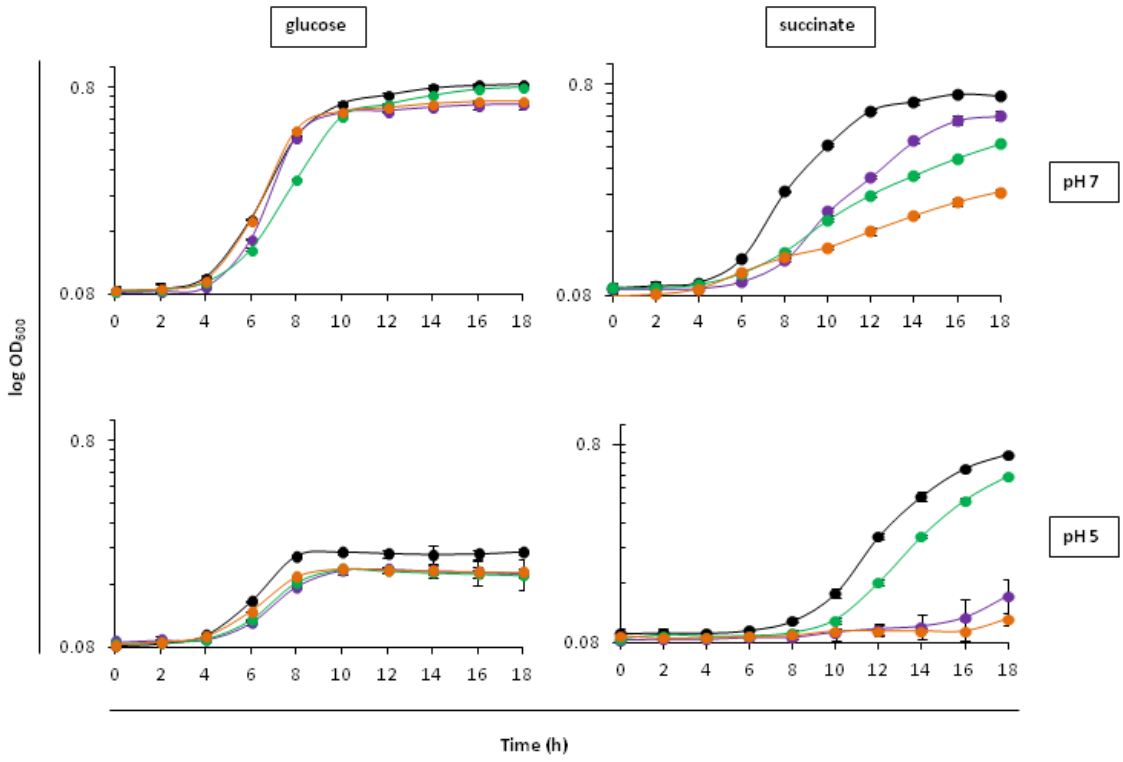

Figure 3-5: DauA plays a role in succinate transport and/or metabolism at pH 5.

Normalized number of BW25113 (black), Δ*dauA* (purple), Δ*dctA* (green) and Δ*dctA*/Δ*dauA* (orange) cells were grown in eM9 minimal medium supplemented with 50 mM glucose (right panel) or succinate (left panel) as the sole carbon source at pH 7 (upper panel) or pH 5 (lower panel). Growth curves were recorded at 600 nm using a Bio Tek microplate reader (average of four independent experiments, error bars represent the standard deviation).

3.2.2.1.2 Protein production

In order to understand the above results at the molecular level the production of DauA and DctA at pH 7 or pH 5 was studied, when succinate was used as the sole carbon source.

DNA encoding a C-terminal 6xHis epitope tag was introduced onto the chromosomally encoded *dauA* by pMAK vector-based recombination using the oligonucleotide pairs EKO307/EKO308 and EKO309/EKO310 in the parental strain (BW25113) and EK83 (Δ*dctA*) backgrounds to give strains EK169 (DauA-H_6) and EK161 (DauA-H_6, Δ*dctA*) respectively. Similarly, using the oligonucleotide pairs EKO311/EKO312 and EKO313/EKO314, a C-terminal 6xHis epitope tag was fused to the chromosomally encoded *dctA* in the wild type (BW25113) and EK9 (Δ*dauA*) backgrounds to generate strains EK178 (DctA-H_6) and EK180 (DctA-H_6, Δ*dauA*) respectively.

It has been shown that correct localization of tagged proteins does not automatically guarantee their functionality (Swulius & Jensen, 2012). In order to check that the C-terminal tags introduced in DauA and DctA do not affect their function, the growth rates of the strains was measured in eM9 minimal medium supplemented with 50 mM succinate at pH 7 or pH 5 (Fig. 3-6). At pH 7, (Fig. 3-6; upper left panel) strains EK169, EK161 and EK178, EK180 showed similar growth to the corresponding strains producing the native forms of DauA and DctA, respectively. At pH 5 (Fig. 3-6; lower left panel), the EK180 strain, which carries a *dauA* deletion, was unable to grow as was observed for EK83 expressing untagged DctA. The rest of the tagged variants grew normally. In the glycerol supplemented medium, at both pHs, all four strains grew equally and at a normal rate (Fig. 3-6; upper and lower right panel). These results show

that the introduction of the histidine tag fusions at the C-terminus of either DctA or DauA does not affect significantly their function.

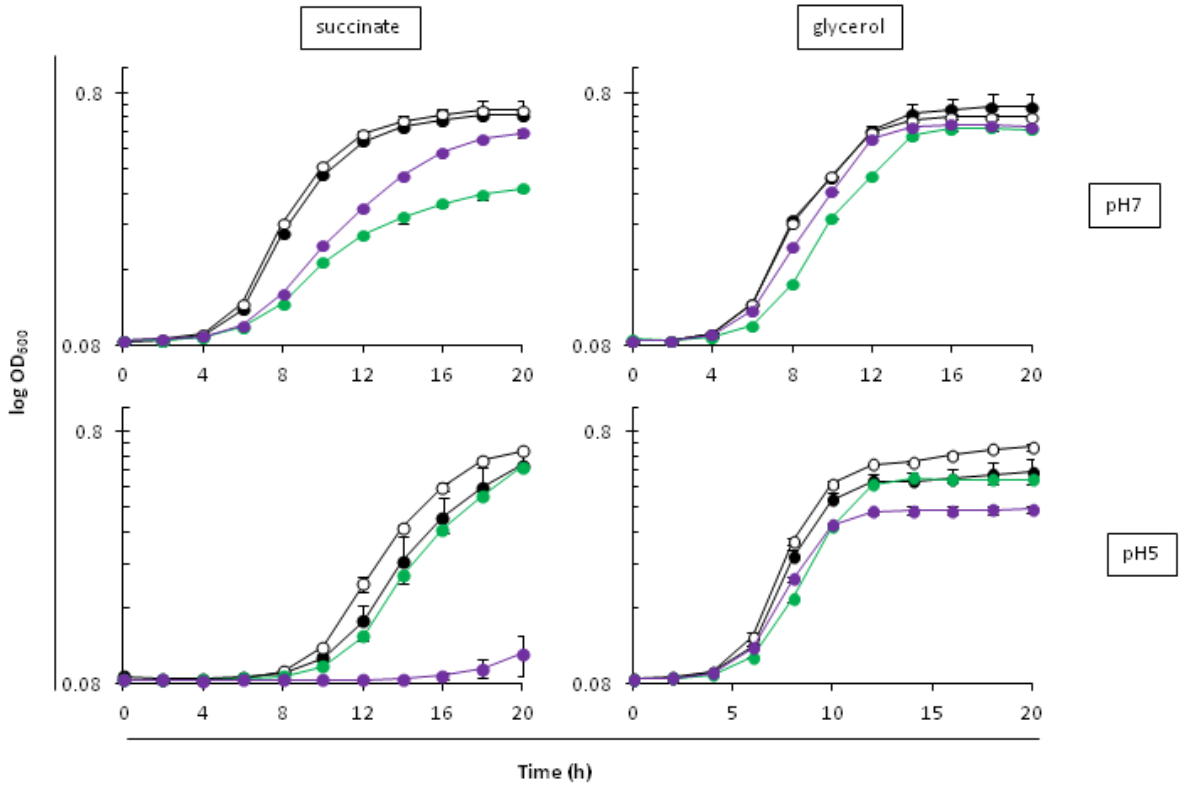

Figure 3-6: Chromosomally-encoded his- tagged variants of DauA and DctA are functional.

Strains EK169 (DauA-H6; black), EK161 (DauA- H6, Δ*dctA*;green) producing a his-tagged variant of DauA from the native chromosomal locus, EK178 (DctA-H6; white) and EK180 (DctA-H6, Δ*dauA*; purple) producing a his-tagged variant of DctA from the native chromosomal locus, were grown in eM9 minimal medium supplemented with 50 mM succinate (left panel) or glycerol (right panel) as the sole carbon source at pH 7 (upper panel) or pH 5 (lower panel). Growth curves were recorded at 600 nm using microplates (average of four independent experiments, error bars represent the standard deviation).

Next, the correct targeting into the membrane of both proteins was confirmed by western immunoblotting. Strains EK169 (DauA-H_6) and EK178 (DctA-H_6) were grown in M9 minimal medium supplemented with glucose as the sole carbon source at pH 7 overnight. The next day the cells were washed twice and cultured for six more hours in

M9 minimal medium supplemented with 50 mM succinate as the sole carbon source at pH 7, pelleted, sonicated and fractionated to membrane and soluble fractions. The presence of DctA or DauA was monitored by western immunoblot using anti-His antibodies in whole cell (WC), soluble (SF) and membrane (M) fractions. TatC, a membrane protein constitutively produced (Jack *et al.*, 2001), was used as loading control and to validate the fractionation protocol used.

In EK169 and EK178 we detected signals for DctA-H_6, DauA-H_6 and TatC only in the membrane fraction, showing that the proteins are correctly targeted to the membrane (Fig. 3-7). DauA-H_6 has a predicted mass of 59.2 kDa and DctA-H_6 of 45.3 kDa, but they were detected at approximately 40 kDa and 35 kDa respectively. This discrepancy in membrane protein migration on SDS-PAGE is common and is likely due to the anomalous SDS-loading capacity and partial unfolding of hydrophobic proteins (Rath *et al.*, 2009).

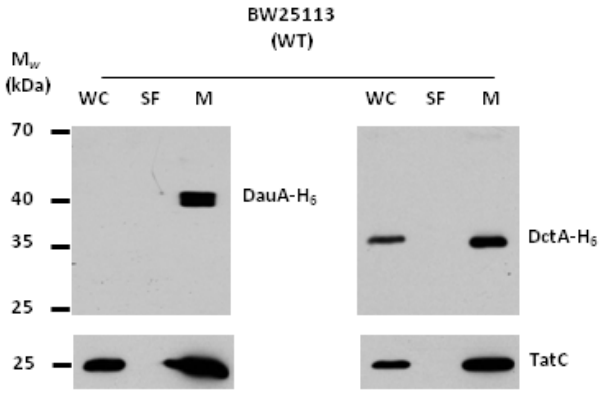

Figure 3-7: DauA-H_6 and DctA-H_6 are correctly targeted at the membrane.

Whole cell (WC), soluble (SF) and membrane (M) fractions were prepared from EK169 (BW25113, encoding for a His- tagged version of DauA from the native chromosomal locus; left panel) and EK178 (BW25113 encoding for a chromosomal His- tagged version of DctA; right panel). Cells were grown for 6 h aerobically in M9 minimal medium supplemented with 50 mM succinate as the sole carbon source at pH 7. Cell pellets were fractionated into membranes and soluble fractions, followed by anti-His immunoblotting. The same membranes were then stripped with a mild treatment and re-probed with a polyclonal anti-TatC antibody as a control.

The investigation on DctA and DauA expression was then continued by comparing succinate-grown cells at pH 7 and pH 5. Interestingly, DauA was clearly present in the membranes of cells grown at both conditions in the wild type and *ΔdctA* backgrounds (Fig. 3-8; upper panel). DctA-H_6 was detected only in cells grown at pH 7, whereas no protein was present in cells grown in succinate at pH 5 (Fig. 3-8; lower panel). When the presence of DctA in wild type was compared to the one in the Δ*dauA* strain at pH 7 the production of DctA appears to decrease in the absence of *dauA*. This observation might indicate a potential interplay between the expression of DctA and DauA.

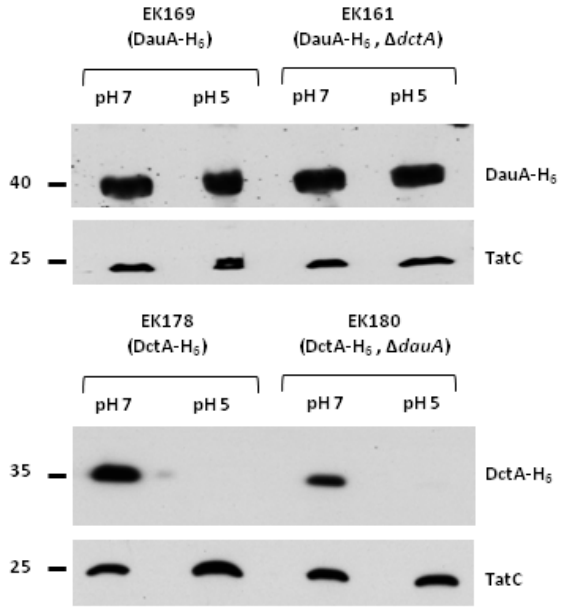

Figure 3-8: Immunoblot detection of DauA and DctA during growth in succinate at pH 7 or pH 5.

Anti-His immunoblot of membrane fractions of EK169 (DauA-H_6**),** EK161 (DauA-H_6**,** Δ*dctA*), EK178 (DctA-H_6**)** and EK180 (DctA-H_6, Δ*dauA*) cells grown for 6 h in M9 minimal medium supplemented with 50 mM succinate as the sole carbon source at pH 5 or pH 7. The same membranes were subsequently stripped and re-hybridized with a polyclonal anti-TatC antibody as a control.

3.2.2.2 Under anaerobic conditions

3.2.2.2.1 Phenotypic analysis

In order to assess whether DauA is involved in anaerobic metabolism we collaborated with Julian Witan and Prof. Gottfried Unden of the University of Mainz (Germany). BW25113, Δ*dauA* (EK9), Δ*dctA* (EK83), Δ*dctA*/Δ*dauA* (EK96) and Δ*dcuABC* strains were grown under anaerobic conditions in eM9 minimal medium supplemented with 50 mM glycerol and 20 mM fumarate at pH 7 (Fig. 3-9; left panel) and pH 5 (Fig. 3-9; right panel). The cell growth was monitored at regular time points in cultures incubated at 37°C in degassed media in infusion bottles with rubber stoppers under N_2. No significant differences were observed in the anaerobic growth of Δ*dauA* (EK9), Δ*dctA* (EK83) and Δ*dctA*/Δ*dauA* (EK96) compared to the wild type rate, whereas the effect of the *dcuABC* mutation (the only anaerobic C_4-dicarboxylate uptake system described so far) was drastic.

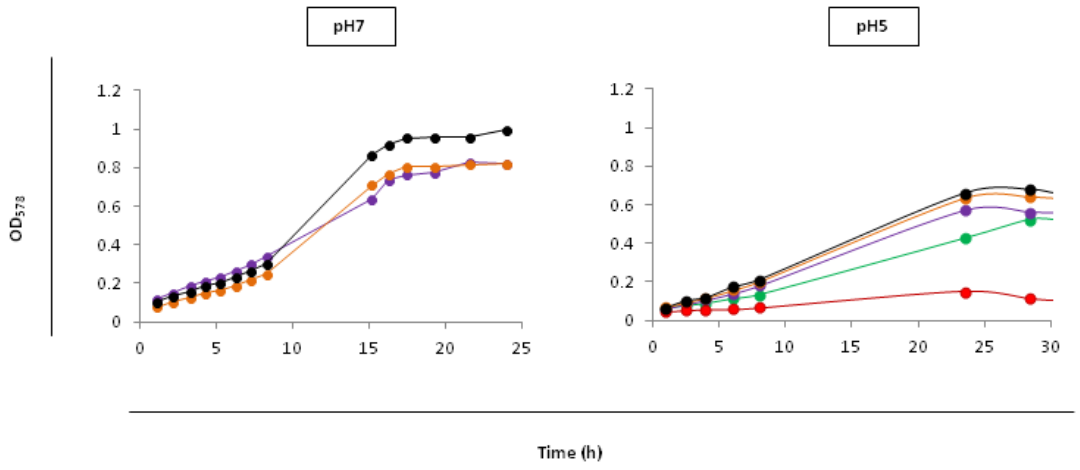

Figure 3-9: Effect of DauA on anaerobic growth.

BW25113 (black), Δ*dauA* (purple), Δ*dctA* (green) and Δ*dctA*/Δ*dauA* (orange) and Δ*dcuABC* (red) cells were grown in eM9 minimal medium supplemented with 50 mM glycerol and 20 mM of the effector fumarate at pH 7 (left panel) and pH 5 (right panel) under anaerobic conditions. The cell growth was monitored at regular time points in culture incubated at 37°C in degassed media in infusion bottles with rubber stoppers under N_2 (experiment performed by Julian Witan).

3.2.2.2.2 Protein production

The absence of *dauA* has no obvious effect on the cell growth under anaerobic conditions. To test whether this is a result of DauA not being expressed or being inactive, the expression of DauA and DctA was monitored after overnight growth in LB (aerobic conditions) or LB supplemented with 0.4% glucose as standing liquid cultures (anaerobic conditions). The 6xHis epitope tag in vector pEK163 was replaced with a FLAG epitope tag by site-directed mutagenesis (using the oligonucleotide pair EKO367/EKO368) and introduced to strain EK169 as described before, to give strain EK182 (DauA-H_6, DctA-FLAG). Cells were pelleted, sonicated and fractionated to membrane and soluble fractions. The presence of DctA or DauA was monitored by western immunoblotting using anti-FLAG or anti-His antibodies, respectively, in whole cell (WC), soluble (SF) and membrane (M) fractions. Again, TatC was used as loading control, since the oxygen condition of the cells does not affect its expression (Jack et al., 2001). Under aerobic conditions, DauA seems to be highly expressed (Fig. 3-10; top panel), while its production is greatly reduced under anaerobic conditions. This reduction might indicate a level of regulation. As expected, DctA expression (Fig. 3-10; lower panel) was repressed in both conditions since it has been shown to be associated strictly with aerobic C_4-dicarboxylate metabolism. Summarizing the above results, it might be hypothesized that DauA is produced constitutively regardless of pH or carbon source the cells are grown in. However, under anaerobic conditions DauA production is clearly reduced suggesting that DauA might be under the inhibitory regulation of ArcBA or FNR.

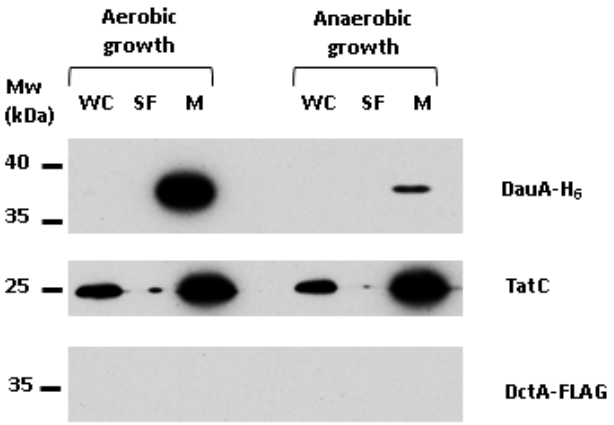

Figure 3-10: DauA and DctA aerobic and anaerobic growth.

Whole cell (WC), soluble (SF) and membrane (M) fractions were prepared from EK182 (DauA-H_6, DctA-FLAG). Cells were grown overnight aerobically in LB or anaerobically in LB supplemented with 0.4% glucose. Cell pellets were fractionated into membranes and soluble fractions, followed by anti-His, anti-FLAG and anti-TatC immunoblotting. Protein extract concentration was normalized and the same amount was loaded in each lane.

3.2.3 DauA is a succinate transporter

3.2.3.1 Time course of DauA- and DctA-dependent succinate accumulation

Janausch *et al.* (Janausch *et al*., 2001) suggested in their study the existence of another succinate carrier (other than DctA) active at acid pH. They based this hypothesis on their observation that a quintuple *E. coli* mutant lacking all known C_4-dicarboxylate transporters (DctA, DcuA, DcuB, DcuC, DcuD) is still able to transport succinate under aerobic conditions at acidic pH.

To confirm whether DauA is the missing succinate transporter an *in vivo* succinate uptake assay was developed. Cells were incubated with [^{14}C]-succinate for up to 6 minutes. Samples were taken periodically and the assay was terminated by filtering the cells on nitrocellulose membrane under a constant vacuum and rigorously washed. Accumulation of [^{14}C]-succinate in the cell was determined using a scintillation counter.

Firstly, succinate accumulation was assessed in cells grown in M9 succinate at pH 5 for 6 hours. It was shown in previous experiments (Fig. 3-8), that under these conditions DctA is not expressed, thus it was hypothesised that succinate uptake is DauA-dependent. The accumulation of [^{14}C]-succinate was measured over time in BW25113, Δ*dauA*, Δ*dctA* and Δ*dctA*/Δ*dauA* cells. Under these conditions, the uptake activity measured was linear over the time course of the experiment and used for V_o calculation. Fig. 3-11 (left panel) shows that succinate uptake activity of wild type (0.043 ±0.007 $\mu mol^{-1}min^{-1}g^{-1}$ dry weight) was 1.4 times higher than the activity measured in Δ*dctA* cells. On the other hand, the uptake rate measured in Δ*dauA* and Δ*dctA*/Δ*dauA* cells was negligible (0.008 ± 0.003 and 0.008 ±0.01 $\mu mol^{-1}min^{-1}g^{-1}$ dry weight, respectively). These results indicate that DauA act as the main succinate transporter at pH 5.

Secondly, it was investigated whether DauA was active at pH 7. Previous western immunoblotting analysis (Fig. 3-8) indeed indicates that DauA is present when cells are grown in succinate at pH 7. Therefore BW25113, Δ*dctA*, Δ*dauA* and Δ*dctA*/Δ*dauA* cells were grown at pH 7 and the accumulation of [^{14}C]-succinate was measured (Fig 3-11; right panel). The uptake rate of succinate in BW25113 cells was 0.546 ± 0.084 $\mu mol^{-1}min^{-1}g^{-1}$ dry weight, while as expected the succinate uptake in Δ*dctA* and Δ*dctA*/Δ*dauA* was negligible. The uptake rate in Δ*dauA* was six times lower compared to the wild type. It can be concluded from the above experiment that at pH 7 (i) DctA is the major succinate transporter and (ii) although DauA seems inactive in transporting succinate, its presence might be necessary to measure optimal DctA activity. These latter results agree with previous western immunoblot analysis (Fig. 3-8) that shows interplay between the expression of DauA and DctA.

The total rate of uptake at pH 7 is 10 times higher than at pH 5 in BW25113 cells. Hence, it could be hypothesized that DauA may transport succinate at a lower rate than DctA.

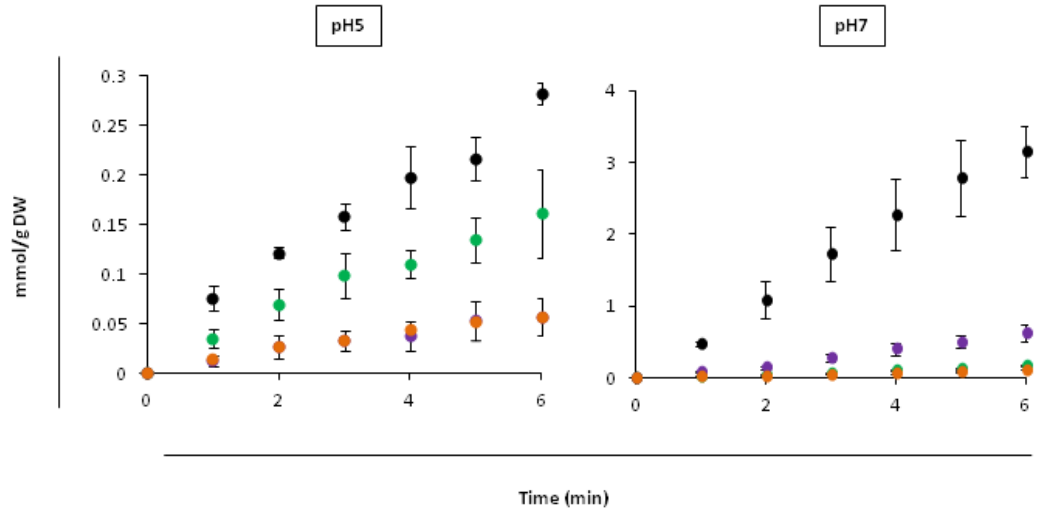

Figure 3-11: Time dependence of [^{14}C] - succinate accumulation.

In vivo succinate uptake assays for BW25113 (black), Δ*dauA* (purple), Δ*dctA* (green) and Δ*dctA*/Δ*dauA* (orange) cells after growth for 6 h in M9 minimal medium supplemented with 50 mM succinate as the sole carbon source at pH 7 (right panel) or pH 5 (left panel). The accumulation of 40 µM [^{14}C]-succinate was measured over time. The average of six independent test series is presented. Error bars represent standard deviation.

3.2.3.2 Kinetics of DauA- and DctA-dependent succinate accumulation

In order to determine the apparent kinetic parameters of DctA and DauA, the transport activity was measured using increasing succinate concentrations (from 40 μM up to 5mM) for each strain growing in succinate at pH 5 or pH 7. The measurements for the double mutant Δ*dctA*/Δ*dauA* were subtracted in each condition. The uptake rates for each condition were calculated and the reaction velocity was plotted as a function of the substrate concentration. The results (Fig 3-12) show that [^{14}C]-succinate accumulation measured in both conditions follow an apparent Michaelis-Menten kinetics, consistent with carrier-mediated transport mechanism. Using the GraphPad Prism 6 Enzyme Kinetics module the measurements were fitted using a Michaelis-Menten equation ($V_o=V_{max}[S]/K_m+[S]$). The Michaelis constant (K_m) and the maximum uptake rate (V_{max}) determined using the Hanes-Woolf transformation ($[S]/V_0=(1/V_{max})[S]+(K_m/V_{max})$ (Table 3-1).

At pH 5 (Fig. 3-12; left panel), a condition under which DctA is not expressed, BW25113 and Δ*dctA* cells demonstrate similar [^{14}C]-accumulation rates. The activity measured in the Δ*dauA* strain shows linear kinetics against increasing concentrations of succinate, which may be due to a diffusion process, activity of a very low-affinity and uncharacterized transport system, or non-specific binding of the substrate to the membrane.

At pH 7, the kinetics of succinate uptake measured in Δ*dctA* cells is linear against the substrate concentrations and uptake rates are negligible when compared to the rates measured in wild type cells. This confirmed that at pH 7 DctA is the main active succinate transporter. Interestingly, the transport activity measured in the Δ*dauA* strain is significantly reduced compared to the wild type (Fig. 3-12). These observations point

toward a DauA-dependent optimum DctA production and/or activity as previously suggested (Fig. 3-8 and 3-11).

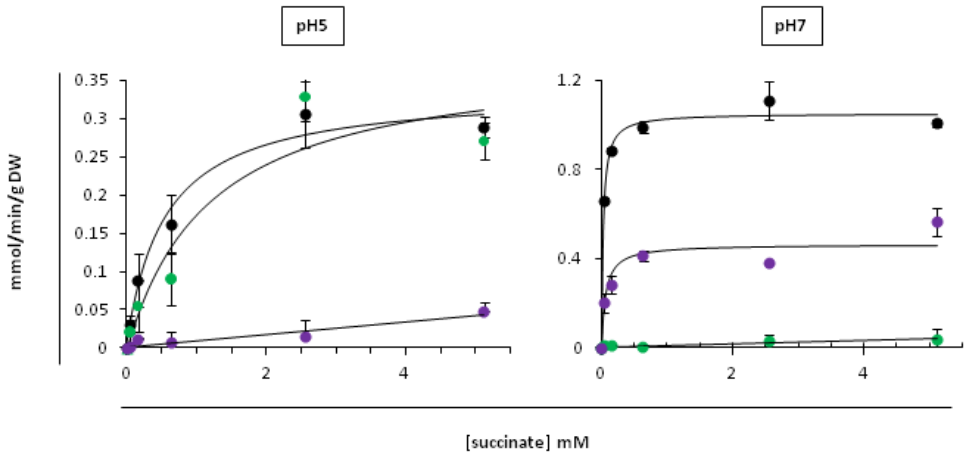

Figure 3-12: Concentration dependence of [^{14}C] - succinate uptake.

In vivo succinate uptake assays for wild type (black), Δ*dauA* (purple), and Δ*dctA* (green) cells after growth for 6 h in M9 minimal medium supplemented with 50 mM succinate as the sole carbon source at pH 7 (right panel) or pH 5 (left panel). The activity measured for Δ*dctA*/Δ*dauA* was subtracted in each case. The average of six independent test series is presented. Error bars represent standard deviation. (The uptake rates of each strain remained linear over the time of measurement)

In Table 3-1 the apparent kinetic parameters for DauA and DctA are shown. The K_m for DauA is 20 times lower compared to DctA and the K_m for DctA agrees with previous studies (20–30 μM) (Lo *et al.*, 1972) validating our results.

Table 3-1: Apparent DauA and DctA kinetic parameters

		$K_{m(app)}$ (mM)	**$V_{max(app)}$ ($mmol^{-1}min^{-1}g^{-1}DW$)**	**R^2**
pH 7	WT	0.025±0.005	1.05±0.02	0.99
	ΔdauA	0.040±0.019	0.45±0.03	0.92
pH 5	WT	0.56±0.15	0.34±0.02	0.96
	ΔdctA	1.19±0.84	0.38±0.02	0.98

3.2.3.3 DauA is able to transport mono- and di-carboxylates

DctA has been characterised as a transporter able to recognise and transport only the di-carboxylate form of succinate (Gutowski & Rosenberg, 1975), while it has been suggested that the missing acidic succinate transporter should only transport the mono-carboxylate form (Janausch *et al*., 2001). This is due to the fact that at pH 7 the main succinate species (95%) is the di-protonated form and whereas at pH 5 it is the mono-protonated (72%) (Fig.3-13A). The above results show that DauA is only active at pH 5 and therefore an assay was developed to test whether DauA could transport only the mono-carboxylated form of succinate.

The first step was to use this assay to test whether DctA transports only the di-carboxylate form of succinate and consequently confirm the validity of our approach. For that, BW25113, Δ*dauA* and Δ*dctA*/Δ*dauA* cells were grown in succinate pH 7 for 6 hours, conditions under which DctA is the main transporter. After the cells were washed the [^{14}C]-succinate uptake rate was measured. The rate measured for the double mutant Δ*dctA*/Δ*dauA* was subtracted in each case. The logic was that at pH 5 the amount of available di-carboxylate form of succinate decreases and thus the uptake rate at pH 7 should be notably higher than at pH 5. Fig. 3-13B shows the ratio of the [^{14}C]-succinate uptake activity at pH 7 over the activity measured at pH 5 for wild type and Δ*dauA* strains. It is clear that the activity measured at pH 7 is seven and four times higher, respectively, than the activity measured at pH 5. This result indicates that DctA is able to transport only succinate di-carboxylate.

Next step was the study of the ability of DauA to transport mono-protonated and/or di-protonated succinate. For that the same approach as before was followed. BW25113, Δ*dctA* and Δ*dctA*/Δ*dauA* cells were grown in succinate pH 5 for 6 hours, conditions

under which it has been shown that DauA is the main transporter. After the cells were washed the [^{14}C]-succinate uptake rate was measured. The rate measured for the double mutant Δ*dctA*/Δ*dauA* was subtracted in each case. The hypothesis was that at pH 5 the amount of available mono-carboxylate succinate increases and thus, if DauA is able to transport only mono-protonated succinate the uptake rate at pH 5 should be notably higher than at pH 7. However, if DauA transports only di-protonated succinate the uptake activity at pH 7 should be higher than the activity measured at pH 5. Finally, if DauA is able to transport both species of succinate it was expected to be able to measure the same rate of succinate uptake for both pHs. Fig. 3-13C shows the ratio of the [^{14}C]-succinate uptake activity at pH 7 over the activity measured at pH 5 for the parental and Δ*dctA* strains. It is clear that the uptake rate measured both at pH 7 and pH 5 is the same (ratio=1) indicating that DauA is able to transport both mono- and di- carboxylate forms of succinate.

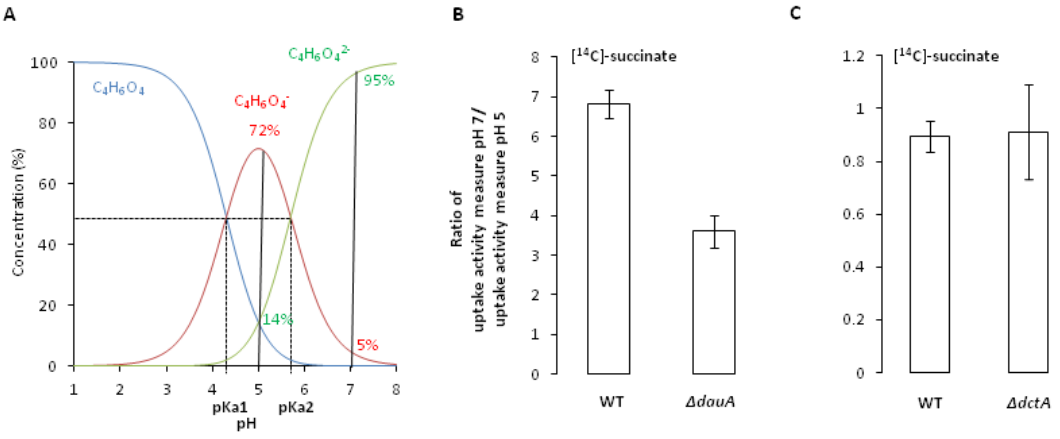

Figure 3-13: Protonation state of DctA and DauA.

(A) Species distribution diagram of succinate protonation state. pH dependence of the concentration (expressed as %). (B) Ratio of the [^{14}C]-succinate (10 µM) uptake activity at pH 7 over the activity measured at pH 5 for wild type and Δ*dauA* strains grown in M9 minimal medium supplemented with 50 mM succinate as the sole carbon source at pH 7. (C) Ratio of the [^{14}C]-succinate (10 µM) uptake activity for wild type and Δ*dctA* strains grown at pH 5 in M9 minimal medium supplemented with 50 mM succinate as the sole carbon source. In each case, the activity of Δ*dctA*/Δ*dauA* strain measured under the same growth and assay conditions was subtracted. The results are the average of at least four independent test series. Error bars represent the standard deviation.

3.2.4 DauA can transport other C_4-dicarboxylates

It is known that DctA is able to transport a variety of C_4-dicarboxylic acids (succinate, fumarate, malate, oxaloacetate, and aspartate) and the monocarboxylic acid orotate. Thus, the next question was to investigate whether DauA is able to transport other C_4-dicarboxylic acids. In order to do that the uptake of [^{14}C]-succinate was measured in the presence of other unlabelled carboxylic acids. It is known from previous results that at pH 5 only DauA is expressed and it is involved in succinate transport. If DauA is able to transport another dicarboxylic acid an inhibition of [^{14}C]-succinate accumulation is expected in the presence of the unlabelled dicarboxylic acid. Figure 3-14A shows the uptake of [^{14}C]-succinate (40 μM) for wild type and Δ*dctA* strain in the presence of 15 different unlabelled dicarboxylic acids (2mM). A strong inhibition of DauA-dependent succinate uptake was measured in the presence of aspartate and fumarate in the wild type and Δ*dctA* strain. Weaker inhibition was observed in the presence of butyrate. These results suggest that DauA might be able to transport aspartate and fumarate.

Next, an attempt to validate this competition assay was made by confirming previous studies showing that DctA is able to transport succinate, fumarate and malate, aspartate and oxaloacetate. The same procedure as above was repeated measuring the inhibition of [^{14}C]-succinate by other carboxylic acids in BW25113 and Δ*dctA* cells grown in succinate at pH 7, when DctA is the main succinate transporter. As expected, the uptake of radiolabelled succinate was strongly inhibited by aspartate, fumarate, malate and oxaloacetate in both strains (Fig. 3-14B). The weak effect of butyrate that was observed was reported also before (Janausch *et al.*, 2001), but remains unexplained. These results indicate that DctA might be able to transport succinate, fumarate, malate, aspartate and

oxaloacetate, validating our inhibition approach to determine other substrates transported by DauA.

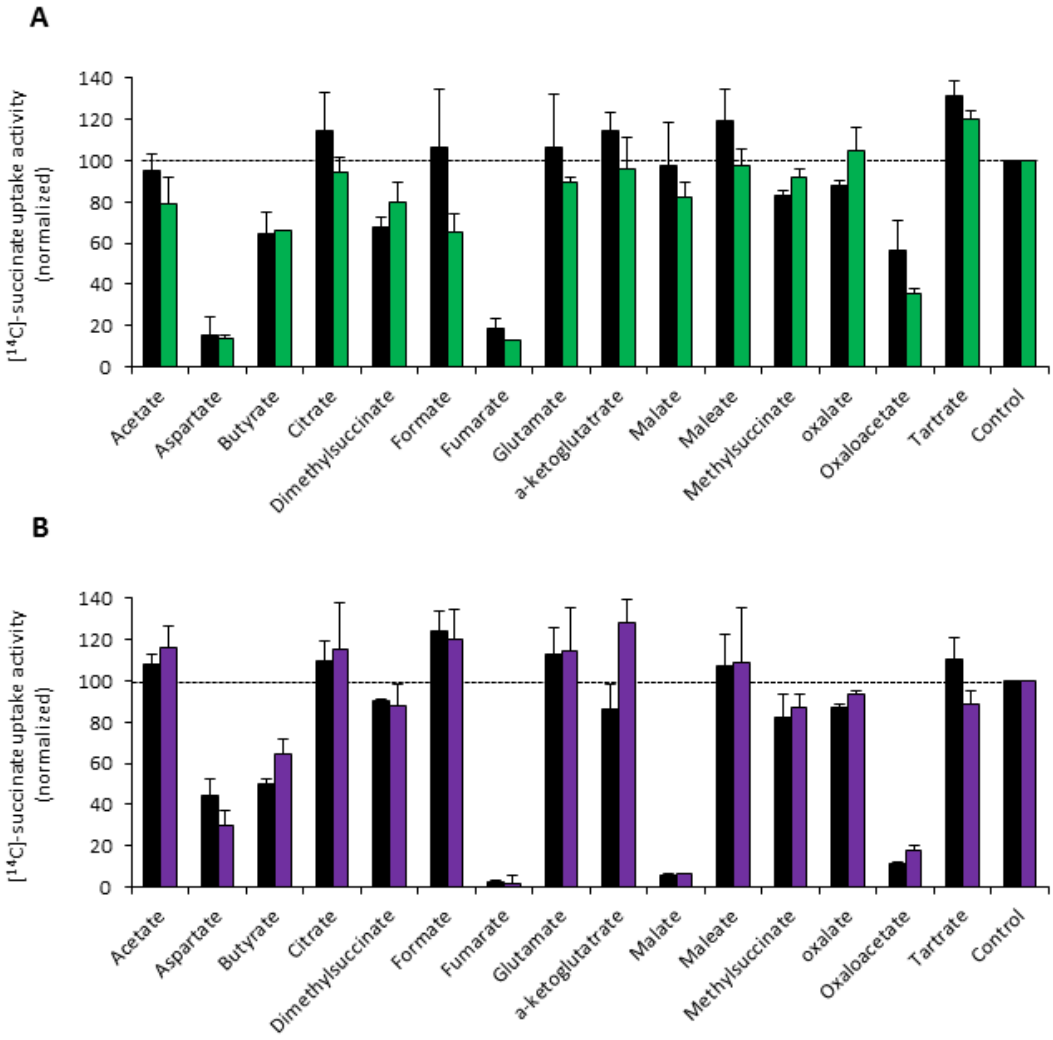

Figure 3-14: Inhibition of DctA- and DauA dependent [^{14}C] - succinate uptake activity in the presence of various carboxylic acids.

[^{14}C]-succinate uptake (40 µM) followed the addition of different carboxylic acids (2 mM). **(A)** BW25113 (wild type; black bars) and EK83 (*ΔdctA*; green bars) cells were grown for 6 h in M9 minimal medium supplemented with 50 mM succinate as the sole carbon source at pH 5 before the measurement. **(B)** BW25113 (wild type; black bars) and EK9 (Δ*dauA*; purple bars) cells were grown in the above conditions but at pH 7 before the measurement. All results (average of six independent series) were normalized to the control (value set at 100%). The activity measured for Δ*dctA*/Δ*dauA* was subtracted in each case. (Control values: BW25113$_{pH\ 7}$ 0.537 mmol/min/g DW, BW25113$_{pH\ 5}$ 0.035 mmol/min/g DW, Δ*dauA*$_{pH\ 7}$ 0.1 mmol/min/g DW, Δ*dctA*$_{pH\ 5}$ 0.025 mmol/min/g DW). Error bars represent the standard deviation.

3.2.4.1 Fumarate metabolism

The competition assay results suggest that DauA might be able to transport fumarate and aspartate. However, these potential substrates might be able to bind to the transporter without being actually transported, and thus prevent the transport of [^{14}C]-succinate. Firstly, to establish that fumarate is being transported by DauA, the accumulation of [^{14}C]-fumarate was directly measured in BW25113, Δ*dctA* and Δ*dauA* cells grown in succinate at pH 5, when DauA is the main succinate transporter. The accumulation rates of [^{14}C]-fumarate in Δ*dctA* cells were comparable to wild type levels, while in the Δ*dauA* background accumulation was negligible (Fig. 3-15; white bars). These results suggest that DauA is able to transport fumarate.

Accumulation rates of [^{14}C]-fumarate were also measured in the same strains for cells grown in succinate at pH 7. Accumulation of [^{14}C]-fumarate is clearly DctA-dependent under this condition, confirming that it is the main fumarate transporter (Fig. 3-15; grey bars). In Δ*dauA* the [^{14}C]-fumarate accumulation rate was decreased approximately four times compared to the wild type confirming our previous results that DauA is necessary for DctA expression and/or activity.

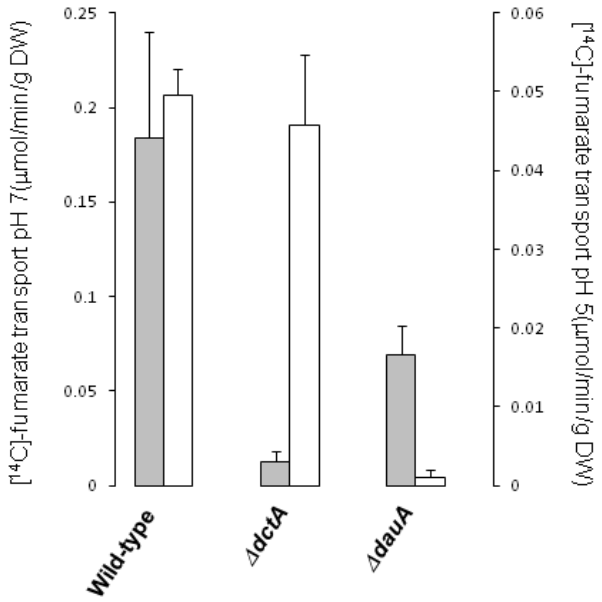

Figure 3-15: DctA- and DauA- dependent [^{14}C] - fumarate uptake activity.

[^{14}C]-fumarate uptake (40 mM final concentration) in BW25113 (wild type), EK9 (Δ*dauA*) and EK83 (Δ*dctA*) strains following growth of cells for 6 hrs in M9 minimal medium supplemented with 50 mM succinate as the sole carbon source at either pH 7 (grey bars) or pH 5 (white bars). The activity measured in the EK96 (Δ*dctA*/Δ*dauA*) strain was subtracted in each case. All results are the averages of at least 6 independent test series. Error bars represent the standard deviation. (Experiment performed by Arnaud Javelle)

Next step was to understand further the DauA fumarate transport and study the ability of DauA to transport fumarate mono- or di-carboxylate. At pH 7 only (99.6%) fumarate di-carboxylate is present while at pH 5 this concentration decreases slightly (73.9%) (Fig. 3-16A). BW25113, Δ*dctA* and Δ*dctA*/Δ*dauA* strains were grown for six hours in the presence of succinate pH 5. The cells were washed and the [^{14}C]-fumarate uptake activity was measured at pH 7 and pH 5. The rate measured for the double mutant Δ*dctA*/Δ*dauA* was subtracted in each case. The [^{14}C]-fumarate uptake activity of wild-type and Δ*dctA* strains was the same if measured at pH 7 or pH 5 confirming transport of both mono- and dicarboxylate forms (Fig. 3-16B).

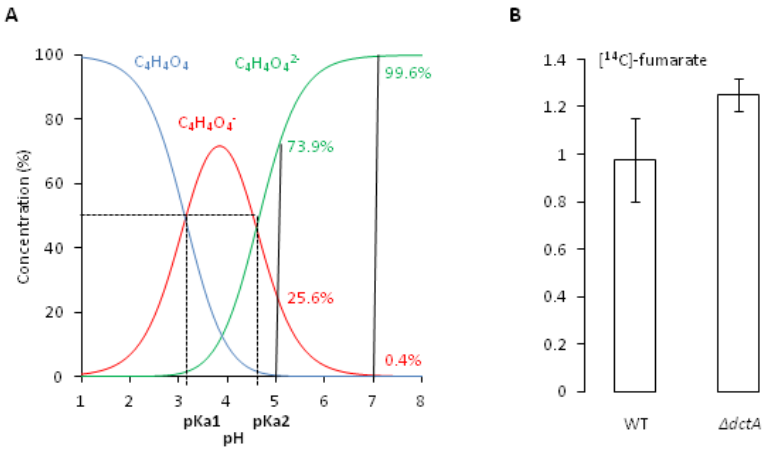

Figure 3-16: Protonation state of DctA and DauA in fumarate.

(A) Protonation state of fumarate. pH dependence of the concentration (expressed as %). (B) Ratio of the [^{14}C]-fumarate (10 µM) uptake activity for wild type and Δ*dctA* strains grown at pH 5 in M9 minimal medium supplemented with 50 mM succinate as the sole carbon source. In each case, the activity of Δ*dctA*/Δ*dauA* strain measured under the same growth and assay conditions was subtracted. The results are the average of at least four independent test series. Error bars represent the standard deviation (Experiment performed by Arnaud Javelle).

Next, the focus was turned to fumarate metabolism. It is known that DctA is the only fumarate transporter at pH 7 and in previous results it was shown that DauA is able to transport fumarate at pH 5. The growth of BW25113, Δ*dctA*, Δ*dauA* and Δ*dctA*/Δ*dauA* strains was compared in eM9 minimal medium supplemented with 50 mM fumarate as the sole carbon source, at pH 7 and pH 5. Unexpectedly, BW25113 and Δ*dauA* cells grew at comparable rates while Δ*dctA* and Δ*dctA*/Δ*dauA* growth was impaired at both conditions (Fig. 3-17A). This result was confusing and apparently disagrees with the fumarate transport assays. To investigate this further DctA and DauA production under the same conditions was studied.

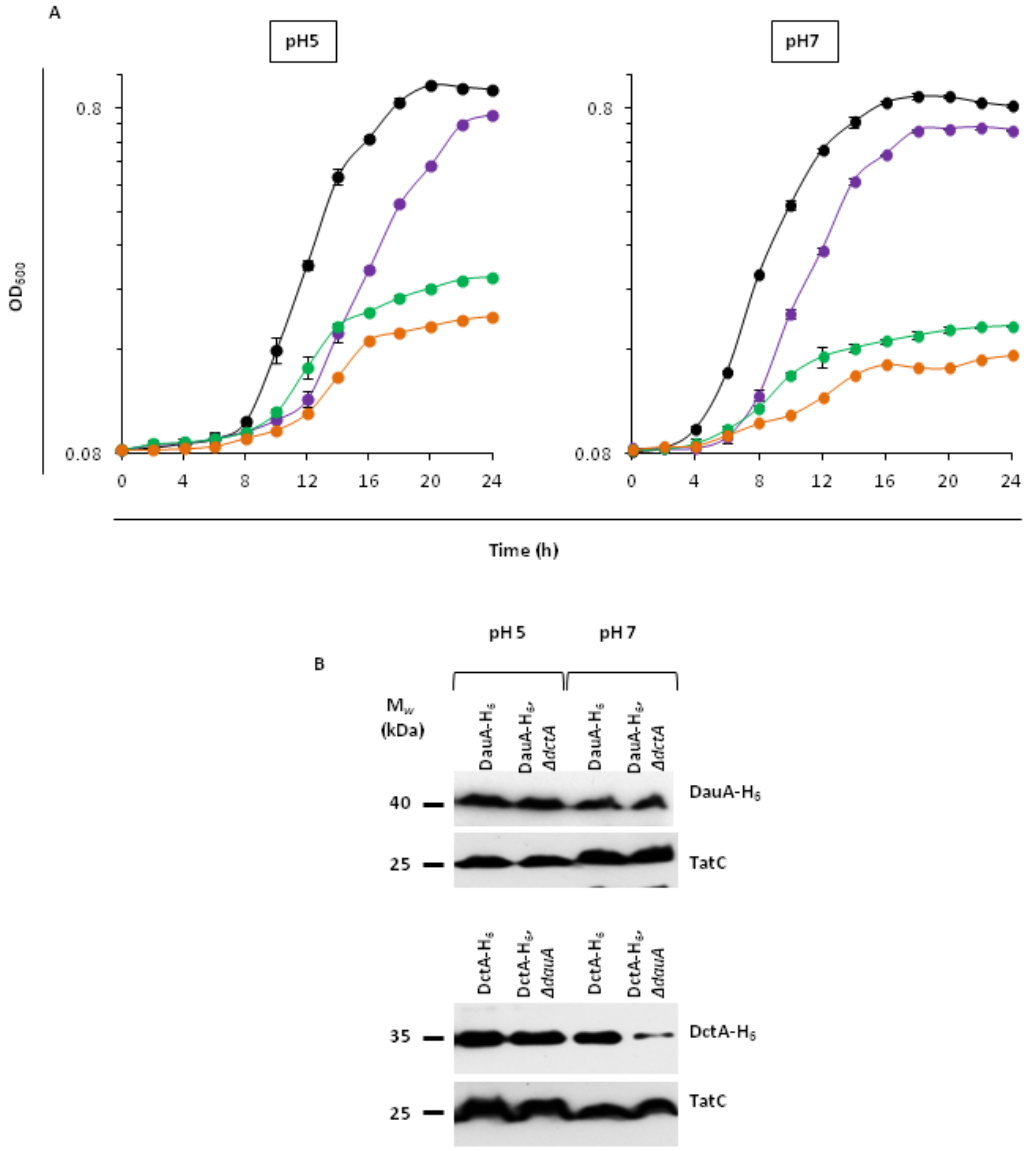

Figure 3-17: DauA and fumarate metabolism.

(A) BW25113 (black ●), Δ*dauA* (purple), Δ*dctA* (green) and Δ*dctA*/Δ*dauA* (orange) cells were grown in eM9 minimal medium supplemented with 50 mM fumarate as the sole carbon source at pH 5 (left panel) or pH 7 (right panel). Growth curves were recorded at 600 nm using microplates (average of four independent experiments, error bars represent the standard deviation).

(B) Membrane fractions were prepared from EK169 (DauA-H_6**),** EK161 (DauA-H_6**,** Δ*dctA*), EK178 (DctA-H_6**)** and EK180 (DctA-H_6, Δ*dauA*) cells grown for 6 h in M9 minimal medium supplemented with 50 mM fumarate as the sole carbon source at pH 5 or pH 7. Samples were harvested, fractioned and subjected to SDS – PAGE followed by Western immunoblotting with an anti-His antibody. The same membranes were subsequently stripped and re-hybridized with a polyclonal anti-TatC antibody as a control.

The production of DctA and DauA was monitored in EK169 (DauA-H_6), EK161 (DauA-H_6, Δ*dctA*), EK178 (DctA-H_6) and EK180 (DctA-H_6, Δ*dauA*) cells grown for 6 h in M9 minimal medium supplemented with 50 mM fumarate as the sole carbon source at pH 5 or pH 7. At pH 5, both DctA and DauA are expressed in an apparent comparable level. At pH 7, again, both proteins are present (as in the case of succinate) with a minor reduction of DctA production in the absence of DauA (Fig. 3-17B). These results show that the presence of active DctA at pH 5 may explain why the Δ*dauA* mutant is able to grow with fumarate at acidic pH but not with succinate. It is not completely understood why Δ*dctA* cells do not grow at pH 5 in the presence of fumarate, although DauA is present and active.

3.2.4.2 Aspartate metabolism

The investigation was continued on other C_4-dicarboxylic acids transported by DauA with aspartate uptake assays. As previously, the accumulation of [^{14}C]-aspartate was directly measured in cells grown in succinate at pH 5 or pH 7. The aspartate accumulation rates of BW25113, Δ*dctA* and Δ*dauA* cells were comparable for both pHs (Figure 3-18).

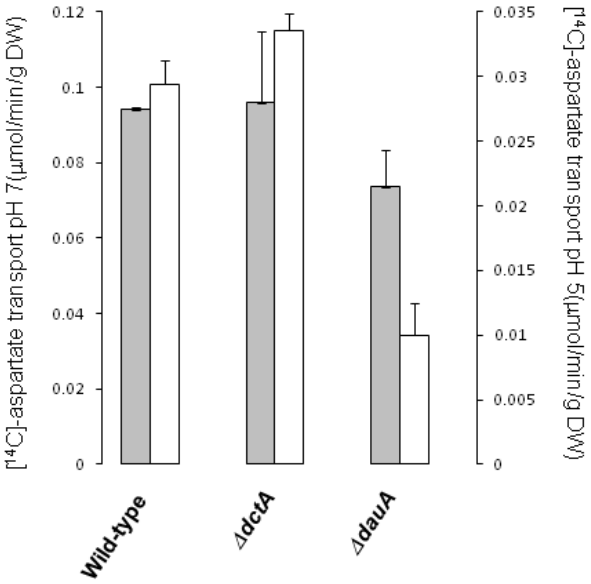

Figure 3-18: DctA- and DauA- dependent [^{14}C]- aspartate uptake activity.

[^{14}C]-aspartate uptake (40 mM final concentration) in BW25113 (wild type), EK9 (Δ*dauA*) and EK83 (Δ*dctA*) strains following growth of cells for 6 hrs in M9 minimal medium supplemented with 50 mM succinate as the sole carbon source at either pH 7 (grey bars) or pH 5 (white bars). The activity measured in the EK96 (Δ*dctA*/Δ*dauA*) strain was subtracted in each case. All results are the averages of at least 6 independent test series. Error bars represent the standard deviation. (Experiment performed by Arnaud Javelle)

In addition when the growth of wild type, Δ*dctA*, Δ*dauA* and Δ*dctA*/Δ*dauA* strains grown in eM9 minimal medium supplemented with 50 mM aspartate as the sole carbon source was monitored, at pH 7 and pH 5, no significant difference was observed

between wild type and Δ*dauA* cells. The growth measured for Δ*dctA* and the double mutant was clearly low but not abolished (Fig. 3-19). These results, as expected, indicate that DctA and DauA are not the only aspartate transporters in *E. coli*, since at least two more aspartate uptake systems have been identified.

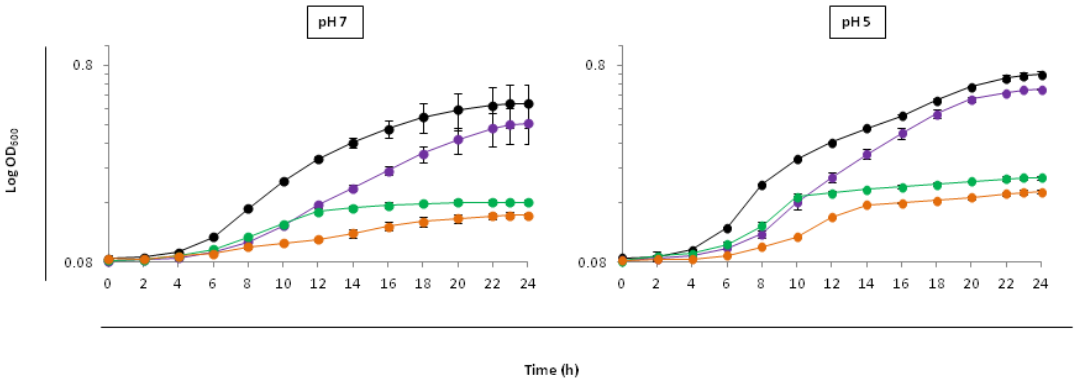

Figure 3-19: DauA and L-aspartate metabolism.

BW25113 (black ●), Δ*dauA* (purple), Δ*dctA* (green) and Δ*dctA*/Δ*dauA* (orange) cells were grown in eM9 minimal medium supplemented with 50 mM L- aspartic acid as the sole carbon source at pH 7 (left panel) or pH 5 (right panel). Growth curves were recorded at 600 nm using microplates (average of four independent experiments, error bars represent the standard deviation).

3.2.5 Identification of DauA regulatory function

A series of interesting results have been obtained that indicate interplay between DauA and DctA expression and/or activity. First of all, Δ*dauA* cells growing on solid MOPS minimal medium (pH 7) supplemented with succinate as the sole carbon source (Fig. 3-4), conditions under which DctA is the main succinate transporter, show a growth defect phenotype similar to Δ*dctA* strain. Similarly, in liquid eM9 succinate medium at pH 7 (Fig. 3-5), the Δ*dauA* strain demonstrates a prolonged lag phase compared to the wild type growth rate. Secondly, the succinate uptake rate of Δ*dauA* cells grown at pH 7 (Fig. 3-12) was significantly reduced compared to the wild type activity. Finally, the production of DctA after growth in M9 succinate pH 7 for 6 hours (Fig. 3-8) is notably reduced in Δ*dauA* compared to the wild type strain. Taken together these four lines of evidence suggest that in the absence of *dauA* the activity and/or expression of DctA is highly affected. To explore this hypothesis further, an in-frame, un-marked and non-polar *dauA* deletion was constructed by P1 transduction in the *E. coli* IMW385 background [MC4100, λ(Φ*dctA'–'lacZ*)hyb, *bla*; A. Kleefeld and G. Unden, unpublished] to give strain EK111. To test the effect of the *dauA* deletion on the transcription of *dctA*, the β-galactosidase activity was measured in strains grown in M9 minimal medium supplemented with 50 mM succinate as the sole carbon source, at pH 7 or pH 5. In accordance with previous observations, at pH 5 the activity of *dctA'-'lacZ* was not detectable above background level. On the other hand, at pH 7 in the wild type strain *dctA'-'lacZ* activity was clearly detect but this activity was significantly reduced by twofold in the Δ*dauA* mutant (Fig. 3-17). Based on these observations it can be hypothesized that there is interplay between the presence/activity of DauA and the expression of DctA.

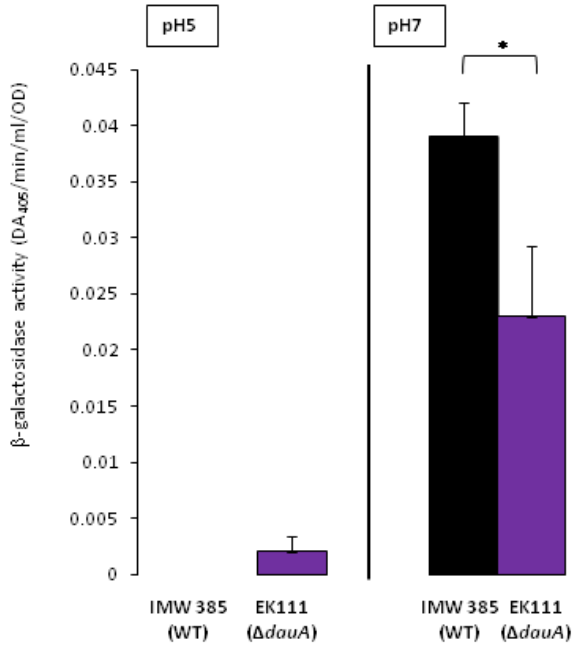

Figure 3-20: Effect of chromosomal *dauA* deletion on the transcription of *dctA*.

Wild type (black bars) and EK111 (purple bars) strains were grown aerobically for 6 hours in M9 minimal medium supplemented with 50 mM succinate as the sole carbon sources at pH 5 or pH 7. The β-galactosidase activity was measured. All results are the average of at least 4 independent test series. Error bars represent the standard deviation. (* t-test $P<0.05$)

3.3 Discussion

While the amount of information on eukaryotic members of the SCL26A/SulP family constantly increases, the role of the prokaryotic homologues had remained unclear. Many bacterial species have been shown to express multiple SulP homologues. In *E. coli* only one SulP protein (DauA) has been identified, but its physiological role remained unknown. In this part of the study an attempt to characterize the role of DauA using both global metabolic approaches and phenotypic characterisation was made.

Ab initio prediction methods remain highly speculative in the absence of other evidence, hence bioinformatics gene function predictions are essentially limited to what we already know experimentally from other systems. Initially, the SulP family had been described as sulphate transporters. However, experimental data on human homologues identified them as versatile transporters of monovalent and divalent anions (Dorwart *et al*., 2008b), it is therefore reasonable to expect that the SulP family in prokaryotes can transport or exchange various substrates. According to this hypothesis, studies on two prokaryotic SulP transporters characterised these proteins as bicarbonate (Price *et al*., 2004) or nitrate transporters (Maeda *et al.*, 2006). Moreover, published data seem to indicate that *E. coli* DauA has no role in sulphate metabolism (Zolotarev *et al.*, 2008).

Babu *et al.* (Babu *et al.*, 2010) in a study describing the structure of the soluble DauA (YchM) STAS domain, proposed that DauA is a bicarbonate transporter involved in fatty acid metabolism. They based their hypothesis on the fact that DauA co-crystallised with acyl carrier protein (ACP). However, direct evidence of such an activity is lacking and attempts to repeat these results and detect DauA-dependent bicarbonate uptake have failed. A following study from the same group contradicts their first findings as they have been unable to reproduce their bicarbonate transport assay (Taddese, 2013).

Furthermore, phylogenetic analysis performed by our group (Fig. 1-4) and others (Felce & Saier, 2004; Price & Howitt, 2011) shows that DauA clusters away from the bicarbonate/carbonate subfamily of the SLC26/SulP transporters.

The technology of Phenotypic Microarrays was used to determine a global metabolic profile of the *E. coli* cell under various nutrient conditions. The advantage of measuring the respiration of the cells instead of growth is the sensitivity of the method, a cell may respond metabolically by respiring but not growing. For example, *Staphylococcus* species give a respiratory response to N-sources but are not able to grow on single N-sources (Bochner, 2009). The second advantage of measuring respiration is that it allows the measurement of more cellular pathways. For example, *E. coli* has a formate dehydrogenase pathway that can be detected by respiration but not by growth. It can respire and generate energy with formate, but it cannot grow on formate because it is not able to convert this carbon compound into the larger molecules that it needs to grow (Bochner, 2009). Finally, a study in *Pseudomonas aeruginosa* has proved that the PM analysis represents an invaluable tool for the characterization of membrane transport proteins (Johnson *et al.*, 2008).

The results of the PM analysis comparing Δ*dauA* and parental strains indicated a role for DauA in succinate metabolism (Fig. 3-2). *E. coli* cells are able to grow aerobically on C_4-dicarboxylates as the sole carbon and energy sources by employing the well characterized DctA transport systems. DctA is the most active C_4-dicarboxylate carrier under aerobic conditions but it has been shown that Δ*dctA* regain growth on succinate at acidic conditions (Davies *et al.*, 1999; Janausch *et al.*, 2001). The presence of an uncharacterised carrier was suggested since the diffusion rates of succinate at acidic pH are not sufficient to support growth (Janausch *et al.*, 2001). DauA was confirmed as the

missing succinate transporter at acidic pH by showing a growth defect phenotype in Δ*dauA* cells (Fig. 3-4 and 3-5) and by developing radiolabelled succinate *in vivo* uptake assays (Fig. 3-11 and 3-12). It was shown that cells growing in succinate as the sole carbon source at pH 5 do not produce DctA while DauA is expressed and active (Fig. 3-8). However, these results should be interpreted with caution since the pH of the M9 medium was not stabilized and potentially was altered at the point of sampling.

Careful study of the kinetic properties of DctA- and DauA-dependent succinate transport requires the development of an *in vitro* assay using purified proteins reconstituted in liposomes. However, *in vivo* assays allow determination of the apparent kinetic parameters by measuring the [^{14}C]-succinate accumulation in the whole cell. The apparent K_m measured (25-40 μM, Table 3-1) for the DctA-dependent succinate transport is similar to the value measured by others in a previous study (20-30 μM) (Lo *et al.*, 1972), validating the transport assay in this study. The comparison of the values of the kinetic parameters for DctA and DauA reveal that DauA has a weaker affinity for succinate. Also, in the whole cell assay system the DauA maximal transport rate is lower than DctA (Table 3-1).

Furthermore, Janausch *et al.* (Janausch *et al.*, 2001) suggested that the missing acidic transporter is a secondary monocarboxylic acid carrier driven by proton motive force. The transport measured in their study had characteristic carrier properties since it was sensitive to uncouplers and was inhibited in the presence of monocarboxylates. It was shown that DauA matches this description and that the protonation state of succinate does not affect the transport ability of DauA in contrast to DctA which is able to transport only dicarboxylic succinate (Fig. 3-13) (Gutowski & Rosenberg, 1975; Karinou et al., 2013).

These competition assays suggested that DauA has different substrate specificity compare to DctA and that it is able to transport fumarate (Fig. 3-14). Although, it was able to measure significant reduction in [^{14}C]-fumarate uptake at pH 5 in the absence of DauA (Fig. 3-15) it was not possible to detect any growth defect when cells where grown under the same conditions with fumarate as the sole carbon source (Fig. 3-17). It has been shown that DctA is expressed both at pH 5 and at pH 7 (Fig. 3-17) and that fumarate remains mostly in its dicarboxylate form at these pHs (Fig. 3-16), indicating that DctA is potentially able to perform transport at both conditions. DcuSR two-component regulatory system responds to succinate and fumarate dicarboxylate (Kneuper *et al.*, 2005). Fumarate is 74% in di-carboxylic form at pH 5. This might explain why *dctA* is expressed in fumarate at pH 5 (Fig. 3-17) but not in succinate (Fig. 3-8), as it has been shown by western immunoblot analysis.

The competition assay results showed that DauA is also able to transport aspartate but no significant difference on growth was observed (Fig. 3-19). These results were expected since two additional aspartate transport systems have been characterised in *E. coli*. A high affinity aspartate transporter, *ast* system, which is weakly inhibited by glutamate, has been described (Kay & Kornberg, 1971). Furthermore, it has been shown that DctA is able to transport aspartate with low affinity for the substrate (Schellenberg & Furlong, 1977).

This is the first report of a SLC26A/SulP member acting on C_4-dicarboxylic acid uptake. However, six members of the SLC26A proteins expressed in humans have been shown to transport oxalate, a C_2-dicarboxylic acid (Mount & Romero, 2004). It is possible that these transporters share common features with the bacterial DauA-like

proteins paving the way to establish *E. coli* DauA as a paradigm for the ubiquitous SLC26A/SulP family of transporters.

It has been reported that in the absence of DauA the expression and/or activity of DctA is clearly reduced indicating that DauA not only acts as a transporter but plays a regulatory role in C_4-dicarboxylic acid metabolism (Fig. 3-4, 3-5, 3-8, 3-12 and 3-20). In *E. coli* C_4-dicarboxylic acid metabolism is controlled by extracellular substrates, via the DcuSR two-component system (Kneuper *et al.*, 2005; Scheu *et al.*, 2010), and by endogenous signals via the cytoplasmic regulatory system TtdR and DmlR that induced the genes for L-tartrate fermentation and D-malate degradation, respectively (Kim *et al.*, 2009; Lukas *et al.*, 2010; Oshima & Biville, 2006). With regard to this, we can speculate a role for DauA and specifically the cytoplasmic STAS domain in a potential sensing mechanism related to C_4-dicarboxylic acid metabolism. Currently the function of the STAS domain in bacterial SulP proteins is unknown. However, it has been shown that other proteins containing STAS domains can function as sensors, interaction/transduction modules and ligand-activated transcription factors (Sharma *et al.*, 2011a). Clearly further studies are required to clarify the role of DauA and its STAS domain in C_4-dicarboxylic acid metabolism.

Taken together the results of this part of the present study allow to propose a model of the DauA bifunctional role (Fig. 3-21):

- At pH 7 in the presence of succinate or fumarate under aerobic conditions, DauA is expressed but inactive as a transporter, DctA is the main uptake system. DauA is essential for optimal expression and activity of DctA; as observed from the reduced *dctA* expression, DctA production and succinate/fumarate DctA-dependent transport. Interestingly, it seems that the activity and regulatory

functions of DauA are not linked. It is not clear yet how and why DauA is inactive as a C_4-dicarboxilic acid transporter at pH 7 and whether it transports another substrate.

- At pH 5 in the presence of succinate under aerobic conditions, DauA is the main transporter. It has weaker affinity and lower apparent transport rate for succinate than DctA. DctA is not produced because the DcuS component of the DcuSR system seems to bind only di-carboxylates and at pH 5 succinate is mainly present as a mono-carboxylate (Cheung & Hendrickson, 2008; Kneuper *et al.*, 2005).

  At pH 5 in the presence of fumarate under aerobic conditions, both DauA and DctA are produced and active. DauA is able to transport both mono- and di-carboxylate fumarate while DctA only transports di-carboxylate fumarate. Under these conditions DauA has no apparent regulatory effect on DctA.

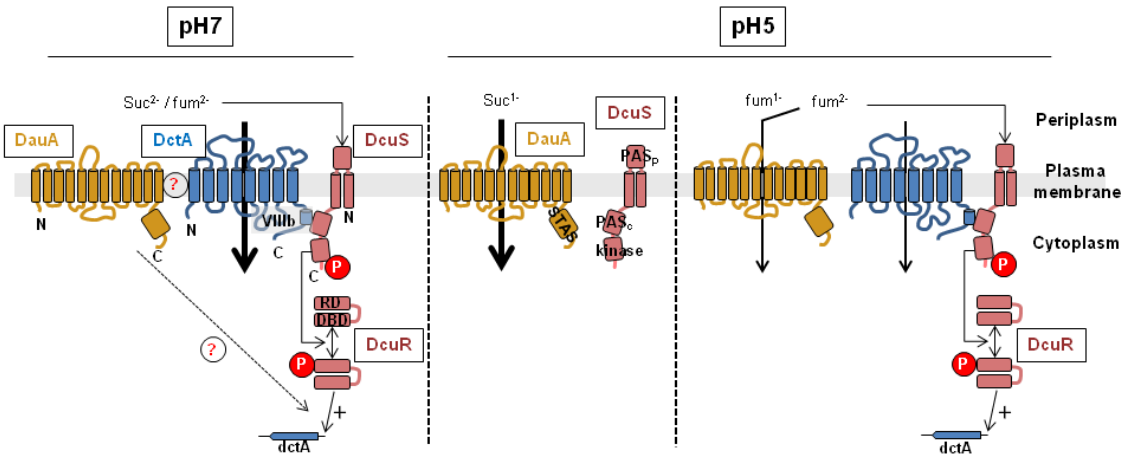

Figure 3-21: Working model for the physiological role of DauA.

DauA ensures the optimal absorption of C_4-dicarboxylic acids at various pHs either by impacting the transcription of *dctA* at pH 7 or by acting as a transporter at acidic pH. At pH 7, C_4-dicarboxylic acid (succinate or fumarate) is bound to DctA and DcuS, helix VIIIb of DctA interacts with the PASc domain of DcuS and, as a result, the transcription of *dctA* is activated via phosphorylation of the response regulator DcuR (Witan *et al.*, 2012). DauA is expressed and plays a role in the transcription of *dctA*. It seems that DauA is not active, or has only low level activity for substrate transport. At pH 5 in the presence of succinate, succinate mono-carboxylates cannot activate DcuSR and *dctA* is not transcribed. DauA is expressed and active. In the presence of fumarate both DauA and DctA are present and active. DauA transports mono- and di- carboxylate species of fumarate while Dcta is able to transport only di-carboxylate fumarate. For simplicity DauA and DcuS which are dimmers and DctA, a trimer, are represented as monomers. The topology of DauA has been predicted using Octopus (http://octopus.cbr.su.se/). DBD, DNA-binding domain; PASc, cytoplasmic Per-ARNT-Sim domain; PASp, periplasmic Per-ARNT-Sim domain; RD, receiver domain; STAS, Sulphate Transporter and Anti-Sigma antagonist domain.

4 Identification of proteins that may interact with DauA

4.1 Introduction

Most of the proteins inside the cell are organised in active complexes rather than as isolated units. Protein-protein interactions are vital for numerous cellular processes, from DNA replication to signal transduction and metabolism (Moraes & Reithmeier, 2012).

Secondary active transporters are able to interact with:

1. **Other transporters,** resulting in co-regulation mechanisms. Several mammalian members of the SLC26 family have been shown to interact with the CFTR chloride channel, mutually regulating their transport activities (Lamprecht *et al*., 2009).

2. **Enzymes** which metabolise the transported substrate. The interactions occurring between membrane transporters and enzymes has led to the concept of "membrane transport metabolons" (Moraes & Reithmeier, 2012). An example of membrane transport metabolon is the acid resistance GadBC system. *gadC* encodes for the glutamate/γ- aminobutyrate (GABA) antiporter and *gadB* for a glutamate decarboxylase which consumes a proton to convert glutamate to 4-aminobutanoate and CO_2. In *E. coli*, this system is involved in the cytoplasmic pH homeostasis (Castanie-Cornet *et al*., 1999; Foster, 2004).

3. **Proteins** involved in regulation of metabolism.

Interactions with **membrane-integrated sensors**. The two-component regulatory system DcuS/R is responsible for sensing and responding to C_4-

dicarboxylic acids. It has been shown that the histidine kinase DcuS requires accessory proteins for optimal function. Under aerobic conditions the secondary transporter DctA physically interacts with DcuS and acts as a co-sensor of C_4-dicarboxylic acids (Witan *et al*., 2012a).

i. Interactions with **transcription regulators**. AmtB is a high affinity ammonium transporter (Javelle *et al.*, 2007). *amtB* forms an operon with *glnK*, a gene encoding a small signal transduction protein. Under excess ammonium conditions, AmtB sequesters GlnK at the membrane preventing it from activating the transcription of genes involved in nitrogen assimilation (Javelle *et al.*, 2004).

ii. Interaction with **transcription factors**. The phosphoenolpyruvate–carbohydrate phosphotransferase system (PTS) is responsible for the transport and simultaneous phosphorylation of various sugars into the cell (Gorke & Stulke, 2008). Mlc is a global repressor of sugar degradation genes (Plumbridge, 1999). In the presence of glucose, the glucose-specific permease PstG sequesters Mlc to the membrane so it does not bind to the operator sequences of the respective genes (Lee *et al.*, 2000).

DauA, acts as a C_4-dicarboxylic acid transporter expressed both at acidic and neutral pH. Interestingly, in a *dauA* mutant grown in succinate at pH7, the main succinate transporter, DctA, shows reduced expression, production and activity (Fig. 3-17, 3-9 and 3-10). These results suggest interplay between DauA and DctA (Karinou *et al.*, 2013).

The aims of this chapter are to identify and characterise any physical interactions between DauA and DctA and/or DcuS. Firstly, the bacterial two-hybrid (BTH) system was used as a genetic approach. Secondly, attempts to validate any interactions were made by co-purification of the two proteins encoded from their native chromosomal locus. Thirdly, DctA and DauA localization was monitored by fluorescence microscopy and finally, further efforts were made to characterize any other potential proteins interacting with DauA by mass spectrometry analysis.

4.2 Results

4.2.1 Investigating the interaction of DauA with components of the C_4-dicarboxylic acid metabolism in vivo

4.2.1.1 A genetic approach: Bacterial two-hybrid (BTH) studies

As a first step towards identification of a potential interaction between DauA and DctA and/or DcuS, a BTH system was used. This technique relies on the functional reconstitution of adenylate cyclase (CyaA) from the separate T18 and T25 domains in an *E. coli cyaA*$^-$ reporter strain. Two putative interacting proteins are fused with complementary fragments of adenylate cyclase (T25 or T18). If the two proteins interact the T18 and T25 domains are brought together restoring the adenylate cyclase activity, resulting in the production of cAMP. The cAMP activates the expression of the reporter gene *lacZ* which encodes the enzyme β-galactosidase. Hence, the potential interaction between the two candidate proteins is detected by measuring the β-galactosidase activity. In the BTH system, the two candidate proteins to be tested for interaction can be N- or C-terminal fused with the T18 or T25 domain of CyaA (Karimova *et al.*, 1998).

Previous work in our group has shown that expression of DauA may be affected by fusions in its N-terminus. For that reasons it was decided to use the plasmids pUT18 and pKNT25 that result in C-terminal fusions of the T18 and T25 domain respectively. The DctA and DcuS constructs were kindly provided by Prof. Gottfried Unden (University of Mainz, Germany). In this assay as positive control the pair DctA-DcuS was used, which have been recently shown to interact with each other (Witan *et al.*, 2012a). The background activity (negative control) was determined by non-interacting pairs (Fig. 4-1B).

Figure 4-1A shows the β-galactosidase activity measured when various T25 and T18 fusion proteins were co-expressed in the reporter *cyaA*$^-$ strain. Interestingly, the activity measured for the pairs DauA-T18/DctA-T25 (1202 Miller units) and DcuS-T18/DauA-T25 (960 Miller units) were 5 and 4 times higher respectively than the positive control DcuS-T18/DctA-T25 (252 Miller units), and more than 8 times higher than the background activity (below 150 Miller units). The reversed pairs DauA-T18/DcuS-T25 (408 Miller units) and DctA-T18/DauA-T25 (412 Miller units) also showed high β-galactosidase activity, suggesting DauA does indeed interact with both DctA and DcuS. One concern when expressing membrane proteins from the high copy plasmid pUT18 is that they might saturate the cell membrane resulting in non-specific interactions. To verify that interactions between DauA and DctA and/or DcuS are specific, the interaction between DauA and another membrane protein, AmtB, were tested. AmtB is an ammonium transporter which is not known to interact with any components of the C_4-dicarboxylic acid metabolism. The β-galactosidase activity measured when DauA and AmtB were co-expressed in the reporter strain *cyaA*$^-$ was below the background level (150 Miller units), suggesting the observed DauA interactions with DctA and DcuS are indeed specific. The above results suggest that DauA may physically interact with both DctA and DcuS. The BTH reporter strain *cyaA*$^-$ expresses chromosomally encoded DctA and DcuS. It is possible that the chromosomally encoded proteins interact with the plasmid encoded ones. This means that *i.e.* the interaction with DctA brings DauA in close proximity with DcuS and thus gives positive result in the BTH study.

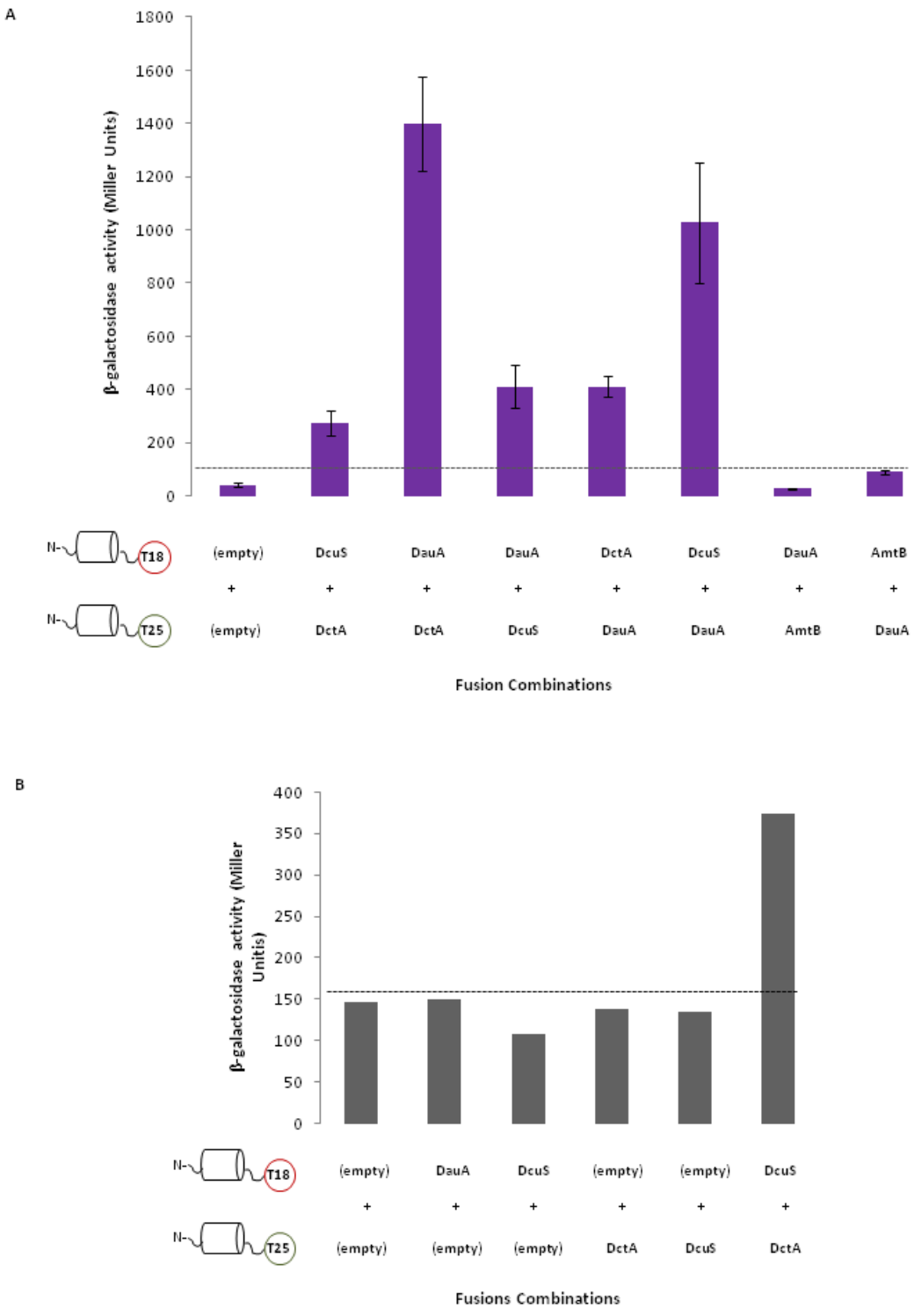

Figure 4-1: Interaction of DauA with components of C_4-dicarboxylic acid metabolism using the bacterial two-hybrid system.
(A) β-galactosidase activity assay was used to quantify the BTH results. BTH101 (*cyaA*$^-$ reporter strain) cells co-transformed with the respective plasmid pairs. The activity was determined after growth in LB supplemented with the appropriate antibiotics. The activity measured for the pair DctA-T25/DcuS-18 was used as a positive control. All the results are the average of at least five independent biological repeats. Error bars represent standard error of the mean. (B) The background activity was measured by non-interacting pairs and was determined as being below 150 Miller units. The data presented are representative of one experiment. The horizontal dotted line denotes the background activity.

4.2.1.2 A biochemical approach: co-purification

The bacterial two-hybrid studies indicate a specific interaction between DauA and DctA. Next, it was sought to confirm this interaction with an alternative biochemical method. For that purpose the strain EK182, harbouring a chromosomally encoded His-tagged version of DauA and a chromosomally encoded FLAG-tagged version of DctA, was used. The cells were grown overnight in LB supplemented with succinate as an inducer for DctA expression and DauA was purified by immobilized metal ion affinity chromatography (IMAC). The elution fractions were further purified by FLAG affinity chromatography. The presence of DauA and/or DctA in the fractions was monitored by western immunoblotting using anti-His or anti-FLAG antibodies. The hypothesis was that if the two proteins interact, after the initial IMAC purification both proteins will be able to be detected in the fractions. Furthermore, if the elution fractions were re-purified using an anti-FLAG matrix it should be still able to detect both DauA and DctA (Fig. 4-2A).

After the initial IMAC purification DauA was detected in the elution fractions (Fig. 4-2B; top left panel). The membrane was subsequently stripped and blotted using anti-FLAG antibody, revealing the presence of DctA (Fig. 4-2B; lower left panel). Next, these elution fractions were purified using an anti-FLAG matrix. The western blot analysis of separate membranes for each antibody showed that DauA (Fig. 4-2B; top right panel) and DctA (Fig. 4-2B; lower right panel) were present in the samples. At this point it has to be noted that the results presented above are from one experiment and further investigation is needed to firmly confirm the interaction between DauA and DctA. An intriguing question concerns the apparent molecular mass shift for both proteins after the second purification. This protein aggregation can be explained by the chosen elution method. For this experiment, proteins were eluded from the FLAG

matrix using an extremely acidic buffer potentially causing the molecular mass shift. Finally, I was not able to detect DcuS on the same elution fraction using specific anti-DcuS antibodies, provided from Prof. Gottfried Unden (University of Mainz, Germany). It is expected that more proteins will be co-purified with DauA as it was indicated by SDS-PAGE analysis (data not shown).

The results of the above experiment reinforced the hypothesis that DauA and DctA form a complex.

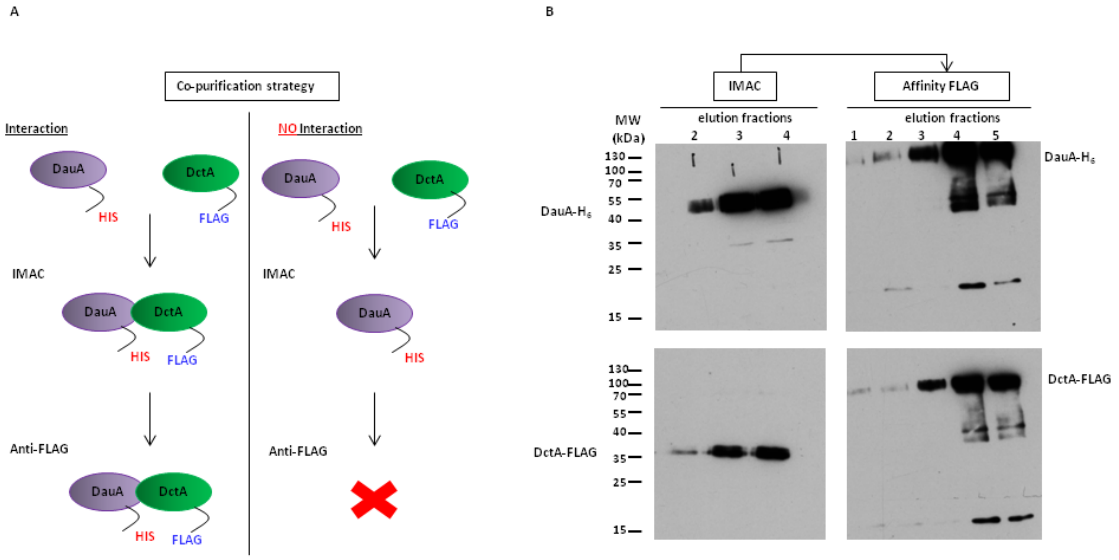

Figure 4-2: DauA and DctA form a complex.
(A) Schematic representation of the purification strategy used to confirm DauA-DctA interactions. (B) Chromosomally encoded C-terminally His-tagged DauA was purified by IMAC. Elution fractions were analyzed by western immunoblotting using an anti-His antibody (top panel) and anti-FLAG antibody. The IMAC elution fractions were re-purified by FLAG affinity chromatography and analysed by western immumoblotting.

4.2.1.3 Co-localization studies using fluorescence microscopy

In addition to the BTH and the co-purification studies, the localization of DauA was investigated using fluorescence microscopy. For that purpose we collaborated with Philipp Steinmetz and Prof. Gottfried Unden (University of Mainz, Germany).

To monitor the localization of DauA, the double mutant strain Δ*dctA*/Δ*dauA* (EK96) was transformed with the plasmids pMW2031 (pBAD30: H_6-*yfp (A206K)-dauA*), pMW526 (pBAD30: H_6-*yfp-dctA*) or co-transformed with pMW2031 and pMW1194 (pBAD18: H_6-*dctA*-H_6). The single mutant Δ*dcuS* (IMW480: MG1655, but *dcuS*::cam^R) was also transformed with plasmid pMW2031. The cells were grown aerobically overnight in LB and then diluted 1/50 and further grown to the exponential phase. Next, the cells were induced with 333 µM L-arabinose for an hour. 5 µl of the culture was washed and resuspended in 1x PBS buffer and fixed on a microscope slide that was freshly coated with a thin layer of 1% agarose and covered with a cover slip.

DauA-YFP expressed alone (Fig. 4-3A) localises at the poles of the cells and this polar localization seems not to be massively affected by the absence of DcuS (Fig. 4-3C). When DctA-YFP was expressed alone it presented a homogenous diffused localization (Fig. 4-3B). Interestingly, when both DauA-YFP and DctA were co-expressed, DauA was distributed homogenously in the membrane (Fig. 4-3D).

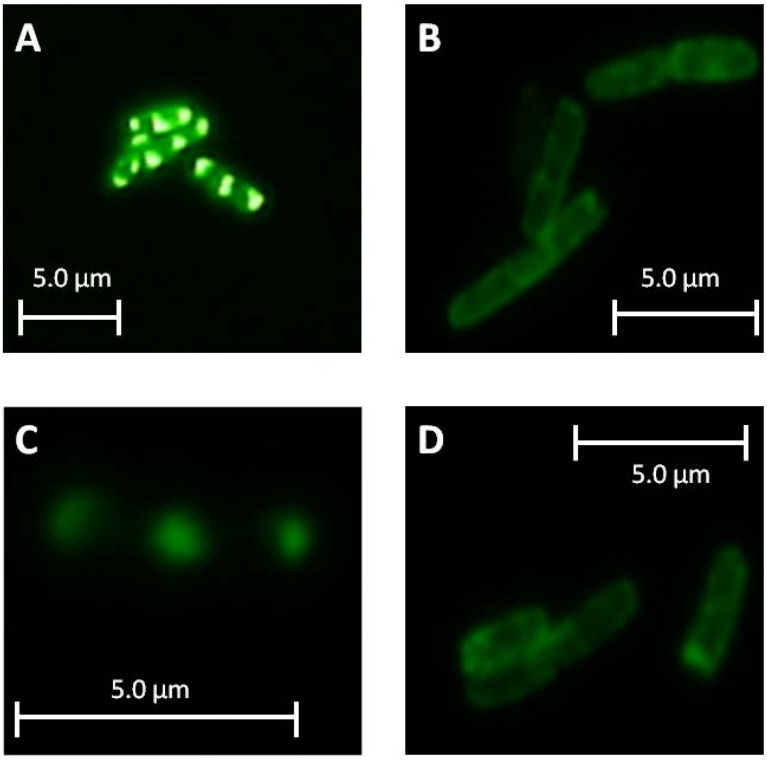

Figure 4-3: Localisation of DauA-YFP.
In vivo fluorescence microscopy of (A) Δ*dctA*/Δ*dauA* cells expressing DauA-YFP, (B) Δ*dctA*/Δ*dauA* cells expressing DctA-YFP, (C) Δ*dcuS* cells expressing DauA-YFP and (D) Δ*dctA*/Δ*dauA* cells co-expressing DauA-YFP and DctA. A Keyence Biozero BZ-8000 microscope was used. (Experiment performed by Philipp Steinmetz)

First of all, it has to be noted that despite the fact that the proteins are expressed from a high copy plasmid that potentially affects the native localization of the proteins, these experiments were performed to test the DauA-DctA interaction and not to study their native cell localization. The loss of DauA polar localization can be interpreted by its interaction with diffused localized DctA. This might suggest that DauA and DctA interact physically. However, an alternative explanation could be that over-expression of DctA disturbs some interaction required for polar localization of over-expressed DauA.

4.2.2 Screening for additional interacting partners by mass spectrometry

The BTH combined with the biochemical analysis and microscopy observations strongly indicated that DauA interacts with DctA. To reinforce this hypothesis and identify more proteins that might interact with DauA, a less biased approach was adopted. The strategy was to identify proteins that co-elute with DauA when DauA was purified expressed at the native level from the chromosome. For that purpose BW25113 and EK182 (DauA-H_6, DctA-FLAG) cells were used. The cells were grown overnight in LB supplemented with succinate as an inducer of DctA at pH 7, and DauA was purified initially by IMAC. The elution fractions of two biological replicates were analysed by nano-liquid chromatography on-line coupled to mass spectrometry (nLC-MS/MS). Proteins identified in the non-tagged strain grown under the same conditions were considered non-specific interactions with the Co^{2+}-affinity column and they were subtracted from the list. Proteins that were present in both biological replicates but not in the control sample (non-tagged strain), were considered as potential DauA interacting partners.

Table 4-1 lists the proteins which potentially interact with DauA. Firstly, DctA was identified further supporting the hypothesis that DauA interacts with DctA and hence validating our method. The low sequence coverage and small number of unique peptide detected for DctA and DauA might be due to the difficulty in analysing integral membrane proteins by nLC-MS/MS. Consistent with this analysis is the fact that for the other integral membrane proteins identified a maximum of 6 unique peptides covering less than 30% of the sequences were detected. Interestingly, two proteins, GadB a dicarboxylic acid transporter and GadX a transcriptional regulator, belonging to the glutamic acid-dependent (GDAR) acid resistance system were identified.

Table 4- 1: Potential DauA interacting partners identified by nLS-MS-MS

GI number	Gene name	Description	Unique peptides detected		Sequence covered %		Subcellular localization
			Assay 1	Assay 2	Assay 1	Assay 2	
90111235	*dauA*	C4-dicarboxylic acid transporter DauA	12	5	19	7	Cell inner membrane
16131144	*accC*	Biotin carboxylase (EC 6.3.4.14) (Acetyl-CoA carboxylase subunit A) (ACC) (EC 6.4.1.2)	12	2	35	6	Cytoplasm
16128722	*aroG*	Phospho-2-dehydro-3-deoxyheptonate aldolase, Phe-sensitive (EC 2.5.1.54)	6	1	26	5	Cytoplasm
16131604	*atpF*	ATP synthase subunit b (ATP synthase F(0) sector subunit b) (ATPase subunit I) (F-type ATPase subunit b) (F-ATPase subunit b)	3	2	23	16	Cell inner membrane
16129210	*cls*	Cardiolipin synthase (CL synthase) (EC 2.7.8.-)	6	2	15	5	Cell inner membrane
90111650	*dapF*	Diaminopimelate epimerase (DAP epimerase) (EC	4	1	22	5	Cytoplasm

		5.1.1.7)					
16129452	*gadB*	Glutamate decarboxylase beta (GAD-beta) (EC 4.1.1.15)	28	14	40	28	Cytoplasm (neutral pH), membrane(acid pH)
16131400	*dctA*	Aerobic C4-dicarboxylate transport protein	1	2	2	3	Cell inner membrane
16132200	*deoB*	Phosphopentomutase (EC 5.4.2.7)	2	2	2	5	Cytoplasm
16130275	*fadI*	3-ketoacyl-CoA thiolase (EC 2.3.1.16) (ACSs) (Acetyl-CoA acyltransferase)	1			4	Cytoplasm
16131388	*gadX*	HTH-type transcriptional regulator GadX	6	2	31	5	Cytoplasm
16129095	*hflD*	High frequency lysogenization protein HflD	5	1	27	7	Cell inner membrane
16129170	*prs*	Ribose-phosphate pyrophosphokinase (RPPK) (EC 2.7.6.1)	11	1	40	4	Cytoplasm
16131091	*lptB*	Lipopolysaccharide export system ATP-binding protein LptB (EC 3.6.3.-)	5	1	32	8	Cell inner mebrane
16131944	*melR*	Melibiose operon regulatory protein	4	2	13	8	Cytoplasm
16131352	*nikE*	Nickel import ATP-binding protein NikE	3	1	14	5	Peripheral membrane

		(EC 3.6.3.24)					protein
16129083	*cobB*	NAD-dependent protein deacylase (EC 3.5.1.-)	6	3	31	17	Cytoplasm
16131919	*phnO*	Protein PhnO (EC 2.3.1.-)	3	3	22	16	ND*
16130105	*fruA*	PTS system fructose-specific EIIBC component (EIIBC-Fru) [Includes: Fructose-specific phosphotransferase enzyme IIB component (EC 2.7.1.69)	1	1	3	2	Cell inner membrane
16131495	*rfaZ*	Lipopolysaccharide core biosynthesis protein RfaZ	3	1	15	3	ND*
16129049	*rluC*	Ribosomal large subunit pseudouridine synthase C (EC 5.4.99.24)	1	3	3	9	Cytoplasm
16130734	*rppH*	RNA pyrophosphohydrolase (EC 3.6.1.-) ((Di)nucleoside polyphosphate hydrolase) (Ap5A pyrophosphatase)	4	1	38	5	cytoplasm
16131190	*rpsQ*	30S ribosomal protein S17	1	1	7	9	Cytoplasm
16131825	*rsd*	Regulator of sigma D	2	3	13	17	Cytoplasm

16130501	*srmB*	ATP-dependent RNA helicase SrmB (EC 3.6.4.13)	1	1	3	4	Cytoplasm
90111354	*uvrC*	UvrABC system protein C	8	1	19	2	Cytoplasm
16128214	*yafM*	Uncharacterized protein YafM	1	1	11	11	ND*
16128754	*ybhL*	Inner membrane protein YbhL	1	1	3	3	Cell inner membrane
16128884	*ycaR*	UPF0434 protein YcaR	2	1	35	15	ND*
16131833	*zraS*	Sensor protein ZraS (EC 2.7.13.3)	2	1	6	3	Cell inner membrane

*: Not Determined

4.2.3 Identifying domains of DauA required for interaction with DctA

So far, four different lines of evidence (Fig. 4-1, Fig. 4-2, Fig. 4-3 and Table 4-1) suggest that DauA interacts with DctA. Next, we wanted to identify the domains that participate in the interaction. For eukaryotic homologues, it appears that the STAS domain is important for the interactions with other proteins (Sharma *et al*., 2011a).

For that reason the potential involvement of DauA STAS domain in the interaction was tested. In order to do that, the BTH approach was used. Constructs expressing DauA lacking the STAS domain ($DauA_{1-444}$) were generated and constructs expressing only the STAS domain fused to the T18 or the T25 domain of the adenylate cyclase. Furthermore, it has been shown that the helix 8b of DctA is necessary for the interaction with DcuS (Witan *et al*., 2012a) and it was sought to test if this is the case for the interaction between DauA and DctA. The plasmid pMW1647 which harbours the TM8

of DctA fused at the N-terminus with MalE, and on the C-terminus of helix 8b to T25 was used (Fig. 4-4). MalE is involved in maltose uptake and only active in the periplasm. When this construct was expressed, it was able to confer growth on maltose to a MalE mutant, meaning that MalE of the fusion has periplasmic location (Witan *et al*., 2012a).

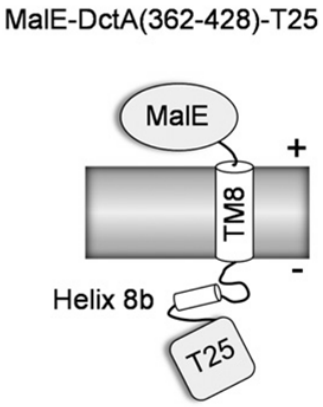

Figure 4-4: Topology of the MalE-DctA(362-428)-T25 fusion protein.
Topology of MalE -DctA Helix 8b fusion relative to the cytoplasmic membrane (Witan *et al*., 2012a).

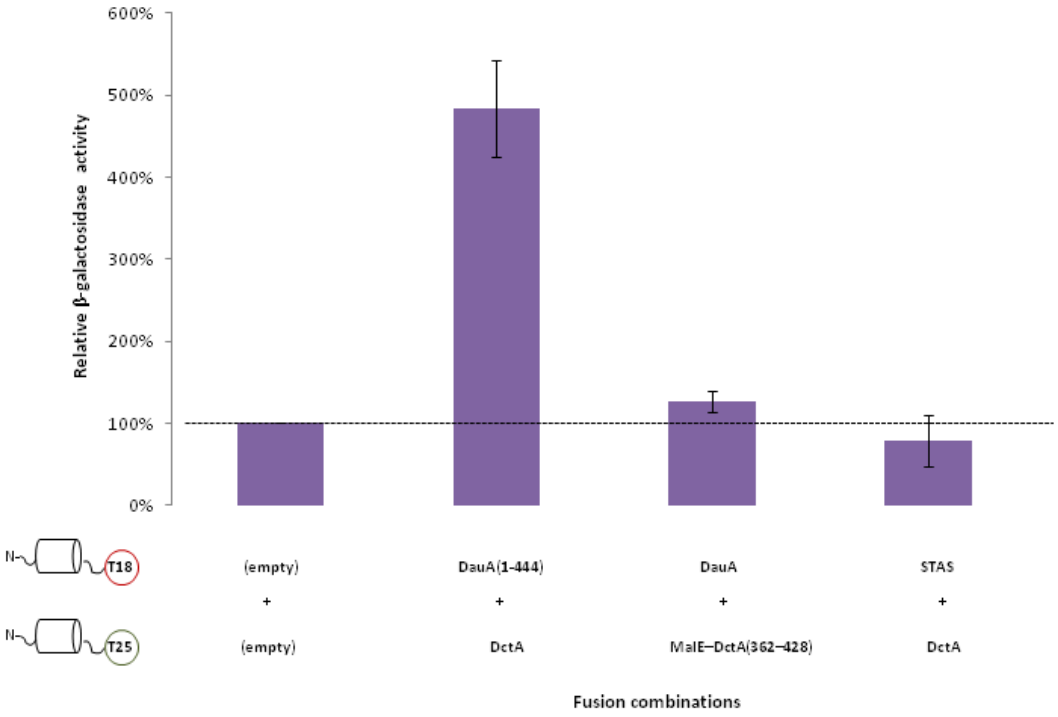

Figure 4-5: DauA sites required for interaction with DctA.
β-galactosidase activity was used to quantify the interactions. BTH101 cells co-transformed with the respective plasmid pairs. The activity was determined after growth in LB supplemented with the appropriate antibiotics. The activity measured from strain co-transformed with the two empty plasmids was used as a negative control (dotted line). Activities are presented as percentage relative to the negative control. All results are the average of at least three independent biological repeats. Error bars represent the standard deviation.

The β-galactosidase activity indicated a clear interaction of DauA $_{(1\text{-}444)}$ with DctA. Furthermore, no interaction was detected between DauA and the helix 8b of DctA. Finally, the isolated STAS domain does not seem to interact with DctA (Fig. 4-5).

These results suggest that DauA and DctA interact primarily via their transmembrane domain. The STAS domain of DauA may represent a potential secondary point of interaction with another protein.

4.3 Discussion

DauA is a succinate transporter active at acidic pH. At pH 7, in the absence of DauA, the expression and/or activity of DctA, the main succinate transporter, is clearly reduced indicating that DauA not only acts as a transporter but also plays a regulatory role in C_4-dicarboxylic acid metabolism (Karinou *et al*., 2013). In this chapter it was sought to explore this hypothesis further by characterising any potential interactions between DauA and components of the C_4-dicarboxylic acid metabolism using a combination of genetic and biochemical methods.

The bacterial two-hybrid system has been widely used for protein-protein interactions studies. The ability to screen libraries of potential interacting candidates and the ease of identifying protein domains that interact have made this method a standard approach for the identification of protein pairs (Phizicky & Fields, 1995).

The results of the bacterial two-hybrid analysis between DauA and DctA indicated a specific interaction between the two proteins (Fig. 4-1) and it was further confirmed by co-purification (Fig. 4-2, Table 4-1). The interaction between DauA and DctA seems to be mediated via the transmembrane domains of the two proteins (Fig. 4-5). These observations suggest an interesting dual role for DauA in succinate metabolism with transport and regulatory functions. Furthermore, localization studies might suggest a polar localization for DauA when it is over-expressed alone whereas co-expression of DauA and DctA led to a relatively uniform distribution across the membrane that might be following the normal DctA localization (Fig. 4-3). However, these studies should be interpreted with caution as they do not prove any interaction and the localization might be an artefact of the protein over-expression.

Numerous membrane transporters have already been described as bifunctional proteins with a carrier function and a role in metabolic regulation.

In *E. coli*, DctA and another C_4-dicarboxylic acid transporter, DcuB, form complexes with the sensor kinase DcuS under aerobic and anaerobic conditions respectively. In these functional sensor units, DctA and DcuB act as co-sensors by directly modulating the activity of DcuS (Davies *et al.*, 1999; Kleefeld *et al.*, 2009; Witan *et al.*, 2012a). Having the above in mind, it is quite tempting to speculate that DauA might play similar roles. It was shown that under the conditions used in this study DctA expression is dependent on the DcuS/R two component regulatory system (Fig. 5-10). Therefore, it is possible that DauA modifies the expression of *dctA* via DcuS/R. To answer these questions it will be necessary to identify the hierarchy of the DauA-DctA-DcuS complex, i.e. if DauA interacts with both DctA and DcuS or the interaction with DctA brings DauA in close proximity with DcuS and vice versa. In order to do so, BTH analysis should be used with reporter strains in which DauA, DctA and DcuS have been deleted. This way the interactions between the proteins expressed from the plasmids can be assessed without the intervention of the chromosomally expressed homologues.

The regulatory function of transporters can also be mediated via their interaction with transcriptional factors. In *E. coli*, such activity has been described for LysP, a lysine-specific permease involved in pH homeostasis. LysP interacts with the transcriptional activator CadC. In the presence of lysine, CadC is released into the cytoplasm and activates the transcription of the *cadBA* operon (Tetsch *et al.*, 2008). Interestingly, the co-purification/mass spectrometry analysis showed that DauA interacts with at least four cytoplasmic regulators: GadX, MelR, Rsd and HflD (Table 4-1). GadX is a HTH-

type dual transcriptional regulator (Shin *et al.*, 2001). GadX has been identified primarily as one of the regulators of the glutamate-induced acid resistance (GDAR) system in *E.coli* (Tramonti *et al.*, 2002). The production of GadX is induced by a variety of stimuli (pH, growth phase, medium composition, oxygen levels and salt stress) and regulates the transcription of a broad range of genes, not necessarily linked to acid resistance (De Biase *et al.*, 1999; Hommais *et al.*, 2004; Lei *et al.*, 2011; Nishino *et al.*, 2008; Shin *et al.*, 2001). GadX is encoded in a region called the acid fitness island (AFI) (Hommais *et al.*, 2004), which also contains the most important genes involved in the acid resistance response in *E. coli* (Tucker *et al.*, 2002). These genes are organised in operons: *slp-yhiF*, *hdeAB-yhiD*, *gadE-mtdEF*, *gadXW* and *gadAX*. Tramonti *et al.* (Tramonti *et al.*, 2008) have showed in a recent study that GadX binds in the promoter region of *slp-yhiF*, *hdeAB* and *gadE-mtdEF* and suggest that it acts as counter-silencer. Hence, the interaction between DauA and GadX is of particular interest:

Firstly, it has been suggested that YhiF, a LuxR-type transcriptional regulator, is involved in a DcuS/R-independent expression of DctA, acting as a negative regulator (Boogerd *et al.*, 1998). YhiF is encoded within the AFI and under the direct transcriptional regulation of GadX. It is tempting to speculate that any DauA effects on DctA expression are due to a regulatory circuit involving GadX and YhiF.

Secondly, the identification by mass spectrometry of two proteins involved in the glutamate-dependent acid resistance system, GadX and GadB, links DauA and succinate metabolism to acid resistance. It has been reported previously that carboxylic acids provide a protective benefit on *E. coli* survival in acidic environments by inducing two amino acid-dependent acid resistance systems (Guilfoyle & Hirshfield, 1996). Recently, it has been shown that the dicarboxylic acid oxalate is able to induce moderate acid tolerance response via the GadE response regulator (Fontenot *et al.*,

2013). Based on the above, we can hypothesise that DauA might be involved in a succinate inducible acid stress tolerance system.

Another interesting potential DauA protein partner identified by the mass spectrometry analysis is the protein Rsd (Regulator of sigma D). This protein is an anti-sigma factor for the primary sigma factor RpoD that negatively regulates RpoD-mediated transcription induction for the transition to the stationary growth phase. It has been suggested that under stress conditions Rsd binds to RpoD promoting alternative sigma factors to take over transcription (Jishage & Ishihama, 1998; Jishage & Ishihama, 1999). Given the similarities between the SLC26A STAS domain and the anti-sigma-factor antagonist SpoIIAA in *B.subtilis* (Aravind & Koonin, 2000), we can speculate that DauA STAS might act as an antagonist for the anti-sigma-factor Rsd. We can hypothesis that under normal conditions DauA STAS sequesters Rsd to the membrane and thus preventing its interaction with RpoD. Under stressed conditions sensed by DauA, Rsd is released which in turn binds to RpoD and the transcription is switched to alternative sigma subunits.

We can suggest a working model for the DauA/DctA sensor complex and function in the presence of succinate under aerobic conditions:

- At pH 7, DctA is the main uptake system. DauA interacts with the transcriptional regulator GadX. The DauA-GadX interaction prevents the induction of the negative regulator YhiF, which inhibits *dctA* transcription. The physiological meaning of the DauA-DctA interaction is not clear yet. We can hypothesise that DauA is necessary for optimal activity of the DctA/DcuS sensor unit or that DauA responds to a yet unknown stimulus and transmits the signal to the sensor kinase DcuS.

- At pH 5, DauA releases GadX which induces YhiF and thus inhibits *dctA* transcription. Now DauA is active and the only succinate transporter.

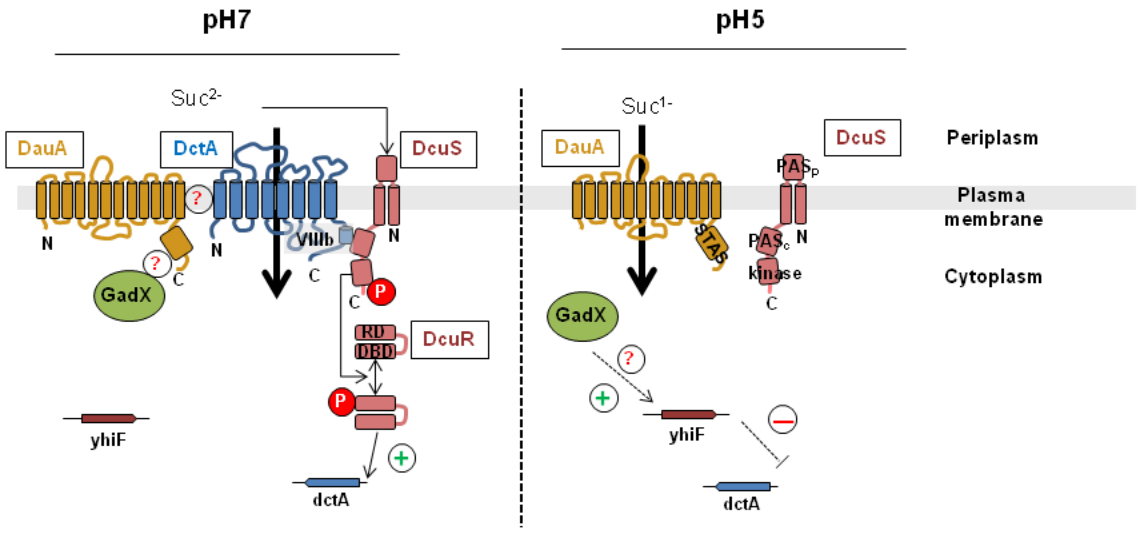

Figure 4- 6: Hypothetical model of the DauA/DctA complex function.
At pH7, DauA interacts with DctA via their transmembrane domains. GadX is sequestered at the membrane hence dctA transcription is not inhibited by YhiF. At pH 5, DauA senses the acidic pH and releases GadX in the cytoplasm which in turn activates YhiF. YhiF inhibits the expression of *dctA*.

5 Investigating the expression of DauA

5.1 Introduction

Studies on the SLC26 transporters have mainly focused in their physiological function and mechanistic aspects of the transport. The eukaryotic homologues of this family have been better characterized and a variety of regulatory mechanisms has been described, such as on the translational, protein trafficking and post-translational level. The C-terminal STAS domain has been shown to play an important role in gene expression and regulation but the regulatory interaction identified are still unclear (Alper & Sharma, 2013; Dorwart *et al*., 2008b; Sharma *et al*., 2011a).

It has been shown that DauA, the *E.coli* SLC26 homologue, is a succinate transporter active at acidic pH with regulatory function in C_4-dicarboxylate metabolism (Karinou et al., 2013). Some of the transporters belonging in the C_4-dicarboxylate metabolism are highly regulated by the oxygen levels of the cell and their expression is induced by the presence of C_4-dicarboxylic acids via the DcuS/R two-component regulatory system (Janausch *et al*., 2002).

In this chapter, it was sought to characterise *dauA* expression. At first, genes co-transcribed with *dauA* in an operon were investigated and an attempt was made to identify potential promoters and regulators. Next, *dauA* specific promoters were identified and using transcriptional fusions the conditions affecting the expression of *dauA* were investigated. Finally, it was investigated whether *dauA* expression is affected by the same conditions regulating genes of the C_4-dicarboxylate metabolism.

5.2 Results

5.2.1 Identification of genes co-transcribed with dauA

5.2.1.1 The *prs-dauA* operon

The *dauA* gene lies only 125 bp downstream of *prs*, a gene that encodes the phosphoribosylpyrophosphate (P-Rib-PP) synthetase (Fig. 5-1). P-Rib-PP synthetase catalyses the synthesis of phosphoribosylpyrophosphate, a precursor in pyrimidine nucleotides, purine nucleotides, histidine and tryptophan synthesis (Post *et al.*, 1993). The genetic proximity of *dauA* and *prs* is concerved in Enterobacteriaceae, as identified using the computational software STRING 8 (data not shown) (Jensen *et al.*, 2009). Based on the chromosomal location of *dauA* we hypothesized that *dauA* forms an operon with *prs*.

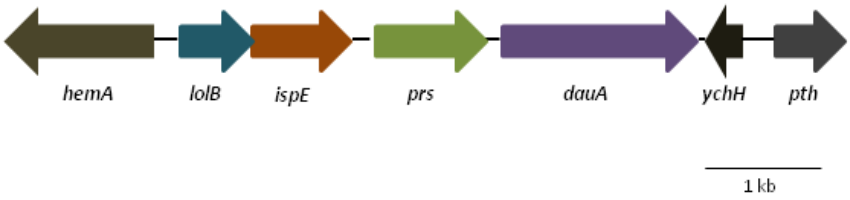

Figure 5-1: Schematic representation of the *dauA* locus.
The organisation of the genes on the chromosomes is depicted on scale. *hemA*, Glutamyl-tRNA reductase; *lolB*, Outer-membrane lipoprotein; *ispE*, 4-diphosphocytidyl-2-C-methyl-D-erythritol kinase; *prs*, ribose-phosphate diphosphokinase; *dauA*, dicarboxylic acid transporter; *ychH*, stress induced protein; *pth*, peptidyl-tRNA hydrolase.

In order to test our hypothesis we analysed cDNA synthesised from RNA extracted from both wild type and *ΔdauA* cells by RT-PCR. cDNA was synthesised using random hexamers. Primer pairs (a: EKO70/EKO71, b: EKO72/EKO73, c: EKO74/EKO75) were designed to amplify specific fragments inside *dauA*, *prs* and the intergenic region

between these two genes. As a negative control, the sample was subjected to the same treatment without the addition of reverse transcriptase to confirm the absence of genomic DNA contamination.

The amplification of the intergenic region indicates a single mRNA transcript for both genes, suggesting that *dauA* and *prs* form an operon (Fig. 5-2). Further studies are required to elucidate the physiological role of the *prs-dauA* operon.

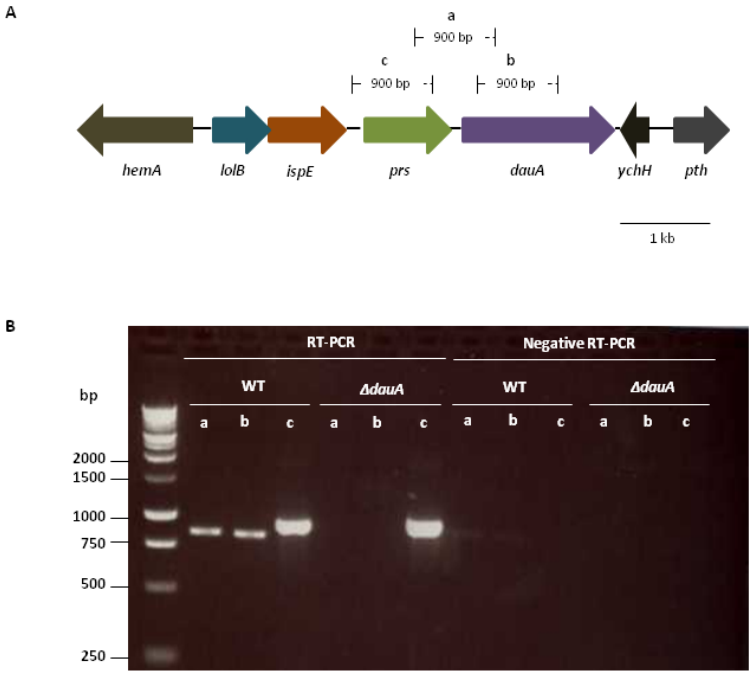

Figure 5-2: Identifying a *prs-dauA* operon by RT-PCR analysis.
RT- PCR analysis confirmed the existence of a *dauA*- *prs* operon. (A) Schematic map of the *dauA* region and the primers used for the RT-PCR analysis: (a) for the intergenic region between *dauA* and *prs*, (b) for *dauA* and for (c) *prs*. All the primers were designed to amplify equal fragments of 900 bp. (B) RNA extracts from wild type and mutant cells were analysed by RT- PCR. Negative RT-PCR (RT-PCR without the addition of reverse transcriptase) was also performed to confirm the absence of genomic DNA contamination in the samples. The organisation of the genes on the chromosomes is depicted on scale. *hemA*, Glutamyl-tRNA reductase; *lolB*, Outer-membrane lipoprotein; *ispE*, 4-diphosphocytidyl-2-C-methyl-D-erythritol kinase; *prs*, ribose-phosphate diphosphokinase; *dauA*, dicarboxylic acid transporter; *ychH*, stress induced protein; *pth*, peptidyl-tRNA hydrolase.

5.2.1.2 Identifying potential promoters for the *prs-dauA* operon

It has been shown that the *prs* gene is transcribed from 2 promoters, $prsp^1$ and $prsp^2$ (Fig. 5-3A), with $prsp^2$ being the primary promoter, under the regulation of the purine repressor PurR (Post *et al.*, 1993). RT-PCR analysis was performed to identify whether $prsp^1$ or $prsp^2$ controls the expression of the *prs-dauA* operon (Fig. 5-3).

RNA was extracted from wild type (BW28113) cells and cDNA generated by random hexamer was used as template for specific primers amplifying fragments before $prsp^1$ (EKO92/EKO95), before $prsp^2$ (EKO92/EKO95) and after $prsp^2$ (EKO94/EKO95). Sample subjected to the same treatment without the addition of reverse transcriptase was used as a negative control to confirm the absence of genomic DNA contamination. Genomic DNA was used as a PCR template to ensure that the fragments amplified from cDNA correspond to the correct size.

A single mRNA transcript was detected by RT-PCR when a primer amplifying downstream $prsp^2$ was used (Fig. 5-3). This indicates that the *prs-dauA* operon may be under the control of the $prsp^2$ promoter. However, it should be noted that the absence of detectable mRNA transcript from $prsp^1$ might potentially be due to the lack of sufficient template length. Further analyses are needed to confirm this hypothesis and it cannot be ruled out that another promoter, in between $prsp^1$ and $prsp^2$, regulates the transcription of the *prs-dauA* operon.

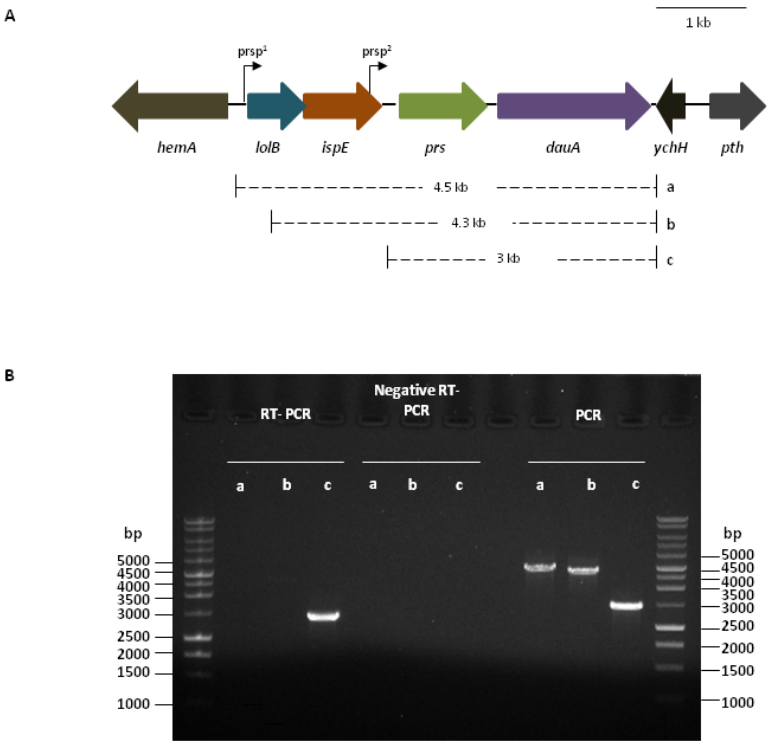

Figure 5-3: Identifying potential promoters for the *prs-dauA* operon.
RT-PCR analysis confirmed prsp^2 as a possible promoter for the *prs-dauA* operon. (A) Schematic map of the *dauA* region, promoter sites prsp^1 and prsp^2 and the primers used for the RT-PCR analysis, (a) upstream of prsp^1, (b) downstream of prsp^1, and (c) downstream of prsp^2. (B) RNA extract from wild type strain was tested using the corresponding primers. Negative RT-PCR (RT-PCR without the addition of reverse transcriptase) was also performed to confirm the absence of genomic DNA. Additionally, PCR screening was performed using the same primers on genomic DNA from wild type cells. The organisation of the genes on the chromosomes is depicted on scale. *hemA*, Glutamyl-tRNA reductase; *lolB*, Outer-membrane lipoprotein; *ispE*, 4-diphosphocytidyl-2-C-methyl-D-erythritol kinase; *prs*, ribose-phosphate diphosphokinase; *dauA*, dicarboxylic acid transporter; *ychH*, stress induced protein; *pth*, peptidyl-tRNA hydrolase.

5.2.1.3 Identifying potential regulators for the *prs-dauA* operons

In order to identify potential regulators for the *prs-dauA* operon, studies were initially focused on the repressor PurR. PurR is the primary regulatory protein that coordinates expression of the genes involved in the biosynthesis of purine nucleotides with the availability of purines. It has been shown that the repressor PurR binds a Pur Box upstream the -35 region of prsp[2]. Moreover, *prs-lacZ* translational fusion is increased two to three-fold in a *purR* mutant (He *et al.*, 1993). The RT-PCR analysis in a *purR* mutant did not indicate any regulation of the *prs-dauA* operon by PurR (data not shown). However, RT-PCR analysis is not the method of choice to detect a two to three-fold variation of the mRNA quantity as indicated by the *prs-lacZ* translational fusion.

Prs activity and stability requires inorganic phosphate (Hove-Jensen *et al.*, 1986). The Pho regulon is a global regulator of phosphate metabolism in *E. coli*. It is controlled by the two-component regulatory system PhoB/R which responds to variations of phosphate concentration. Phosphate independent controls of PhoB have also been observed, related to the carbon and energy sources (Fig. 5-4) (Lamarche *et al.*, 2008). We wanted to test whether the *prs-dauA* operon is under the control of the Pho regulon and whether this control is dependent on the phosphate availability. For that purpose WT, *ΔphoB* and *ΔphoR* cells were grown aerobically in LB medium overnight at 37^{o}C. The next day, the cells were washed twice and grown in a phosphate-free buffer (MOPS phosphate free) at 37^{o}C for 5 hours until they reached an OD_{600} of 0.5, RNA from each strain was then extracted and analysed by RT- PCR.

Each strain was tested by RT-PCR for expression of the *prs-dauA* operon and of *phoA*, the gene which encodes for the alkaline phosphatase, a classical indicator of the *pho* genes activation by PhoB. The *tat* operon was used as a negative control due to its constitutive expression (Jack et al., 2001). The non-expression of a transcript for the

prs-dauA operon (Fig. 5-3) from prsp[1] promoter was used as a positive control to ensure that the RNA sample was not contaminated by genomic DNA.

In the absence of *phoB* the transcription of the *prs-dauA* operon decreases, while this is not the case in the *ΔphoR* cells (Fig. 5-4). These results suggest that the *prs-dauA* operon is under a phosphate independent PhoB regulation (Fig. 5-4A). Further studies are needed in order to identify the pathway of PhoB induction. A CreC-dependent activation of PhoB (Fig. 5-4A) would be the first working hypothesis.

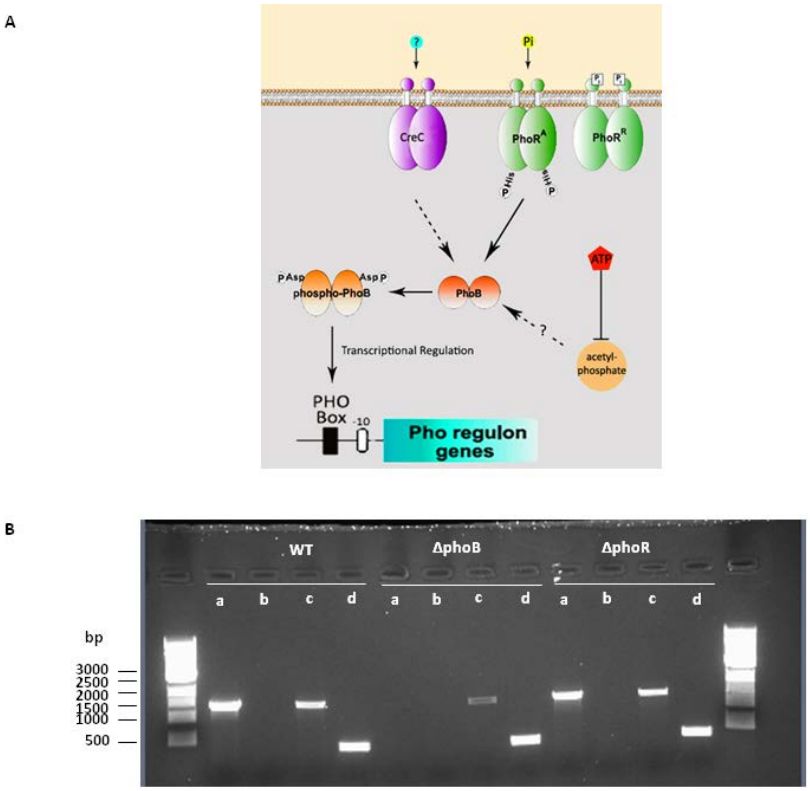

Figure 5- 4: Identification of *prs-dauA* operon regulators.
The *prs-dauA* operon may be under inorganic phosphate (Pi)-independent PhoB regulation. (A) Regulation of the Pho regulon. PhoB controls the expression of the Pho regulon genes. It can be activated by PhoR in response to phosphate limitation, or by carbon and energy sources levels via CreC and acetyl phosphate, respectively (adapted by Lamarche *et al*., 2008). (B) WT, *ΔphoB* and *ΔphoR* cells were grown under phosphate starvation conditions and RT-PCR was performed for the expression of the *prs-dauA* operon. Also, the strains were tested for the expression of *phoA*, the expression of *prs-dauA* operon from prsp[1] promoter as a negative control and the expression of *tat* as a positive control. Lanes a: *phoA* expression; b: expression of prsp[1]- *dauA* transcript; c: expression of *prs-dauA* operon; d: *tat* expression.

5.2.2 Studying dauA expression in C_4-diacarboxlate metabolism

5.2.2.1 Identification of *dauA* promoters

Bacterial genes belonging to the same metabolic pathway with related functions are usually organised in operons. However, more studies are necessary to elucidate the physiological role of a *prs-dauA* operon. Multiple internal gene specific promoters can exist in a single operon resulting in differential gene expression for flexible adaptation to external environmental stimuli (Okuda *et al.*, 2007). Thus, the next step in the investigation of the *dauA* regulation and expression was to identify and study *dauA* specific promoters.

The upstream region between promoter prsp[2], responsible for the expression of *prs-dauA* (Fig. 5-3), and the translational start site of *dauA*, was used as input to identify potential promoter sites in the computational software BPROM (Softberry Inc., Mt. Kisco, NY). The location on the chromosome and sequence of the three potential promoters identified is shown in Fig. 5-5.

In order to identify the active *dauA* promoter under the conditions used throughout this study, *lacZ* transcriptional fusions were generated containing *dauA* upstream region. The 1377 bp, 809 bp and 490 bp *dauA* upstream region including the first *dauA* codon was cloned to plasmid pJL28 using primer pairs EKO411/EKO414, EKO412/EKO414 and EKO413/EKO414 respectively, generating plasmids pEK201, pEK202 and pEK203. The primer EKO414 was used to alter the translational start codon GTG to ATG for maximal efficiency (O'Donnell & Janssen, 2001).

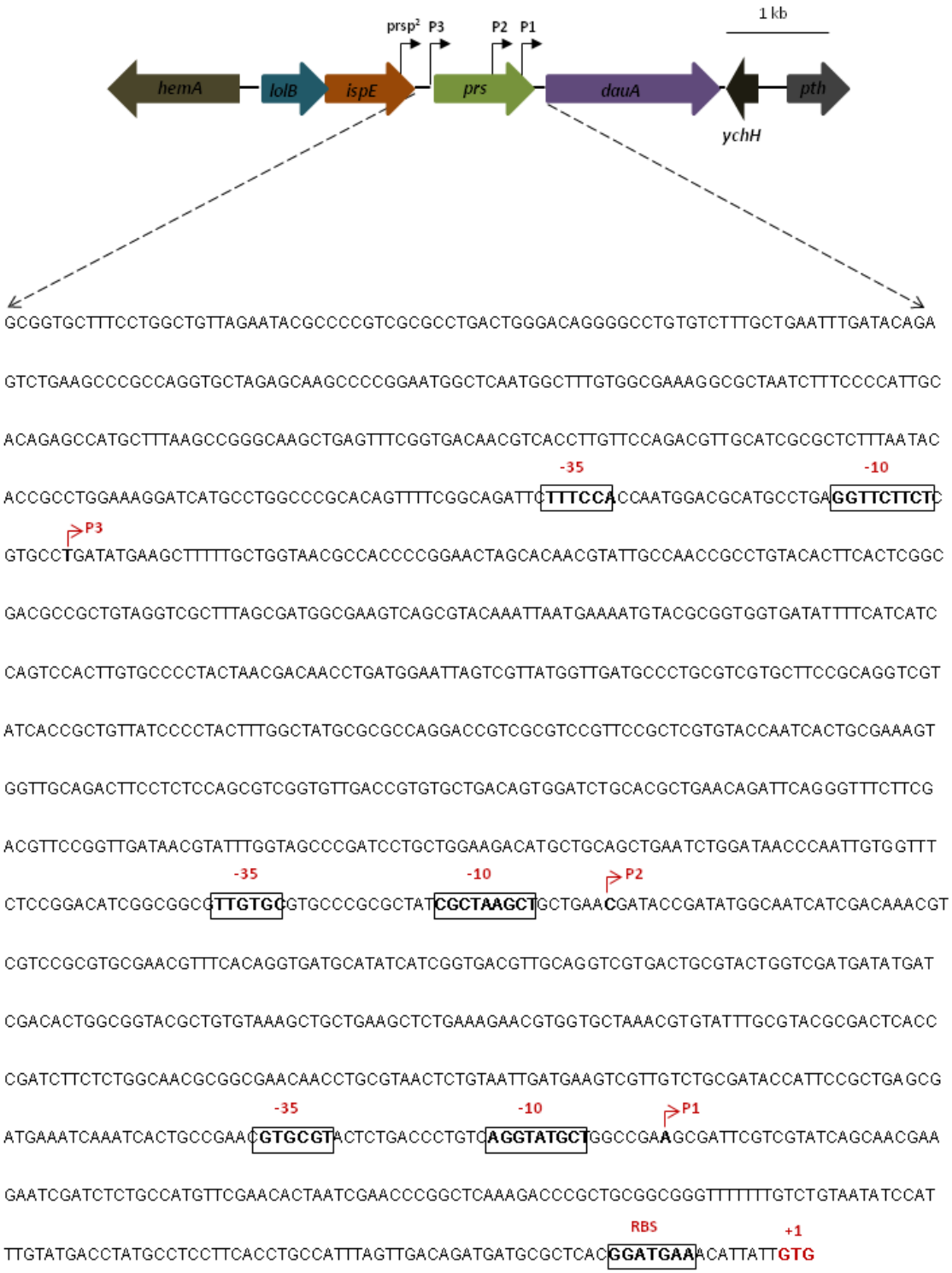

Figure 5-5: Schematic map of *dauA* region and predicted promoters.
The organisation of the genes on the chromosome is depicted on scale. The sequence upstream *dauA* (after promoter prsp[2]) was used as input for the prediction of potential *dauA* specific promoters using BPROM (http://linux1.softberry.com/berry.phtml). Potential RNA polymerase binding sites, -10 and -35, and Ribosomal Binding Site (RBS) are boxed. Potential transcription start sites are indicated with red stalked arrows. The translational start codon is highlighted in red. *hemA*, Glutamyl-tRNA reductase; *lolB*, Outer-membrane lipoprotein; *ispE*, 4-diphosphocytidyl-2-C-methyl-D-erythritol kinase; *prs*, ribose-phosphate diphosphokinase; *dauA*, dicarboxylic acid transporter; *ychH*, stress induced protein; *pth*, peptidyl-tRNA hydrolase.

Wild type (BW25113) cells were transformed with plasmids pEK201, pEK202 and pEK203 and grown overnight in M9 minimal medium supplemented with glucose as the sole carbon source at pH 7. The next day the cells were washed twice and cultured for six more hours in M9 minimal medium supplemented with 50 mM succinate as the sole carbon source at pH 7 or pH 5. Samples were taken at t=0 before the cells were transferred in the succinate supplemented medium, at t=6 after 6 hours of growth and the β-galactosidase activity was measured. BW25113 strain containing the empty pJL28 plasmid was used as negative control and the strain IMW385 containing a chromosomal *dctA'-'lacZ* fusion as positive control.

β-galactosidase activity was detected for all three constructs under both conditions (M9 succinate pH 7 or pH 5) (Fig. 5-6). At pH 7, *dctA* expression was induced in the presence of succinate (Fig. 5-6A) as it has been shown in previous studies (Davies et al., 1999). In accordance with previous observations, at pH 5 the activity of *dctA'–'lacZ* was not detectable above background level (Fig. 5-6B).

The constructs were designed to contain increasing length of *dauA* upstream regions. As a result plasmid pEK201 contains all three predicted promoters, plasmid pEK202 contains promoters P2 and P1, and plasmid pEK203 harbours the proximal promoter P1. One-way ANOVA statistical analysis was used to compare the three promoters activity and identify the potential *dauA* promoter under the conditions used. No statistical significant difference was detected in the activity of the promoters at pH7 t=0 (p=0.161), pH7 t=6 (p=0.080), pH5 t=0 (p=0.092) nor pH5 t=6 (0.095), indicating that the proximal promoter P1 might be the active specific *dauA* promoter. 5'RACE analysis is necessary to confirm these results.

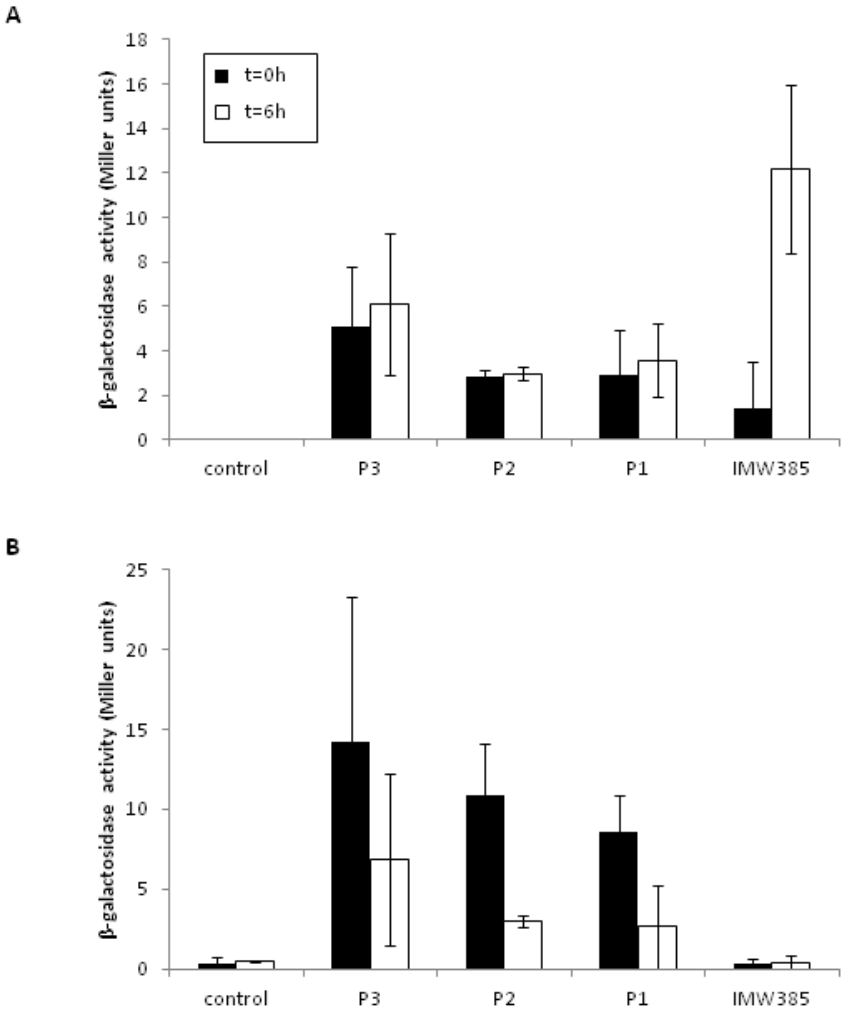

Figure 5-6: Identification of *dauA* specific promoter.
BW25113 cells containing empty pJL28 plasmid (control) or plasmids pEK201 (P3), pEK202 (P2) and pEK203 (P1) were grown aerobically for 6 hours in M9 minimal medium supplemented with 50 mM succinate as the sole carbon sources at (A) pH7 or (B) pH5. The strain IMW385 harbouring a *dctA'-'lacZ* chromosomal fusion was tested under the same conditions as positive control. The β-galactosidase activity was measured. All results are the average of three independent biological repeats. Error bars represent the standard deviation.

5.2.2.2 Regulation by pH

DauA is a succinate transporter active under acidic conditions with a bifunctional role in DctA regulation and/or expression. DauA was detected both at pH 7 and pH 5 (Karinou *et al.*, 2013). Furthermore, the results in Chapter 4 suggest that DauA might be involved in a succinate inducible acid stress tolerance system.

In order to study whether *dauA* expression is pH-regulated, cells transformed with the empty plasmid pJL28, plasmid EK203 harbouring the potential *dauA* P1 promoter and strain IMW385 containing a chromosomal *dctA'-'lacZ* fusion were grown overnight in M9 minimal medium supplemented with glucose at pH 5, pH 6, pH 7 or pH 8. The next day cells were harvested and β-galactosidase activity was measured. The activity measured for cells transformed with empty pJL28 plasmid was used as a negative control. *dctA* expression is strongly repressed in the presence of glucose via the cAMP-CRP complex (Davies *et al*., 1999) and thus the activity detected for IMW385 was bellow background level (Fig. 5-7).

One-way ANOVA statistical analysis was used to compare the *dauA* promoter activity at different pHs. Pairwise Multiple Comparison showed that there is no significant difference between the promoter activities ($p > 0.050$) except for the activity between pH5 and pH8 ($p = 0.025$).

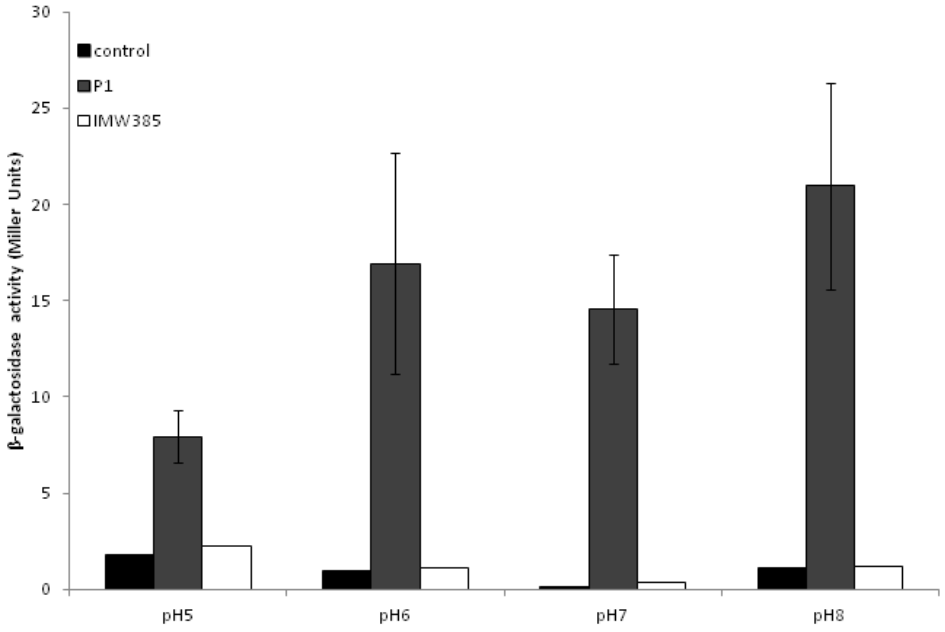

Figure 5-7: Studying the effect of pH in *dauA* expression.
BW25113 cells containing empty pJL28 plasmid (control) or plasmid pEK203 (P1) were grown aerobically overnight in M9 minimal medium supplemented with 50 mM glucose as the sole carbon sources at pH 5, pH 6, pH 7 or pH 8. The strain IMW385 harbouring a *dctA*'-'*lacZ* chromosomal fusion was tested under the same conditions. The β-galactosidase activity was measured. Results are the average of three independent biological repeats. Error bars represent the standard deviation

5.2.2.3 Regulation by growth phase

To obtain better understanding on factors affecting the regulation of *dauA* expression, I monitored the β-galactosidase activity of cells grown in M9 minimal medium supplemented with glucose at pH 7 for 18 hours.

The results presented in Fig. 5-8 show that the expression of *dauA* is increased 3-fold in stationary phase (21.6 Miller units) compared to the activity measured at the early-log phase (7.3 Miller units). These results are consistent with a growth-phase-dependent regulation of *dauA* expression. The expression of *dctA* in the presence of glucose followed a CRP-mediated repression as observed before (Davies *et al.*, 1999).

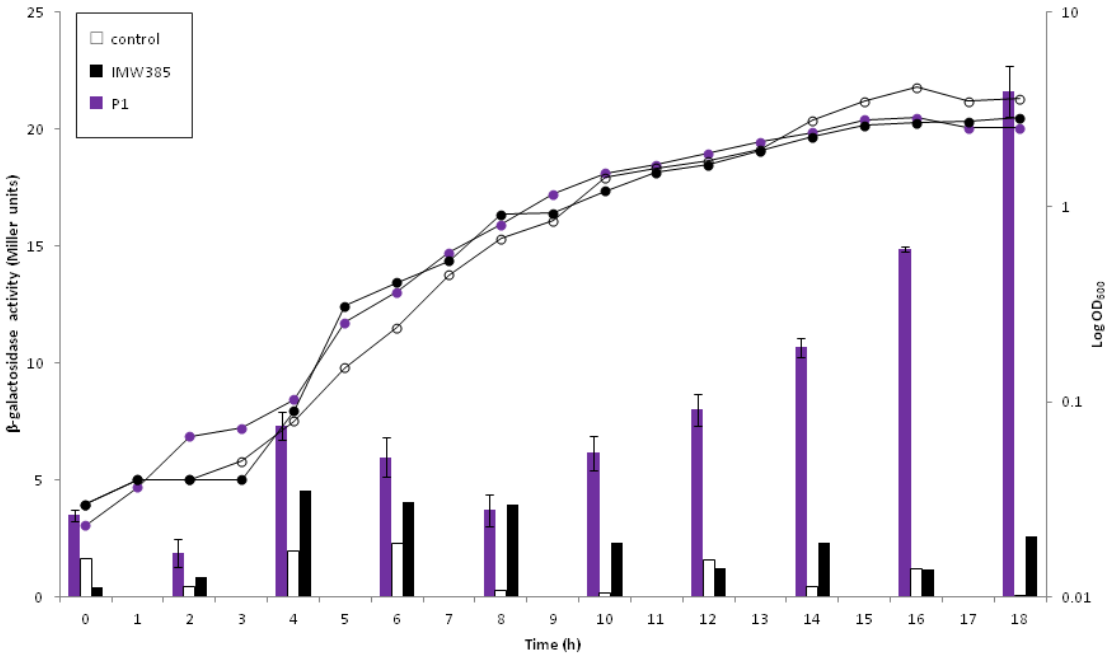

Figure 5-8: Aerobic expression of *dauA* during growth in M9 glucose pH 7.
The β-galactosidase activity (bars) and growth (lines) of EK203 (P1), IMW385 and the empty vector (control), are shown after aerobic growth at 37°C in M9 minimal medium supplemented with 50 mM glucose as the sole carbon source. Average of three independent cultures; error bars represent the standard deviation.

The production of DauA was further monitored by western immunoblotting. Strain EK182 carrying His-tagged DauA variant and a FLAG-tagged DctA variant was grown for 8 hours in LB and samples were harvested hourly. Cells were pelleted, sonicated and fractionated to membrane and soluble fractions. The presence of DauA and DctA was monitored in the membrane fraction by western immunoblot using anti-His and anti-FLAG antibodies respectively. TatC, a membrane protein constitutively produced was used as loading control.

DctA was detected and the expression pattern was similar to previous studies (Davies *et al.*, 1999). However, DauA was not detected in the same samples (Fig 5-9). The cells tested in this assay were still in the exponential phase which might explain the absence of DauA in the membranes. Taken together, these results might indicate that *dctA* expression is induced in stationary phase. However, the fact that DauA was not detected in the membranes after growth in LB might be the result of the complexity of the medium. Further experiments will be needed to monitor the production of DauA in M9 supplemented with glucose at pH 7 and compare these results with the *dauA* expression in Fig. 5-8.

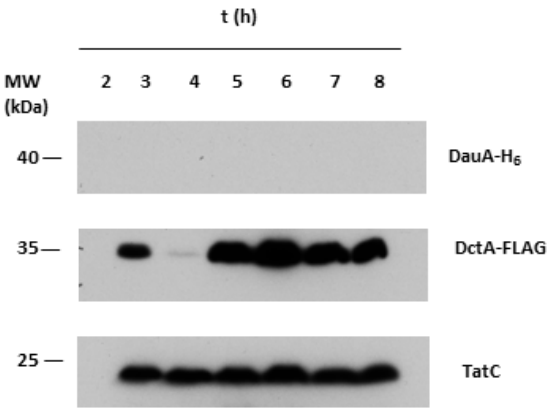

Figure 5-9: Immunoblot detection of DauA and DctA during growth in LB at pH 7.
Membrane fractions were prepared from strain EK182, encoding chromosomal C-terminally His-tagged DauA and FLAG-tagged DctA variants. Cells were grown in LB for 8 hours and samples were taken hourly. Cell pellets were fractionated into membranes and soluble fractions, followed by anti-His, anti-FLAG and anti-TatC immunoblotting. Protein extract concentration was normalized and the same amount was loaded in each lane.

5.2.2.4 Regulation of *dauA* expression by the two-component regulatory system DcuS/R

Under aerobic conditions, *dctA* expression is induced by the DcuS/R two-component regulatory system in the presence of C_4-dicarboxylic acids (Davies et al., 1999; Golby et al., 1999; Zientz et al., 1998). The next step was to test if there is induction of DauA production depending on DcuS/R activity.

Strains EK182 (DauA-H_6, DctA-FLAG) and EK184 (*ΔdcuS*, DauA-H_6, DctA-FLAG) were grown overnight in M9 minimal medium supplemented with glucose as the sole carbon source. The next day, cells were washed and cultured for 6h in M9 minimal medium supplemented with 50 mM succinate at pH 7 or pH 5. The detection of DauA and DctA was monitored in the membranes using anti-His and anti-FLAG antibodies respectively. TatC was used as loading control.

DctA was not detected in the *ΔdcuS* background or at pH5, suggesting that under these conditions *dctA* expression is tightly dependent on the DcuS/R two-component system. On the other hand, the production of DauA remained at the same levels in the wild type or *ΔdcuS* strain indicating that *dauA* expression is not affected by DcuS/R under the conditions used.

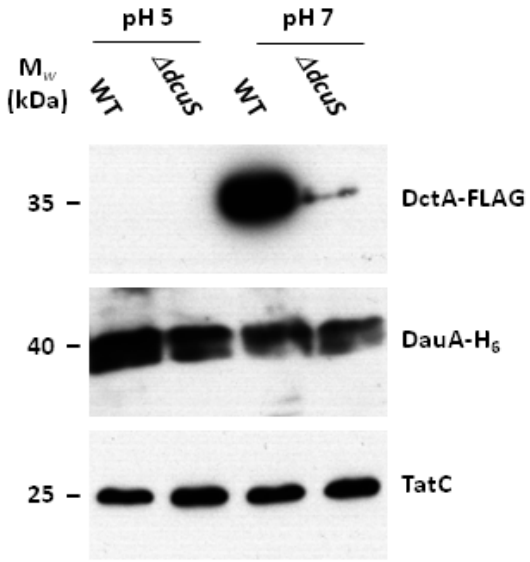

Figure 5- 10: Effect of DcuS on *dauA* expression.
Strains EK182 (DauA-H_6, DctA-FLAG) and EK184 (*ΔdcuS*, DauA-H_6, DctA-FLAG) were grown for 6h in M9 minimal medium supplemented with 50 mM succinate as the sole carbon source at pH5 or pH7. Cell pellets were fractionated into membranes and soluble fractions, followed by anti-His, anti-FLAG and anti-TatC immunoblotting. Protein extract concentration was normalized and the same amount was loaded in each lane.

5.3 Discussion

Studies on the expression of eukaryotic SLC26 homologues identified transcriptional and post translational level of regulation. However, the lack of comprehensive information on the physiological role of the bacterial homologues limits the ability to study their regulation. In this part of the current work an attempt was made to understand the regulation of *dauA* expression. Due to time constrictions only a small number of conditions were tested but preliminary experiments gave some interesting results.

Based on the fact that *prs* is immediately upstream (125 bp) of *dauA*, a gene involved in nucleotide metabolism (Post *et al.*, 1993), it was hypothesised that *dauA* and *prs* may form an operon. This hypothesis was tested and confirmed by RT-PCR analysis (Fig. 5-2). The bacterial genome organisation usually favours the operon formation of genes involved in the same metabolic pathway (Okuda *et al*., 2007) however further studies are needed to clarify whether Prs and DauA are also metabolically linked.

It is known from the literature that *prs* is transcribed from two promoters: $prsp^1$ and $prsp^2$, the latter being located 302 bp upstream the translational start site (Post *et al*., 1993). The RT-PCR analysis indicated that $prsp^2$ may be the promoter from which the *prs-dauA* operon is transcribed (Fig. 5-3). However, it cannot be ruled out that the lack of detectable product could be the result of the inability to generate a RT-PCR product longer than 3 kb. Further studies by 5'RACE analysis is needed to confirm these results.

It has been shown that PurR, the global repressor of the purine biosynthetic pathway, binds on a Pur Box upstream the -35 region of $prsp^2$, causing a two- to three- fold transcription repression of *prs* (He *et al.*, 1993). However, it was not able to identify similar regulation for the *prs-dauA* operon by RT-PCR (data not shown). A more

sensitive and quantitative method such as qRT-PCR should be used to confirm these results.

The *pho* genes are regulated by the two-component regulatory system PhoB/R. PhoR is a membrane sensor kinase that responds to periplasmic phosphate concentration variations. PhoB is a DNA-binding protein that regulates the transcription of the genes belonging to the *pho* regulon. Under phosphate starvation conditions, PhoR is autophosphorylated and in turn phosphorylates PhoB, which activates the transcription of the *pho* genes. It has been shown that PhoB can be induced directly or indirectly by other stress responses not related to phosphate limitation (Lamarche *et al*., 2008). Based on the requirement of inorganic phosphate for Prs activity and stability (Hove-Jensen *et al*., 1986) it was examined whether the *prs-dauA* operon is under the PhoB/R transcriptional control. The RT-PCR results show that the *prs-dauA* operon was sensibly downregulated in *ΔphoB* cells compared to a wild type background (Fig. 5-4). However, no difference was observed under the same condition in the *ΔphoR* background. These results indicate that the *prs-dauA* operon may be under phosphate independent PhoB regulation. The results presented in this study identified DauA as an acidic succinate transporter and no physiological role has been identified in the phosphate metabolism. Nonetheless, *pho* regulon induction by stringent response, directly or indirectly via the alternative sigma factor RpoS (Lamarche *et al.*, 2008) might explain the phosphate independent PhoB regulation of *prs-dauA*.

Next, in order to study the *dauA* expression related to the physiological role of DauA in succinate metabolism, a *dauA* specific promoter was identified by computational and transcriptional fusion analysis, located 178 bp upstream the translational start of DauA (Fig. 5-5 and 5-6). Previous results indicated that DauA is produced constitutively regardless of pH or carbon source the cells are grown in. However, monitoring the

expression of *dauA* in M9 glucose at pH7 revealed that a 3-fold induction in the stationary phase indicating a growth-phase-dependent regulation (Fig. 5-8). Furthermore, under aerobic conditions, DauA seems to be highly expressed, while its production is significantly reduced under anaerobic conditions (Fig. 3-10). This reduction might indicate a level of regulation and that DauA might be under the inhibitory regulation of FNR or ArcBA.

The effect of pH in the expression of DauA has been further studied at the transcriptional level. No significant difference was observed in the expression of *dauA* grown in M9 supplemented with glucose at various pHs (Fig. 5-7). The reduced β-galactosidase activity measured at pH5 might not necessarily reflect reduced *dauA* expression. In principal, β-galactosidase activity measured in transcriptional fusions is proportional to the transcriptional rate of the tested gene. However, caution is needed in the interpretation of the results (Pessi *et al.*, 2001; Silhavy & Beckwith, 1985). The β-galactosidase enzyme has optimal activity at pH7 and this activity decreases as the pH decreases. When the β-galactosidase enzyme is incubated at pH5 and then transferred at pH7 the recovery of its activity is not attained immediately (Tenu *et al.*, 1971). Therefore, the reduced activity observed in cells grown at pH5 might be a result of the impaired enzyme activity and not of the decreased gene expression. The difference in the expression of *dauA* under various pH conditions should be verified using qRT-PCR.

Finally, the effect on *dauA* expression of the DcuS/R two-component regulatory system, which is responsible for C_4-dicarboxylate gene induction, was tested (Fig. 5-10). The results showed that the production of DauA is not affected by the presence of DcuS indicating that either *dauA* is not under the DcuS/R regulatory control or that under the conditions used the response regulator DcuR is activated by another sensor kinase.

To summarise, preliminary results on the expression of *dauA* suggested that *dauA* is induced during stationary phase but it is not affected by the carbon source used or the pH applied in the medium. In contrast to *dctA*, *dauA* expression is not affected by DcuS/R. Future studies are necessary to identify the condition and specific regulations of *dauA* expression. A potential operon has been identified with *prs* which might be under a phosphate independent PhoB regulatory control.

6 Concluding Remarks and Future Perspectives

6.1 DauA is an acidic succinate transporter

The SLC26/SulP family is a ubiquitous superfamily of anion transporter proteins conserved from bacteria to man. Members of this family possess a wide variety of functions and a wide substrate repertoire transporting anions ranging from halides to bicarbonate (Dorwart *et al.*, 2008b; Mount & Romero, 2004). The functional importance of this family is illustrated by the fact that several inherited human diseases are caused by mutations in SLC26 genes (Mount & Romero, 2004).

Although these proteins are present in almost all bacteria their physiological function is unknown. The only comprehensive functional and topological analysis of a bacterial SulP protein concerns the bicarbonate transporter BicA from *Synechococcus* (Shelden *et al.*, 2010). In cyanobacteria, these proteins have been characterised as a low affinity Na^+-dependent HCO_3^- transporter (Price & Howitt, 2011; Price *et al.*, 2004).

Studying the physiological role and function of membrane proteins in simpler organisms, such as the model organism *Escherichia coli*, has been proven crucial in our understanding of different physiological phenomena in more complex systems. In *E. coli* only one SulP homologue, YchM has been identified. A phylogenetic analysis of bacterial SulP proteins (Fig. 1-4) showed that YchM clusters independently from the BicA and BicA-like proteins, indicating that YchM may not act as a bicarbonate transporter. Therefore, the overall aim of this project was to use a combination of genetic and biochemical approaches to investigate the substrate and physiological role of YchM.

The work presented here has identified that YchM is an aerobic succinate transporter and thus, *ychM* was re-named as *dauA* (for dicarboxylic acid uptake system A). It was confirmed that DauA is a succinate transporter at acidic pH by showing a growth defect phenotype of *ΔdauA* cells (Fig. 3-4 and 3-5) and by developing a succinate *in vivo* uptake assays (Fig. 3-11 and 3-12). The comparison of the values of the kinetic parameters for DctA, the only aerobic succinate transporter identify so far, and DauA revealed that DauA has a weaker affinity for succinate and a lower maximal transport rate (Table 3-1). Furthermore, it was showed that the transport ability of DauA is not affected by the protonation state of succinate in contrast to DctA which is able to transport only succinate dicarboxylate (Fig. 3-13). The competition assays suggested that DauA has different substrate specificity compare to DctA and that it is able to transport fumarate (Fig. 3-14). Finally, it was reported that in the absence of DauA the expression and/or activity of DctA is clearly reduced indicating that DauA not only acts as a transporter but plays a regulatory role in C_4-dicarboxylic acid metabolism. Interestingly, it seems that the activity and regulatory functions of DauA are not linked.

Future work should include the development of an *in vitro* assay using purified proteins reconstituted in liposomes to study the kinetic properties of DctA- and DauA-dependent succinate transport. Site-directed mutagenesis can be used to identify residues necessary for the succinate uptake or regulatory function of DauA. The regulatory effect of DauA on *dctA* expression can be further quantified using qRT-PCR. Ultimately, structural and topological studies will help in our understanding of the mechanistic aspects of a DauA-dependent succinate transport.

6.2 DauA interacts with DctA

The first part of this work showed that DauA is a succinate transporter active at acidic pH. At pH7, in the absence of DauA, the expression and/or activity of DctA, the main succinate transporter, is clearly reduced indicating that DauA not only acts as a transporter but also plays a regulatory role in C_4-dicarboxylic acid metabolism (Karinou *et al.*, 2013). It was sought to explore this hypothesis further by characterising any potential interactions between DauA and components of the C_4-dicarboxylic acid metabolism.

Bacterial two-hybrid analysis and co-purification studies confirmed a specific interaction between DauA and DctA (Fig. 4-1 and 4-2). Furthermore, localization studies indicated that DauA and DctA interact physically (Fig. 4-3). Preliminary results in the identification of specific domains responsible for this interaction suggested that the interaction seems to be mediated via the transmembrane domains of the two proteins (Fig. 4-4).

The identification by mass spectrometry of two proteins involved in the glutamate-dependent acid resistance system, GadX and GadB, links DauA and succinate metabolism to acid resistance (Table 4-1). It can be hypothesised that DauA might be involved in a succinate inducible acid stress tolerance system. Moreover, the transcriptional regulator YhiF is involved in a DcuS/R-independent expression of *dctA*, acting as a negative regulator. YhiF is encoded within the AFI and under the direct transcriptional regulation of GadX. It is tempting to speculate that any DauA effects on DctA expression are due to a regulatory circuit involving GadX and YhiF. These observations suggest an interesting dual role for DauA in succinate metabolism with transport and regulatory functions.

Combining the results of the first two parts of this study a hypothetical working model for the DauA physiological function can be proposed (Fig. 6-1):

- At pH7 in the presence of succinate under aerobic conditions, DauA is expressed but inactive as a transporter, DctA is the main uptake system. DauA interacts with the transcriptional regulator GadX. The DauA-GadX interaction prevents the induction of the negative regulator YhiF, which inhibits *dctA* transcription. The physiological meaning of the DauA-DctA interaction is not clear yet. It can be hypothesised that DauA is necessary for optimal activity of the DctA/DcuS sensor unit or that DauA responds to a yet unknown stimulus and transmits the signal to the sensor kinase DcuS.
- ❖ At pH5 in the presence of succinate under aerobic conditions, DauA is the main transporter. It has weaker affinity and lower apparent transport rate for succinate than DctA. DauA releases GadX which induces YhiF and thus inhibits *dctA* transcription.

Future work should be focused on the validation of this model. First, it will be necessary to identify the hierarchy of the DauA-DctA-DcuS complex by BTH studies using reporter strains lacking the chromosomally produced DauA, DctA and DcuS. Also, these interactions should be further confirmed biochemically. Second, it will be necessary to identify the specific interacting domains of DauA and DctA by site directed mutagenesis and BTH studies. Furthermore, it will be quite informative to study if the interaction between DauA and DctA is induced by different pH or carbon sources giving us a better understanding of the physiological role of the complex. Third, the protein interacting candidates identified by mass spectrometry should be validated both by BTH analysis and co-purification studies. Specifically identification of an interaction between DauA and GadX will reinforce our hypothesis on the regulatory

function of DauA. Identification of specific domains in this interaction and specifically the role of the STAS domain will be necessary for the validation of the DauA regulatory function. Finally, this model can be further investigated by identifying direct interactions of the regulatory protein YhiF or GadX with the *dctA* promoter using computational approaches and Electrophoretic Mobility Shift Analysis (EMSA).

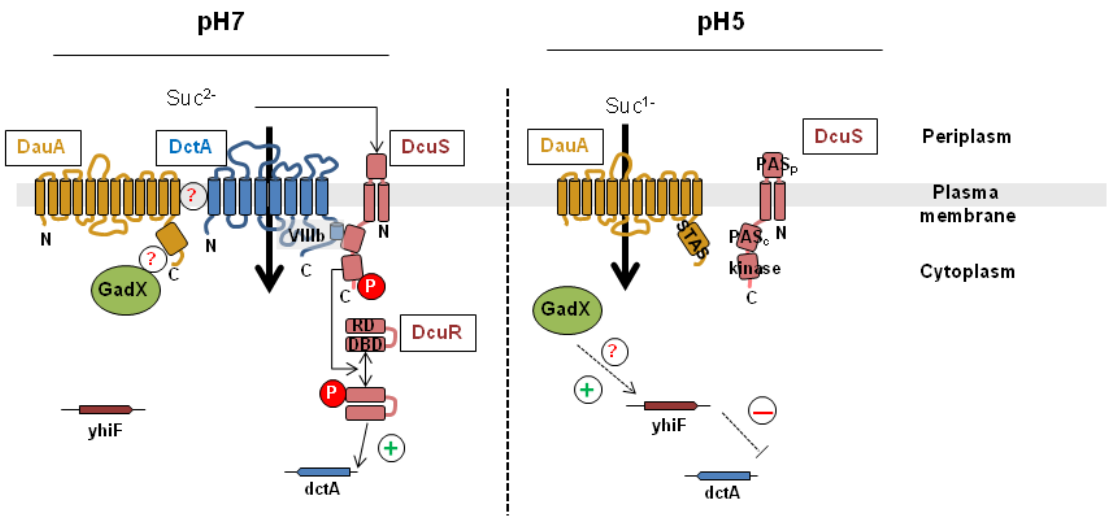

Figure 6-1: Working model for the physiological function of DauA in the C_4-dicarboxylic acid metabolism.

6.3 Elucidating *dauA* regulation

The lack of physiological and functional characterisation of the bacterial SLC26 homologues has not allowed further investigation into their expression and regulation. For the last part of this work an attempt was made to investigate the expression and regulation of DauA. Although, this is an on-going project interesting preliminary results have been obtained regarding the expression of DauA.

Based on the chromosomal proximity of *prs* and *dauA* it was hypothesised that they form an operon. This hypothesis was confirmed by RT-PCR (Fig. 5-2) and it was identified that $prsp^2$ might be the potential promoter of the *prs-dauA* operon (Fig. 5-3). Also, in an attempt to identify potential operon regulators it was shown that the *prs-dauA* operon might be under a phosphate independent PhoB regulation (Fig. 5-4). Next, specific *dauA* expression in C_4-dicarboxylic metabolism was identified. Computation analysis indicated the presence of three promoters directly upstream *dauA* (Fig. 5-5) and fusion studies identified that P1 is the *dauA* specific promoter (Fig. 5-6). Further results indicated that DauA is produced constitutively regardless of pH (Fig. 5-7) or carbon source the cells are grown in. However, monitoring the expression of *dauA* in M9 glucose at pH7 revealed that a 3-fold induction in the stationary phase indicating a growth-phase-dependent regulation (Fig. 5-8). Furthermore, under aerobic conditions, DauA seems to be highly expressed, while its production is significantly reduced under anaerobic conditions (Fig. 3-10). This reduction might indicate a level of regulation and that DauA might be under the inhibitory regulation of FNR or ArcBA. Finally, in contrast to *dctA*, *dauA* expression is not under the DcuS/R regulatory control (Fig. 5-10).

They are many unanswered questions regarding the conditions affecting the expression of *dauA*. First, $prsp^2$ should be validated as the *prs-dauA* operon promoter by 5'RACE.

PhoB can be confirmed as a regulator for the operon by EMSA. Further studies are needed to understand the physiological role of such an operon and if it is affected by phosphate independent induction of the *pho* regulon. This can be tested initially by translation fusions and qRT-PCR in *ΔcreC* strains. Second, to confirm that P1 is a *dauA* specific promoter 5' RACE is necessary. Once, the promoter is confirmed we can screen for potential regulators by computational methods. Candidate regulators can be validated by EMSA. Identifying regulators involved in pH homeostasis and growth phase induction are of particular interest. Also, we can test whether *dauA* regulates its own expression by promoter fusions. Finally, more sensitive quantification methods, such as qRT-PCR can be used to confirm the difference in expression of *dauA* under different growth condition. Elucidating the conditions regulating the expression of *dauA* combined with the results we have obtain so far will allow us a better understanding of the DauA physiological role.

7 References

Alper, S.L. & A.K. Sharma, (2013) The SLC26 gene family of anion transporters and channels. *JMAM* **34**: 494-515.

Alvarez, B.V., D.M. Kieller, A.L. Quon, D. Markovich & J.R. Casey, (2004) Slc26a6: a cardiac chloride-hydroxyl exchanger and predominant chloride-bicarbonate exchanger of the mouse heart. *J Physiol* **561**: 721-734.

Aravind, L. & E.V. Koonin, (2000) The STAS domain - a link between anion transporters and antisigma-factor antagonists. *Curr Biol : CB* **10**: R53-55.

Baba, T., T. Ara, M. Hasegawa, Y. Takai, Y. Okumura, M. Baba, K.A. Datsenko, M. Tomita, B.L. Wanner & H. Mori, (2006) Construction of Escherichia coli K-12 in-frame, single-gene knockout mutants: the Keio collection. *Mol Syst Biol* **2**: 2006 0008.

Babu, M., J.F. Greenblatt, A. Emili, N.C. Strynadka, R.A. Reithmeier & T.F. Moraes, (2010) Structure of a SLC26 anion transporter STAS domain in complex with acyl carrier protein: implications for E. coli YchM in fatty acid metabolism. *Structure* **18**: 1450-1462.

Bai, J.P., A. Surguchev, S. Montoya, P.S. Aronson, J. Santos-Sacchi & D. Navaratnam, (2009) Prestin's anion transport and voltage-sensing capabilities are independent. *Biophys J* **96**: 3179-3186.

Baker, K.E., K.P. Ditullio, J. Neuhard & R.A. Kelln, (1996) Utilization of orotate as a pyrimidine source by Salmonella typhimurium and Escherichia coli requires the dicarboxylate transport protein encoded by dctA. *J Bacteriol* **178**: 7099-7105.

Bertrand, C.A., R. Zhang, J.M. Pilewski & R.A. Frizzell, (2009) SLC26A9 is a constitutively active, CFTR-regulated anion conductance in human bronchial epithelia. *J Gen Physiol* **133**: 421-438.

Bidart, J.M., C. Mian, V. Lazar, D. Russo, S. Filetti, B. Caillou & M. Schlumberger, (2000) Expression of pendrin and the Pendred syndrome (PDS) gene in human thyroid tissues. *Journal Clin Endocrinol Metab* **85**: 2028-2033.

Bissig, M., B. Hagenbuch, B. Stieger, T. Koller & P.J. Meier, (1994) Functional expression cloning of the canalicular sulfate transport system of rat hepatocytes. *J Biol Chem* **269**: 3017-3021.

Bochner, B.R., (2009) Global phenotypic characterization of bacteria. *FEMS Microbiol Rev* **33**: 191-205.

Boogerd, F.C., L. Boe, O. Michelsen & P.R. Jensen, (1998) atp Mutants of Escherichia coli fail to grow on succinate due to a transport deficiency. *J Bacteriol* **180**: 5855-5859.

Booth, I.R., (2003) Bacterial ion channels. *Genetic engineering* **25**: 91-111.

Buchner, P., H. Takahashi & M.J. Hawkesford, (2004) Plant sulphate transporters: co-ordination of uptake, intracellular and long-distance transport. *J Exp Bot* **55**: 1765-1773.

Casadaban, M.J. & S.N. Cohen, (1979) Lactose genes fused to exogenous promoters in one step using a Mu-lac bacteriophage: in vivo probe for transcriptional control sequences. *PNAS* **76**: 4530-4533.

Castanie-Cornet, M.P., T.A. Penfound, D. Smith, J.F. Elliott & J.W. Foster, (1999) Control of acid resistance in Escherichia coli. *J Bacteriol* **181**: 3525-3535.

Chang, M.H., C. Plata, A. Sindic, W.K. Ranatunga, A.P. Chen, K. Zandi-Nejad, K.W. Chan, J. Thompson, D.B. Mount & M.F. Romero, (2009) Slc26a9 is inhibited by the R-

region of the cystic fibrosis transmembrane conductance regulator via the STAS domain. *J Biol Chem* **284**: 28306-28318.

Chapman, J.M. & L.P. Karniski, (2010) Protein localization of SLC26A2 (DTDST) in rat kidney. *Histochem Cell Biol* **133**: 541-547.

Cherest, H., J.C. Davidian, D. Thomas, V. Benes, W. Ansorge & Y. Surdin-Kerjan, (1997) Molecular characterization of two high affinity sulfate transporters in Saccharomyces cerevisiae. *Genetics* **145**: 627-635.

Chernova, M.N., L. Jiang, D.J. Friedman, R.B. Darman, H. Lohi, J. Kere, D.H. Vandorpe & S.L. Alper, (2005) Functional comparison of mouse slc26a6 anion exchanger with human SLC26A6 polypeptide variants: differences in anion selectivity, regulation, and electrogenicity. *J Biol Chem* **280**: 8564-8580.

Chernova, M.N., L. Jiang, B.E. Shmukler, C.W. Schweinfest, P. Blanco, S.D. Freedman, A.K. Stewart & S.L. Alper, (2003) Acute regulation of the SLC26A3 congenital chloride diarrhoea anion exchanger (DRA) expressed in Xenopus oocytes. *J Physiol* **549**: 3-19.

Cheung, J. & W.A. Hendrickson, (2008) Crystal structures of C4-dicarboxylate ligand complexes with sensor domains of histidine kinases DcuS and DctB. *J Biol Chem* **283**: 30256-30265.

Choi, B.Y., H.M. Kim, T. Ito, K.Y. Lee, X. Li, K. Monahan, Y. Wen, E. Wilson, K. Kurima, T.L. Saunders, R.S. Petralia, P. Wangemann, T.B. Friedman & A.J. Griffith, (2011) Mouse model of enlarged vestibular aqueducts defines temporal requirement of Slc26a4 expression for hearing acquisition. *J Clin Invest* **121**: 4516-4525.

Compton, E.L., E. Karinou, J.H. Naismith, F. Gabel & A. Javelle, (2011) Low resolution structure of a bacterial SLC26 transporter reveals dimeric stoichiometry and mobile intracellular domains. *J Biol Chem* **286**: 27058-27067.

Coutts, G., G. Thomas, D. Blakey & M. Merrick, (2002) Membrane sequestration of the signal transduction protein GlnK by the ammonium transporter AmtB. *The EMBO journal* **21**: 536-545.

Currall, B., D. Rossino, H. Jensen-Smith & R. Hallworth, (2011) The roles of conserved and nonconserved cysteinyl residues in the oligomerization and function of mammalian prestin. *J Neurophysiol* **106**: 2358-2367.

Datsenko, K.A. & B.L. Wanner, (2000) One-step inactivation of chromosomal genes in Escherichia coli K-12 using PCR products. *PNAS* **97**: 6640-6645.

Davies, S.J., P. Golby, D. Omrani, S.A. Broad, V.L. Harrington, J.R. Guest, D.J. Kelly & S.C. Andrews, (1999) Inactivation and regulation of the aerobic C(4)-dicarboxylate transport (dctA) gene of Escherichia coli. *J Bacteriol* **181**: 5624-5635.

De Biase, D., A. Tramonti, F. Bossa & P. Visca, (1999) The response to stationary-phase stress conditions in Escherichia coli: role and regulation of the glutamic acid decarboxylase system. *Mol Microbiol* **32**: 1198-1211.

Detro-Dassen, S., M. Schanzler, H. Lauks, I. Martin, S.M. zu Berstenhorst, D. Nothmann, D. Torres-Salazar, P. Hidalgo, G. Schmalzing & C. Fahlke, (2008) Conserved dimeric subunit stoichiometry of SLC26 multifunctional anion exchangers. *J Biol Chem* **283**: 4177-4188.

Dorwart, M.R., N. Shcheynikov, J.M. Baker, J.D. Forman-Kay, S. Muallem & P.J. Thomas, (2008a) Congenital chloride-losing diarrhea causing mutations in the STAS domain result in misfolding and mistrafficking of SLC26A3. *J Biol Chem* **283**: 8711-8722.

Dorwart, M.R., N. Shcheynikov, Y. Wang, S. Stippec & S. Muallem, (2007) SLC26A9 is a Cl(-) channel regulated by the WNK kinases. *J Physiol* **584**: 333-345.

Dorwart, M.R., N. Shcheynikov, D. Yang & S. Muallem, (2008b) The solute carrier 26 family of proteins in epithelial ion transport. *Physiology* **23**: 104-114.

Du, L., C. Sanchez, M. Chen, D.J. Edwards & B. Shen, (2000) The biosynthetic gene cluster for the antitumor drug bleomycin from Streptomyces verticillus ATCC15003 supporting functional interactions between nonribosomal peptide synthetases and a polyketide synthase. *Chem Biol* **7**: 623-642.

Dubyak, G.R., (2004) Ion homeostasis, channels, and transporters: an update on cellular mechanisms. *Adv Physiol Educ* **28**: 143-154.

Errington, J., (2003) Regulation of endospore formation in Bacillus subtilis. *Nat Rev Microbiol* **1**: 117-126.

Felce, J. & M.H. Saier, Jr., (2004) Carbonic anhydrases fused to anion transporters of the SulP family: evidence for a novel type of bicarbonate transporter. *J Mol Microbiol Biotech* **8**: 169-176.

Fitzpatrick, K.L., S.D. Tyerman & B.N. Kaiser, (2008) Molybdate transport through the plant sulfate transporter SHST1. *FEBS letters* **582**: 1508-1513.

Fong, P., (2011) Thyroid iodide efflux: a team effort? *Journal Physiol* **589**: 5929-5939.

Fontenot, E.M., K.E. Ezelle, L.N. Gabreski, E.R. Giglio, J.M. McAfee, A.C. Mills, M.N. Qureshi, K.M. Salmon & C.G. Toyota, (2013) YfdW and YfdU are required for oxalate-induced acid tolerance in Escherichia coli K-12. *J Bacteriol* **195**: 1446-1455.

Foster, J.W., (2004) Escherichia coli acid resistance: tales of an amateur acidophile. *Nature reviews. Microbiology* **2**: 898-907.

Galamb, O., F. Sipos, N. Solymosi, S. Spisak, T. Krenacs, K. Toth, Z. Tulassay & B. Molnar, (2008) Diagnostic mRNA expression patterns of inflamed, benign, and malignant colorectal biopsy specimen and their correlation with peripheral blood results. *Cancer Epidem Biomar* **17**: 2835-2845.

Golby, P., S. Davies, D.J. Kelly, J.R. Guest & S.C. Andrews, (1999) Identification and characterization of a two-component sensor-kinase and response-regulator system (DcuS-DcuR) controlling gene expression in response to C4-dicarboxylates in Escherichia coli. *J Bacteriol* **181**: 1238-1248.

Golby, P., D.J. Kelly, J.R. Guest & S.C. Andrews, (1998) Transcriptional regulation and organization of the dcuA and dcuB genes, encoding homologous anaerobic C4-dicarboxylate transporters in Escherichia coli. *J Bacteriol* **180**: 6586-6596.

Gorke, B. & J. Stulke, (2008) Carbon catabolite repression in bacteria: many ways to make the most out of nutrients. *Nat Rev Microbiol* **6**: 613-624.

Guilfoyle, D.E. & I.N. Hirshfield, (1996) The survival benefit of short-chain organic acids and the inducible arginine and lysine decarboxylase genes for Escherichia coli. *Lett Appl Microbiol* **22**: 393-396.

Gutowski, S.J. & H. Rosenberg, (1975) Succinate uptake and related proton movements in Escherichia coli K12. *Biochem J* **152**: 647-654.

Haila, S., J. Hastbacka, T. Bohling, M.L. Karjalainen-Lindsberg, J. Kere & U. Saarialho-Kere, (2001) SLC26A2 (diastrophic dysplasia sulfate transporter) is expressed in developing and mature cartilage but also in other tissues and cell types. *J Histochem Cytochem* **49**: 973-982.

Hallworth, R. & M.G. Nichols, (2012) Prestin in HEK cells is an obligate tetramer. *J Neurophysiol* **107**: 5-11.

Hamilton, C.M., M. Aldea, B.K. Washburn, P. Babitzke & S.R. Kushner, (1989) New method for generating deletions and gene replacements in Escherichia coli. *J Bacteriol* **171**: 4617-4622.

Harwood, C.R. & S.M. Cutting, (1990) *Molecular biological methods for Bacillus*. Wiley New York:.

Hastbacka, J., A. de la Chapelle, M.M. Mahtani, G. Clines, M.P. Reeve-Daly, M. Daly, B.A. Hamilton, K. Kusumi, B. Trivedi, A. Weaver & et al., (1994) The diastrophic

dysplasia gene encodes a novel sulfate transporter: positional cloning by fine-structure linkage disequilibrium mapping. *Cell* **78**: 1073-1087.

Hastbacka, J., A. Superti-Furga, W.R. Wilcox, D.L. Rimoin, D.H. Cohn & E.S. Lander, (1996) Atelosteogenesis type II is caused by mutations in the diastrophic dysplasia sulfate-transporter gene (DTDST): evidence for a phenotypic series involving three chondrodysplasias. *Am J Hum Genet* **58**: 255-262.

Hatzios, S.K. & C.R. Bertozzi, (2011) The regulation of sulfur metabolism in Mycobacterium tuberculosis. *PLoS pathogens* **7**: e1002036.

Hawkesford, M.J. & L.J. De Kok, (2006) Managing sulphur metabolism in plants. *Plant Cell Environ* **29**: 382-395.

Hayashi, H. & Y. Yamashita, (2012) Role of N-glycosylation in cell surface expression and protection against proteolysis of the intestinal anion exchanger SLC26A3. *Am J Physiol* **302**: C781-795.

He, B., K.Y. Choi & H. Zalkin, (1993) Regulation of Escherichia coli glnB, prsA, and speA by the purine repressor. *J Bacteriol* **175**: 3598-3606.

Hecker, M., J. Pane-Farre & U. Volker, (2007) SigB-dependent general stress response in Bacillus subtilis and related gram-positive bacteria. *Ann Rev Microbiol* **61**: 215-236.

Heneghan, J.F., A. Akhavein, M.J. Salas, B.E. Shmukler, L.P. Karniski, D.H. Vandorpe & S.L. Alper, (2010) Regulated transport of sulfate and oxalate by SLC26A2/DTDST. *American journal of physiology. Cell Physiol* **298**: C1363-1375.

Herrou, J. & S. Crosson, (2011) Function, structure and mechanism of bacterial photosensory LOV proteins. *Nature reviews. Microbiology* **9**: 713-723.

Hoglund, P., C. Holmberg, P. Sherman & J. Kere, (2001) Distinct outcomes of chloride diarrhoea in two siblings with identical genetic background of the disease: implications for early diagnosis and treatment. *Gut* **48**: 724-727.

Hommais, F., E. Krin, J.Y. Coppee, C. Lacroix, E. Yeramian, A. Danchin & P. Bertin, (2004) GadE (YhiE): a novel activator involved in the response to acid environment in Escherichia coli. *Microbiology* **150**: 61-72.

Hove-Jensen, B., K.W. Harlow, C.J. King & R.L. Switzer, (1986) Phosphoribosylpyrophosphate synthetase of Escherichia coli. Properties of the purified enzyme and primary structure of the prs gene. *J Biol Chem* **261**: 6765-6771.

Jack, R., M. De Zamaroczy & M. Merrick, (1999) The signal transduction protein GlnK is required for NifL-dependent nitrogen control of nif gene expression in Klebsiella pneumoniae. *J Bacteriol* **181**: 1156-1162.

Jack, R.L., F. Sargent, B.C. Berks, G. Sawers & T. Palmer, (2001) Constitutive expression of Escherichia coli tat genes indicates an important role for the twin-arginine translocase during aerobic and anaerobic growth. *J Bacteriol* **183**: 1801-1804.

Jackson, G.C., L. Mittaz-Crettol, J.A. Taylor, G.R. Mortier, J. Spranger, B. Zabel, M. Le Merrer, V. Cormier-Daire, C.M. Hall, A. Offiah, M.J. Wright, R. Savarirayan, G. Nishimura, S.C. Ramsden, R. Elles, L. Bonafe, A. Superti-Furga, S. Unger, A. Zankl & M.D. Briggs, (2012) Pseudoachondroplasia and multiple epiphyseal dysplasia: a 7-year comprehensive analysis of the known disease genes identify novel and recurrent mutations and provides an accurate assessment of their relative contribution. *Hum Mutat* **33**: 144-157.

Janausch, I.G., O.B. Kim & G. Unden, (2001) DctA- and Dcu-independent transport of succinate in Escherichia coli: contribution of diffusion and of alternative carriers. *Arch Microbiol* **176**: 224-230.

Janausch, I.G. & G. Unden, (1999) The dcuD (former yhcL) gene product of escherichia coli as a member of the DcuC family of C4-dicarboxylate carriers: lack of evident expression. *Arch Microbiol* **172**: 219-226.

Janausch, I.G., E. Zientz, Q.H. Tran, A. Kroger & G. Unden, (2002) C4-dicarboxylate carriers and sensors in bacteria. *Biochim Biophys Acta* **1553**: 39-56.

Javelle, A., D. Lupo, X.D. Li, M. Merrick, M. Chami, P. Ripoche & F.K. Winkler, (2007) Reprint of "Structural and mechanistic aspects of Amt/Rh proteins" [J. Struct. Biol. 158 (2007) 472-481]. *J Struct Biol* **159**: 243-252.

Javelle, A., E. Severi, J. Thornton & M. Merrick, (2004) Ammonium sensing in Escherichia coli. Role of the ammonium transporter AmtB and AmtB-GlnK complex formation. *J Biol Chem* **279**: 8530-8538.

Jennings, M.L. & J. Cui, (2012) Inactivation of Saccharomyces cerevisiae sulfate transporter Sul2p: use it and lose it. *Biophys J* **102**: 768-776.

Jensen, L.J., M. Kuhn, M. Stark, S. Chaffron, C. Creevey, J. Muller, T. Doerks, P. Julien, A. Roth, M. Simonovic, P. Bork & C. von Mering, (2009) STRING 8--a global view on proteins and their functional interactions in 630 organisms. *Nucleic Acids Res* **37**: D412-416.

Jishage, M. & A. Ishihama, (1998) A stationary phase protein in Escherichia coli with binding activity to the major sigma subunit of RNA polymerase. *PNAS* **95**: 4953-4958.

Jishage, M. & A. Ishihama, (1999) Transcriptional organization and in vivo role of the Escherichia coli rsd gene, encoding the regulator of RNA polymerase sigma D. *J Bacteriol* **181**: 3768-3776.

Johnson, D.A., S.G. Tetu, K. Phillippy, J. Chen, Q. Ren & I.T. Paulsen, (2008) High-throughput phenotypic characterization of Pseudomonas aeruginosa membrane transport genes. *PLoS genetics* **4**: e1000211.

Jurk, M., P. Schramm & P. Schmieder, (2013) The blue-light receptor YtvA from Bacillus subtilis is permanently incorporated into the stressosome independent of the illumination state. *Biochem Bioph Res Co* **432**: 499-503.

Karimova, G., J. Pidoux, A. Ullmann & D. Ladant, (1998) A bacterial two-hybrid system based on a reconstituted signal transduction pathway. *PNAS* **95**: 5752-5756.

Karinou, E., E.L. Compton, M. Morel & A. Javelle, (2013) The Escherichia coli SLC26 homologue YchM (DauA) is a C(4)-dicarboxylic acid transporter. *Mol Microbiol* **87**: 623-640.

Kay, W.W. & H.L. Kornberg, (1971) The uptake of C4-dicarboxylic acids by Escherichia coli. *Eur J Biochem* **18**: 274-281.

Kim, O.B., J. Reimann, H. Lukas, U. Schumacher, J. Grimpo, P. Dunnwald & G. Unden, (2009) Regulation of tartrate metabolism by TtdR and relation to the DcuS-DcuR-regulated C4-dicarboxylate metabolism of Escherichia coli. *Microbiology* **155**: 3632-3640.

Kleefeld, A., (2002) Der Einfluss der C4-Dicarboxylat-Carrier DcuB und DctA auf die DcuSR-abhängige Genregulation in Escherichia coli. In.: Johannes Gutenberg-Universität, Mainz, pp.

Kleefeld, A., B. Ackermann, J. Bauer, J. Kramer & G. Unden, (2009) The fumarate/succinate antiporter DcuB of Escherichia coli is a bifunctional protein with sites for regulation of DcuS-dependent gene expression. *J Biol Chem* **284**: 265-275.

Kneuper, H., I.G. Janausch, V. Vijayan, M. Zweckstetter, V. Bock, C. Griesinger & G. Unden, (2005) The nature of the stimulus and of the fumarate binding site of the fumarate sensor DcuS of Escherichia coli. *J Biol Chem* **280**: 20596-20603.

Ko, S.B., N. Shcheynikov, J.Y. Choi, X. Luo, K. Ishibashi, P.J. Thomas, J.Y. Kim, K.H. Kim, M.G. Lee, S. Naruse & S. Muallem, (2002) A molecular mechanism for aberrant CFTR-dependent HCO(3)(-) transport in cystic fibrosis. *The EMBO journal* **21**: 5662-5672.

Ko, S.B., W. Zeng, M.R. Dorwart, X. Luo, K.H. Kim, L. Millen, H. Goto, S. Naruse, A. Soyombo, P.J. Thomas & S. Muallem, (2004) Gating of CFTR by the STAS domain of SLC26 transporters. *Nat Cell Biol* **6**: 343-350.

Kobayashi, T., T. Sugimoto, K. Saijoh, M. Fujii & K. Chihara, (1997) Cloning and characterization of the 5'-flanking region of the mouse diastrophic dysplasia sulfate transporter gene. *Biochem Bioph Res Co* **238**: 738-743.

Kosiek, O., S.M. Busque, M. Foller, N. Shcheynikov, P. Kirchhoff, M. Bleich, S. Muallem & J.P. Geibel, (2007) SLC26A7 can function as a chloride-loading mechanism in parietal cells. *Pflugers Archiv* **454**: 989-998.

Kramer, J., J.D. Fischer, E. Zientz, V. Vijayan, C. Griesinger, A. Lupas & G. Unden, (2007) Citrate sensing by the C4-dicarboxylate/citrate sensor kinase DcuS of Escherichia coli: binding site and conversion of DcuS to a C4-dicarboxylate- or citrate-specific sensor. *J Bacteriol* **189**: 4290-4298.

Krusell, L., K. Krause, T. Ott, G. Desbrosses, U. Kramer, S. Sato, Y. Nakamura, S. Tabata, E.K. James, N. Sandal, J. Stougaard, M. Kawaguchi, A. Miyamoto, N. Suganuma & M.K. Udvardi, (2005) The sulfate transporter SST1 is crucial for symbiotic nitrogen fixation in Lotus japonicus root nodules. *Plant cell* **17**: 1625-1636.

Lamarche, M.G., B.L. Wanner, S. Crepin & J. Harel, (2008) The phosphate regulon and bacterial virulence: a regulatory network connecting phosphate homeostasis and pathogenesis. *FEMS Microbiol Rev* **32**: 461-473.

Lamprecht, G., V. Gaco, J.R. Turner, D. Natour & M. Gregor, (2009) Regulation of the intestinal anion exchanger DRA (downregulated in adenoma). *Ann NY Acad Sci* **1165**: 261-266.

Lee, S.J., W. Boos, J.P. Bouche & J. Plumbridge, (2000) Signal transduction between a membrane-bound transporter, PtsG, and a soluble transcription factor, Mlc, of Escherichia coli. *The EMBO journal* **19**: 5353-5361.

Lei, G.S., W.J. Syu, P.H. Liang, K.F. Chak, W.S. Hu & S.T. Hu, (2011) Repression of btuB gene transcription in Escherichia coli by the GadX protein. *BMC microbiology* **11**: 33.

Lo, T.C., M.K. Rayman & B.D. Sanwal, (1972) Transport of succinate in Escherichia coli. I. Biochemical and genetic studies of transport in whole cells. *J Biol Chem* **247**: 6323-6331.

Lohi, H., M. Kujala, S. Makela, E. Lehtonen, M. Kestila, U. Saarialho-Kere, D. Markovich & J. Kere, (2002) Functional characterization of three novel tissue-specific anion exchangers SLC26A7, -A8, and -A9. *J Biol Chem* **277**: 14246-14254.

Loughlin, P., M.C. Shelden, M.L. Tierney & S.M. Howitt, (2002) Structure and function of a model member of the SulP transporter family. *Cell Biochem Bioph* **36**: 183-190.

Lowry, O.H., N.J. Rosebrough, A.L. Farr & R.J. Randall, (1951) Protein measurement with the Folin phenol reagent. *J Biol Chem* **193**: 265-275.

Lukas, H., J. Reimann, O.B. Kim, J. Grimpo & G. Unden, (2010) Regulation of aerobic and anaerobic D-malate metabolism of Escherichia coli by the LysR-type regulator DmlR (YeaT). *J Bacteriol* **192**: 2503-2511.

Maeda, S., C. Sugita, M. Sugita & T. Omata, (2006) Latent nitrate transport activity of a novel sulfate permease-like protein of the cyanobacterium Synechococcus elongatus. *J Biol Chem* **281**: 5869-5876.

Makela, S., R. Eklund, J. Lahdetie, M. Mikkola, O. Hovatta & J. Kere, (2005) Mutational analysis of the human SLC26A8 gene: exclusion as a candidate for male infertility due to primary spermatogenic failure. *Mol Hum Reprod* **11**: 129-132.

Malakooti, J., S. Saksena, R.K. Gill & P.K. Dudeja, (2011) Transcriptional regulation of the intestinal luminal Na(+) and Cl(-) transporters. *Biochem J* **435**: 313-325.

Markovich, D., (2011) Physiological roles of renal anion transporters NaS1 and Sat1. *Am J Physiol* **300**: F1267-1270.

Marles-Wright, J. & R.J. Lewis, (2010) The stressosome: molecular architecture of a signalling hub. *Biochem Soc T* **38**: 928-933.

Marzluf, G.A., (1970) Genetic and metabolic controls for sulfate metabolism in Neurospora crassa: isolation and study of chromate-resistant and sulfate transport-negative mutants. *J Bacteriol* **102**: 716-721.

Marzluf, G.A., (1997) Molecular genetics of sulfur assimilation in filamentous fungi and yeast. *Ann Rev Microbiol* **51**: 73-96.

Masuda, S., K.S. Murakami, S. Wang, C. Anders Olson, J. Donigian, F. Leon, S.A. Darst & E.A. Campbell, (2004) Crystal structures of the ADP and ATP bound forms of the Bacillus anti-sigma factor SpoIIAB in complex with the anti-anti-sigma SpoIIAA. *J Mol Biol* **340**: 941-956.

Melvin, J.E., K. Park, L. Richardson, P.J. Schultheis & G.E. Shull, (1999) Mouse down-regulated in adenoma (DRA) is an intestinal Cl(-)/HCO(3)(-) exchanger and is up-regulated in colon of mice lacking the NHE3 Na(+)/H(+) exchanger. *J Biol Chem* **274**: 22855-22861.

Miller, J.H., (1972) *Experiments in molecular genetics*. Cold Spring Harbor Laboratory Cold Spring Harbor, New York.

Minor, J.S., H.Y. Tang, F.A. Pereira & R.L. Alford, (2009) DNA sequence analysis of SLC26A5, encoding prestin, in a patient-control cohort: identification of fourteen novel DNA sequence variations. *PloS one* **4**: e5762.

Mio, K., Y. Kubo, T. Ogura, T. Yamamoto, F. Arisaka & C. Sato, (2008) The motor protein prestin is a bullet-shaped molecule with inner cavities. *J Biol Chem* **283**: 1137-1145.

Moraes, T.F. & R.A. Reithmeier, (2012) Membrane transport metabolons. *Biochim Biophys Acta* **1818**: 2687-2706.

Mount, D.B. & M.F. Romero, (2004) The SLC26 gene family of multifunctional anion exchangers. *Pflugers Archiv* **447**: 710-721.

Mullis, K., F. Faloona, S. Scharf, R. Saiki, G. Horn & H. Erlich, (1986) Specific enzymatic amplification of DNA in vitro: the polymerase chain reaction. *Cold Spring HarB Symp* **51 Pt 1**: 263-273.

Natorff, R., M. Sienko, J. Brzywczy & A. Paszewski, (2003) The Aspergillus nidulans metR gene encodes a bZIP protein which activates transcription of sulphur metabolism genes. *Mol Microbiol* **49**: 1081-1094.

Navaratnam, D., J.P. Bai, H. Samaranayake & J. Santos-Sacchi, (2005) N-terminal-mediated homomultimerization of prestin, the outer hair cell motor protein. *Bioph J* **89**: 3345-3352.

Neidhardt, F.C., P.L. Bloch & D.F. Smith, (1974) Culture medium for enterobacteria. *J Bacteriol* **119**: 736-747.

Nishimori, I., T. Minakuchi, A. Maresca, F. Carta, A. Scozzafava & C.T. Supuran, (2010) The beta-carbonic anhydrases from Mycobacterium tuberculosis as drug targets. *Curr Pharm Design* **16**: 3300-3309.

Nishino, K., Y. Senda & A. Yamaguchi, (2008) The AraC-family regulator GadX enhances multidrug resistance in Escherichia coli by activating expression of mdtEF multidrug efflux genes. *J Infect Chemother* **14**: 23-29.

O'Donnell, S.M. & G.R. Janssen, (2001) The initiation codon affects ribosome binding and translational efficiency in Escherichia coli of cI mRNA with or without the 5' untranslated leader. *J Bacteriol* **183**: 1277-1283.

Ohana, E., N. Shcheynikov, O.W. Moe & S. Muallem, (2013) SLC26A6 and NaDC-1 transporters interact to regulate oxalate and citrate homeostasis. *JASN* **24**: 1617-1626.

Ohana, E., N. Shcheynikov, M. Park & S. Muallem, (2012) Solute carrier family 26 member a2 (Slc26a2) protein functions as an electroneutral SOFormula/OH-/Cl- exchanger regulated by extracellular Cl. *J Biol Chem* **287**: 5122-5132.

Ohana, E., N. Shcheynikov, D. Yang, I. So & S. Muallem, (2011) Determinants of coupled transport and uncoupled current by the electrogenic SLC26 transporters. *J Gen Physiol* **137**: 239-251.

Ohana, E., D. Yang, N. Shcheynikov & S. Muallem, (2009) Diverse transport modes by the solute carrier 26 family of anion transporters. *J Physiol* **587**: 2179-2185.

Okuda, S., S. Kawashima, K. Kobayashi, N. Ogasawara, M. Kanehisa & S. Goto, (2007) Characterization of relationships between transcriptional units and operon structures in Bacillus subtilis and Escherichia coli. *BMC genomics* **8**: 48.

Oshima, T. & F. Biville, (2006) Functional identification of ygiP as a positive regulator of the ttdA-ttdB-ygjE operon. *Microbiology* **152**: 2129-2135.

Ouesleti, S., V. Brunel, H. Ben Turkia, H. Dranguet, A. Miled, N. Miladi, M.F. Ben Dridi, A. Lavoinne, P. Saugier-Veber & S. Bekri, (2011) Molecular characterization of MPS IIIA, MPS IIIB and MPS IIIC in Tunisian patients. *Clin Chim Acta* **412**: 2326-2331.

Pasqualetto, E., R. Aiello, L. Gesiot, G. Bonetto, M. Bellanda & R. Battistutta, (2010) Structure of the cytosolic portion of the motor protein prestin and functional role of the STAS domain in SLC26/SulP anion transporters. *J Mol Biol* **400**: 448-462.

Pessi, G., C. Blumer & D. Haas, (2001) lacZ fusions report gene expression, don't they? *Microbiology* **147**: 1993-1995.

Petrovic, S., S. Barone, J. Xu, L. Conforti, L. Ma, M. Kujala, J. Kere & M. Soleimani, (2004) SLC26A7: a basolateral Cl-/HCO3- exchanger specific to intercalated cells of the outer medullary collecting duct. *Am J Physiol* **286**: F161-169.

Phizicky, E.M. & S. Fields, (1995) Protein-protein interactions: methods for detection and analysis. *Microbiol Rev* **59**: 94-123.

Pilsyk, S. & A. Paszewski, (2009) Sulfate permeasesphylogenetic diversity of sulfate transport. *Acta Bioch Pol* **56**: 375-384.

Plumbridge, J., (1999) Expression of the phosphotransferase system both mediates and is mediated by Mlc regulation in Escherichia coli. *Molecular microbiology* **33**: 260-273.

Poolman, B. & W.N. Konings, (1993) Secondary solute transport in bacteria. *Biochim Biophys Acta* **1183**: 5-39.

Pos, K.M., P. Dimroth & M. Bott, (1998) The Escherichia coli citrate carrier CitT: a member of a novel eubacterial transporter family related to the 2-oxoglutarate/malate translocator from spinach chloroplasts. *J Bacteriol* **180**: 4160-4165.

Post, D.A., B. Hove-Jensen & R.L. Switzer, (1993) Characterization of the hemA-prs region of the Escherichia coli and Salmonella typhimurium chromosomes: identification of two open reading frames and implications for prs expression. *J Gen Microbiol* **139**: 259-266.

Prasad, S., K.A. Kolln, R.A. Cucci, R.C. Trembath, G. Van Camp & R.J. Smith, (2004) Pendred syndrome and DFNB4-mutation screening of SLC26A4 by denaturing high-performance liquid chromatography and the identification of eleven novel mutations. *Am J Med Genet. Part A* **124A**: 1-9.

Price, G.D. & S.M. Howitt, (2011) The cyanobacterial bicarbonate transporter BicA: its physiological role and the implications of structural similarities with human SLC26 transporters. *Biochem Cell Biol* **89**: 178-188.

Price, G.D., F.J. Woodger, M.R. Badger, S.M. Howitt & L. Tucker, (2004) Identification of a SulP-type bicarbonate transporter in marine cyanobacteria. *PNAS* **101**: 18228-18233.

Rath, A., M. Glibowicka, V.G. Nadeau, G. Chen & C.M. Deber, (2009) Detergent binding explains anomalous SDS-PAGE migration of membrane proteins. *PNAS* **106**: 1760-1765.

Regeer, R.R. & D. Markovich, (2004) A dileucine motif targets the sulfate anion transporter sat-1 to the basolateral membrane in renal cell lines. *Am J Physiol* **287**: C365-372.

Reimold, F.R., J.F. Heneghan, A.K. Stewart, I. Zelikovic, D.H. Vandorpe, B.E. Shmukler & S.L. Alper, (2011) Pendrin function and regulation in Xenopus oocytes. *Cell Physiol Biochem* **28**: 435-450.

Royaux, I.E., K. Suzuki, A. Mori, R. Katoh, L.A. Everett, L.D. Kohn & E.D. Green, (2000) Pendrin, the protein encoded by the Pendred syndrome gene (PDS), is an apical porter of iodide in the thyroid and is regulated by thyroglobulin in FRTL-5 cells. *Endocrinology* **141**: 839-845.

Rozenfeld, J., O. Tal, O. Kladnitsky, L. Adler, E. Efrati, S.L. Carrithers, S.L. Alper & I. Zelikovic, (2012) The pendrin anion exchanger gene is transcriptionally regulated by uroguanylin: a novel enterorenal link. *Am J Physiol* **302**: F614-624.

Saier, M.H., Jr., (1998) Molecular phylogeny as a basis for the classification of transport proteins from bacteria, archaea and eukarya. *Adv Microb Physiol* **40**: 81-136.

Saier, M.H., Jr., (2000) A functional-phylogenetic classification system for transmembrane solute transporters. *MMBR* **64**: 354-411.

Saier, M.H., Jr., B.H. Eng, S. Fard, J. Garg, D.A. Haggerty, W.J. Hutchinson, D.L. Jack, E.C. Lai, H.J. Liu, D.P. Nusinew, A.M. Omar, S.S. Pao, I.T. Paulsen, J.A. Quan, M. Sliwinski, T.T. Tseng, S. Wachi & G.B. Young, (1999) Phylogenetic characterization of novel transport protein families revealed by genome analyses. *Biochim Biophys Acta* **1422**: 1-56.

Saier, M.H., Jr. & I.T. Paulsen, (1999) Paralogous genes encoding transport proteins in microbial genomes. *Res Microbiol* **150**: 689-699.

Sambrook, J., E.F. Fritsch & T. Maniatis, (1989) *Molecular cloning*. Cold spring harbor laboratory press New York.

Sandal, N.N. & K.A. Marcker, (1994) Similarities between a soybean nodulin, Neurospora crassa sulphate permease II and a putative human tumour suppressor. *Trends Biochem Sci* **19**: 19.

Schellenberg, G.D. & C.E. Furlong, (1977) Resolution of the multiplicity of the glutamate and aspartate transport systems of Escherichia coli. *J Biol Chem* **252**: 9055-9064.

Scheu, P.D., O.B. Kim, C. Griesinger & G. Unden, (2010) Sensing by the membrane-bound sensor kinase DcuS: exogenous versus endogenous sensing of C(4)-dicarboxylates in bacteria. *Future Microbiol* **5**: 1383-1402.

Schnedler, N., G. Burckhardt & B.C. Burckhardt, (2011) Glyoxylate is a substrate of the sulfate-oxalate exchanger, sat-1, and increases its expression in HepG2 cells. *J Hepat* **54**: 513-520.

Schweinfest, C.W., D.D. Spyropoulos, K.W. Henderson, J.H. Kim, J.M. Chapman, S. Barone, R.T. Worrell, Z. Wang & M. Soleimani, (2006) slc26a3 (dra)-deficient mice display chloride-losing diarrhea, enhanced colonic proliferation, and distinct up-regulation of ion transporters in the colon. *J Biol Chem* **281**: 37962-37971.

Sharma, A.K., A.C. Rigby & S.L. Alper, (2011a) STAS domain structure and function. *Cell Physiol Biochem* **28**: 407-422.

Sharma, A.K., L. Ye, S.L. Alper & A.C. Rigby, (2012) Guanine nucleotides differentially modulate backbone dynamics of the STAS domain of the SulP/SLC26 transport protein Rv1739c of Mycobacterium tuberculosis. *The FEBS journal* **279**: 420-436.

Sharma, A.K., L. Ye, C.E. Baer, K. Shanmugasundaram, T. Alber, S.L. Alper & A.C. Rigby, (2011b) Solution structure of the guanine nucleotide-binding STAS domain of

SLC26-related SulP protein Rv1739c from Mycobacterium tuberculosis. *J Biol Chem* **286**: 8534-8544.

Shcheynikov, N., D. Yang, Y. Wang, W. Zeng, L.P. Karniski, I. So, S.M. Wall & S. Muallem, (2008) The Slc26a4 transporter functions as an electroneutral Cl-/I-/HCO3- exchanger: role of Slc26a4 and Slc26a6 in I- and HCO3- secretion and in regulation of CFTR in the parotid duct. *J Physiol* **586**: 3813-3824.

Sheffield, V.C., Z. Kraiem, J.C. Beck, D. Nishimura, E.M. Stone, M. Salameh, O. Sadeh & B. Glaser, (1996) Pendred syndrome maps to chromosome 7q21-34 and is caused by an intrinsic defect in thyroid iodine organification. *Nat Genet* **12**: 424-426.

Shelden, M.C., S.M. Howitt & G.D. Price, (2010) Membrane topology of the cyanobacterial bicarbonate transporter, BicA, a member of the SulP (SLC26A) family. *Mol Membr Biol* **27**: 12-23.

Shibagaki, N. & A.R. Grossman, (2006) The role of the STAS domain in the function and biogenesis of a sulfate transporter as probed by random mutagenesis. *J Biol Chem* **281**: 22964-22973.

Shibagaki, N. & A.R. Grossman, (2010) Binding of cysteine synthase to the STAS domain of sulfate transporter and its regulatory consequences. *J Biol Chem* **285**: 25094-25102.

Shin, S., M.P. Castanie-Cornet, J.W. Foster, J.A. Crawford, C. Brinkley & J.B. Kaper, (2001) An activator of glutamate decarboxylase genes regulates the expression of enteropathogenic Escherichia coli virulence genes through control of the plasmid-encoded regulator, Per. *Mol Microbiol***41**: 1133-1150.

Silhavy, T.J. & J.R. Beckwith, (1985) Uses of lac fusions for the study of biological problems. *Microbiol Rev* **49**: 398-418.

Six, S., S.C. Andrews, G. Unden & J.R. Guest, (1994) Escherichia coli possesses two homologous anaerobic C4-dicarboxylate membrane transporters (DcuA and DcuB) distinct from the aerobic dicarboxylate transport system (Dct). *J Bacteriol* **176**: 6470-6478.

Stewart, A.K., B.E. Shmukler, D.H. Vandorpe, F. Reimold, J.F. Heneghan, M. Nakakuki, A. Akhavein, S. Ko, H. Ishiguro & S.L. Alper, (2011) SLC26 anion exchangers of guinea pig pancreatic duct: molecular cloning and functional characterization. *Am J Physiol* **301**: C289-303.

Swulius, M.T. & G.J. Jensen, (2012) The helical MreB cytoskeleton in Escherichia coli MC1000/pLE7 is an artifact of the N-Terminal yellow fluorescent protein tag. *J Bacteriol* **194**: 6382-6386.

Taddese, R., (2013) Role of the STAS domain of the E. coli anion transporter YchM. In.: University of Toronto, pp.

Takahashi, H., A. Watanabe-Takahashi, F.W. Smith, M. Blake-Kalff, M.J. Hawkesford & K. Saito, (2000) The roles of three functional sulphate transporters involved in uptake and translocation of sulphate in Arabidopsis thaliana. *Plant* **23**: 171-182.

Tang, Y., Z. Cao, E. Livoti, U. Krauss, K.E. Jaeger, W. Gartner & A. Losi, (2010) Interdomain signalling in the blue-light sensing and GTP-binding protein YtvA: a mutagenesis study uncovering the importance of specific protein sites. *Photochem Photobiol Sci* **9**: 47-56.

Tenu, J.P., O.M. Viratelle, J. Garnier & J. Yon, (1971) pH dependence of the activity of beta-galactosidase from Escherichia coli. *Eur J Biochem* **20**: 363-370.

Tetsch, L., C. Koller, I. Haneburger & K. Jung, (2008) The membrane-integrated transcriptional activator CadC of Escherichia coli senses lysine indirectly via the interaction with the lysine permease LysP. *Mol Microbiol* **67**: 570-583.

Thakker, C., I. Martinez, K.Y. San & G.N. Bennett, (2012) Succinate production in Escherichia coli. *Biotech J* **7**: 213-224.

Toure, A., P. Lhuillier, J.A. Gossen, C.W. Kuil, D. Lhote, B. Jegou, D. Escalier & G. Gacon, (2007) The testis anion transporter 1 (Slc26a8) is required for sperm terminal differentiation and male fertility in the mouse. *Hum Mol Genet* **16**: 1783-1793.

Toure, A., L. Morin, C. Pineau, F. Becq, O. Dorseuil & G. Gacon, (2001) Tat1, a novel sulfate transporter specifically expressed in human male germ cells and potentially linked to rhogtpase signaling. *J Biol Chem* **276**: 20309-20315.

Tramonti, A., M. De Canio & D. De Biase, (2008) GadX/GadW-dependent regulation of the Escherichia coli acid fitness island: transcriptional control at the gadY-gadW divergent promoters and identification of four novel 42 bp GadX/GadW-specific binding sites. *Mol Microbiol* **70**: 965-982.

Tramonti, A., P. Visca, M. De Canio, M. Falconi & D. De Biase, (2002) Functional characterization and regulation of gadX, a gene encoding an AraC/XylS-like transcriptional activator of the Escherichia coli glutamic acid decarboxylase system. *J Bacteriol* **184**: 2603-2613.

Tucker, D.L., N. Tucker & T. Conway, (2002) Gene expression profiling of the pH response in Escherichia coli. *J Bacteriol* **184**: 6551-6558.

Ullmann, R., R. Gross, J. Simon, G. Unden & A. Kroger, (2000) Transport of C(4)-dicarboxylates in Wolinella succinogenes. *J Bacteriol* **182**: 5757-5764.

Unden, G. & J. Bongaerts, (1997) Alternative respiratory pathways of Escherichia coli: energetics and transcriptional regulation in response to electron acceptors. *Biochim Biophys Acta* **1320**: 217-234.

Unden, G. & A. Kleefeld, (2004) C4-Dicarboxylate degradation in aerobic and anaerobic growth, Module 3.4. 5 In R. Curtiss III (Editor in Chief), EcoSal-Escherichia coli and Salmonella. *Cellular and Molecular Biology.(Online) http://www. ecosal. org. ASM Press, Washington, DC.*

van de Kamp, M., E. Pizzinini, A. Vos, T.R. van der Lende, T.A. Schuurs, R.W. Newbert, G. Turner, W.N. Konings & A.J. Driessen, (1999) Sulfate transport in Penicillium chrysogenum: cloning and characterization of the sutA and sutB genes. *J Bacteriol* **181**: 7228-7234.

Vincourt, J.B., D. Jullien, F. Amalric & J.P. Girard, (2003) Molecular and functional characterization of SLC26A11, a sodium-independent sulfate transporter from high endothelial venules. *FASEB* **17**: 890-892.

Wang, X., S. Yang, S. Jia & D.Z. He, (2010) Prestin forms oligomer with four mechanically independent subunits. *Brain Res* **1333**: 28-35.

Wang, Z., S. Petrovic, E. Mann & M. Soleimani, (2002) Identification of an apical Cl(-)/HCO3(-) exchanger in the small intestine. *Am J Physiol* **282**: G573-579.

Wedenoja, S., E. Pekansaari, P. Hoglund, S. Makela, C. Holmberg & J. Kere, (2011) Update on SLC26A3 mutations in congenital chloride diarrhea. *Hum Mutat* **32**: 715-722.

Weinstock, G.M., (2002) Transduction in gram-negative bacteria.

Witan, J., J. Bauer, I. Wittig, P.A. Steinmetz, W. Erker & G. Unden, (2012a) Interaction of the Escherichia coli transporter DctA with the sensor kinase DcuS: presence of functional DctA/DcuS sensor units. *Mol Microbiol* **85**: 846-861.

Witan, J., C. Monzel, P.D. Scheu & G. Unden, (2012b) The sensor kinase DcuS of Escherichia coli: two stimulus input sites and a merged signal pathway in the DctA/DcuS sensor unit. *Biol Chem* **393**: 1291-1297.

Xie, Q., R. Welch, A. Mercado, M.F. Romero & D.B. Mount, (2002) Molecular characterization of the murine Slc26a6 anion exchanger: functional comparison with Slc26a1. *Am J Physiol* **283**: F826-838.

Yanisch-Perron, C., J. Vieira & J. Messing, (1985) Improved M13 phage cloning vectors and host strains: nucleotide sequences of the M13mp18 and pUC19 vectors. *Gene* **33**: 103-119.

Ye, H., X.Q. Zhang, S. Broughton, S. Westcott, D. Wu, R. Lance & C. Li, (2011) A nonsense mutation in a putative sulphate transporter gene results in low phytic acid in barley. *Funct Integr Genomic* **11**: 103-110.

Yoshimoto, N., H. Takahashi, F.W. Smith, T. Yamaya & K. Saito, (2002) Two distinct high-affinity sulfate transporters with different inducibilities mediate uptake of sulfate in Arabidopsis roots. *Plant* **29**: 465-473.

Yusa, A., K. Miyazaki, N. Kimura, M. Izawa & R. Kannagi, (2010) Epigenetic silencing of the sulfate transporter gene DTDST induces sialyl Lewisx expression and accelerates proliferation of colon cancer cells. *Cancer Res***70**: 4064-4073.

Zheng, J., G.G. Du, C.T. Anderson, J.P. Keller, A. Orem, P. Dallos & M. Cheatham, (2006) Analysis of the oligomeric structure of the motor protein prestin. *J Biol Chem* **281**: 19916-19924.

Zheng, J., W. Shen, D.Z. He, K.B. Long, L.D. Madison & P. Dallos, (2000) Prestin is the motor protein of cochlear outer hair cells. *Nature* **405**: 149-155.

Zientz, E., J. Bongaerts & G. Unden, (1998) Fumarate regulation of gene expression in Escherichia coli by the DcuSR (dcuSR genes) two-component regulatory system. *J Bacteriol* **180**: 5421-5425.

Zientz, E., I.G. Janausch, S. Six & G. Unden, (1999) Functioning of DcuC as the C4-dicarboxylate carrier during glucose fermentation by Escherichia coli. *J Bacteriol* **181**: 3716-3720.

Zientz, E., S. Six & G. Unden, (1996) Identification of a third secondary carrier (DcuC) for anaerobic C4-dicarboxylate transport in Escherichia coli: roles of the three Dcu carriers in uptake and exchange. *J Bacteriol* **178**: 7241-7247.

Zolotarev, A.S., M. Unnikrishnan, B.E. Shmukler, J.S. Clark, D.H. Vandorpe, N. Grigorieff, E.J. Rubin & S.L. Alper, (2008) Increased sulfate uptake by E. coli overexpressing the SLC26-related SulP protein Rv1739c from Mycobacterium tuberculosis. *Comp Biochem Phys A* **149**: 255-266.

8 Appendices

8.1 Appendix A: Media, Buffers and Solutions

Luria–Bertani (LB) broth (1l)	10 g Casein
	5 g Yeast extract
	5 g NaCl
MacConkey agar (1l) pH7.1	17 g Peptone
	3 g Proteose Peptone
	10 g Lactose
	5 g NaCl
	1 mg Crystal Violet
	30 mg Neutral Red
	1.5 g Bile Salts
	13.5 g Agar
1x M9 minimal medium* (1l)	6 g Na_2HPO_4 (anhydrous)
	3 g KH_2PO_4
	0.5 g NaCl
	1 g NH_4Cl
	1 ml $MgSO_4$ (1 M)
	1 ml $CaCl_2$ (0.1 M)

Enriched M9 (eM9) minimal medium* (1l)

	1x M9 minimal medium
	10 ml Acid-hydrolysed casein (10%)
	5 ml L-tryptophan (1%)

*pH 7.4

1x MOPS minimal medium (1l)*	100 ml MOPS mixture (10x)
	10 ml K_2HPO_4 (0.132 M)
10x MOPS mixture (1l)	83.72 g MOPS
	7.17 g tricine
	10 ml $FeSO_4 \cdot 7\ H_2O$ (0.01 M)
	50 ml NH_4Cl (1.9 M)
	10 ml K_2SO_4 (0.276 M)
	0.25 ml $CaCl_2 \cdot 2\ H_2O$ (0.02 M)
	2.1 ml $MgCl_2$ (2.5 M)
	100 ml NaCl (5 M)
	0.2 ml Micronutrient stock
Micronutrient stock (50 ml)	0.009 g $(NH_4)_6Mo_7O_{24} \cdot 4\ H_2O$
	0.062 g H_3BO_3
	0.018 g $CoCl_2$

	0.006 $CuSO_4$
	0.04 g $MnCl_2$
	0.007 g $ZnSO_4$

*pH 7.4

gDNA extraction

Lysis buffer	0.1 M NaCl
	0.05 M EDTA (pH 7.5)

P1 lysate preparation and transduction

MC buffer	0.1 M $MgSO_4$
	5 mM $CaCl_2$
R plates	LB broth
	0.1% glucose
	2 mM $CaCl_2$
	1.2% agar
LBMC soft agar	LB broth
	5 mM $CaCl_2$
	10 mM $MgSO_4$

	0.65% agar
TGYES medium	1% tryptone 0.5% yeast extract 1% NaCl 0.2% glucose

β-galactosidase activity assay

Z-buffer (1l)	8.52 g Na_2HPO_4 (anhydrous) 6.24 g NaH_2PO_4 0.75 g KCl 0.25 g $MgSO_4 \cdot 7\ H_20$

SDS-PAGE

Solution 2	1.5 M Tris-HCl, pH 8.8 0.3% SDS
Solution 3	0.5 M Tris-HCl, pH 6.8 0.4% SDS
Running buffer	25 mM Tris-HCl (pH 8.3) 192 mM Glycine 0.1 % (w/v) SDS
5x SDS loading buffer	2.25 ml Tris-HCl (1 M), pH 6.8

	5 ml Glycerol
	0.5 g SDS
	5 mg Bromophenol blue
	2.5 ml DTT (1 M)

Coomassie staining

Coomassie stain	50 % (v/v) Ethanol
	7.5 % (v/v) Acetic Acid
	0.1 % (w/v) Coomassie Brilliant Blue
Coomassie destain	50 % (v/v) Methanol
	10 % (v/v) Acetic Acid

Protein purification

Lysis buffer	Buffer A
	10 µg/ml DNase
	10 mM $MgCl_2$
	200 µg/ml PMSF
Buffer A	50 mM Tris, pH 8
	300 mM NaCl
	10% glycerol

Buffer B	50 mM Tris, pH 8
	300 mM NaCl
	10% glycerol
	500 mM imidazole
Wash buffer 1	50 mM Tris, pH 8
	300 mM NaCl
	10% glycerol
	25 mM imidazole
	0.03% DDM
Wash buffer 2	50 mM Tris, pH 8
	300 mM NaCl
	10% glycerol
	35 mM imidazole
	0.03% DDM
Elution buffer	Buffer B
	0.03% DDM

Western immunobloting

10x TBS (1l), pH 7.6	24.2 g Tris base
	80 g NaCl

1x TBST (1l)	100 ml 10x TBS 1 ml Tween 20
1x Transfer buffer (1l)	3.04 g Tris base 14.44 g glycine 20 ml MeOH

Membrane stripping

Stripping buffer (1l), pH 2.2	15 g glycine 1 g SDS 10 ml Tween 20

8.2 Papers published from this study

THE JOURNAL OF BIOLOGICAL CHEMISTRY VOL. 286, NO. 30, pp. 27058–27067, July 29, 2011

Low Resolution Structure of a Bacterial SLC26 Transporter Reveals Dimeric Stoichiometry and Mobile Intracellular Domains*[S]

Received for publication, March 28, 2011, and in revised form, May 26, 2011 Published, JBC Papers in Press, June 9, 2011, DOI 10.1074/jbc.M111.244533

Emma L. R. Compton[†1], **Eleni Karinou**[†2], **James H. Naismith**[§], **Frank Gabel**[¶], **and Arnaud Javelle**[†3]

From the [†]*Division of Molecular Microbiology, College of Life Sciences, University of Dundee, Dundee DD1 5EH, United Kingdom, the* [§]*Biomedical Sciences Research Complex, University of St. Andrews, North Haugh, St. Andrews KY16 9ST, United Kingdom, and the* [¶]*Institut de Biologie Structurale Commissariat à l'Energie Atomique, CNRS, Université Joseph Fourier, 41 rue Jules Horowitz, 38027 Grenoble, France*

The SLC26/SulP (solute carrier/sulfate transporter) proteins are a superfamily of anion transporters conserved from bacteria to man, of which four have been identified in human diseases. Proteins within the SLC26/SulP family exhibit a wide variety of functions, transporting anions from halides to carboxylic acids. The proteins comprise a transmembrane domain containing between 10–12 transmembrane helices followed a by C-terminal cytoplasmic sulfate transporter and anti-sigma factor antagonist (STAS) domain. These proteins are expected to undergo conformational changes during the transport cycle; however, structural information for this family remains sparse, particularly for the full-length proteins. To address this issue, we conducted an expression and detergent screen on bacterial Slc26 proteins. The screen identified a *Yersinia enterocolitica* Slc26A protein as the ideal candidate for further structural studies as it can be purified to homogeneity. Partial proteolysis, co-purification, and analytical size exclusion chromatography demonstrate that the protein purifies as stable oligomers. Using small angle neutron scattering combined with contrast variation, we have determined the first low resolution structure of a bacterial Slc26 protein without spectral contribution from the detergent. The structure confirms that the protein forms a dimer stabilized via its transmembrane core; the cytoplasmic STAS domain projects away from the transmembrane domain and is not involved in dimerization. Supported by additional biochemical data, the structure suggests that large movements of the STAS domain underlie the conformational changes that occur during transport.

The SLC26/SulP[4] proteins are a superfamily of anion transporters conserved from bacteria to man (1). The human genome encodes at least 10 SLC26 proteins that play critical roles in cell physiology and are medically important, being implicated in genetic diseases such as diastrophic dysplasia, congenital chloride diarrhea, Pendred syndrome, and nonsyndromic deafness (2, 3). Proteins within the SLC26/SulP family exhibit a wide variety of functions, transporting anions ranging from halides to carboxylic acids. The molecular basis for this diversity, however, is poorly understood and structural information is extremely limited. A model of the transmembrane region containing 12 transmembrane helices has been published for the *Synechococcus* Slc26 protein BicA, and it has been proposed that this topology may apply across the family (4). A conserved stoichiometry within the family is the subject of debate as several members, across multiple species, have been reported to form dimers and/or tetramers (5–7). The only high resolution structural data available to date is for the cytoplasmic sulfate transporter and anti-sigma factor antagonist (STAS) domain, which is fused to the C terminus of the transmembrane domain (8–10).

SLC26 transporters must undergo sequential conformational changes during the transport cycle as typified by prestin (SLC26A5), the cochlear protein that enables animals to efficiently detect high frequency sounds (11, 12). Upon binding and/or transporting Cl^-/HCO_3^-, prestin transduces a major conformational change into considerable mechanical force leading to a change in the length of the cochlear outer hair cells. Although the motor function of prestin may have evolved at the expense of its transport abilities (12), its electromotile function has evolved from the ability of this protein family to undergo dramatic molecular rearrangements (11, 13). Thus, characterizing the architecture of SLC26 transporters is of particular interest, paving the way to an understanding of their domain organization, structure, and associated conformational changes. Negative stain electron microscopy has been used to generate a low resolution structure of the full-length prestin from rat (5), revealing an apparent bullet-shaped molecule, however; in this case, it was difficult to judge the level of contribution of the associated detergent to the overall structure.

In this work, we have used small angle neutron scattering (SANS) combined with contrast variation to mask the deter-

* This work was supported by grants from Tenovus Scotland (T08/26), the Royal Society (2008/R2), and the Medical Research Council (G1000054).
[S] The on-line version of this article (available at http://www.jbc.org) contains supplemental Figs. S1–S3.
[1] Supported by the College of Life Science (University of Dundee).
[2] Supported by a Biotechnology and Biological Sciences Research Council Doctoral Training Grant BB/F017022/1.
[3] Supported by a Scottish government/Royal Society of Edinburgh personal research fellowship. To whom correspondence should be addressed: Div. of Molecular Microbiology, College of Life Sciences, University of Dundee, Dundee DD1 5EH, UK. Tel.: 44-1382-386-203; Fax: 44-1382388-216; E-mail: ajavelle@dundee.ac.uk.
[4] The abbreviations used are: SulP, sulfate permease; SANS, small angle neutron scattering; STAS, sulfate transporter and anti-sigma antagonist; IMAC, immobilized metal affinity chromatography; SEC, size exclusion chromatography; TEV, tobacco etch virus; CLC, chloride channel.

gent and obtain a low resolution model of a purified SLC26 protein alone in solution, giving the first insight into the domain organization of this important protein family. The structure of the *Y. enterocolitica* Slc26A2 protein shows a homodimer stabilized via its transmembrane core. Our low resolution structure, combined with other structural and biochemical information, provides a structural model for the conformational changes associated with the transport cycle in SLC26/SulP proteins.

EXPERIMENTAL PROCEDURES

Expression and Purification of YeSlc26A2—The GFP gene in the pWaldo-TEV-GFPe plasmid (14) was removed by PCR using two oligonucleotides (5′-ctggaagtacaggttttcggatccagg-3′ and 5′-aacctgtacttccagggtaaaaagcttgcggcccatcatcatcC-3′) to generate the plasmid pArno. The *Y. enterocolitica Yeslc26a2* gene (YE0973) was cloned into pArno between XhoI and BamHI sites using two oligonucleotides: 5′-atgcctcgagaatgtgcaggttttaaaatca-3′ (XhoI site underlined) and 5′-atgcggatccctcaaatttccgctgagacg-3′ (BamHI site underlined).

YeSlc26A2 was overexpressed in *Escherichia coli* strain C41(DE3) and induced with 0.1 mM isopropyl 1-thio-β-D-galactopyranoside for 16 h. Cells were lysed by French press in a buffer containing 50 mM Tris-HCl, pH 8.0, 500 mM NaCl, 2 mM β-mercaptoethanol, 10% glycerol (immobilized metal affinity chromatography (IMAC) buffer) plus 0.2 mM PMSF, 10 μg/ml DNase, 2 mM $MgCl_2$. The membrane fraction was solubilized with 2% *n*-dodecyl β-D-maltoside (Anatrace) and loaded onto a Co^{2+}-affinity column (HisTrap, GE Healthcare). The column was washed with IMAC buffer containing 55 mM imidazole, 0.03% *n*-dodecyl β-D-maltoside, and the YeSlc26A2 protein was eluted using a linear 55–500 mM imidazole gradient. YeSlc26A2 was incubated with TEV protease (10/1 w/w ratio) at 4 °C, and the IMAC purification was repeated to remove noncleaved protein and the His-tagged TEV protease. YeSlc26A2 was further purified by gel filtration in 50 mM Tris-HCl, pH 8.0, 150 mM NaCl, 0.1% Fos-choline-12 (Anatrace). The purified YeSlc26A2 was concentrated by ultrafiltration with a nominal molecular mass limit of 100 kDa (Centricon 100-K, Millipore), then diluted to 4.94 mg/ml in 50 mM Tris-HCl, pH 8.0, 150 mM NaCl, 0.1% Fos-choline-12, 11% D_2O, and dialyzed against the same buffer.

Expression and Purification of YeSlc26A2 STAS Domain—The YeSlc26A2 STAS domain (amino acids 381–483) was cloned into the pEHISTEV plasmid (15) between the NcoI and XhoI sites using two oligonucleotides: 5′-atgccatggtggcgcatgtgatttatgcagag-3′ (NcoI site underlined) and 5′-atgcctcgagttactctcaaatttccgctgag-3′ (XhoI site underlined). The protein was overexpressed in *E. coli* BL21(DE3) cells and purified under the same conditions as the full-length protein except that the detergent was excluded.

Co-purification of His and FLAG-tagged YeSlc26A2—C-terminally FLAG-tagged *Yeslc26a2* was synthesized by PCR using the following primers 5′-atgcgagctcaggaggaatacaccatgtggcaggttttaaaatcaccaaaac-3′ (SacI site underlined) and 5′-atgctctagatcatttatcatcatcatctttataatccgtcaaatttccgctgagacggct-3′ (XbaI site underlined) to clone into plasmid pBAD33 (16) using the SacI/XbaI sites. The sequence encoding C-terminally His-tagged *Yeslc26a2* was introduced in between SmaI and SacI sites in pBADCHIS (15). *Yeslc26a2* was synthesized by PCR using *Yeslc26a2* in pArno as a template (see above) and the following primers 5′-atgcccgggatgtggcaggttttaaaatcacc-3′ (SmaI site underlined) and 5′-atgcgagctctcagtggtggtggtggtgatgatgatgggc-3′ (SacI site underlined). C41(DE3) cells were transformed (or cotransformed) with the pBADCHIS plasmid encoding the C-terminally His-tagged version and/or the pBAD33 plasmid harboring the C-terminal FLAG-tagged version of YeSlc26A2. Cells were induced using 0.02% arabinose and then harvested and lysed by French press, and membranes were solubilized as described above. The solubilized membranes were split into two fractions and incubated with Co^{2+}-loaded Sepharose beads or anti-FLAG M2 affinity gel (Sigma). The Sepharose beads were washed stepwise with IMAC A buffer containing 25 and 35 mM imidazole and YeSlc26A2-His_8 was eluted with 500 mM imidazole. The anti-FLAG M2 affinity gel was washed with IMAC A buffer and YeSlc26A2-FLAG was eluted with 0.1 mM glycine, pH 3.5. Samples were analyzed on SDS-PAGE. For the gel filtration analysis of the His/FLAG tag YeSlc26A2 oligomer, the oligomer was purified by IMAC as described in "Purification of YeSlc26A2" with the exclusion of the TEV proteolysis and second IMAC step.

SANS Experiments and Raw Data Reduction—All samples were measured at 6 °C at the SANS instrument D22 at the Institute Laue-Langevin (Grenoble, France). Raw data were reduced with the Institute Laue-Langevin software package and PRIMUS.

SANS Data Analysis—All samples were measured on instrument D22 at the Institute Laue-Langevin (Grenoble, France) in Hellma® quartz cuvettes 100QS with 1-mm optical path length. The sample temperature was kept at 6 °C during the exposure times. Scattering data from all samples were recorded at two instrumental detector/collimator configurations, 2m/2m and 8m/8m, using a neutron wavelength of $\lambda = 6$ Å. At each configuration, the H_2O/D_2O buffers, the empty beam, an empty quartz cuvette, as well as a boron sample (electronic background) were measured. Exposure times varied between 20 min (empty cell, boron) and 2 h (YeSlc26A2 at 11% D_2O) according to sample and instrument setup. Transmissions were measured during 3-min exposure times for each sample. The raw data were reduced (detector efficiency, electronic background, angular averaging) using a standard Institute Laue-Langevin software package. Finally, the corrected scattered intensities $I(Q)$ ($Q = (4\pi/\lambda)\sin\theta$, where 2θ is the scattering angle) from the two different Q ranges were merged, and the respective buffer signals were subtracted using the program "PRIMUS."

Contrast Variation Series and Structural Properties of Fos-choline-12 Detergent—To find the contrast match-point of Fos-choline-12 a contrast series of Fos-choline-12 ($C = 5$ mg/ml) at 0, 10, 50, 90, and 100% D_2O were measured and used to plot $(I(0)/(T_sC))^{1/2}$ as a function of percentage of D_2O in the solvent (T_s, sample transmission; I, intensity). The measured transmissions T_s of the samples were 0.5286 (0% D_2O), 0.5593 (10% D_2O), 0.6906 (50% D_2O), 0.8592 (90% D_2O), and 0.9164 (100% D_2O). The respective $I(0)$ values determined were as follows (in the same order): 0.014, 0.001, 0.16, 0.771, and

1.217. The Fos-choline-12 contrast match point was determined by the intersection of a linear fit through all points with the abscissa (Fig. 2*B*).

Molecular Weight, Radii of Gyration of YeSlc26A2 Determined by SANS—The radii of gyration R_g and the intensities in the forward scattering direction, $I(0)$, of all samples were extracted by the Guinier approximation.

$$\ln[I(Q)] = \ln[I(0)] - 1/3R_g^2Q^2 \quad \text{(Eq. 1)}$$

The validity of the Guinier approximation, $R_gQ \leq 1.3$, was verified and fulfilled in each case.

The protein molecular weight, was determined from the $I(0)$ intensity at 11% D_2O using absolute calibration against H_2O under the assumption that the detergent (free micelles and bound) had a negligible contribution at the contrast match point.

Molecular weight of YeSlc26A2 determined by SANS—The protein molecular weight, M_w, was determined from the $I(0)$ intensity in 11% D_2O (17) under the assumption that the detergent (free micelles and protein bound) has a negligible contribution at the contrast conditions measured.

$$M = \frac{I_{inc}(0)}{I(0)} \frac{f4\pi T_s}{1 - T_w} N_A C t 10^{-3} \left[\left(\frac{1}{V} \sum_i b - \rho_N^o \right) V \right]^2 \quad \text{(Eq. 2)}$$

$I(0)$ is the coherent macromolecular scattering in the forward direction, $I_{inc}(0)$ is the incoherent scattering from the solvent in the forward direction, T_s and T_w are the transmissions of the sample and of water, respectively, C is the protein concentration in mg/ml, t is the thickness of the quartz cuvette in cm, f is a correction factor for the anisotropicity of the solvent scattering as a function of neutron wavelength, $\sum_i b$ is the scattering length density of the protein in cm (calculated from (18)), ρ_N^o is the solvent neutron scattering density in cm^{-2}, and V is the solvent-displaced protein volume in cm^3. The values used were as follows: $f = 0.82$; $t = 0.1$ cm, $I(0) = 0.0432$, $I_{inc}(0) = 1.00$, $T_S = 0.567$, $T_W = 0.531$, $N_A = 6.023 \cdot 10^{23}$, $C = 4.94$ mg/ml, $V = 6.582 \cdot 10^{-20}$ cm^3, $\sum_i b = 1.21 \cdot 10^{-9}$ cm, and $\rho_N^o = 1.77 \cdot 109$ cm^{-2}. (The solvent scattering density was calculated for 10.6% D_2O, which was determined experimentally from the transmission analysis.)

Low Resolution Models Determined by Ab Initio Analysis Using DAMMIN—We used the program DAMMIN (19) to generate a low resolution envelope of YeSlc26A2 from the 5 mg/ml SANS data at the contrast match point of the Fos-choline-12 detergent. We used several variations of the program parameters using either default or expert mode with and without P2 symmetry to model the data up to $Q_{max} = 0.141$ $Å^{-1}$. Beyond this Q value, the experimental data were too noisy to support a modeling procedure. The DAMMIN input files were generated using the program GNOM imposing the restraints $p(r = 0) = 0$ and $p(r = D_{max}) = 0$ for the pair distance distribution function. The values of D_{max} were varied between 110 and 130 Å. As a quality control, the radii of gyration determined from the pair distribution analyses were compared with that determined by the Guinier analysis of the SANS data (R_g = 40.7 ± 4.1 Å). The best results were obtained for $D_{max} = 120$ Å, yielding a radius of gyration of 38.5 ± 2.6 Å from the $p(r)$ function. Although DAMMIN only generates a single model, its mirror image molecule would also fulfill exactly the same criteria. Without independent information, it is impossible to judge which stereoisomer is correct. We used the fit to the recently published SLC26A6 model to select which DAMMIN model to use (20). MmSLC26A6 coordinates were supplied by Dr. Ehud Ohana (National Institutes of Health, Bethesda, MD).

RESULTS

YeSlc26A2 Purifies as Stable Oligomer—Mammalian integral membrane proteins are notoriously difficult to handle; thus, studies on prokaryotic homologues have proven crucial in characterizing the structure and function of their human counterparts (21). We cloned 27 genes encoding bacterial proteins (Fig. 1) that carried the SLC26 signatures (Prosite 01130) and cytoplasmic STAS domains (InterPro 002645). A subsequent expression and detergent screen identified the *Y. enterocolitica* protein YP001005307.1 (hereafter referred to as YeSlc26A2) as the ideal candidate for further structural studies as it can be purified to homogeneity in the detergent Fos-choline-12 and elutes as a single, stable and symmetrical peak from size exclusion chromatography (Fig. 2*A*). A first indication as to the oligomeric state of YeSlc26A2 came from its behavior during IMAC. Deliberate partial proteolysis of YeSlc26A2 expressed with a TEV protease-cleavable, C-terminal His-tag yielded a mixture of His-tagged and untagged proteins, as judged by SDS-PAGE (Fig. 2*B*) and Western immunoblot (data not shown). When purified by IMAC, the majority of the untagged protein flowed through the column. However, a small amount remained tightly bound and eluted with the tagged protein under high imidazole conditions, suggesting that YeSlc26A2 formed oligomers comprising tagged and untagged proteins (Fig. 2*B*). To further investigate the oligomeric state of YeSlc26A2, C-terminally FLAG- and His-tagged versions were co-expressed and purified by parallel IMAC and anti-FLAG affinity chromatography. When expressed in isolation the proteins were eluted from their expected affinity matrix and showed no cross-reactivity (Fig. 2*C*). However, when co-expressed the FLAG-tagged protein was eluted from the IMAC matrix, and the His-tagged protein was eluted from the Anti-FLAG matrix, a result strongly indicative that YeSlc26A2 forms mixed His-/FLAG-tagged oligomers (Fig. 2*C*). Size exclusion chromatography of the oligomeric His/FLAG proteins showed a single symmetrical peak containing both His- and FLAG-tagged proteins with no protein present at the void volume confirming that stable oligomers were formed rather than aggregates (Fig. 2*D*). The related distribution coefficient (K_{av}) corresponded to a mass of ~180 kDa, suggesting a trimeric or dimeric state (monomer, 54.4 kDa) (Fig. 2*D* and supplemental Fig. S1).

SANS Data Demonstrate YeSlc26A2 Is a Dimer—A critical problem in deriving low resolution structural information from purified membrane proteins is the complex nature of a sample that contains both free detergent micelles and protein surrounded by detergent. Most commonly used techniques are unable to differentiate between the protein and detergent, thus making data collection from the protein alone difficult. SANS,

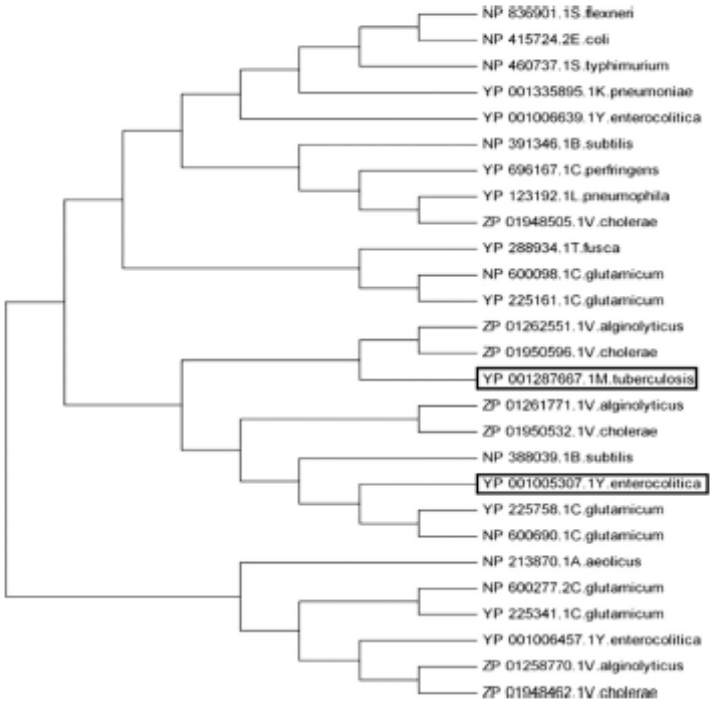

FIGURE 1. **Phylogenetic relationships of the 27 bacterial SulP/SLC26A proteins used for the initial expression screen.** Complete amino acid sequences were aligned with ClustalW and the tree was constructed by the neighbor-joining method using Mega (version 2.1). GenBank™ accession numbers are indicated. The *Y. enterocolitica* Slc26A2 (YP001005307.1) and the *M. tuberculosis* we used to model the STAS domain are boxed.

however, can distinguish between the protein and detergent when used in combination with contrast variation: at the correct contrast match point, *i.e.* hydrogen/deuterium ratio, the scattering signal from the detergent is minimal, making the detergent invisible under favorable conditions (22). First, to determine the contrast match point of Fos-choline-12 experimentally, we recorded scattering curves of Fos-choline-12 solutions without protein at varying H_2O/D_2O contrast ratios. The scattering curve at 100% D_2O is the most representative of the unmatched detergent and indicative of compact, globular micellar structures with a radius of gyration of 17 Å (Fig. 3*A*). Importantly, the weakest signal was observed at 10% D_2O (Fig. 3*A*), very close to our experimentally determined contrast match-point at 11% D_2O (Fig. 3*B*). The scattering curve is flat without any variations of intensity outside the noise of the signal (Fig. 3*A*), an important indication that Fos-choline-12 can be matched homogeneously by contrast variation. Second, SANS data were collected for purified YeSlc26A2 in Fos-choline-12 at 0, 11 and 100% D_2O (Fig. 3*C*). Both the 0 and 100% D_2O data sets contain contributions from the free micelles because we did not explicitly determine the volume fractions of free detergent, we did not further analyze these data sets but focused instead on the 11% D_2O data set where the detergent contributions were matched and therefore invisible. From the scattering data, the molecular weight (calculated by $I(0)$ analysis) and solvent excluded volume (calculated by Porod analysis) of the protein at 11% D_2O were calculated to be 103 kDa and 125,000 $Å^3$, corresponding, respectively, to 1.94 and 1.9 times the theoretical values for a monomer (Table 1) demonstrating that YeSlc26A2 is a dimer under the experimental conditions.

YeSlc26A2 Model Reveals Multidomain Organization—The program DAMMIN was used to generate low resolution models of YeSlc26A2. For all parameter variations (see "Experimental Procedures"), all models generated showed very similar symmetrical, S-shaped envelopes (Fig. 4*A*). The presence of this symmetry indicates that such symmetry is genuine. When P2 symmetry was applied during DAMMIN modeling (Fig. 4*B*), the fit of the model against the experimental data improved (χ^2 = 0.367 compared with 0.370 without imposed symmetry) (Fig. 3*D*). The solvent-excluded volume (140,000 ± 10,000$Å^3$) and radius of gyration (38.5 ± 2.6Å) of the model were consistent with those derived from the scattering data (125,000 ± 25,000$Å^3$ and 40.7 ± 4.1Å, respectively), another indication that the model correctly represents the YeSlc26A2 structure. The solvent excluded volume of the model corresponded to 2.1 times the predicted volume of the monomer (Table 1), again supporting a dimeric stoichiometry. The main bulk of the protein in our SANS envelope, encompassing the dimerization

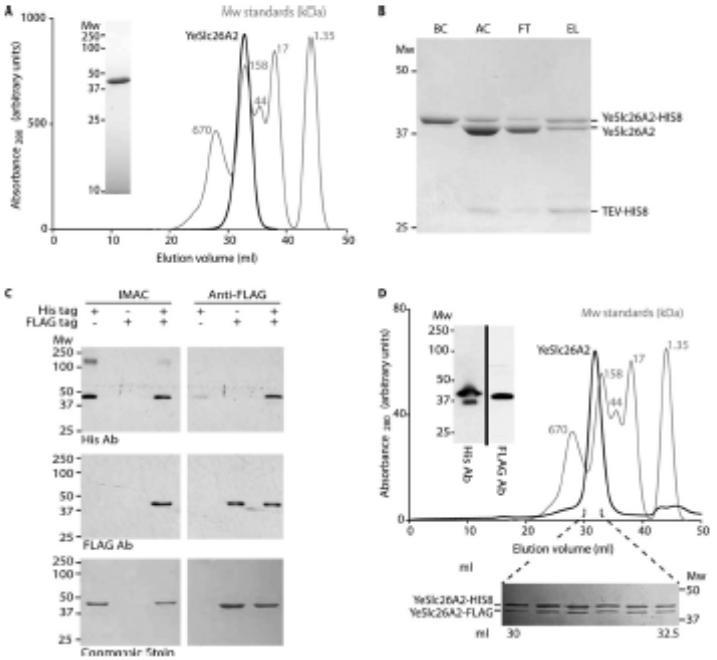

FIGURE 2. **Oligomerization of YeSlc26A2.** *A*, gel filtration trace (Superose 6 10/60) of YeSlc26A2 used to collect the SANS data. *Inset*, SDS-PAGE Coomassie Blue-stained gel of Superose 6 peak fraction. *B*, a mixture of His-tagged and untagged YeSlc26A2 was analyzed by IMAC. Samples (*BC*, before cleavage; *AC*, after cleavage; *FT*, IMAC flow-through; *EL*, IMAC elution) were analyzed by Coomassie Blue-stained SDS-PAGE. *C*, C-terminally His-tagged (His tag) and FLAG-tagged (FLAG tag) YeSlc26A2 were expressed or co-expressed and purified by parallel IMAC or anti-FLAG affinity chromatography as indicated in the table *above* the gels. Eluates were analyzed by Western blotting using an anti-His antibody (*top panel*), anti-FLAG antibody (*middle panel*), or visualized with Coomassie Blue (*bottom panel*). The additional band at 200 kDa observed on the *top panel* is only present in this preparation and is due to a contamination. *D*, the coexpressed His-/FLAG-tagged protein was analyzed by gel filtration on a Superose 6 10/60 column. Molecular mass standard proteins (thyroglobulin, 670 kDa; γ-globulin, 158 kDa; ovalbumin, 44 kDa; myoglobin, 17 kDa; vitamin B12, 1.35 kDa) are shown for comparison. *Inset*, fractions from the gel filtration peak were pooled and analyzed by Western blotting using anti-His (*left*) or anti-FLAG antibodies (*right*). The additional *lower band* on the *left* is only present in this preparation and is due to a contamination. The gel *below* the gel filtration trace represents 0.5-ml fractions collected during the elution of the His/FLAG oligomer. *Mw*, molecular mass marker (kDa). The gel filtration traces of the molecular mass standards have been normalized.

domain, lies mostly within a plane that corresponds to the depth of a membrane bilayer (~30 Å) with two globular domains extending from this plane (Fig. 4*B*), thus revealing a multidomain organization.

YeSlc26A Forms a Homodimer Stabilized via Its Transmembrane Core—To determine the organization of the transmembrane and C-terminal, soluble STAS domains within the structure, we created a model of the YeSlc26A2 STAS domain. The backbone traces of the high resolution STAS domain structures from *E. coli*, *Mycobacterium tuberculosis*, and rat prestin superimpose very closely (8–10), indicative of a common fold despite their limited levels of amino acid sequence identity. The reasonable sequence identity (21%, Fig. 5*A*) between the STAS domains of YeSlc26A2 and Rv1739c allowed us to model the STAS domain of YeSlc26A2 using SwissProt software (Fig. 5*B*).

The STAS domains must project away from the membrane into the cytoplasm, thus, we considered two regions as possible STAS domain locations: either the two distal arms or the bulbous dimerization domain in the center of the structure (Fig. 4*B*). We overexpressed and purified the YeSlc26A2 STAS domain and then analyzed it using analytical size exclusion chromatography (Fig. 6). The YeSlc26A2 STAS domain eluted predominantly in a monodisperse peak corresponding to 13.8 kDa (predicted monomer mass, 14.6 kDa) (Fig. 6). Thus, similar to the STAS domains of the SLC26 proteins of *E. coli* (8), *M. tuberculosis* (10), and rat prestin (9), the YeSlc26A2 STAS domain purified as a monomer, showing no propensity to dimerize. These observations suggest that the STAS domains are located within the arms of the envelope rather than comprising the dimerization interface. To biochemically verify our model, in particular the position of the STAS domain within the solvent exposed arms of the envelope, we treated the purified YeSlc26A2 with trypsin and analyzed the peptides released by mass spectrometry (supplemental Fig. S2). The large majority of the peptides identified lie within the STAS domain, with the few other trypsin cleavable sites being within predicted exposed loops (supplemental Fig. S2).

To position the STAS model within the arm of the DAMMIN envelope, we applied the following constraints (Fig. 7*B*). First,

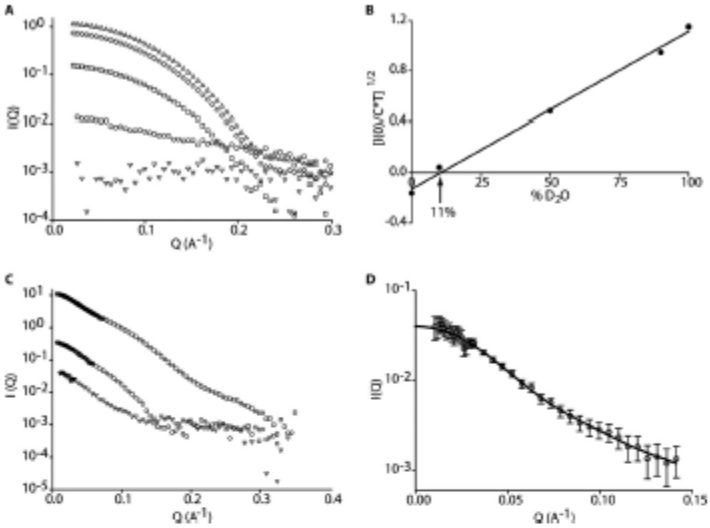

FIGURE 3. **Small angle neutron scattering analysis.** *A*, Fos-choline-12 SANS contrast variation series 0% (○), 10% (▽), 50% (□), 90% (◇), and 100% (△) D_2O. *B*, experimental determination of the Fos-choline-12 contrast match point. *C*, SANS contrast series of the protein-detergent complex (○) 0%, (▽) 11%, and (□) 100% D_2O. *D*, fit of the DAMMIN (*line*) model (P2, D_{max} = 120 Å, expert mode) against the experimental YeSlc26A2 SANS data (*open circles*). In all panels, *Q* is the scattering vector, and *I* represents intensity.

TABLE 1

Predicted and calculated YeSlc26A2 particle properties

	Monomer (Theoretical)	SANS (11% D_2O)	Ratio (monomer:SANS)	P2 DAMMIN model	Ratio (Monomer:DAMMIN)
Mw (kDa)	53.1	103, 10–15% error	1.94	N.A.	
Solvent-excluded volume (Å^3)	66,000	125,000, ±25,000	1.9	140,000 ± 10,000	2.1
Radius of gyration (Å)	N.A.	40.7 ± 4.1		38.5 ± 2.6	

N.A., not applicable.

the N-terminal residues must be close to the bulk of the envelope; second, residues corresponding to those proposed to constitute a juxtamembrane binding surface in the rat prestin STAS and Rv1739c STAS structures were accordingly oriented; third, YeSlc26A2 residues corresponding to those identified in GDP/GTP binding in Rv1739c were assumed to be solvent-exposed.

A recent study of mouse SLC26A6 suggested that its closest structural homologue is the *E. coli* CLC transporter, clc-ec1, and a model of SLC26A6 based upon the clc-ec1 fold has been generated (20). CLC proteins contain a conserved essential glutamate that maps to an essential glutamate residue in the Slc26A6 model (20) also present in YeSlc26A2 (supplemental Fig. S3). CLC proteins are dimeric; thus, we also fitted the proposed SLC26A6 dimer model into the bulky, dimerization domain of our SANS envelope (Fig. 7*C*).

DISCUSSION

The primary goal of this study was to obtain clear insights into the domain architecture of the important SLC26/SulP family of transporters. However, large, human membrane proteins are challenging to handle for biochemical characterization. Thus, studies on prokaryotic homologues have proven crucial in gaining structural information for their human counterparts. Moreover, due to their fragile nature and the general difficulties in overexpressing and purifying the necessary quantities, structural characterization of integral membrane proteins is notoriously difficult. Contrast-matched, SANS is an ideal technique for studying these as it (i) circumvents the need for well-ordered three-dimensional crystals and (ii) allows the construction of a three-dimensional model of membrane protein alone but stabilized in the protein-detergent complex. Thus, it can be expected that this technique will gain increasing popularity in the future among the community of scientists working on the structural biology of membrane proteins. In this study, we have succeeded in obtaining the first low resolution model of a SLC26A/SulP protein in solution with no detergent contribution giving the first clear insight into their domain architecture.

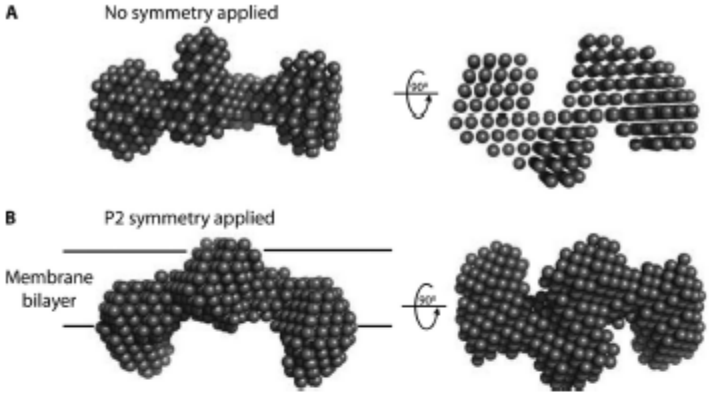

FIGURE 4. ***Ab initio* envelopes of YeSlc26A2.** *A*, P1 (no symmetry applied). *B*, P2 DAMMIN models of YeSlc26A2 using D_{max} = 120 Å and Q_{max} = 0.141 Å^{-1}. The models on the *right* are generated from the ones on the *left* by a rotation of 90 degrees around their long axes.

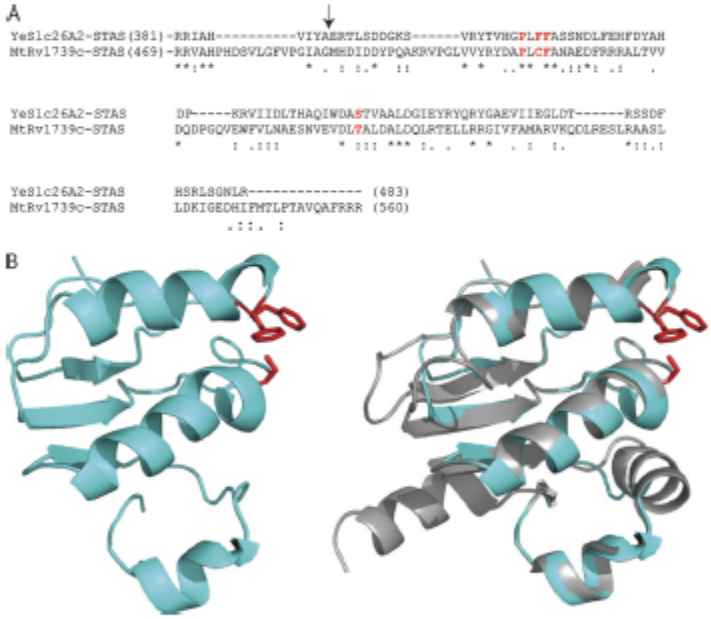

FIGURE 5. **Modeling of the YeSlc26A2 STAS domain.** *A*, amino acid sequence alignment of YeSlc26A2 and *M. tuberculosis* Rv1739c STAS domain generated using ClustalW. *Numbers* in *parentheses* are the amino acid residues encompassing each STAS domain. The residues in *red* have been proposed to constitute a juxtamembrane binding surface in Rv1739c. The *asterisk*, *semicolon*, and *period* under sequences mark positions of complete sequence conservation, conserved substitutions, and semiconserved substitution, respectively. The *arrow* marks the start of the model (*B*) YeSlc26A2 STAS model generated using Swiss-Model (*left*). No optimizing of threading energy was necessary. The model and the structure of the STAS domain of TbRc1739c (*grey*) are superimposed (*right*).

Oligomeric State of YeSlc26A2—The partial proteolysis, co-purification, and analytical size exclusion chromatography presented in this study, together with the three independent analyses of SANS data, *i.e.* molecular weight determination by $I(0)$ analysis, solvent-excluded volume by POROD analysis, and DAMMIN modeling, demonstrate that YeSlc26A purifies as a stable dimer. This is also supported by the symmetry observed during DAMMIN modeling; the symmetric features were present without imposing any symmetry options during the annealing process, a good indication that such symmetry is genuine. The oligomeric state, as well as whether a common stoichiometry is conserved among the SLC26/SulP superfamily,

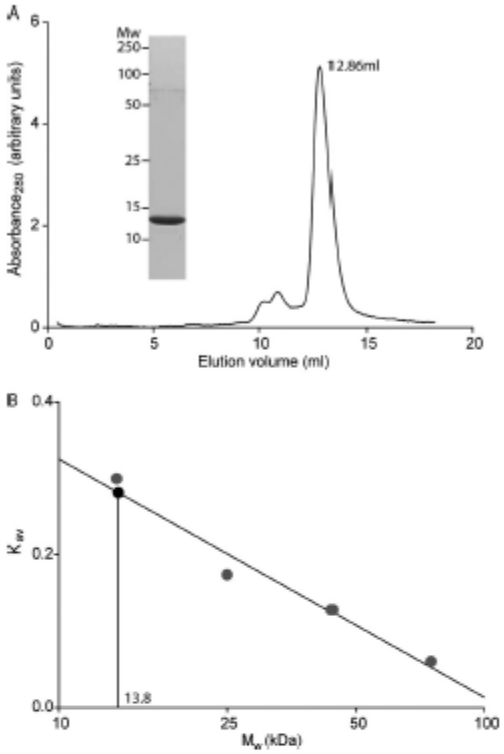

FIGURE 6. **Purification of the YeSlc26A2 STAS domain.** *A*, analytical gel filtration of the purified YeSlc26A2 STAS domain on a Superdex 75 10/30 column. *Inset*, SDS-PAGE Coomassie Blue-stained gel of Superdex 75 (10 × 30) peak fractions. *B*, determination of the YeSlc26A2 STAS domain molecular weight. K_{av} values were calculated from the equation $K_{av} = (V_e - V_0)/(V_t - V_0)$ where V_e is the elution volume of each protein, V_0 is the column void volume, and V_t is the total bed volume. *Mw*, molecular mass.

remains a subject of debate. Initial studies of gerbil prestin using Native PAGE and yeast two-hybrid systems suggested a tetrameric state (23), a hypothesis subsequently supported by single particle analysis (5). Recently however, Wang *et al.* (7) used the charge density of prestin in gerbil outer hair cells to conclude that a tetrameric state was possible, but that their data would also be consistent with a dimer. In contradiction to the original hypothesis, Detro-Dassen *et al.*, (6) used copurification, blue native PAGE and chemical cross-linking to show that human SLC26A3, rat, and zebrafish prestin, as well as a SLC26 homologue from *Pseudomonas aeruginosa*, form dimers with the monomers working in parallel. They conclude that a dimeric subunit is the general prokaryotic and eukaryotic SLC26 isoform. Our results support this latter hypothesis.

YeSlc26A2 Domain Architecture—Our SANS-derived envelope allows us to determine the domain organization of YeSlc26A2. We fitted a model of the soluble, C-terminal STAS domain and a model of the mouse SLC26A6 protein, generated from the ClC-ec1 fold, into our *ab initio* envelope. As the YeSlc26A2 STAS domain, similar to those of the SLC26 proteins of *E. coli* (8), *M. tuberculosis* (10), and rat prestin (9), purified as a monomer, we attempted to fit it into the distal arms of the DAMMIN model rather than the central dimerization domain.

Given the limited information available, only proposed juxtamembrane and substrate binding residues in the *M. tuberculosis* and rat prestin STAS structures, the fit of the STAS model into its proposed position is excellent (Fig. 7*C*). This location is also in agreement with a FRET study (24) that indicated that the N terminus rather than the C terminus of prestin is important for oligomerization.

Further proteolysis/mass spectrometry analysis indicates that the STAS domain is not protected by detergent micelles, but exposed to the solvent and hence susceptible to trypsin proteolysis, whereas the transmembrane domain appears protected by the micelles. Locating the STAS domains in the distal arms of the envelope leaves the bulk of the structure, which corresponds to the depth of a membrane bilayer, to contain the transmembrane region. Into this region, we fitted the recent CLC-derived, dimeric mouse SLC26A6 model. Overall, this model appears to fit the proposed transmembrane region of the YeSlc26A2 envelope well: the shape is similar, the dimer interfaces superimpose well, and the translocation pore is within the boundary of the YeSlc26A2 envelope. Most helices are entirely contained within the envelope, and those that are not are clustered tightly along the periphery of the envelope, and importantly, none overlap with the STAS domain model (Fig. 7*C*). These data cannot tell us about the relationship between the SLC26 and CLC proteins, and we do not imply here that YeSlc26A2 belongs to the CLC family; however, this modeling does demonstrate that the proposed transmembrane region of our SANS-derived envelope is similar in size to a dimeric helix bundle membrane protein with 12 transmembrane helices.

Functional Implications for SLC26A/SulP Family—The *Y. enterocolitica* Slc26A2 protein shows a homodimer stabilized via its transmembrane core. The cytoplasmic STAS domain projects away from the transmembrane domain and is not involved in dimerization. This domain organization has functional implications for the SLC26A/SulP protein family and provides a structural model for the conformational changes associated with the transport cycle in SLC26/SulP proteins.

Although there may have been an inverse relationship between motor and transport functions during the evolution of prestin (12), the electromotile function of prestin evolved from the ability of these proteins to undergo dramatic conformational changes (11, 13). A three-dimensional reconstruction from EM data showed a compact bullet-shaped molecule for rat prestin (5), which is clearly very different from what we observed in the YeSlc26A2 model. However, changes in membrane potential were observed by FRET to induce significant movement of the C-terminal tail of prestin (25). This is reminiscent of cyclic nucleotide-modulated (26) and CLC channels (27), where conformational rearrangements of intracellular

Low Resolution Structure of a Bacterial SLC26A Protein

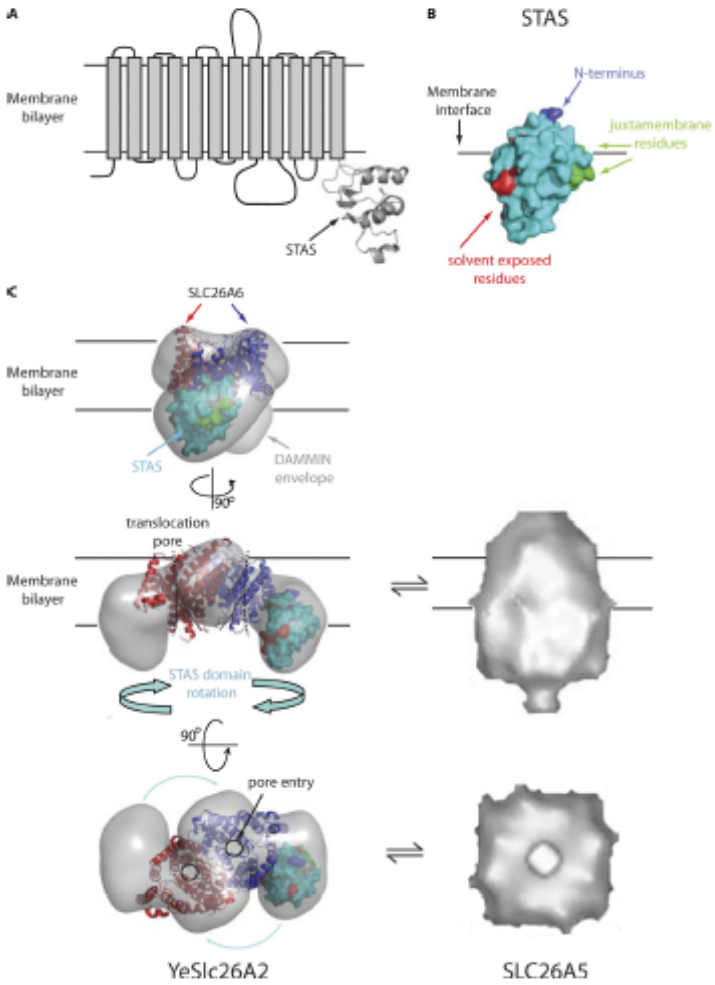

FIGURE 7. **Domain architecture of YeSlc26A2.** *A*, domain organization of YeSlc26A2 showing a transmembrane region of 12 α-helices and a model of the cytoplasmic STAS domain generated from sequence alignment with the *M. tuberculosis* STAS domain. *B*, surface representation of STAS domain, the N terminus is highlighted in *blue*, proposed juxtamembrane residues are highlighted in *green*, and solvent-exposed residues are highlighted in *red*. *C*, *left panel*, docking of SLC26A6 transmembrane model (based on ClC-ec1) and STAS domain model into the P2 DAMMIN envelope, viewed from the plane of the membrane (*top* and *middle*) and above the membrane (*bottom*). *Blue arrows* indicate possible movement of the STAS domains to form the more contracted conformation observed in the EM reconstruction of SLC26A5/prestin (right panel-adapted from Mio *et al.* (5)).

domains is coupled to gating of the channels. Comparing the two structures (prestin *versus* YeSlc26A2) may offer structural insight into the conformational changes occurring during the transport cycle of the SLC26A/SulP family, varying in length in the plane of the membrane between "contracted" (Prestin) and "expanded" (YeSlc26A2) conformations via a large rotational movement of the two STAS domains (Fig. 7*C*). Such large conformational changes may explain how prestin transduces a change in membrane potential into the considerable mechanical force, leading to a length change of outer hair cells. Contrast-matched SANS measurements on purified prestin (5), in the presence or absence of Cl^-/HCO_3^-, is an ideal technique to answer these essential questions.

In conclusion, we have demonstrated that YeSlc26A2 in solution is a dimer stabilized via its transmembrane domain, adding support to the hypothesis that a dimeric stoichiometry is a common feature within the family. The cytoplasmic STAS domain projects away from the transmembrane domain and is not involved in dimerization. Our model, combined with other biochemical information, strongly implicates that large move-

ments of the STAS domain underlie the conformational changes that occur during transport.

Acknowledgments—We thank Professors Daan van Aalten and Mike Merrick, Dr. Joseph Mindell, Professor Tracy Palmer, Professor Frank Sargent, and Professor Fritz Winkler for constructive criticism of the manuscript; Dr. XiaoDan Li and P. Callow for technical help. We thank Institute Laue-Langevin for beam time on D22.

REFERENCES

1. Sater, M. H., Jr., Eng, B. H., Fard, S., Garg, J., Haggarty, D. A., Hutchinson, W. J., Jack, D. L., Lai, E. C., Liu, H. J., Nusinew, D. P., Omar, A. M., Pao, S. S., Paulsen, I. T., Quan, J. A., Sliwinski, M., Tseng, T. T., Wachi, S., and Young, G. B. (1999) *Biochim. Biophys. Acta* **1422,** 1–56
2. Dorwart, M. R., Shcheynikov, N., Yang, D., and Muallem, S. (2008) *Physiology* **23,** 104–114
3. Mount, D. B., and Romero, M. F. (2004) *Pflugers Arch.* **447,** 710–721
4. Shelden, M. C., Howitt, S. M., and Price, G. D. (2010) *Mol. Membr. Biol.* **27,** 12–23
5. Mio, K., Kubo, Y., Ogura, T., Yamamoto, T., Arisaka, F., and Sato, C. (2008) *J. Biol. Chem.* **283,** 1137–1145
6. Detro-Dassen, S., Schänzler, M., Lauks, H., Martin, I., zu Berstenhorst, S. M., Nothmann, D., Torres-Salazar, D., Hidalgo, P., Schmalzing, G., and Fahlke, C. (2008) *J. Biol. Chem.* **283,** 4177–4188
7. Wang, X., Yang, S., Jia, S., and He, D. Z. (2010) *Brain Res.* **1333,** 28–35
8. Babu, M., Greenblatt, J. F., Emili, A., Strynadka, N. C., Reithmeier, R. A., and Moraes, T. F. (2010) *Structure* **18,** 1450–1462
9. Pasqualetto, E., Aiello, R., Gesiot, L., Bonetto, G., Bellanda, M., and Battistutta, R. (2010) *J. Mol. Biol.* **400,** 448–462
10. Sharma, A. K., Ye, L., Baer, C. E., Shanmugasundaram, K., Alber, T., Alper, S. L., and Rigby, A. C. (2011) *J. Biol. Chem.* **286,** 8534–8544
11. Schaechinger, T. J., and Oliver, D. (2007) *Proc. Natl. Acad. Sci. U.S.A.* **104,** 7693–7698
12. Tan, X., Pecka, J. L., Tang, J., Okoruwa, O. E., Zhang, Q., Betsel, K. W., and He, D. Z. (2011) *J. Neurophysiol.* **105,** 36–44
13. Stewart, C. E., and Hudspeth, A. J. (2000) *Proc. Natl. Acad. Sci. U.S.A.* **97,** 454–459
14. Drew, D. E., von Heijne, G., Nordlund, P., and de Gier, J. W. (2001) *FEBS Lett.* **507,** 220–224
15. Lin, Y., Kimpler, L. A., Natsmith, T. V., Lauer, J. M., and Hanson, P. I. (2005) *J. Biol. Chem.* **280,** 12799–12809
16. Guzman, L. M., Belin, D., Carson, M. J., and Beckwith, J. (1995) *J. Bacteriol.* **177,** 4121–4130
17. Jacrot, B., and Zaccai, G. (1981) *Biopolymers* **20,** 2413–2426
18. Jacrot, B. (1976) *Rep. Prog. Phys.* **39,** 911–953
19. Svergun, D. I. (1999) *Biophys. J.* **76,** 2879–2886
20. Ohana, E., Shcheynikov, N., Yang, D., So, I., and Muallem, S. (2011) *J. Gen. Physiol.* **137,** 239–251
21. Gouaux, E., and Mackinnon, R. (2005) *Science* **310,** 1461–1465
22. Heller, W. T. (2010) *Acta Crystallogr. D. Biol. Crystallogr.* **66,** 1213–1217
23. Zheng, J., Du, G. G., Anderson, C. T., Keller, J. P., Orem, A., Dallos, P., and Cheatham, M. (2006) *J. Biol. Chem.* **281,** 19916–19924
24. Navaratnam, D., Bai, J. P., Samaranayake, H., and Santos-Sacchi, J. (2005) *Biophys. J.* **89,** 3345–3352
25. Gleitsman, K. R., Tateyama, M., and Kubo, Y. (2009) *Am. J. Physiol. Cell Physiol.* **297,** C290–298
26. Zagotta, W. N., Olivier, N. B., Black, K. D., Young, E. C., Olson, R., and Gouaux, E. (2003) *Nature* **425,** 200–205
27. Bykova, E. A., Zhang, X. D., Chen, T. Y., and Zheng, J. (2006) *Nat. Struct. Mol. Biol.* **13,** 1115–1119

Molecular Microbiology (2012) ■ doi:10.1111/mmi.12120

The *Escherichia coli* SLC26 homologue YchM (DauA) is a C_4-dicarboxylic acid transporter

Eleni Karinou,[1] Emma L. R. Compton,[1] Mélanie Morel[2] and Arnaud Javelle[1]*
[1]*Division of Molecular Microbiology, College of Life Sciences, University of Dundee, Dundee DD1 5EH, UK.*
[2]*Unité Mixte de Recherches INRA UHP 1136 Interaction Arbres Microorganismes, IFR 110 Ecosystèmes Forestiers, Agroressources, Bioprocédés et Alimentation, Faculté des Sciences et Technologies, Nancy Université BP 70239, 54506 Vandoeuvre-lès-Nancy Cedex, France.*

Summary

The SLC26/SulP (solute carrier/sulphate transporter) proteins are a ubiquitous superfamily of secondary anion transporters. Prior studies have focused almost exclusively on eukaryotic members and bacterial members are frequently classified as sulphate transporters based on their homology with SulP proteins from plants and fungi. In this study we have examined the function and physiological role of the *Escherichia coli* Slc26 homologue, YchM. We show that there is a clear YchM-dependent growth defect when succinate is used as the sole carbon source. Using an *in vivo* succinate transport assay, we show that YchM is the sole aerobic succinate transporter active at acidic pH. We demonstrate that YchM can also transport other C_4-dicarboxylic acids and that its substrate specificity differs from the well-characterized succinate transporter, DctA. Accordingly *ychM* was re-designated *dauA* (dicarboxylic acid uptake system A). Finally, our data suggest that DauA is a protein with transport and regulation activities. This is the first report that a SLC26/SulP protein acts as a C_4-dicarboxylic acid transporter and an unexpected new function for a prokaryotic member of this transporter family.

Introduction

Under aerobic conditions, facultative anaerobic bacteria such as *Escherichia coli* can take up succinate from the environment for use as a carbon and energy source. However, under anaerobic conditions, succinate represents the end-product of fumarate respiration and is thus excreted into the growth medium. *E. coli* possesses a battery of five import/export systems for succinate transport, namely DctA, DcuA, DcuB, DcuC, DcuD, each of which is expressed differently under aerobic or anaerobic conditions (Janausch *et al.*, 2002).

Aerobically, exogenous succinate is transported into the cell by the well-studied C_4-dicarboxylate transporter system, DctA. DctA belongs to the dicarboxylate/amino acid:cation symporter (DAACS, TC2.A.23) family, which act as proton symporters. DctA can also transport fumarate, malate, aspartate, tartrate and orotate (Kay and Kornberg, 1971; Baker *et al.*, 1996). Expression of *dctA* in response to C_4-dicarboxylic acid is induced by the DcuSR two-component system (Zientz *et al.*, 1998; Davies *et al.*, 1999; Golby *et al.*, 1999). The membrane-bound sensor kinase (DcuS) binds C_4-dicarboxylates and stimulates phosphorylation of the cytoplasmic response regulator (DcuR) which activates expression of genes involved in C_4-dicarboxylate metabolism, including DctA (Zientz *et al.*, 1998; Davies *et al.*, 1999; Golby *et al.*, 1999). A recent study demonstrated that there is a direct interaction between DcuS and helix VIIIb of DctA, mediated by the cytoplasmic PAS domain of DcuS, and it has been proposed that the transporter acts as co-sensor by directly modulating the activity of DcuS (Davies *et al.*, 1999; Witan *et al.*, 2012).

Anaerobically, succinate is excreted into the growth medium by DcuA and DcuB, which are carriers from the C_4-dicarboxylate uptake family (Dcu, TC2.A.61). These transporters are capable of C_4-dicarboxylate exchange and uptake but operate preferentially as fumarate/succinate antiporters, excreting the latter. Interestingly, like DctA, DcuB also interacts with DcuS, and has been proposed to act as co-sensor by directly modulating the activity of DcuS in a similar manner to DctA but under anaerobic conditions (Davies *et al.*, 1999; Kleefeld *et al.*, 2009; Witan *et al.*, 2012). The DcuC and DcuD transporters belong to a separate family of C_4-dicarboxylate efflux systems (DcuC, TC2.A.61), DcuC acts as a proton/succinate co-exporter, while the function of DcuD is still unclear (Janausch *et al.*, 2002).

DctA is the most active carrier under aerobic conditions with a *dctA* mutant presenting a clear phenotypic growth defect when C_4-dicarboxylates are used as sole carbon

Accepted 3 December, 2012. *For correspondence. E-mail ajavelle@dundee.ac.uk; Tel. (+44) 1382 386 203; Fax (+44) 1382 388 216.

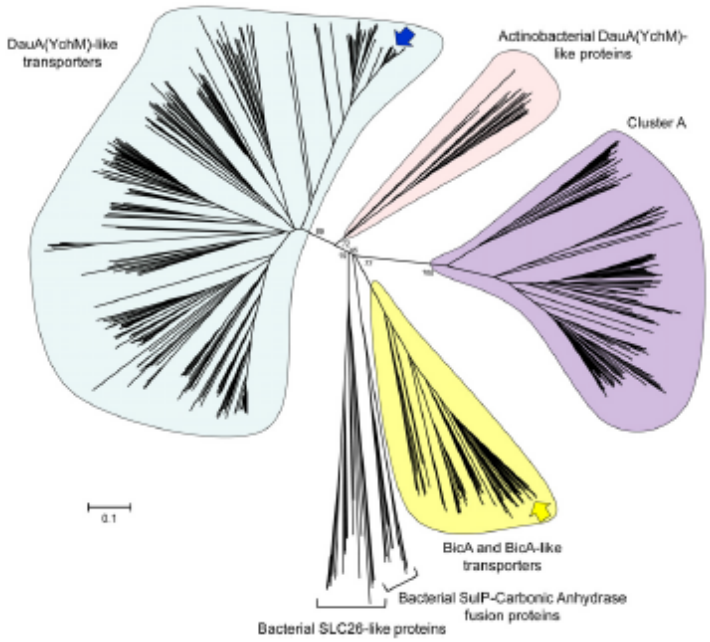

Fig. 1. Phylogenetic tree of DauA (YchM) homologues in bacteria.
Neighbour-joining tree of 766 DauA-related sequences retrieved from the NCBI database using BLASTP. The blue and yellow arrows refer to DauA from *E. coli* and BicA from *Synechococcus* sp. respectively. Sequences from Actinobacteria, Bacteroidetes, Chlorobi, Chlamydiae, Cyanobacteria, Firmicutes, Proteobacteria and Spirochaetes are reported. Cluster A is a separate group without any functional annotation, composed of sequences from Actinobacteria, Bacteroidetes, Cyanobacteria and Proteobacteria. Bootstrap values are reported only for main clusters. The scale marker represents 0.1 substitutions per residue.

source (Davies *et al*., 1999). However, it has been shown that a single *dctA* and a quintuple *dctA*, *dcuA*, *dcuB*, *dcuC*, *dcuD* mutant retained aerobic growth on succinate at acidic pH, indicating the presence in *E. coli* of an additional, unknown succinate transporter (Janausch *et al*., 2001). Attempts to identify this extra transporter have, to date, been unsuccessful.

The Solute Carrier 26 (SLC26; animals) and sulphate transporter (SulP; plants and fungi) family is a ubiquitous superfamily of secondary anion transporters conserved from bacteria to man (Saier *et al*., 1999). These proteins comprise an integral membrane domain containing 10–12 transmembrane helices followed by a C-terminal cytoplasmic Sulphate Transporter and Anti-Sigma factor antagonist (STAS) domain (Shelden *et al*., 2010). Using small angle neutron scattering combined with contrast variation, we have recently shown that a *Yersinia enterocolitica* Slc26 homologue forms a dimer stabilized via its transmembrane core; the cytoplasmic STAS domain projects away from the transmembrane domain and is not involved in dimerization (Compton *et al*., 2011). Proteins within this family exhibit a wide variety of functions, transporting anions ranging from halides to bicarbonate. The human genome encodes at least 10 SLC26 proteins that play critical roles in cell physiology and are medically important, being implicated in genetic diseases such as diastrophic dysplasia, congenital chloride diarrhoea, Pendred syndrome and nonosyndromic deafness (Mount and Romero, 2004; Dorwart *et al*., 2008). In plants and fungi, SulP proteins are primarily sulphate uptake transporters, with mutations in the encoding genes leading to auxotrophic phenotypes in fungi (Marzluf, 1997; Hawkesford and De Kok, 2006).

Although these proteins are present ubiquitously among bacteria (Fig. 1), their physiological functions are almost completely unknown. The only comprehensive physiological and topological analysis of a bacterial Slc26/SulP protein concerned the *Synechococcus* Slc26 homologue BicA, which has been reported to act as a Na^+-dependent bicarbonate transporter (Price *et al*., 2004; 2011; Price and

Howitt, 2011). Bacterial Slc26/SulP proteins are frequently classified as sulphate transporters based on their homology with SulP proteins from plants and fungi. The only evidence to support this view comes from a study of the *Mycobacterium tuberculosis* SLC26 homologue Rc1739c which when overproduced in *E. coli* stimulated sulphate transport (Zolotarev *et al*., 2007). However, given the wide variety of substrates transported and the diverse physiological roles of the SLC26/SulP proteins, particularly in humans, it is impossible to predict their function based solely on sequence similarity. Thus there is clearly a need for the functional characterization of additional members of the bacterial Slc26 protein family.

Recently, a crystal structure of the isolated STAS domain from the *E. coli* Slc26 homologue YchM was reported (Babu *et al*., 2010). Surprisingly, the YchM STAS domain co-crystallized in an apparent complex with acyl-carrier protein (ACP), leading the authors to propose that YchM, like the *Synechococcus* SLC26 homologue BicA, was a bicarbonate transporter and that it was involved in fatty acid metabolism. However, an exhaustive phylogenetic analysis of bacterial SLC26 homologues clearly shows that *E. coli* YchM clusters independently from the BicA/BicA-like proteins (Fig. 1). We therefore took an unbiased approach to elucidate the substrate and physiological role of *E. coli* YchM. In this study we show that there is a clear YchM-dependent growth defect when succinate is used as the sole carbon source. Using an *in vivo* succinate transport assay, we show that YchM is the sole aerobic succinate transporter active at acidic pH and that although it can also transport other C_4-dicarboxylic acids it has a different substrate spectrum to DctA. Therefore we have re-named *ychM* as *dauA* (for dicarboxylic acid uptake system A) and this designation is used from here on in. Finally, our data suggest that DauA may impact upon DctA expression and/or activity. Taken together, these results demonstrate that DauA is the previously uncharacterized succinate transporter identified in *E. coli* and point towards a role for DauA in the regulation of C_4-dicarboxylate metabolism. This is the first report that a SLC26/SulP protein acts as a C_4-dicarboxylic acid transporter, an unexpected new function for a prokaryotic member of this transporter family.

Results

A ΔdauA mutant presents a clear growth defect phenotype on succinate

As a first step towards identifying the physiological role of DauA we constructed an in-frame deletion of *dauA* in the *E. coli* BW25113 strain background to give strain EK1 and used phenotypic microarray (PM) technology to compare the metabolic activity of the wild-type versus the Δ*dauA* mutant under a wide range of metabolic conditions. To assay phenotypes during aerobic metabolism, a tetrazolium salt was used that is reduced by dehydrogenases and reductases produced by cells to yield a formazan dye, which indicates that the cells are actively metabolizing a substrate. No colour change implies that the cells are not metabolically active and the substrate of interest, for example a specific carbon source, is not capable of being metabolized (Bochner, 2009).

The first substrates we tested were different sulphur sources. However, no significant difference in the metabolic activity between the wild-type and Δ*dauA* strains was observed when either sulphate or a range of other sulphur sources were tested (Fig. S1), indicating that DauA does not play an essential role in sulphur assimilation. We therefore next switched our attention to testing different carbon sources as substrates. Unexpectedly, and in contrast to the wild-type strain, the Δ*dauA* strain was metabolically inactive when succinate was used as sole carbon source (Fig. 2; open symbols). However both strains were equally metabolically active when other carbon sources such as glucose, fructose, maltose and glycerol were tested (Fig. 2; open symbols). This indicates that the difference in phenotype observed when succinate was present as the sole carbon source is due to the inability of the Δ*dauA* strain to specifically metabolize succinate and does not result from a general problem of carbon metabolism. In these experiments citrate was use as a negative control since *E. coli* is not able to use citrate as carbon source under aerobic conditions.

The *dauA*-dependent metabolic phenotype was next confirmed by measuring growth rates with succinate as sole carbon source. Using MOPS minimal growth medium, the Δ*dauA* mutant was unable to grow with added succinate, whereas normal growth was observed for all other added carbon sources tested for both strains (Fig. 2; closed symbols). Taken together these results indicate that DauA is involved in succinate metabolism.

DauA is involved in succinate metabolism

During aerobic growth, exogenous succinate is transported into *E. coli* by the well-studied C_4-dicarboxylate transporter system DctA. A Δ*dctA* mutant shows poor growth on minimal medium containing succinate as the sole carbon source at pH 7; however, the strain shows almost wild-type growth using succinate at acidic pH (≤6) (Janausch *et al*., 2001). This suggests that *E. coli* possesses an additional succinate transporter that is active at acidic pH and we therefore hypothesized that DauA may be involved in this transport process.

To assess whether this was the case, we constructed an in-frame deletion of *dctA* in the *E. coli* BW25113 and EK1 (Δ*dauA*) strain backgrounds to give strains EK2

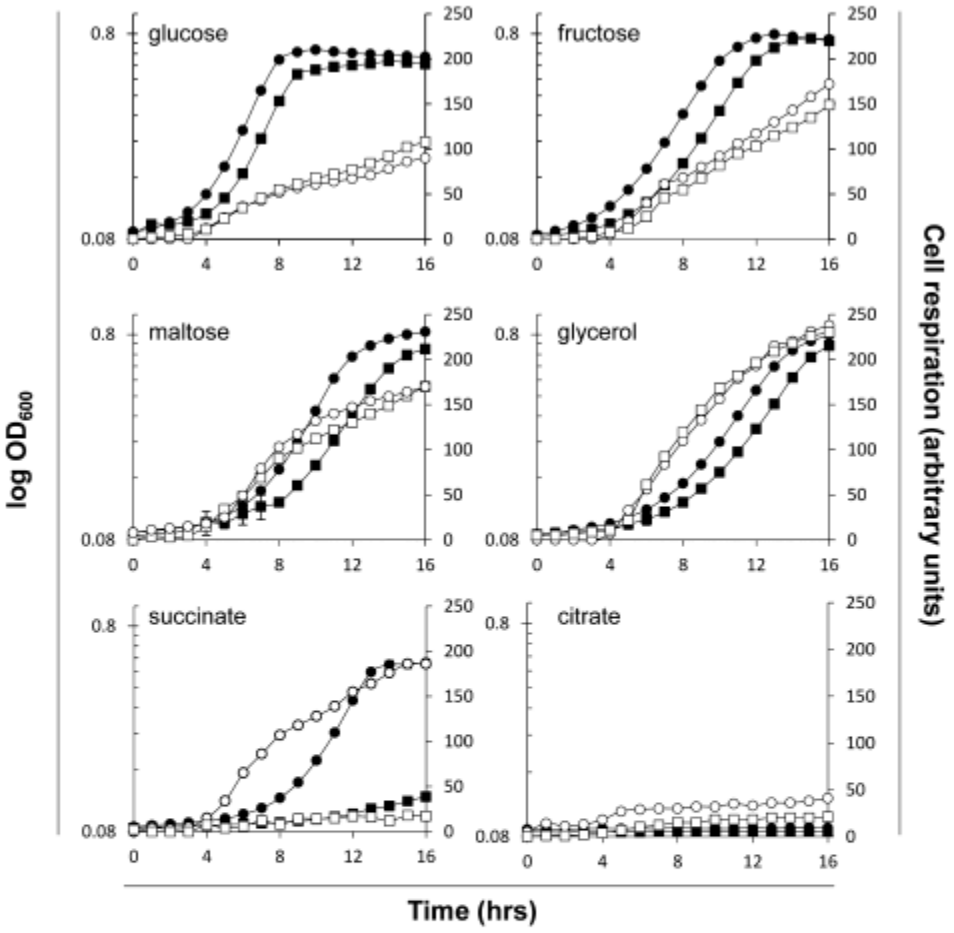

Fig. 2. Identification of a DauA-dependent growth phenotype.
Strains BW25113 (wild-type; circles) and EK1 (Δ*dauA*; squares) were grown in MOPS minimal medium pH 7 supplemented with 50 mM of the indicated carbon sources. Growth curves at 600 nm were recorded using microplates (closed symbols). Cell respiration (open symbols) was measured in a different set of experiments by following the production of formazan dye spectrophotometrically at 590 nm. Growth curves are the averages of four independent test series, error bars represent the standard deviation. One representative experiment for the Phenotypic Microarray is shown.

(BW25113, Δ*dctA*) and EK3 (BW25113, Δ*dauA*/Δ*dctA*) respectively. We then tested the growth phenotype of the wild-type and the isogenic Δ*dauA*, Δ*dctA* and Δ*dauA*/Δ*dctA* strains on agar plates made using MOPS minimal medium and supplemented with 50 mM of either glucose or succinate as the sole carbon source. After 24 h of aerobic growth at 37°C, only the wild-type strain grew on the succinate-supplemented plates, although all four strains grew equally well in the presence of glucose (Fig. 3A, left panel). After 48 h, the individual Δ*dctA* and Δ*dauA* mutant strains showed some growth on the succinate-supplemented plates, but very weak growth was observed for the Δ*dctA*/Δ*dauA* strain (Fig. 3A, right panel).

Next we compared aerobic growth of the same four strains in liquid eM9 medium (which is M9 minimal medium containing 0.1% hydrolysed casein) containing

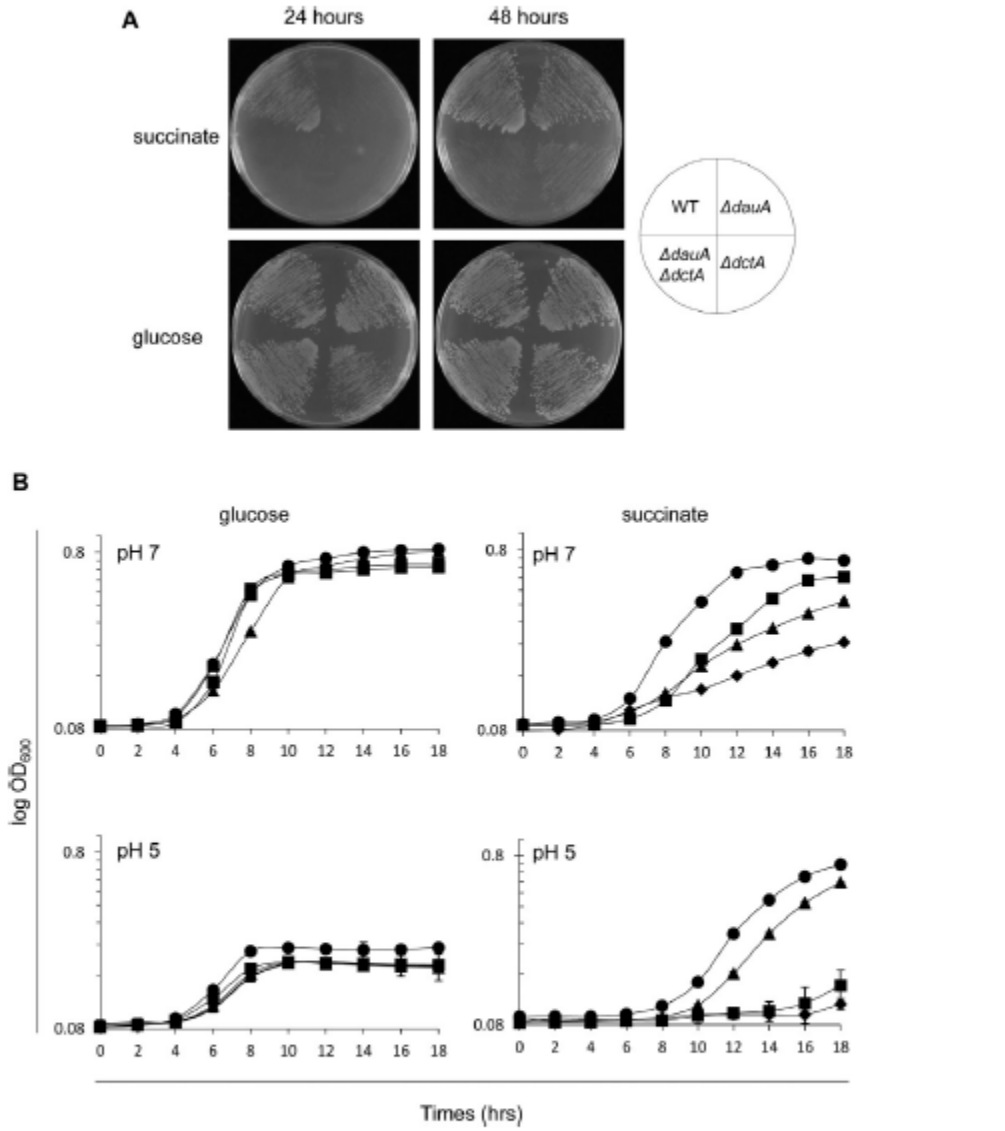

Fig. 3. DauA is involved in succinate metabolism.
A. Growth of the wild-type and isogenic Δ*dctA*, Δ*dauA* and Δ*dctA*/Δ*dauA* strains on MOPS minimal medium agar plates (pH 7) supplemented with 50 mM of either succinate or glucose as sole the carbon source. The plates were incubated for 24 h (left hand photograph) or 48 h (right hand photograph) at 37°C.
B. The wild-type (●), Δ*dctA* (▲), Δ*dauA* (■) and Δ*dctA*/Δ*dauA* (♦) strains were grown in eM9 minimal medium (pH 5 or pH 7 as indicated) containing either 50 mM glucose (left panels) or 50 mM succinate (right panels) as the sole carbon source. Growth curves at 600 nm were recorded using microplates. All results are the averages of at least four independent test series. Error bars represent the standard deviation.

50 mM glucose or 50 mM succinate as the carbon source, at pH 7 and pH 5. The strains grew equally well on glucose at pH 7, while all grew poorly on glucose at pH 5 (Fig. 3B). The poor growth on glucose at acidic pH is most likely due to glucose repression of the acid resistance system (Castanie-Cornet *et al.*, 1999) since all of the strains grew normally on glycerol at pH 5 (Fig. S2). In media containing succinate, at pH 7, the Δ*dauA* strain did not grow quite as well as the wild-type strain, while the Δ*dctA* strain grew less well than the Δ*dauA* strain and the double mutant showed the poorest growth. Very interestingly, at pH 5, the wild-type and Δ*dctA* strains showed a similar growth rate whereas Δ*dauA* and Δ*dauA*/Δ*dctA* were devoid of any growth. Taken together these results indicate that DauA plays a role in succinate transport and/or metabolism at pH 5.

DauA is produced at pH 5 and pH 7, whereas DctA is produced primarily at pH 7

The results presented above indicate that DauA is required to support growth on succinate, primarily at pH 5. We therefore sought to examine the production of DauA and DctA at pH 5 and pH 7, when succinate was supplied as the sole carbon source. To this end we introduced DNA encoding a C-terminal 6xHis epitope tag onto the chromosomally encoded *dauA* in the BW25113 (wild-type) and EK2 (Δ*dctA*) strain backgrounds to give strains EK4 and EK5 respectively. Likewise we similarly introduced DNA encoding a C-terminal 6xHis epitope tag onto the chromosomally encoded *dctA* in the BW25113 (wild-type) and EK1 (Δ*dauA*) strains, producing strains EK6 and EK7 respectively.

We first confirmed that the introduction of this epitope tag onto either DauA or DctA did not grossly affect protein function by assessing the growth of these strains in eM9 medium supplemented with succinate at pH 5 or pH 7 (Fig. S2). At pH 7, strains EK4 (DauA-H_6) and EK6 (DctA-H_6) showed similar growth to the analogous strains producing the native forms of DauA and DctA, and likewise strains EK5 (DauA-H_6, Δ*dctA*) and EK7 (DctA-H_6, Δ*dauA*) behaved similarly to the strains producing untagged proteins. Again at pH 5, the EK4 (DauA-H_6), EK5 (DauA-H_6, Δ*dctA*) and EK6 (DctA-H_6) strains grew normally whereas the EK7 (DctA-H_6, Δ*dauA*) strain was unable to grow, giving similar growth phenotypes to the analogous strains producing the native forms of DauA and DctA. These results indicate that the introduction of the histidine tag fusions at the C-terminus of DctA and DauA does not appear to grossly impair their functions.

In order to investigate the presence of DctA and DauA in succinate-grown cells at pH 5 and pH 7, strains EK4 (DauA-H_6), EK6 (DctA-H_6), EK5 (DauA-H_6, Δ*dctA*) and EK7 (DctA-H_6, Δ*dauA*) were grown overnight in M9 medium containing glucose as carbon source, washed twice and subsequently cultured for 6 h on M9 minimal medium containing succinate at pH 7 or pH 5. We monitored whole cell (WC), soluble fraction (SF) and membrane (M) fractions for the presence of DctA or DauA by Western blot using anti-His antibodies. TatC is a membrane protein known to be constitutively produced (Jack *et al.*, 2001) and was used as a loading control. In all of the strains tested, signals for DctA-H_6, DauA-H_6 and TatC were only detected in the membrane fraction, indicating that the proteins were correctly targeted to the membrane (Fig. 4A). DauA-H_6 (predicted mass, 59.2 kDa) and DctA-H_6 (predicted mass, 45.3 kDa) were detected at approximate molecular masses of ~40 kDa and ~35 kDa respectively. It should be noted that anomalous migration of membrane protein on SDS-PAGE is common and is likely due to the anomalous SDS-loading capacity and partial unfolding of hydrophobic proteins (Rath *et al.*, 2009).

Interestingly it was clear that DauA-H_6 was present in membranes of cells grown both at pHs and in the *dctA*$^+$ and Δ*dctA* strain backgrounds (Fig. 4B). Conversely, while DctA-H_6 was detected when the strains were grown at pH 7, no protein was detected when the cells were grown in the presence of succinate at pH 5. Unexpectedly, it also appeared that less DctA-H_6 was present at pH 7 in the strain where *dauA* was deleted. This latter observation might suggest that the presence and/or activity of DauA can affect the expression of *dctA*. To investigate this further, we constructed an in-frame deletion of *dauA* in *E. coli* strain IMW385 [As MC4100, λ(Φ*dctA'–'lacZ*)hyb, *bla*; A. Kleefeld and G. Unden, unpublished] to give strain EK8 and assessed the activity of the single copy *dctA'–'lacZ* fusion after growth of the strains in an identical manner to those used for the Western blot analysis above. Consistent with the lack of detectable DctA-H_6 at pH 5, activity of the *dctA'–'lacZ* fusion was not detectable above the background level at pH 5 (Fig. S3). At pH 7, expression of *dctA'–'lacZ* was clearly observed and this activity was approximately twofold lower in the Δ*dauA* mutant background (Fig. S3). This is entirely consistent with the results of the Western blot analysis of DctA-H_6, and indicates that there is some interplay between the presence/activity of DauA and the production of DctA.

DauA acts as a succinate transporter

The results presented above are consistent with the idea that DauA transports succinate. In order to obtain firm evidence that this is indeed the case, we developed an *in vivo* succinate uptake assay. Uptake and cellular accumulation of [^{14}C]-succinate were measured by incubating cells with [^{14}C]-succinate for up to 6 min, samples were removed periodically and cells were captured by vacuum filtration onto polycarbonate filters. The filter-trapped cells

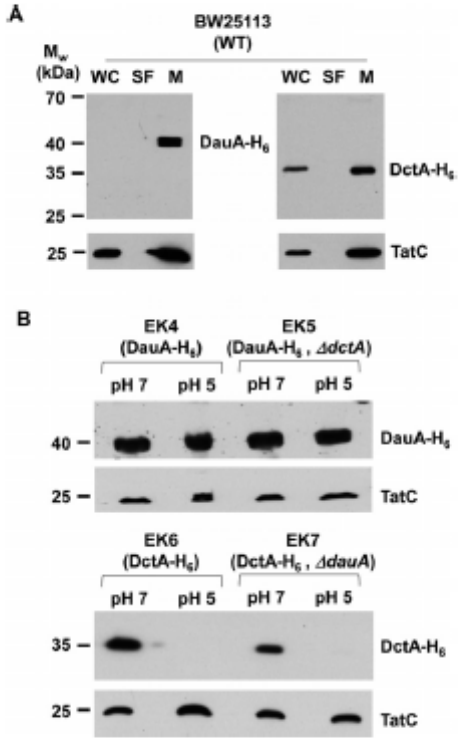

Fig. 4. DauA-H_6 is detectable during growth with succinate at pH 5 or pH 7, while DctA-H_6 is only present at pH 5.
A. Whole cells (*WC*), soluble fraction (*SF*) and membrane (*M*) fractions were prepared from the wild-type strain (BW25113) producing a his-tagged variant of DauA (left panel) or DctA (right panel) from the native chromosomal locus. Cells were grown for 6 h in M9 minimal medium (pH 7) supplemented with 50 mM succinate as the sole carbon source. Samples were harvested, fractionated into membrane and soluble fractions as described in *Experimental procedures*, and subjected to SDS-PAGE followed by Western blotting with an anti-His antibody. The same membranes were subsequently stripped and re-hybridized with a polyclonal anti-TatC antibody as a control.
B. Membrane fractions were prepared from strains EK4 (DauA-H_6), EK5 (DauA-H_6, Δ*dctA*), EK6 (DctA-H_6) and EK7 (DctA-H_6, Δ*dauA*) after growth for 6 h in M9 minimal medium supplemented with 50 mM succinate as the sole carbon source at either pH 7 or pH 5. Samples were subjected to SDS-PAGE, followed by Western blotting with an anti-His antibody. The same membranes were subsequently stripped and re-hybridized with a polyclonal anti-TatC antibody as a control.

were subsequently washed thoroughly and the level of radioactivity present on the filter, and thus associated with the cells, was then measured.

We have shown in the previous section that after growth in the presence of succinate at pH 5 only DauA, and not DctA, is present (Fig. 4B and Fig. S3). Therefore, these accumulation assays were initially performed following growth of cells for 6 h in the presence of succinate at pH 5 using equal-sized inocula of the wild-type, Δ*dctA*, Δ*dauA* and Δ*dctA*/Δ*dauA* strains. As shown in Fig. 5A, the [^{14}C]-succinate uptake activity was linear over the time period of measurement for all of the strains tested. The uptake activity for the wild-type strain was 0.043 ± 0.007 μmol^{-1} min^{-1} g^{-1} dry weight and was 1.4 times lower in Δ*dctA* strain. A negligible uptake rate was measured for the Δ*dauA* and Δ*dauA*/Δ*dctA* cells (0.008 ± 0.003 and 0.008 ± 0.001 μmol^{-1} min^{-1} g^{-1} dry weight respectively). The activity measured in the absence of DctA and the negligible uptake in the absence of DauA is strong evidence that DauA acts as a succinate transporter and that it is the major route for succinate import under these growth conditions.

We have also shown that in the wild-type and Δ*dctA* strains DauA was present when cells were grown in the presence of succinate at pH 7 (Fig. 4B). Therefore, in order to determine whether DauA plays a role in succinate uptake at pH 7, the wild-type, Δ*dctA*, Δ*dauA* and Δ*dauA*/Δ*dctA* strains were cultured in the presence of succinate at pH 7 and [^{14}C]-succinate uptake was measured. Again, as observed previously, the uptake activity was linear over the time period of measurement for all strains (Fig. 5A). The succinate uptake rate in the wild-type cells was 0.546 ± 0.084 μmol^{-1} min^{-1} g^{-1} dry weight and was almost negligible in the Δ*dctA* and Δ*dauA*/Δ*dctA* cells. This shows that under these growth conditions, DauA is largely inactive and DctA is the main succinate transporter. Although DauA appears not to be active in succinate transport under these growth conditions, the [^{14}C]-succinate uptake activity measured in the Δ*dauA* cells was six times lower than in the wild-type. This result is consistent with our previous findings that in the absence of DauA, *dctA* is not fully expressed (Fig. 4B; Fig. S3).

Comparison of the [^{14}C]-succinate uptake rates measured in wild-type cells grown in the presence of succinate at pH 5 (when DauA is the main transporter) and pH 7 (when DctA is the main transporter) shows that the total rate of uptake is around 10 times lower at pH 5. This suggests that DauA may transport succinate at a lower rate than DctA. Although an *in vitro* assay using purified protein reconstituted into liposomes would be necessary to precisely compare the uptake rates of DctA and DauA, we explored the kinetic parameters of DauA-dependent uptake compared with DctA-dependent uptake in whole cells by measuring the rates of [^{14}C]-succinate accumulation for each of the four strains, grown at pH 7 or pH 5, over a substrate concentration range of 40 μM to 5 mM. For each pH growth condition, the background rate of uptake measured in the Δ*dauA*/Δ*dctA* strain was sub-

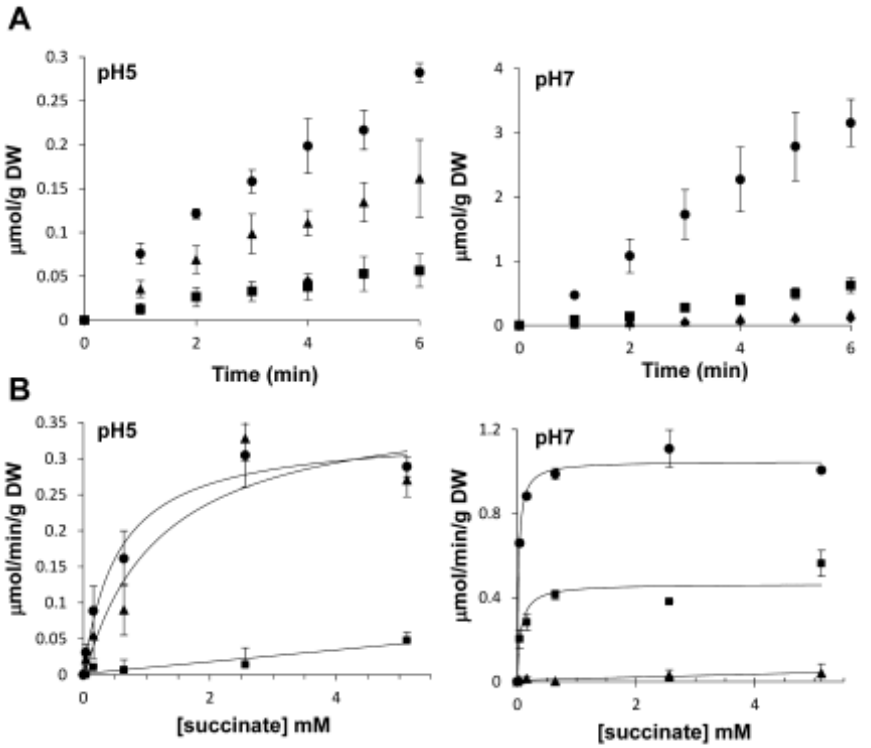

Fig. 5. Development of an *in vivo* succinate transport assay.
A. Time dependence of [^{14}C]-succinate accumulation in BW25113 (wild-type; ●), EK1 (Δ*dauA*; ■), EK2 (Δ*dctA*; ▲) and EK3 (Δ*dctA*/Δ*dauA*; ♦) strains.
B. Concentration dependence of ^{14}[C]-succinate uptake in BW25113 (wild-type; ●), EK1 (Δ*dauA*; ■) and EK2 (Δ*dctA*; ▲). The activity measured for strain EK3 (Δ*dctA*/Δ*dauA*) was subtracted in each case. Measurements were taken following growth of cells for 6 h in M9 minimal medium supplemented with 50 mM succinate as the sole carbon source at either pH 5 (left panels) or pH 7 (right panels). The ^{14}[C]-succinate uptake rate were linear over the time period of measurement (15 s–6 min).
All results are the averages of at least six independent test series. Error bars represent the standard deviation.

tracted from the rates obtained for the other strains and the results presented in Fig. 5B.

At pH 5, [^{14}C]-succinate accumulation in the wild-type and Δ*dctA* strains follows Michaelis–Menten-type kinetics, consistent with carrier-mediated transport (Fig. 5B). The very low residual transport activity in the Δ*dauA* strain shows linear kinetics with increasing succinate concentrations ($R^2 = 0.96$), which may result from either a diffusion process, the activity of a very low-affinity, uncharacterized transporter, or non-specific binding of the substrate to the membrane. The measurements obtained for the wild-type and Δ*dctA* strains were fitted to Michaelis–Menten kinetics and the apparent half-saturation constant (K_m) and maximum uptake rate (V_m), reflecting DauA activity, were derived from a Hanes–Woolf plot of the data (Table 1).

In order to compare the apparent kinetic parameters of DauA with those of DctA, the same uptake assays were

Table 1. Kinetics parameters for DauA and DctA.

		K_m (mM)	V_m (mmol^{-1} min^{-1} g^{-1} DW)	R^2
pH 7	WT	0.025 ± 0.005	1.05 ± 0.02	0.99
	Δ*dauA*	0.040 ± 0.019	0.45 ± 0.03	0.92
pH 5	WT	0.56 ± 0.15	0.34 ± 0.02	0.96
	Δ*dctA*	1.19 ± 0.84	0.38 ± 0.09	0.98

performed after growth of cells on succinate at pH 7, conditions under which DctA is the main active succinate transporter. In the wild-type and Δ*dauA* strains, succinate accumulation also follows Michaelis–Menten-type kinetics, again consistent with carrier-mediated transport (Fig. 5B). The apparent kinetic parameters, derived from a Hanes–Woolf plot of the data, are presented Table 1. In the Δ*dctA* mutant, the uptake rate was very low and increased linearly with increasing succinate concentrations (R^2 = 0.92) (Fig. 5B), again consistent with either of a diffusion process, the activity of a very low-affinity uncharacterized transporter, or non-specific binding of the substrate to the membrane, and thus confirming that under these growth conditions DctA is the major succinate transporter.

The analysis of the apparent kinetic parameters for DauA and DctA in the whole cell assay reveal that, first, the K_m values measured after growth at pH 7, reflecting DctA activity, are very similar to those determined for succinate transport *in vivo* by others (20–30 μM; Lo *et al*., 1972), validating our transport assay. Second, comparison of the kinetic parameters obtained for the wild-type strain after growth at pH 5 (reflecting DauA activity) and pH 7 (reflecting DctA activity) suggests that DauA has a weaker affinity for succinate. The results also indicate that DauA has a lower apparent maximal transport rate than DctA in this whole cell assay system. Finally, the significantly reduced V_m measured in the Δ*dauA* strain compared with the wild-type strain after growth with succinate at pH 7 confirms the reduction of *dctA* expression that we have observed in the absence of DauA (Fig. 4 and Fig. S3). This indicates that DauA is necessary at pH 7 for optimum DctA production and activity.

DauA can transport other C_4-dicarboxylic acids

DctA has been shown to transport a broad spectrum of substrates, including succinate, fumarate, malate, aspartate and oxaloacetate (Janausch *et al*., 2002). Therefore, in order to gain information about DauA specificity, the uptake of [^{14}C]-succinate (40 μM final concentration) in wild-type and Δ*dctA* strains was measured in the presence of various unlabelled carboxylic acids (2 mM final concentration) after growth of cells in the presence of succinate at pH 5. The rate of uptake measured for the negative control strain Δ*dauA*/Δ*dctA* under the same conditions was subtracted in each case. We reasoned that if DauA is able to transport any of the other carboxylic acids tested, we would expect to observe severe inhibition of succinate accumulation in the presence of the large excess of competitor. As shown in Fig. 6A, succinate uptake in both strains was severely inhibited by the presence of excess aspartate or fumarate. Oxaloacetate and butyrate gave a weak inhibition of succinate transport (≈40%) and no significant inhibition was observed in the presence of malate (Fig. 6A, Table S1). These results indicate that although DauA is able to transport aspartate and fumarate the inability of malate to inhibit succinate uptake suggests that DauA has differing substrate specificity to DctA.

In order to confirm previous observations that DctA can indeed transport succinate, fumarate, malate, aspartate and oxaloacetate (Janausch *et al*., 2002), the same experiment was repeated using the wild-type and Δ*dauA* strains after growth with succinate at pH 7. As expected, succinate uptake in both strains was inhibited by aspartate, fumarate, malate and oxaloacetate, in agreement with the previously reported specificity of DctA (Fig. 6B and Table S1) (Kay and Kornberg, 1971). The weak inhibition measured in the presence of butyrate has been previously reported (Janausch *et al*., 2001).

To validate our inhibition studies and confirm that DauA is indeed able to transport fumarate and aspartate, we directly measured [^{14}C]-fumarate and [^{14}C]-aspartate accumulation in the wild-type, Δ*dctA* and Δ*dauA* strains after growth in the presence of succinate at pH 5 (where we have already shown that DauA is the major transporter). As before, the background rate measured for the Δ*dauA*/Δ*dctA* strain under the same conditions was subtracted from the rate we measured for each of the other strains. The [^{14}C]-fumarate and [^{14}C]-aspartate accumulation rates measured in the wild-type and Δ*dctA* cells, shown in Fig. 7, were comparable and again the radioactive accumulation measured in the Δ*dauA* cells was negligible for fumarate and very low for aspartate. These results confirm that DauA is able to transport fumarate and aspartate at pH 5.

Finally, in order to confirm that when the cells are grown in the presence of succinate at pH 7 DauA is necessary for correct DctA expression and/or activity, [^{14}C]-fumarate accumulation was measured. Similar to our previous findings for succinate transport, the [^{14}C]-fumarate accumulation rate measured in the wild-type was also approximately four times higher than the rate measured in the Δ*dauA* cells. This result confirms that DctA expression and/or activity is impaired in the absence of DauA. In contrast, aspartate accumulation in the three strains was comparable. This result was expected as *E. coli* possesses at least two additional aspartate transport systems that are active at pH 7 (Schellenberg and Furlong, 1977).

DauA is able to transport mono- and di-carboxylates

The net charge of a C_4-dicarboxylate varies from −2 (i.e. the di-carboxylate form) to 0 (i.e. the dicarboxylic acid form) according to the pKa of the two carboxylic acid groups (Table S1). Succinate is present mainly as a

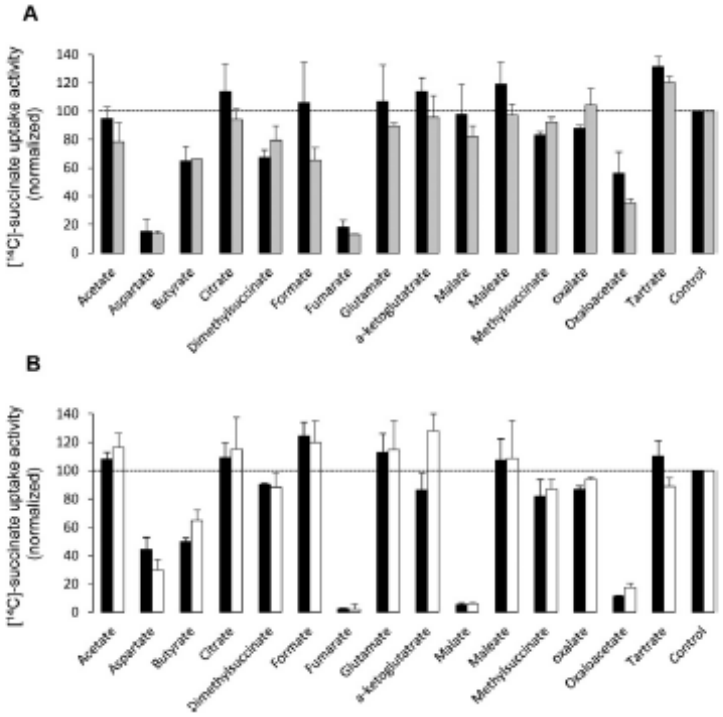

Fig. 6. Inhibition of DctA- and DauA-dependent [^{14}C]-succinate uptake activity in the presence of various carboxylic acids. [^{14}C]-succinate uptake (final concentration 40 µM) in (A) BW25113 (wild-type; black bars), and EK2 (Δ*dctA*; grey bars) strains and (B) BW25113 (wild-type; black bars) and EK1 (Δ*dauA*; white bars) strains upon addition of different carboxylic acids (2 mM final concentration). Measurements were taken following growth of cells for 6 h in M9 minimal medium supplemented with 50 mM succinate as the sole carbon source at either pH 5 (A) or pH 7 (B). All results are the averages of at least six independent test series and normalized to the control value which was set to 100%. The activity measured in the Δ*dctA*/Δ*dauA* strain was subtracted. (Control value: $WT_{pH\ 7}$ 0.537 µmol^{-1} min^{-1} g^{-1} DW, $WT_{pH\ 5}$ 0.035 µmol^{-1} min^{-1} g^{-1} DW, $\Delta DauA_{pH\ 7}$ 0.1 µmol^{-1} min^{-1} g^{-1} DW, $\Delta DctA_{pH\ 5}$ 0.025 µmol^{-1} min^{-1} g^{-1} DW). Error bars represent the standard deviation.

di-carboxylate at pH 7 and mono-carboxylate at pH 5 (Fig. S4). Since our results show that DauA is only active when the cells have been grown in the presence of succinate at pH 5, this would be consistent with the explanation that DauA can only transport the mono-carboxylate form of succinate. Inversely, the succinate transporters from the DAACS family characterized so far, including *E. coli* DctA, appear to recognize and transport only di-carboxylates (Gutowski and Rosenberg, 1975).

We therefore developed an assay to test whether DauA could transport the mono-carboxylate form of succinate. We first used the assay to confirm that DctA transports the di-carboxylate form of succinate. To this end we grew the BW25113 (wild-type), EK1 (Δ*dauA*) and EK3 (Δ*dauA*/Δ*dctA*) strains for 6 h in the presence of succinate at pH 7 (where we have already shown that DctA is the major transporter), washed them and then performed the [^{14}C]-succinate transport assay (10 µM final concentration) in a buffer of pH 5 or pH 7. As before, the rate measured for the EK3 (Δ*dauA*/Δ*dctA*) strain under the same conditions was subtracted from the rates for the other strains. When the external pH shifts from 7 to 5, the concentration of succinate di-carboxylate decreases seven times, therefore, if DctA transports only succinate di-carboxylate, and because the total succinate concentration (10 µM) is below the K_m we have measured (Table 1), we expect that the uptake activity at pH 7 would be significantly higher than at pH 5. The results in Fig. 8A clearly show that in the wild-type and the Δ*dauA* cells grown in the presence of succinate at pH 7, the [^{14}C]-succinate uptake activity is

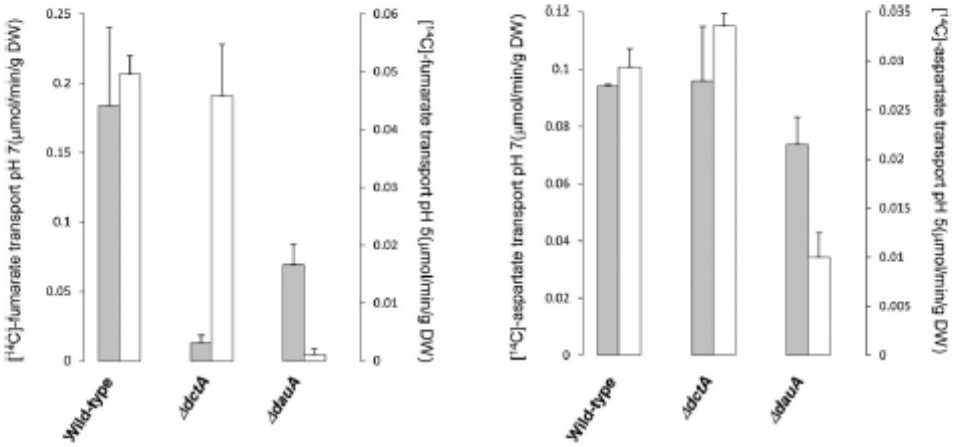

Fig. 7. DctA- and DauA-dependent [14C]-fumarate and [14C]-aspartate uptake activity.
[14C]-fumarate (left panel) and [14C]-aspartate (right panel) uptake (40 µM final concentration) in BW25113 (wild-type), EK1 (Δ*dauA*) and EK2 (Δ*dctA*) strains was measured as in Fig. 5A following growth of cells for 6 h in M9 minimal medium supplemented with 50 mM succinate as the sole carbon source at either pH 7 (grey bars) or pH 5 (white bars). The activity measured in the EK3 (Δ*dctA*/Δ*dauA*) strain was subtracted in each case. All results are the averages of at least six independent test series. Error bars represent the standard deviation.

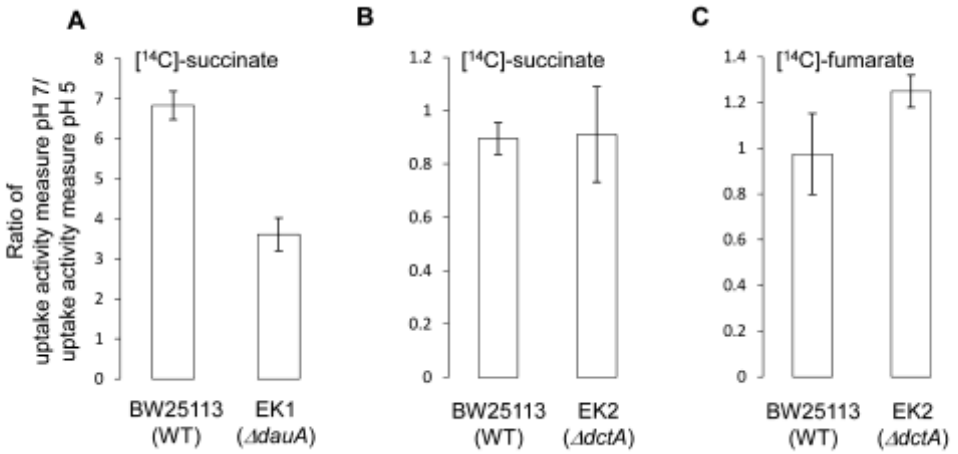

Fig. 8. Protonation state of DctA and DauA substrates.
A. Ratio of the [14C]-succinate (10 µM) uptake activity at pH 7 over the activity measured at pH 5 for strains BW25113 (wild-type) and EK1 (Δ*dauA*) that had previously been grown at pH 7 in M9 minimal medium supplemented with 50 mM succinate as the sole carbon source.
B and C. (B) Ratio of the [14C]-succinate (10 µM) or (C) [14C]-fumarate (10 µM) for strains BW25113 (wild-type) and EK2 (Δ*dauA*) that had previously been grown at pH 5 in M9 minimal medium supplemented with 50 mM succinate as the sole carbon source.
In each case, the activity of strain EK3 (Δ*dctA*Δ*dauA*), measured under the same growth and assay conditions, was subtracted. The results are the average of at least four independent test series. Error bars represent the standard deviation.

seven and four times higher, respectively, if measured at pH 7 compared with pH 5. This result confirms that DctA is able to transport only succinate di-carboxylate.

We next used this approach to elucidate the protonation state of succinate that can be transported by DauA. To this end we grew the BW25113 (wild-type), EK2 (Δ*dctA*) and EK3 (Δ*dauA*/Δ*dctA*) strains for 6 h in the presence of succinate at pH 5 (where we have already shown that DauA is the major transporter), washed them and then performed the [^{14}C]-succinate transport assay in a buffer of pH 5 or pH 7. As before, the rate measured for the EK3 (Δ*dauA*/Δ*dctA*) strain under the same conditions was subtracted from the rates for the other strains. When the external pH shifts from 7 to 5, the concentration of succinate di-carboxylate decreases seven times while the concentration of succinate mono-carboxylate increases 15 times (Fig. S4). Therefore, if DauA transports only succinate mono-carboxylate, and because the total succinate concentration (10 µM) is below the K_m we have measured (Table 1), we expect that the uptake activity at pH 5 would be higher than at pH 7. If DauA transports only succinate di-carboxylate, we expect that the uptake activity at pH 5 would be lower than at pH 7, and if DauA transports both succinate mono- and di-carboxylates, we expect to see the same succinate uptake activity at both pHs. The results in Fig. 8B clearly show that in wild-type and Δ*dctA* cells grown in the presence of succinate at pH 5, the [^{14}C]-succinate uptake activity is the same if measured at pH 7 or pH 5 (ratio = 1 for both strains in Fig. 8B). This result indicates that DauA is able to transport both mono- and di-carboxylate forms of succinate.

We have shown in Fig. 7 that DauA is able to transport fumarate. To confirm that DauA can also transport the mono- and di-carboxylate form of fumarate, we measured the [^{14}C]-fumarate uptake activity of cells grown in the presence of succinate at pH 5. When the external pH shifts from 7 to 5, the concentration of fumarate di-carboxylate decreases 1.4 times while the concentration of fumarate mono-carboxylate increases 64 times (Fig. S4). However, in close agreement with what we observed for succinate transport, the [^{14}C]-fumarate uptake activity of the wild-type and Δ*dctA* strains was the same if measured in buffer at pH 7 or pH 5 (since the ratio is very close to 1 for both strains in Fig. 8C), again confirming transport of both mono- and di-carboxylate forms.

DauA production is not dependent on the DcuSR activity

Expression of *dctA* is induced by the DcuSR two-component system in response to C_4-dicarboxylic acid (Zientz *et al.*, 1998; Davies *et al.*, 1999; Golby *et al.*, 1999). To examine whether DauA production is also dependent on the activity of DcuSR, we introduced DNA encoding a C-terminal FLAG epitope tag onto the chromosomally encoded *dctA* in strain EK4 (DauA-H$_6$), to give strain EK9 (DauA-H$_6$, DctA-FLAG). We then constructed an in-frame deletion of *dcuS* in the EK9 (DauA-H$_6$, DctA-FLAG) strain background, giving strain EK10 (DauA-H$_6$, DctA-FLAG, Δ*dcuS*). To investigate the presence of DctA and DauA in succinate-grown cells at pH 5 and pH 7, strains EK9 (DauA-H$_6$, DctA-FLAG) and EK10 (DauA-H$_6$, DctA-FLAG, Δ*dcuS*) were grown overnight in M9 medium containing glucose as the carbon source, washed twice with M9 medium lacking carbon source and subsequently cultured for 6 h in M9 minimal medium containing succinate at pH 7 or pH 5. We monitored membrane fractions for the presence of DctA or DauA by Western blot using anti-FLAG or anti-His antibodies respectively. Again TatC was used as a loading control. The Western blot analysis (Fig. 9) shows that under these conditions, DctA is not produced in a Δ*dcuS* background or at pH 5, and we can therefore conclude that under these conditions *dctA* expression is totally dependent on the activity of the DcuSR two-component system. However, DauA is produced at the same level in the wild-type or Δ*dcuS* strains, which indicates that *dauA* expression is not dependent on DcuSR under the conditions we have used in these experiments.

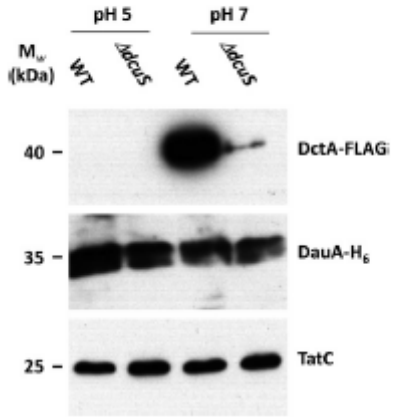

Fig. 9. DauA production is not dependent on the DcuSR activity. Membrane fractions were prepared from strain EK9 (DauA-H6, DctA-FLAG) and EK10 (DauA-H$_6$, DctA-FLAG, Δ*dcuS*) following growth of cells for 6 h in M9 minimal medium at pH 5 or pH 7 supplemented with 50 mM succinate as the sole carbon source. Samples were subjected to SDS-PAGE, followed by Western blotting with an anti-His antibody. The same membranes were subsequently stripped and re-hybridized with anti-FLAG and then stripped and re-hybridized with a polyclonal anti-TatC antibody as a control.

Discussion

DauA is a protein with transport and regulation activity

The SLC26/SulP (solute carrier/sulphate transporter) proteins are a ubiquitous superfamily of anion transporters. Prior studies on this family of transporters have focused overwhelmingly on eukaryotic members, particularly as some of the human members are implicated in genetic diseases (Mount and Romero, 2004; Dorwart *et al.*, 2008). Despite the fact that these proteins are present in almost all bacteria (Fig. 1), their physiological functions are almost completely unknown. In this study we have identified *E. coli* DauA as a previously undiscovered class of C_4-dicarboxylic acid transporters. Although this is the first report that a member of the SLC26/SulP family acts as a C_4-dicarboxylic acid uptake system, it should be noted that from the 10 SLC26A proteins expressed in humans, six have been shown to transport oxalate, a C_2-dicarboxylic acid (Mount and Romero, 2004). These transporters (Slc26A1, 3, 6, 7, 8 and 9) act as oxalate/chloride or oxalate/sulphate exchangers (Mount and Romero, 2004; Dorwart *et al.*, 2008), it is therefore possible that these transporters share common features with the bacterial DauA-like proteins, paving the way to establish *E. coli* DauA as a paradigm for the ubiquitous SLC26/SulP transporter family. Further studies using an *in vitro* system will be necessary to define the energetics of DauA transport activity.

A previous study describing the structure of the soluble DauA (YchM) STAS domain led the authors to propose that DauA is a bicarbonate transporter involved in fatty acid metabolism (Babu *et al.*, 2010). However, direct proof of this activity is so far lacking and phylogenetic analysis by ourselves and others (Fig. 1) (Felce and Saier, 2004; Price and Howitt, 2011) shows that DauA does not belong to the subfamily of bicarbonate/carbonate transporters from the SLC26A/SulP family, consistent with the likelihood that the primary function of DauA is not bicarbonate transport. In support of this we have repeatedly failed to detect any DauA-dependent bicarbonate accumulation under conditions where the protein is clearly active for succinate and fumarate transport (data not shown), making it unlikely that bicarbonate is a major substrate for DauA.

The results we report here indicate that DauA is not only acting as a transporter, but also plays a role in the regulation of C_4-dicarboxylic acid metabolism, as illustrated by the reduced expression and/or activity of DctA in the absence of DauA. Under aerobic conditions and in response to external C_4-dicarboxylic acids, expression of *dctA* is stimulated by the DcuSR two-component system (Zientz *et al.*, 1998; Davies *et al.*, 1999; Golby *et al.*, 1999). Moreover we have shown that under the experimental conditions we have used in this study, the expression of DctA is completely dependent on DcuSR. It is, therefore, plausible that DauA modifies the expression of *dctA* via DcuSR. Such a dual role as a transporter and a sensor has already been described for two other *E. coli* C_4-dicarboxylic acid transporters, DctA and DcuB, where DcuS interacts with DctA or DcuB to form a functional sensor unit under aerobic and anaerobic conditions respectively (Davies *et al.*, 1999; Kleefeld *et al.*, 2009; Witan *et al.*, 2012). It should also be noted that other secondary carriers such as the lysine-specific permease, LysP (Tetsch *et al.*, 2008), the hexose phosphate transporter, UhpC (Schwoppe *et al.*, 2003) and the ABC transporters PstSCAB2 (the high-affinity phosphate transporter) (Wanner, 1996) and MalEFGK (the maltose translocation system) (Antoine *et al.*, 2005) also act as co-sensors of membrane-bound transcriptional activators and histidine kinases, reflecting the fact that co-sensing by membrane-bound transporters is an increasingly common phenomenon. It is therefore tempting to speculate that DauA acts as a co-sensor of DcuS.

In addition to the DcuSR two-component system that controls exogenous induction of genes required for general C_4-dicarboxylic acid metabolism by extracellular substrates (Kneuper *et al.*, 2005; Scheu *et al.*, 2010), *E. coli* contains two other regulators that control specific pathways of C_4-dicarboxylate metabolism. The cytoplasmic regulatory systems TtdR and DmlR control endogenous induction of the genes for L-tartrate fermentation and D-malate degradation respectively (Oshima and Biville, 2006; Kim *et al.*, 2009; Lukas *et al.*, 2010). Therefore, C_4-dicarboxylate metabolism in *E. coli* is regulated by a combination of exogenous and endogenous signals which regulate the expression of the pathways of general and specific C_4-dicarboxylate metabolism for metabolic integration (Scheu *et al.*, 2010). In light of the dual exogenous/endogenous sensing of C_4-dicarboxylate, a role for DauA and specifically the cytoplasmic STAS domain in a potential sensing mechanism related to C_4-dicarboxylic acid metabolism is very attractive. The function of the STAS domain in bacterial SLC26/SulP proteins is currently unknown; however, studies on other proteins containing STAS domains have shown that they function as sensors, interaction/transduction modules and ligand-activated transcription factors (Sharma *et al.*, 2011). Therefore, the STAS domain of DauA appears to be a prime candidate for a sensing function. Clearly further studies are required to clarify the role of DauA and its STAS domain in C_4-dicarboxylate-mediated regulation.

Taken together, the results presented in this study allow us to develop a model for DauA function (Fig. 10):

At pH 7 in the presence of succinate, DctA is the main transporter and DauA is inactive under these conditions. However, in the Δ*dauA* strain we observe a reduced growth phenotype with succinate, a significant decrease

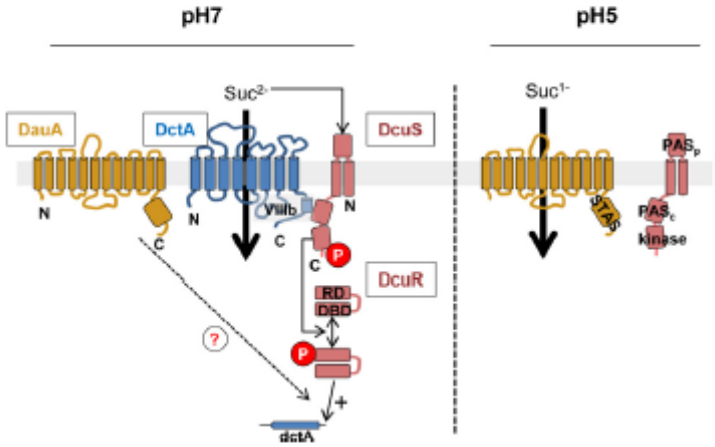

Fig. 10. Working model for the physiological role of DauA: DauA ensures the optimal absorption of C_4-dicarboxylic acids at various pHs either by impacting the transcription of *dctA* at pH 7 or by acting directly as a transporter at acidic pH.
At pH 7, C_4-dicarboxylic acid is bound to DctA and DcuS, helix VIIIb of DctA interacts with the PAS_c domain of DcuS and, as a result, the transcription of *dctA* is activated via the phosphorylation of the response regulator DcuR (Witan *et al.*, 2012). DauA is expressed and plays a role in the transcription of *dctA*. It seems that DauA is not active, or has only low level activity for succinate transport.
At pH 5 in the presence of succinate, succinate mono-carboxylates cannot activate DcuS/R and *dctA* is not transcribed. DauA is expressed and active. For simplicity DauA and DcuS which are dimers and DctA, a trimer, are represented as monomers. The topology of DauA has been predicted using Octopus (http://octopus.cbr.su.se/). BDB, DNA-binding domain; PAS_c, cytoplasmic Per-ARNT-Sim domain; PAS_p, periplasmic Per-ARNT-Sim domain; RD, receiver domain; STAS, Sulphate Transporter and Anti-Sigma antagonist domain.

of *dctA* expression, DctA protein in the membrane and DctA-dependent transport activity. This shows that under these conditions, DauA is essential for optimal expression and activity of DctA. It is not yet clear why DauA is inactive as a transporter under these conditions, further studies are needed to clarify this point.

At pH 5 in the presence of succinate, DauA is the main transporter under these growth conditions. The kinetic analysis shows that DauA has a weaker affinity and lower apparent transport rate for succinate than DctA, in agreement with previous conclusions (Davies *et al.*, 1999; Janausch *et al.*, 2001). DctA is not produced, most likely because the DcuS component of the DcuSR system seems to only bind di-carboxylates and at pH 5 succinate is mainly present as a mono-carboxylate (Kneuper *et al.*, 2005; Cheung and Hendrickson, 2008). Since a *ΔdcuS* mutant is able to grow under these conditions (our unpublished data and Golby *et al.*, 1999), and the fact that we detect DauA independently of the presence of DcuS (Fig. 9), it is unlikely that *dauA* expression depends strongly on DcuSR.

Experimental procedures

Bacterial strains and growth conditions

The *E. coli* K12 strains and plasmids used in this study are listed in Table 2. Luria–Bertani broth (LB) and LB agar were used for routine bacterial growth and genetic studies (Sambrook *et al.*, 1989). For growth experiments *E. coli* was cultivated in M9 minimal medium (Yanisch-Perron *et al.*, 1985), enriched M9 (eM9) medium (Kramer *et al.*, 2007) or MOPS minimal medium (Neidhardt *et al.*, 1974). All media were supplemented with 50 mM of the specified carbon source. When required, antibiotics where added at the following final concentrations: Ampicillin 100 μg ml^{-1}, Kanamycin 50 μg ml^{-1} and Chloramphenicol 30 μg ml^{-1}.

EK1 and EK2 originate from strains JW5189-1 and JW3469-1 respectively (Table 2) in which the Kan-resistance cassette has been removed using the temperature-sensitive vector pCP20 that encodes the FLP recombinase (Datsenko and Wanner, 2000). Strain EK3 (*ΔdauA/ΔdctA*) was constructed by P1 transduction. A P1 lysate was prepared from JW3469-1 and transduced into EK1 according to standard methods (Miller, 1992). The Kan^R cassette was then subsequently removed using the pCP20-encoded FLP recombinase (Datsenko and Wanner, 2000).

Strains EK4 and EK5 were constructed as follows: a fragment (A) covering the last 501 base pairs (bp) of *dauA* and introducing six histidines before the termination codon was amplified by PCR using primers EKO1 Fw and EKO2 Rv (Table S2) with BW25113 chromosomal DNA as template. The product was digested with XbaI and BamHI. A second fragment (B) covering 500 bp sequence downstream of *dauA* was amplified by PCR using primers EKO3 Fw and EKO4 Rv (Table S2) with BW25113 chromosomal DNA as template. The product was digested with BamHI and PstI. Both frag-

Table 2. Strains and plasmids used in this study.

Strains/plasmids	Genotype	Source
***E. coli* K-12**		
WT (BW25113)	F-, Δ(*araD-araB*)*567*, Δ*lacZ4787*(::*rrnB-3*), λ-, *rph-1*, Δ(*rhaD-rhaB*)*568*, *hsdR514*	Baba *et al.* (2006)
JW5189-1	BW25113, but Δ*dauA724*::kan	Baba *et al.* (2006)
JW3469-1	BW25113, but Δ*dctA783*::kan	Baba *et al.* (2006)
JW4086-1	BM25113, but Δ*dcuS751*::kan	Baba *et al.* (2006)
EK1	BW25113, but Δ*dauA*	This study
EK2	BW25113, but Δ*dctA*	This study
EK3	BW25113, but Δ*dauA*/Δ*dctA*	This study
EK4	BW25113 encoding DauA-His[a]	This study
EK5	EK2 encoding DauA-His[a]	This study
EK6	BW25113 encoding Dcta-His[a]	This study
EK7	EK1 encoding DctA-His[a]	This study
IMW385	MC4100, but λ[Φ(*dctA–lacZ*)*hyb* Amp[R]]	Kleefeld and Unden (unpublished)
EK8	IMW385, but Δ*dauA*	This study
EK9	EK4 encoding DctA-FLAG[b]	This study
EK10	EK9 but Δ*dcuS*	This study
Plasmid		
pBluescript-II KS+	Amp[R]	Stratagene
pCP20	FLP[+], λcI857[+], λp[R] Flp[R], Amp[R], Cam[R]	Datsenko and Wanner (2000)
pMAK705	pSC101 derivative- rep(ts) – Cm[R]	Hamilton *et al.* (1989)

a and b denotes proteins with in-frame C-terminal His tag or FLAG tag fusions respectively.

ments were cloned simultaneously into pBluescript (Stratagene). The *dauA* $(His)_6$-tagged allele was excised by digestion with XbaI and PstI and subcloned into pMAK705. The mutant allele of *dauA* was transferred into the chromosome of BW25113 and EK2 as described (Hamilton *et al.*, 1989) to give strains EK4 and EK5 respectively.

Strains EK5 and EK6 were constructed similarly using the primers EKO5 Fw – EKO6 Rv for fragment A and EKO7 Fw – EKO8 Rv for fragment B (Table S2). The mutant allele of *dctA* was transferred to the chromosome of BW25113 and EK1 to give strains EK5 and EK6 respectively.

Strain EK9 was constructed as follows: primers EKO9 Fw and EKO10 Rv (Table S2) were used to replace by PCR the His-tag with a FLAG tag on the pMAK705 vector carrying the mutated allele of *dctA*. The FLAG tagged mutate allele was transferred into the chromosome of EK4 as described (Hamilton *et al.*, 1989) to give strain EK9.

Strain EK10 was constructed by P1 transduction. A P1 lysate was prepared from JW4086-1 and transduced into EK9 according to standard methods (Miller, 1992). The Kan^R cassette was then subsequently removed using the pCP20-encoded FLP recombinase (Datsenko and Wanner, 2000).

Phenotypic microarrays

The technology of Phenotypic Microarrays (Biolog) was used (Bochner, 2009). Briefly, the strains were grown overnight on LB agar. A cell suspension at a standardized cell density was prepared in MOPS-based minimal medium supplemented with the appropriate nutrient source and a redox dye, tetrazolium violet. One hundred microlitres of this cell suspension was pipetted in a 96-well microtitre plate and measured for 24 h at 37°C in a microtitre plate reader (OMNILOG instrument). Seven hundred non-redundant trophic conditions were screened (Carbon, Nitrogen, Phosphorus and Sulphur metabolism, nutrient supplements, osmotic and pH sensitivity).

Growth experiments

Escherichia coli strains were cultured overnight in eM9 medium supplemented with the appropriate carbon source at pH 7 or 5. The next day the cells were washed twice in eM9 (carbon source free) at pH 5 or pH 7 and diluted to an optical density at 600 nm of 0.05 in 150 µl of eM9 medium containing the appropriate carbon source at the appropriate pH into a 96-well microtitre plate. Growth was monitored for 24 h using a Synergy 2 platereader (Biotek).

β-Galactosidase assays

Escherichia coli strains were cultured overnight in M9 minimal medium containing glucose as sole carbon source. The next day the cells were washed twice in M9 (carbon source free) at pH 5 or pH 7 and diluted to an optical density at 600 nm of 0.6 in M9 medium containing succinate (50 mM) at pH 5 or pH 7. After 6 h, cells were harvested for measurement of β-galactosidase activity. For measurement of β-galactosidase activity, cells were permeabilized with toluene and added to Z buffer (52 g of Na_2HPO_4, 6.24 g of $NaH_2PO_4{\cdot}2H_2O$, 0.75 g of KCl, 0.25 g of $MgSO_4{\cdot}7H_2O$ and 0.7 ml of β-mercaptoethanol per litre) in a total volume of 160 µl. The reaction was started by the addition of 30 µl of 4 mg ml^{-1} *o*-nitrophenyl β-galactoside and the rate of increase of A_{405} (ΔA_{405} min^{-1}) at 37°C was measured immediately in an ELx808 absorbance microplate reader (BioTek). β-Galactosidase activity is reported as ΔA_{405} min^{-1} ml^{-1} OD_{600}^{-1}.

Subcellular fractionation

Cells were grown as for the β-galactosidase assays using the carbon source and pH indicated and fractionated according to procedures described previously (Coutts *et al.*, 2002). The total protein concentration in each fraction was measured using the *DC protein assay* kit (Bio-Rad Laboratories) using bovine serum albumin as the standard.

Western immunoblotting

Western blotting was performed as described previously (Coutts *et al.*, 2002). Proteins were detected using one of the following antibodies: anti-His antibody (Qiagen); anti-FLAG antibody (Sigma) and rabbit polyclonal anti-TatC antibody raised against purified *E. coli* TatC protein (kind gift of T. Palmer).

In vivo *[^{14}C]-succinate, [^{14}C]-fumarate and [^{14}C]-aspartate transport assays*

In vivo transport assays were adapted from Jack *et al.* (1999). Briefly, cells were cultured in the same way as for the β-galactosidase assays using the carbon source and pH indicated. After 6 h, cells were harvested, washed twice in M9 minimal medium without a carbon source, at the appropriate pH and resuspended in the same medium to give a final OD_{600} of 0.6. At zero time, [^{14}C]-aspartate, -fumarate or -succinate (55 mCi mmol^{-1}) was added to give the final concentration specified for each experiment. Samples of 300 µl were taken at 15 s, 30 s, 1, 2, 3, 4, 5 and 6 min and uptake was terminated by filtration through nitrocellulose filters (Millipore type HA; 0.45 µm pore size) under a constant vacuum. The radioactivity present on the filter was determined using a scintillation counter. Data were calibrated by using internal standards spotted on filters and counted in the same experiment.

For the competition experiments, unlabelled competitor (50-fold excess) was added at the same time as the [^{14}C]-labelled substrate (40 µM). For the uptake experiments at pH 7 and pH 5, the cells were cultured in the same way as for the other transport assays, at pH 7 or pH 5, after which they were split in two equal batches, washed quickly twice in M9 minimal medium without a carbon source at pH 7 or 5 and assayed immediately for uptake activity (10 µM substrate). The pH dependence of the concentrations (expressed as %) of the different protonation states of succinate and fumarate were calculated as follows: $[COOH - COOH] = ([H^+]^2)/([H^+]^2 + K_{a1}[H^+] + K_{a1}K_{a2})$, $[COOH - COO^-] = (K_{a1}[H^+])/([H^+]^2 + K_{a1}[H^+] + K_{a1}K_{a2})$, $[COO^- - COO^-] = (K_{a1}K_{a2})/([H^+]^2 + K_{a1}[H^+] + K_{a1}K_{a2})$ with $pKa = -Log_{10}(K_a)$

Phylogenetic analysis

Sequences were obtained from NCBI databases (http://www.ncbi.nlm.nih.gov/) using BLASTP and the DauA (YchM) sequence from *E. coli* as the input sequence. Amino acid sequence alignments were performed with Muscle in MEGA version 5 (Tamura *et al.*, 2011). The evolutionary history was inferred using the Neighbour-Joining method (Saitou and Nei, 1987). The optimal tree with the sum of branch length = 111.73872566 is shown. The percentage of replicate trees in which the associated taxa clustered together in the bootstrap test (1000 replicates) are shown next to the main branches. The tree is drawn to scale, with branch lengths in the same units as those of the evolutionary distances used to infer the phylogenetic tree. The evolutionary distances were computed using the Poisson correction method (Zuckerkandl and Pauling, 1965) and are in the units of the number of amino acid substitutions per site. The analysis involved 766 amino acid sequences. All ambiguous positions were removed for each sequence pair. There were a total of 1868 positions in the final data set. Evolutionary analyses were conducted in MEGA5 (Tamura *et al.*, 2011).

Acknowledgements

We would like to thank Prof. Tracy Palmer for her constructive comments on the manuscript and for providing us with the anti-TatC antibody, Prof. Gottfried Unden for providing strain IMW385 and Lucia Licandro-Lado for technical help. E.K. was supported by a studentship from the Biotechnology and Biological Sciences Research Council doctoral training grant (BB/F017022/1), E.C. by a postdoctoral fellowship from the Medical Research Council (G1000054) and A.J. by a Scottish government/Royal Society of Edinburgh personal research fellowship.

References

Antoine, R., Huvent, I., Chemial, K., Deray, I., Raze, D., Locht, C., and Jacob-Dubuisson, F. (2005) The periplasmic binding protein of a tripartite tricarboxylate transporter is involved in signal transduction. *J Mol Biol* **351:** 799–809.

Baba, T., Ara, T., Hasegawa, M., Takai, Y., Okumura, Y., Baba, M., *et al.* (2006) Construction of *Escherichia coli* K-12 in-frame, single-gene knockout mutants: the Keio collection. *Mol Syst Biol* **2:** 2006.0008.

Babu, M., Greenblatt, J.F., Emili, A., Strynadka, N.C., Reithmeier, R.A., and Moraes, T.F. (2010) Structure of a SLC26 anion transporter STAS domain in complex with acyl carrier protein: implications for *E. coli* YchM in fatty acid metabolism. *Structure* **18:** 1450–1462.

Baker, K.E., Difullio, K.P., Neuhard, J., and Kelln, R.A. (1996) Utilization of orotate as a pyrimidine source by *Salmonella typhimurium* and *Escherichia coli* requires the dicarboxylate transport protein encoded by dctA. *J Bacteriol* **178:** 7099–7105.

Bochner, B.R. (2009) Global phenotypic characterization of bacteria. *FEMS Microbiol Rev* **33:** 191–205.

Castanie-Cornet, M.P., Penfound, T.A., Smith, D., Elliott, J.F., and Foster, J.W. (1999) Control of acid resistance in *Escherichia coli*. *J Bacteriol* **181:** 3525–3535.

Cheung, J., and Hendrickson, W.A. (2008) Crystal structures of C_4-dicarboxylate ligand complexes with sensor domains of histidine kinases DcuS and DctB. *J Biol Chem* **283:** 30256–30265.

Compton, E.L., Karinou, E., Naismith, J.H., Gabel, F., and Javelle, A. (2011) Low resolution structure of a bacterial SLC26 transporter reveals dimeric stoichiometry and

mobile intracellular domains. *J Biol Chem* **286:** 27058–27067.

Coutts, G., Thomas, G., Blakey, D., and Merrick, M. (2002) Membrane sequestration of the signal transduction protein GlnK by the ammonium transporter AmtB. *EMBO J* **21:** 536–545.

Datsenko, K.A., and Wanner, B.L. (2000) One-step inactivation of chromosomal genes in *Escherichia coli* K-12 using PCR products. *Proc Natl Acad Sci USA* **97:** 6640–6645.

Davies, S.J., Golby, P., Omrani, D., Broad, S.A., Harrington, V.L., Guest, J.R., *et al.* (1999) Inactivation and regulation of the aerobic C(4)-dicarboxylate transport (*dctA*) gene of *Escherichia coli*. *J Bacteriol* **181:** 5624–5635.

Dorwart, M.R., Shcheynikov, N., Yang, D., and Muallem, S. (2008) The solute carrier 26 family of proteins in epithelial ion transport. *Physiology (Bethesda)* **23:** 104–114.

Felce, J., and Saier, M.H., Jr (2004) Carbonic anhydrases fused to anion transporters of the SulP family: evidence for a novel type of bicarbonate transporter. *J Mol Microbiol Biotechnol* **8:** 169–176.

Golby, P., Davies, S., Kelly, D.J., Guest, J.R., and Andrews, S.C. (1999) Identification and characterization of a two-component sensor-kinase and response-regulator system (DcuS–DcuR) controlling gene expression in response to C4-dicarboxylates in *Escherichia coli*. *J Bacteriol* **181:** 1238–1248.

Gutowski, S.J., and Rosenberg, H. (1975) Succinate uptake and related proton movements in *Escherichia coli* K12. *Biochem J* **152:** 647–654.

Hamilton, C.M., Aldea, M., Washburn, B.K., Babitzke, P., and Kushner, S.R. (1989) New method for generating deletions and gene replacements in *Escherichia coli*. *J Bacteriol* **171:** 4617–4622.

Hawkesford, M.J., and De Kok, L.J. (2006) Managing sulphur metabolism in plants. *Plant Cell Environ* **29:** 382–395.

Jack, R., de Zamaroczy, M., and Merrick, M. (1999) The signal transduction protein GlnK is required for NifL-dependent nitrogen control of nif expression in *Klebsiella pneumoniae*. *J Bacteriol* **181:** 1156–1162.

Jack, R.L., Sargent, F., Berks, B.C., Sawers, G., and Palmer, T. (2001) Constitutive expression of *Escherichia coli tat* genes indicates an important role for the twin-arginine translocase during aerobic and anaerobic growth. *J Bacteriol* **183:** 1801–1804.

Janausch, I.G., Kim, O.B., and Unden, G. (2001) DctA- and Dcu-independent transport of succinate in *Escherichia coli*: contribution of diffusion and of alternative carriers. *Arch Microbiol* **176:** 224–230.

Janausch, I.G., Zientz, E., Tran, Q.H., Kroger, A., and Unden, G. (2002) C_4-dicarboxylate carriers and sensors in bacteria. *Biochim Biophys Acta* **1553:** 39–56.

Kay, W.W., and Kornberg, H.L. (1971) The uptake of C_4-dicarboxylic acids by *Escherichia coli*. *Eur J Biochem* **18:** 274–281.

Kim, O.B., Reimann, J., Lukas, H., Schumacher, U., Grimpo, J., Dunnwald, P., and Unden, G. (2009) Regulation of tartrate metabolism by TtdR and relation to the DcuS–DcuR-regulated C_4-dicarboxylate metabolism of *Escherichia coli*. *Microbiology* **155:** 3632–3640.

Kleefeld, A., Ackermann, B., Bauer, J., Kramer, J., and Unden, G. (2009) The fumarate/succinate antiporter DcuB of *Escherichia coli* is a bifunctional protein with sites for regulation of DcuS-dependent gene expression. *J Biol Chem* **284:** 265–275.

Kneuper, H., Janausch, I.G., Vijayan, V., Zweckstetter, M., Bock, V., Griesinger, C., and Unden, G. (2005) The nature of the stimulus and of the fumarate binding site of the fumarate sensor DcuS of *Escherichia coli*. *J Biol Chem* **280:** 20596–20603.

Kramer, J., Fischer, J.D., Zientz, E., Vijayan, V., Griesinger, C., Lupas, A., and Unden, G. (2007) Citrate sensing by the C_4-dicarboxylate/citrate sensor kinase DcuS of *Escherichia coli*: binding site and conversion of DcuS to a C_4-dicarboxylate- or citrate-specific sensor. *J Bacteriol* **189:** 4290–4298.

Lo, T.C., Rayman, M.K., and Sanwal, B.D. (1972) Transport of succinate in *Escherichia coli*. I. Biochemical and genetic studies of transport in whole cells. *J Biol Chem* **247:** 6323–6331.

Lukas, H., Reimann, J., Kim, O.B., Grimpo, J., and Unden, G. (2010) Regulation of aerobic and anaerobic d-malate metabolism of *Escherichia coli* by the LysR-type regulator DmlR (YeaT). *J Bacteriol* **192:** 2503–2511.

Marziut, G.A. (1997) Molecular genetics of sulfur assimilation in filamentous fungi and yeast. *Annu Rev Microbiol* **51:** 73–96.

Miller, J.H. (1992) *A Short Course in Bacterial Genetics. A Laboratory Manual and Handbook for* Escherichia coli *and Related Bacteria*. New York: Cold Spring Harbor Laboratory Press.

Mount, D.B., and Romero, M.F. (2004) The SLC26 gene family of multifunctional anion exchangers. *Pflugers Arch* **447:** 710–721.

Neidhardt, F.C., Bloch, P.L., and Smith, D.F. (1974) Culture medium for enterobacteria. *J Bacteriol* **119:** 736–747.

Oshima, T., and Biville, F. (2006) Functional identification of ygiP as a positive regulator of the *tfdA-tfdB-ygjE* operon. *Microbiology* **152:** 2129–2135.

Price, G.D., and Howitt, S.M. (2011) The cyanobacterial bicarbonate transporter BicA: its physiological role and the implications of structural similarities with human SLC26 transporters. *Biochem Cell Biol* **89:** 178–188.

Price, G.D., Woodger, F.J., Badger, M.R., Howitt, S.M., and Tucker, L. (2004) Identification of a SulP-type bicarbonate transporter in marine cyanobacteria. *Proc Natl Acad Sci USA* **101:** 18228–18233.

Price, G.D., Sheiden, M.C., and Howitt, S.M. (2011) Membrane topology of the cyanobacterial bicarbonate transporter, SbtA, and identification of potential regulatory loops. *Mol Membr Biol* **28:** 265–275.

Rath, A., Glibowicka, M., Nadeau, V.G., Chen, G., and Deber, C.M. (2009) Detergent binding explains anomalous SDS-PAGE migration of membrane proteins. *Proc Natl Acad Sci USA* **106:** 1760–1765.

Saier, M.H., Jr, Eng, B.H., Fard, S., Garg, J., Haggerty, D.A., Hutchinson, W.J., *et al.* (1999) Phylogenetic characterisation of novel transport protein families revealed by genome analysis. *Biochim Biophys Acta* **1422:** 1–56.

Saitou, N., and Nei, M. (1987) The neighbor-joining method: a new method for reconstructing phylogenetic trees. *Mol Biol Evol* **4:** 406–425.

Sambrook, J., Fritsch, E.F., and Maniatis, T. (1989) *Molecular Cloning. A Laboratory Manual*. New York: Cold Spring Harbor Laboratory Press.

Schellenberg, G.D., and Furlong, C.E. (1977) Resolution of the multiplicity of the glutamate and aspartate transport systems of *Escherichia coli*. *J Biol Chem* **252:** 9055–9064.

Scheu, P.D., Kim, O.B., Griesinger, C., and Unden, G. (2010) Sensing by the membrane-bound sensor kinase DcuS: exogenous versus endogenous sensing of C(4)-dicarboxylates in bacteria. *Future Microbiol* **5:** 1383–1402.

Schwoppe, C., Winkler, H.H., and Neuhaus, H.E. (2003) Connection of transport and sensing by UhpC, the sensor for external glucose-6-phosphate in *Escherichia coli*. *Eur J Biochem* **270:** 1450–1457.

Sharma, A.K., Rigby, A.C., and Alper, S.L. (2011) STAS domain structure and function. *Cell Physiol Biochem* **28:** 407–422.

Sheiden, M.C., Howitt, S.M., and Price, G.D. (2010) Membrane topology of the cyanobacterial bicarbonate transporter, BicA, a member of the SulP (SLC26A) family. *Mol Membr Biol* **27:** 12–23.

Tamura, K., Peterson, D., Peterson, N., Stecher, G., Nei, M., and Kumar, S. (2011) MEGA5: molecular evolutionary genetics analysis using maximum likelihood, evolutionary distance, and maximum parsimony methods. *Mol Biol Evol* **28:** 2731–2739.

Tetsch, L., Koller, C., Haneburger, I., and Jung, K. (2008) The membrane-integrated transcriptional activator CadC of *Escherichia coli* senses lysine indirectly via the interaction with the lysine permease LysP. *Mol Microbiol* **67:** 570–583.

Wanner, B.L. (1996) Signal transduction in the control of phosphate-regulated genes of *Escherichia coli*. *Kidney Int* **49:** 964–967.

Witan, J., Bauer, J., Wittig, I., Steinmetz, P.A., Erker, W., and Unden, G. (2012) Interaction of the *Escherichia coli* transporter DctA with the sensor kinase DcuS: presence of functional DctA/DcuS sensor units. *Mol Microbiol* **85:** 846–861.

Yanisch-Perron, C., Vieira, J., and Messing, J. (1985) Improved M13 phage cloning vectors and host strains: nucleotide sequences of the M13mp18 and pUC19 vectors. *Gene* **33:** 103–119.

Zientz, E., Bongaerts, J., and Unden, G. (1998) Fumarate regulation of gene expression in *Escherichia coli* by the DcuSR (*dcuSR* genes) two-component regulatory system. *J Bacteriol* **180:** 5421–5425.

Zolotarev, A.S., Unnikrishnan, M., Shmukler, B.E., Clark, J.S., Vandorpe, D.H., Grigorieff, N., *et al*. (2007) Increased sulfate uptake by *E. coli* overexpressing the SLC26-related SulP protein Rv1739c from *Mycobacterium tuberculosis*. *Comp Biochem Physiol A* **149:** 255–266.

Zuckerkandl, E., and Pauling, L. (1965) Molecules as documents of evolutionary history. *J Theor Biol* **8:** 357–366.

Supporting information

Additional supporting information may be found in the online version of this article.